THE STRATIGRAPHY AND SEDIMENTATION OF UPPER CAMBRIAN, PERMO - TRIASSIC AND LOWER TRIASSIC ROCKS ALONG THE NORTHEASTERN MARGIN OF THE DEAD SEA BASIN, JORDAN

A thesis submitted for the degree
of Doctor of Philosophy at
the University of Newcastle upon Tyne

ISSA M. MAKHLOUF

Geology Department

March 1987

University of Newcastle upon Tyne
Newcastle upon Tyne NE1 7RU

ACKNOWLEDGEMENTS

I wish to express my sincere thanks and gratitude to Dr. B.R. Turner, Geology Department, Newcastle University for supervising this work and for his assistance, patience and guidance in the field and for critical reading of the manuscript.

I am also greatly indebted to Prof. A. M. Abed, Geology Department, Jordan University for suggesting the research; for his supervision and guidance in the field and for his continuous encouragement during the progress of this work.

Thanks are due to Prof. J. R. Cann, for his encouragements and for his permission to use the facilities in the Geology Department at Newcastle University. I would also like to extend my thanks to the academic staff at Newcastle University for the fruitful discussions throughout, particularly to Dr. H. Armstrong for his help with the micropalaeontological work.

Many thanks are due to the academic and technical staff of the Geology Department, Jordan University for their general interest in the project and the facilities they kindly offered.

My special thanks go to the Geology Department of Oran University for providing other facilities needed for my work.

I should like to express my gratitude to all those who helped me in carrying out this work: Mr. L. Rhodes and Mr. P. Murry assisted in photomicrography; Mr. P. J. Oakley performed the chemical analyses; Miss. A. Al - Kurdi and Mr. N. Abadi for thin section preparation; Mr. G. Sumadi for X - ray diffraction.

I owe special thanks to my wife, Amal, for the support she gave me during the course of this work.

ABSTRACT

A thick sequence of predominantly terrigenous clastic sediments ranging from Cambrian to Cretaceous in age is exposed along the northeastern margin of the Dead Sea, Jordan. The present study is confined to rocks of Upper Cambrian, Permo - Triassic (Um Irna Formation) and Lower Triassic (Ma'in Formation) age, which attain a total thickness of about 150 m. The lithology, stratigraphy, sedimentary structures, lithofacies and depositional environments of these sediments have been studied in detail.

After deposition of the Early Middle Cambrian marine Burj Formation, a major regressive event occured punctuated by minor transgressive phases, during which the Upper Cambrian sediments were laid down. These lie conformably on the Burj Formation, and are unconformably overlain by the Permo - Triassic Um Irna Formation.

The Upper Cambrian succession consists of a medium - to coarse - grained quartzarenite facies and a subordinate heterolithic facies of siltstone and mudstone with sandy lenses. Internally the arenites are structured by trough cross - bedding arranged in cosets or solitary sets. Foreset dip directions show a unidirectional northwesterly mode. Most of the trough cross - beds are deformed giving rise to penecontemporaneous overturning of the foresets in the down-current

direction. This is attributed to shear stress exerted by a dense sediment - laden current of water moving over the top of seismically liquefied cross - bedded sand.

The Upper Cambrian sediments were deposited on a braidplain and adjacent tidal flats due to periodic shifting of the active part of the braidplain. Reworking of the inactive part of the braidplain by tidal currents and subsidence led to marine incursions and the devel - opment of tidal flats.

The Permo - Triassic Um Irna Formation is conformably overlain by interbedded sandstone, siltstone and mudstone of the Lower Triassic Ma'in Formation. ~~Lithostratigraphically the~~ Um Irna Formation can be divided into a lower and upper member according to grain size and the proportion of sandstone to siltstone and shale in succession. The lower member attains a thickness of 10 m and is characterised by the presence of five sandstone-dominated fining - upward sequences from 0·75 to 2·15 m thick comprising an erosively - based coarse-to fine-grained sandstone overlain by, and laterally intertonguing with, maroon silt - stone and shale. The sandstones are internally structured by small - scale (< 20 cm thick) trough cross - bedding. Foreset azimuths show a unidirectional trend towards the north - northwest.

The upper member also consists of five fining - upward sequences from 4 to 14·5 m thick, each sequence comprising an erosively - based

pebbly sandstone grading up through medium and fine-grained sandstone into maroon siltstone and silty - shale. Trough cross - bedding is the dominant internal structure with foresets directed towards the north - northwest. A characteristic feature of the silty - shale is the presence of abundant ferruginous concretions (pisoliths).

Both members were deposited by fluvial processes. The lower member is attributed to deposition mainly by shallow, low sinuosity sand bed channels draining the distal reaches of a low gradient alluvial plain. The upper member contains a higher proportion of overbank fines (silt and mud) consistent with deposition by a mean - dering fluvial system, while the dominance of pebbly components in the sandy facies and their multilateral and multistorey nature suggests deposition by low sinuosity channels on the more proximal reaches of the braidplain. The nature of the concretions (Fe- pisoliths) suggests that the diagenetic (pedogenic) environment was complex with alternating episodes of leaching, cementation and fracturing during their growth.

The Lower Triassic Ma'in Formation is overlain by the shallow marine Dardur Formation. Two facies are recognised within the Ma'in Formation. The lower Himara Member comprises two facies which are deep maroon in colour and highly bioturbated: a lower sandy facies and an upper heterolithic facies (sand, silt and mud). This member is thought to have been deposited on a tidal flat as evidenced by rhythmic

beds of sand, silt and clay, flaser, wavy and lenticular bedding, herringbone cross - bedding, mudcracks, raindrop imprints, superimposed ripple marks showing interference, and ladder-back forms reflecting shallowing and late stage emergence run off features. The depositional model proposed is one of a microtidal to mesotidal coastline, with a palaeotidal range of 0·45 m to 2·35 m. The coastline is inferred to have been interacting with a braided fluvial plain, which fed in quartzitic sediment from the southeast as indicated by the palaeocurrent pattern.

The upper, more sandy, Nimra Member is cream in colour, more fossiliferous and more calcareous. The proposed depositional model is that of a shallow subtidal shelf receiving clastic sediment by way of river mouths extending seawards as subtidal channels. The shallow open marine nature of the environment is indicated by the presence of ooids, foraminifers, lamellibranchs, echinoids, bryozoans and gastropod fragments cemented mainly by dolomite.

The overall model proposed for the Ma'in Formation is that of an intertidal flat (Himara Member) located between a braided alluvial plain (Um Irna Formation) and a subtidal marine shelf (Nimra Member).

CONTENTS

TABLES

FIGURES

Fig. 3. 7. Heterolithic facies of the Upper Cambrian at section 3 showing ball - and - pillow and wedge shaped structures, intercalated within muds. These may be due to differential loading (drawn from photographs).

Fig. 3. 8. Heterolithic facies of the Upper Cambrian at section 3 showing ball - and - pillow structures. Sandstone masses have sunk down within the mud (drawn from photographs).

Fig. 3. 9. Overturned cross - beds. (a) and (b) are simple recumbent folds with smooth, completely overturned limbs, and fold nose in the middle portion. (c) Slight steepening of the upper part of the cross - bed with the hinge zone located in the upper part which shows slight undulations. (d) The upper part is moderately steepened to form an asymmetrical recumbent fold (right side). The hinge zone is located in the upper part and slightly undulated. (b) and (d) at section 5, (a) and (c) at section 3, (drawn from photographs).

Fig. 3.10. Overturned cross - beds. (a) and (c) are simple recumbent folds (completely overturned limbs) with fold nose near to the lower surface. The lower and upper limbs are almost parallel. (b) and (d) show overturned cosets in which the hinge zone is undulatory. (a) and (d) at section 8, (b) and (c) at section 3, (drawn from photographs).

Fig. 3.11. Overturned cross - bedding. (a) slight steepening of the upper part. (b) Moderate overturning with an undulated hinge zone. (c) Moderate steepening of the upper part of the cross - bed to form asymmetrical recumbent folds. In the upper recumbent fold the hinge zone is located in the upper part. In the lower recumbent fold the hinge zone is located in the middle part. (d) The upper and lower limbs

PLATES

Plate 3. 1. General view showing a vertical sequence of the different rocks under study. Upper Cambrian, Permo - Triassic (Um Irna Formation) and Lower Triassic (Ma'in Formation). The total vertical section in the picture is more than 115 m. Section 6.

Plate 3. 2. General view showing the contact (arrow) between the Middle Cambrian (fine sediments) and the Upper Cambrian (compact sandstones), in the area between Wadi Himara and Wadi Zarqa Ma'in.

Plate 3. 3. General view showing a vertical section of the Upper Cambrian succession at section 5. The sandy facies is brownish and the heterolithic facies is maroon coloured. The total thickness within the picture is nearly 40 metres. Section 5.

Plate 3. 4. Sharp planar contact separating the heterolithic facies below from the sandy facies above. Upper Cambrian, section 5 (hammer is 30 cm long).

Plate 3. 5. Exposure at section 5 illustrating vertically repetitive medium - scale trough cross - bedding. Note overturned cross - beds. Upper Cambrian, sandy facies (hammer is 30 cm long).

Plate 3. 6. Low - angle, tangentially - based cross - bedding in medium - to coarse - grained sandstones. Pebbles and mudclasts are imbricated. View parallel to the palaeocurrent direction (left to right). Upper Cambrian sandy facies, section 5 (hammer is 30 cm long).

Plate 3. 7. Small - scale trough cross - bedding resting on and overlain by massive sandstones in the quartzarenite facies of the

Upper Cambrian at section 5. View parallel to the direction of current (hammer is 30 cm long).

Plate 3. 8. Thick bedded quartzarenites of the Upper Cambrian. Beds are separated by erosional surface (at hammer), section 5, (hammer is 30 cm long).

Plate 3. 9. Sandy unit of the Upper Cambrian, in which the lower part is composed of friable parallel laminated sandy, silty shale. The upper part is composed of compact, trough cross - bedded locally overturned sandstone, current direction is to the left. Section 3, (hammer is 30 cm long).

Plate 3.10. Planar tabular cross - bedded set (at hammer) interbedded within heterolithic facies of the Upper Cambrian. View is parallel to the current direction (left to right) section 8, (hammer is 30 cm long).

Plate 3.11. The uppermost interval of the heterolithic facies of the Upper Cambrian, composed of siltstone, conglomerate lenses and sand - stone. Section 3, (hammer is 30 cm long).

Plate .3.12. Large sandstone pillows within a deep maroon mudstone. The sand layer is broken up into isolated pillows, some of them showing deformation structures. Note that the structure is confined to a specific bed, and it is laterally persistent. Heterolithic facies, Upper Cambrian, section 3, (hammer is 30 cm long).

Plate 3.13. Ball - and - pillow structure and bottom irregularities in sandstone bed ascribed to load casting in interbedded sandstone and shale. Note the predominance of down - facing convexities and the lateral persistence of the deformed layer. Heterolithic facies, Upper

Cambrian, section 3, (hammer is 30 cm long).

Plate 3.14. Bedding surface showing sinuous crested - ripples. Note silty shale lamination (to the left) in the heterolithic facies of the Upper Cambrian at section 3, (hammer is 30 cm long).

Plate 3.15. Bedding surface showing bivalve fossils and bioturbation in a silty shale unit of the heterolithic facies, Upper Cambrian, section 5, (pen is 15 cm long).

Plate 3.16. Thin sandy and silty shale beds of the heterolithic facies, Upper Cambrian, showing the following sedimentary structures; small -, medium - and large - scale ripple marks, cross - lamination, wavy bedding surfaces and load structures. Section 5, (hammer is 30 cm long).

Plate 3.17. Thin rippled beds and laminations of sandy, silty and clayey components comprising part of the heterolithic facies. Note the clay draped ripples and the dissected behaviour of lenses and ripples. Some ripples suggest that they have been piled up and completely rotated (below the pen). Upper Cambrian, section 5, (pen is 15 cm long).

Plate 3.18. Overturned cross - bed forming simple recumbent fold with completely overturned limbs. The fold nose is near to the upper surface. Quartzarenite facies, Upper Cambrian, section 5, (hammer is 30 cm long).

Plate 3.19. Overturned cross - beds forming simple recumbent folds with completely overturned limbs and fold nose near the lower surface. Quartzarenite facies, Upper Cambrian, section 3, (hammer is 30 cm long).

Plate 3.20. Overturned cross - bedding, with a moderate steepening of the upper set to form asymmetrical recumbent fold in which the hinge zone is located in the upper part. In the lower set (at hammer) the hinge zone is located in the middle part. Quartzarenite facies, Upper Cambrian, section 5, (hammer is 30 cm long).

Plate 3.21. S - shaped folds in which double overturning took place in a cross - set, to form a recumbent anticline above a recumbent syncline. Quartzarenite facies, Upper Cambrian, section 3, (hammer is 30 cm long).

Plate 3.22. Vertical section showing the contact (arrow) between the Upper Cambrian and the Permo - Triassic (Um Irna Formation). Note the difference in colour, cross - bedding and weathering surface. Section 3, (hammer is 30 cm long).

Plate 3.23. Close up of plate 2.22 showing the deformed cross - bedding of the Upper Cambrian, section 3, (hammer is 30 cm long).

Plate 3.24. Contorted lamination in medium - grained sandstone indicating hydroplasticity during deformation. In the lower part the foresets are tangential, but truncated sharply at top by a planar surface. Quartzarenite facies, Upper Cambrian, section 5, (hammer is 30 cm long).

Plate 3.25. Contorted and crumpled cross - set with tangential base and truncated top. Note the undisturbed layers above and below. Quartzarenite facies, Upper Cambrian, section 5, (hammer is 30 cm long).

Plate 4. 1. General view showing the uppermost fining-upward sequence of the Um Irna Formation at section 11. The contact with the

Ma'in Formation is shown by the arrow. Section 11.

Plate 4. 2. Vertical section showing the contact (arrow) between the lower and upper Members of the Um Irna Formation at section 12.

Plate 4. 3. Lenticular bedded sandstone interbedded with silty - shale (hammer head) typical of the Lower Member of the Um Irna Formation. Note faint low angle trough cross - beds in sandstone. Section 7, (hammer is 30 cm long).

Plate 4. 4. General view showing the upper part of the Um Irna Formation overlain by the Ma'in Formation at section 11.

Plate 4. 5. Trough cross - bedded sandstone of the Um Irna Formation (Upper Member). View perpendicular to trough axes. Section 11, (hammer is 30 cm long).

Plate 4. 6. Side view parallel to trough axes of plate 4.05, transport from left to right. Trough cross - sets usually start with pebbly bottom - sets. Section 11, (hammer is 30 cm long).

Plate 4. 7. Planar - tabular cross - bedding, composed of Fe - pisoliths, pebbles and large-scale mudclasts, overlying greenish, pisolitic shales (transport to right). This unit marks the top of the Um Irna Formation. Section 11, (pen is 15 cm long).

Plate 4. 8. Trough cross - bedding in the Um Irna Formation (Upper Member) in which the internal laminae are graded and fine - upward. Colour reflects oxidation reduction processes. Section 7, (hammer is 30 cm long).

Plate 4. 9. Silty shale unit composed of Fe - pisoliths up to 3 cm in diameter in the Um Irna Formation, immediately above the Upper

Cambrian rocks, at section 12, (hammer is 30 cm long).

Plate 4.10. Bedding surface showing maroon silty matrix supported oval - shaped pisoliths (iron concretions) with large concentric internal structure (films and nuclei). Some pale reduction haloes are present. Upper Member of the Um Irna Formation at section 12, (coin is 2·5 cm in diameter).

Plate 4.11. Sandstones with carbonaceous material of the Um Irna Formation (Upper Member) at section 6. Note the lower limonitic part, (hammer is 30 cm long).

Plate 4.12. Flaser - bedded, ripple laminated silty - shale. Fe- pisoliths are common, especially in the lower part. Um Irna Formation (Upper Member) at section 13, (hammer is 30 cm long).

Plate 4.13. Photomicrograph of a ferruginous pisolith showing a well developed concentric structure, silty - shale, Upper Member, Um Irna Formation, section 11. Polarised light.

Plate 4.14. Photomicrograph showing a ferruginous pisolith lacking any internal structure. Note dendritic fractures and scattered fine to coarse angular to subrounded quartz grains enclosed within the concretion. Silty - shale, Upper Member, Um Irna Formation, section 11. Polarised light.

Plate 4.15. Photomicrograph of a ferruginous concretion showing a concentric structure. The nucleus is formed by an aggregate of sand-size quartz clastics. Silty - shale, Upper Member, Um Irna Formation, section 11. Polarised light.

Plate 4.16. Photomicrograph of a ferruginous concretion showing

lopsided inclusions of fine to coarse angular to subrounded quartz grains. The pisolith has been flattened during diagenesis. Silty - shale, Upper Member, Um Irna Formation. Polarised light.

Plate 4.17. Photomicrograph showing two generations of ferruginous concretions. To the right a concretion formed by the cementation of accumulated angular to subrounded quartz grains. To the left smaller ferruginous pisoliths showing quartz nuclei. Silty - shale, Upper Member, Um Irna Formation, section 13. Polarised light.

Plate 4.18. Photomicrograph showing some of the enclosed quartz grains fractured into a number of fragments (2 - 5) and then coated by iron oxide. Silty - shale, Upper Member, Um Irna Formation, section 11. Polarised light.

Plate 5. 1. A general view of the Ma'in Formation at section 1, showing the contact (arrow) between the Himara Member (reddish, lower) and the Nimra Member (cream, upper).

Plate 5. 2. Thin rippled beds of silty, very fine-grained sandstone comprising the Himara Member (Ma'in Formation) at section 1. Note the oxidation (red) reduction (cream) colour of sediments (hammer "arrow" is 30 cm long).

Plate 5. 3. Vertical section showing the contact between Um Irna Formation (lower) and Ma'in Formation (upper) see arrow. Below the contact a greenish pisolitic silty shale of the Um Irna Formation is overlain by a bed composed of quartz pebbles, mudclasts and pisoliths. Above the contact the Ma'in Formation begins with rippled silty and sandy laminations which are usually bioturbated, cross - laminated and

mudcracked. Alternations of sand, silt and clay are common. Section 6, (hammer is 30 cm long).

Plate 5. 4. Folded, rhythmic bedding composed of thin clayey, silty and sandy beds. Section 2, (arrow shows hammer 30 cm long for scale).

Plate 5. 5. General view showing the lower part of the Himara Member, consisting mainly of sandy facies below hammer, and silty shale facies above. Bedding surfaces are usually rippled and bioturbated. Note mudcracks at the bottom. Section 1, (hammer is 30 cm long).

Plate 5. 6. Vertical section showing sand infilled desiccation cracks at two levels. Note ripple cross - laminations at top of pen. Section 1, (pen is 15 cm long).

Plate 5. 7. Bedding surface showing mudcrack polygons enhanced by sand infilling. Himara Member, section 1, (pen is 15 cm long).

Plate 5. 8. Underside of thin bedded sandstone showing casts of sand polygons filling eroded mudcracks. Himara Member, section 4.

Plate 5. 9. Bedding surface and vertical section (two dimension) associated with animal trails. Himara Member, section 10, (hammer is 30 cm long).

Plate 5.10. Sinuous ripple marks on bedding surface with abundant horizontal burrows (tracks, trails and smooth - walled meandering tubes) along the troughs. Himara Member, section 10, (hammer is 30 cm long).

Plate 5.11. Sinuous - crested current ripples superimposed obliquely on different bedding surfaces. Note that the ripples having dissimilar crest orientations on different bedding planes. Himara Member, section 1, (hammer is 30 cm long).

Plate 5.12. Linguoid ripple marks on thin bedded sandstone, current from upper left to lower right. Himara Member, section 4, (hammer is 30 cm long).

Plate 5.13. Interference current ripples on bedding surface, top of picture above hammer head. On the left ladder back ripples comprise a secondary train of very small - scale ripples (2 cm wave - length) oriented at 90° to the troughs of the larger ripples (4 cm wavelength). On the right slightly sinuous - crested ripples are shown. Himara Member, section 6, (hammer is 30 cm long).

Plate 5.14. Bedding surface of a fine - grained sandstone showing rain imprints, wrinkle marks and crawling trails. Himara Member, section 7, (pen is 15 cm long).

Plate 5.15. Herringbone cross - bedding above sand infilled desiccation cracks, at base of Himara Member. Note rippling and wavy laminations upward, section 1, (pen is 15 cm long).

Plate 5.16. Micro cross - laminations in the lower part of the Himara Member. Below pen is a claystone horizon. Himara Member, section 6, (pen is 15 cm long).

Plate 5.17. Ripple cross - laminations at base passing upward into parallel laminations within a sandstone bed. Himara Member, section 11, (pen is 15 cm long).

Plate 5.18. Bedding surface showing a fossiliferous bed (coquina) composed of bivalves, in the sandy facies of the Himara Member, section 6, (pen is 15 cm long).

Plate 5.19. Silty - shale facies of the Himara Member showing the

the following sedimentary structures; wavy, rippled, flaser and lent - icular bedding. Note soft sediment deformation features above the pen which may be due to differential compaction (thixotropy) or dewatering processes. Mud draped ripples at the base of pen. Section 1, (pen is 15 cm long).

Plate 5.20. Sequence of interbedded thin sandstone and mudstone exhibiting soft - sediment deformation and balling - up, possibly due to thixotropy. Note rippling and oxidation (red) reduction (cream, greenish) colour of sediments. Himara Member, section 1, (pen is 15 cm long).

Plate 5.21. Interbedded sandstone and shale exhibiting soft - sediment deformation and balling - up, possibly due to thixotropy or a water escape plume. Himara Member, section 4, (hammer is 30 cm long).

Plate 5.22. Bedding surface showing laterally linked and discrete stromatolite structures. Himara Member, section 4. (hammer is 30 cm long).

Plate 5.23. Vertical section showing stacked, linked hemispheroidal stromatolites. Himara Member, section 4, (hammer is 30 cm long).

Plate 5.24. Vertical section showing hemispheroidal stromatolites with clear laminations. Himara Member, section 4, (hammer is 30 cm long).

Plate 5.25. Ripples in alternating sand and silty shale with interbedded deformation structures (balling - up, convolution and pseudonodules) which may be due to thixotropy. Nimra Member, section 11, (pen is 15 cm long).

Plate 5.26. General view showing the upper contact of the Ma'in Formation with the Dardur Formation (arrow). Section 11.

Plate 5.27. Internally rippled rhythmites in the lower part of the Nimra Member, section 11, (hammer is 30 cm long).

Plate 5.28. Alternating calcareous (cream) and non calcareous sandstone (white) comprising the upper part of the Nimra Member. Section 2.

Plate 5.29. Sinuous ripples (symmetrical) on bedding surface, with abundant horizontal burrows, usually along the ripple troughs. Nimra Member, section 1, (pen is 15 cm long).

Plate 5.30. Intrusive igneous sill (at hammer level) embedded between two sandstone layers. Nimra Member, section 1, (hammer is 30 cm long).

Plate 6. 1. Photomicrograph of a medium - grained well - sorted quartzarenite (nearly 96 percent quartz), with well - rounded to sub - rounded quartz, cemented by quartz overgrowth in optical continuity with the detrital grains. The boundaries between detrital core and overgrowth are made very distinct by a continuous line of "dust" particles (commonly clay minerals). Polarised light, sample No. C 0514.

Plate 6. 2. Photomicrograph of a fine - grained moderately well-sorted sublitharenite. Quartz grains are subangular and highly interlocked Intergranular pore space is infilled mainly by iron oxide cement and kaolin (fibrous) matrix (centre). Quartz overgrowths are also visible. Crossed polars, sample No. C 03 20.

Plate 6. 3. Photomicrograph showing a grain of ilmenite (black,

centre), with secondary overgrowths giving rise to the formation of leucoxene (colourless) with euhedral toothed form. Polarised light sample No. C 03 16.

Plate 6. 4. Photomicrograph of a ferruginous pisolitic siltstone of the Um Irna Formation, showing a ferruginous pisolite with quartz nuclei. The matrix is mostly kaolin (white) and iron oxides (black). Polarised light,sample No. U 12 01.

Plate 6. 5. Photomicrograph of a medium - grained sublitharenite , cemented mainly by iron oxides; some of the quartz grains appear to have been reworked. The interstices are occupied partially by kaolin with fibrous and booklet behaviour. Crossed polars, sample No. U 11 00.

Plate 6. 6. Photomicrograph of a medium - grained lithic subarkose, showing the original subrounded grains of quartz modified by authigenic overgrowths. The margin of the original detrital cores is occupied by a film of clay minerals. Polarised light, sample No. U 13 07.

Plate 6. 7. Photomicrograph of a coarse - grained subarkose, cemmented by ferroan dolomite. A dolomite rhomb is well developed (centre). An orthoclase grain (bottom left) shows marked evidence of corrosion by percolating carbonate - rich pore waters. Polarised light, sample No. U 06 05a.

Plate 6. 8. Photomicrograph of a fine - grained lithic subarkose, showing well - sorted, subrounded to subangular quartz grains, with orthoclase and microline (centre right), cemented by iron oxide and quartz authigenic overgrowths. The interstices are occupied partially by kaolin. Crossed polars, sample No. U 06 10.

Plate 6. 9. Photomicrograph of a coarse silty arkose, showing well - sorted, subrounded to subangular quartz grains, with orthoclase and twinned plagioclase (centre), cemented by iron oxide and ferroan dolomite, with some scattered dolomite rhombs (centre). Crossed polars, sample No. H 11 15.

Plate 6.10. Photomicrograph of a coarse silty arkose, consisting of a moderately sorted mixture of angular to subangular quartz and feldspar grains together with a little mica set in a ferroan dolomite cement and clotlike (black) hematite matrix. Abundant, though not clearly shown in the figure, are rhombic dolomite euhedra (centre). Polarised light, sample No. H 07 07.

Plate 6.11. Photomicrograph of a medium - grained calcarenaceous orthoquartzite, cemented by dolomite and showing a fuziform foraminiferal tests (centre) with further recrystallisation. Brachiopod debris (top left) and floating quartz grains in a dolomitic cement are also visible. Polarised light, sample No. N 10 10a.

Plate 6.12. Photomicrograph of a medium - grained calcarenaceous orthoquartzite, cemented by dolomite. Skeletal debris includes bryzoan fragment (centre) showing dolomite recrystallisation. Polarised light, sample No. N 10 10b.

Plate 6.13. Photomicrograph of a medium - grained calcarenaceous orthoquartzite, cemented by dolomite. Moderately - sorted, subrounded quartz grains appear to be floating in the dolomite cement. Spherical ooidshs (algal) with a concentric structure are embedded in dolomitic cement; some of the ooidshs have a single quartz nucleus or a shell

fragment. Polarised light, sample No. N 07 08.

Plate 6.14. Photomicrograph of a calcarenaceous orthoquartzite, showing elongate fragment of lamillibranch, ooïdsh and quartz grains floating in a dolomite cement. Polarised light, sample No. N 07 08.

CHAPTER ONE

INTRODUCTION

CHAPTER ONE

INTRODUCTION

1.1 AREA AND GEOMORPHOLOGY

Jordan, with an area of about 96,500 Km^2, is situated in the north-western part of the Arabian Peninsula, which is bordered by the Mediterranean Sea, the Red Sea, the Indian Ocean and the Arabian Gulf (Fig. 1. 1). Jordan consists of the following morphological units (Bender, 1974):

i. The Northeastern Desert (east of the Mafraq - Azraq - Wadi Sirhan). This consists of (a) the Harrat esh shaba plateau basalts, which are thought to be a southerly extension of the Jabel ed Drouz basalt highland, and which lie at an altitude of more than 1,100m, and (b) the Jordanian limestone plateau lying at an elevation of some 623 m above sea level.

ii. The Azraq - Wadi Sirhan Depression. This depression occurs to the west of the Northeastern Desert. It extends from the southern rim of the Jebel ed Drouz basalt shield and continues south - eastwards across the Azraq Oasis at an elevation of about 500 m above sea level.

iii. The Central Desert Areas of East Jordan. This lies at an elevation of about 1000 m above sea level.

iv. The Escarpment of Ras en Naqab. This reaches altitudes of about 1,700 m above sea level (south - west of Ma'an).

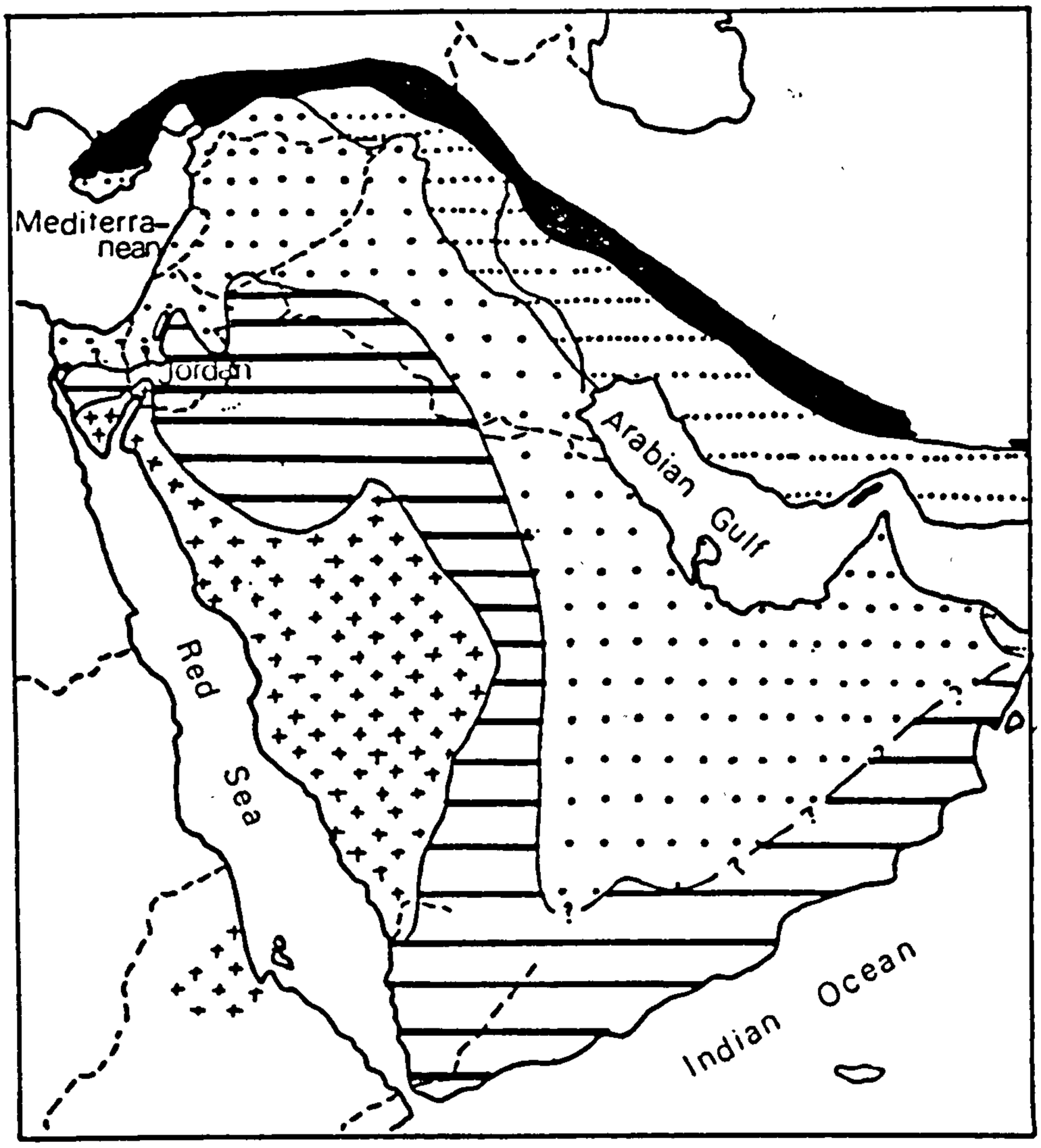

Zone of Neogene autochthonous folding

Zone of marginal troughs in the unstable shelf

Unstable shelf

Stable shelf

Nubo - Arabian Shield

Fig. 1. 1. Tectonic stratigraphic zones of the Arabian Peninsula (from Bender, 1974).

v. The Highlands at the Eastern Rim of the Wadi Araba - Jordan Graben (1,300 m above sea level). These slope gently towards the central plateau in the east, but they have a very steep scarp face overlooking the Dead Sea Rift in the west which lies at an elevation of 402 m below sea level. It is dissected by deep wadis running east - west into the rift.

vi. The Dead Sea Rift Including the Wadi Araba - Dead Sea Basin and The Jordan Valley. This extends for about 360 Km. from the Gulf of Aqaba to Lake Tiberias. The elevation of the southern margin of the Dead Sea is 392 m below sea level. It attains a maximum depth of 402 m. Thus, the deepest point of the whole depression is 793 m below sea level. Along the 105 Km length of the Jordan Valley, the elevation ranges from 407 m below sea level in the south, up to 212 m below sea level at Lake Tiberias in the north (Fig. 1. 2).

1.2 CLIMATE

A mediterranean climate dominates the highlands (700 m above sea level) on both sides of the Jordan River, and in the mountain chains east of the Dead Sea and Wadi Araba Rift. Its influence extends southwards to Shobak. The climate has an average maximum annual temperature of 38·8°C, and an average minimum annual temperature of 0·5°C. The average annual rainfall is more than 300 mm.

A semi-arid climate characterizes the transitional zone between

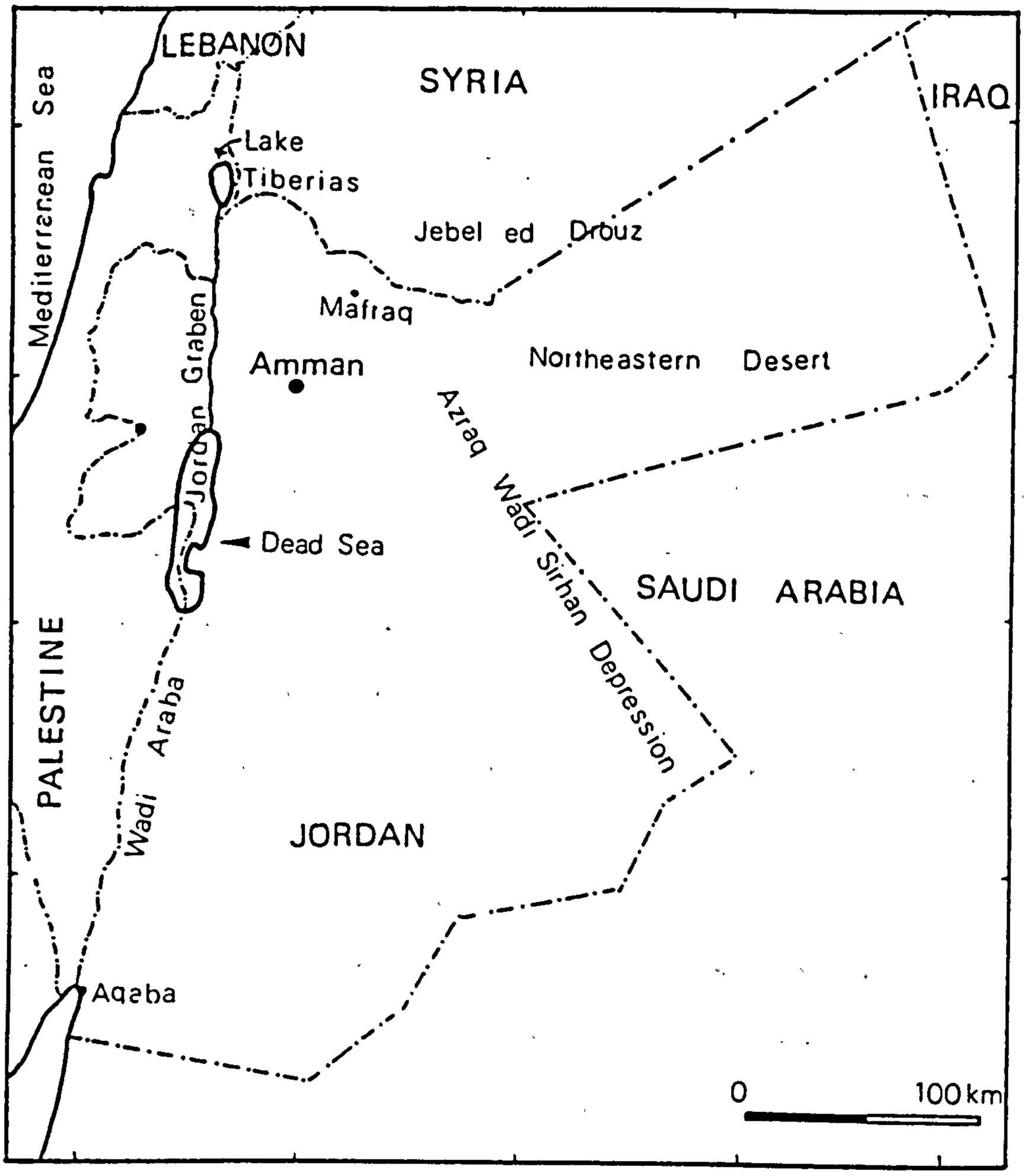

Fig. 1. 2. Map of Jordan, showing major morphological units (from Bender, 1974).

the northern and western highlands and the eastern and southern desert. The average annual maximum temperature is 40°C, and the average annual minimum temperature is -1·6°C. The average annual rainfall is 50 - 300 mm.

An arid climate characterizes the eastern and southern deserts, with an average annual rainfall of less than 50 mm.

1.3 GENERAL CONSIDERATIONS

1.3.1 THE DEAD SEA

The Dead Sea which is 402 m below sea level, is the lowest subaerial point on the earth's surface. It is 79·5 km long and 17·5 km wide. The surface area of the Dead Sea prior to the late fifties was 1000 km^2 and it is divided by the Lisan Peninsula into a northern and southern basin which are connected by a narrow strait (Fig. 1. 3).

The northern basin makes up about 75% (about 756 km^2) of the Dead Sea, and it attains a maximum depth of 400 m on the eastern side. In contrast the southern basin (about 244km^2) is very shallow with a depth of less than 10 m. The catchment area of the Dead Sea extends over some 40,000 km^2 (Bentor 1961; Abed, 1983).

Prior to the middle fifties the Dead Sea was supplied by 1,600 m^3

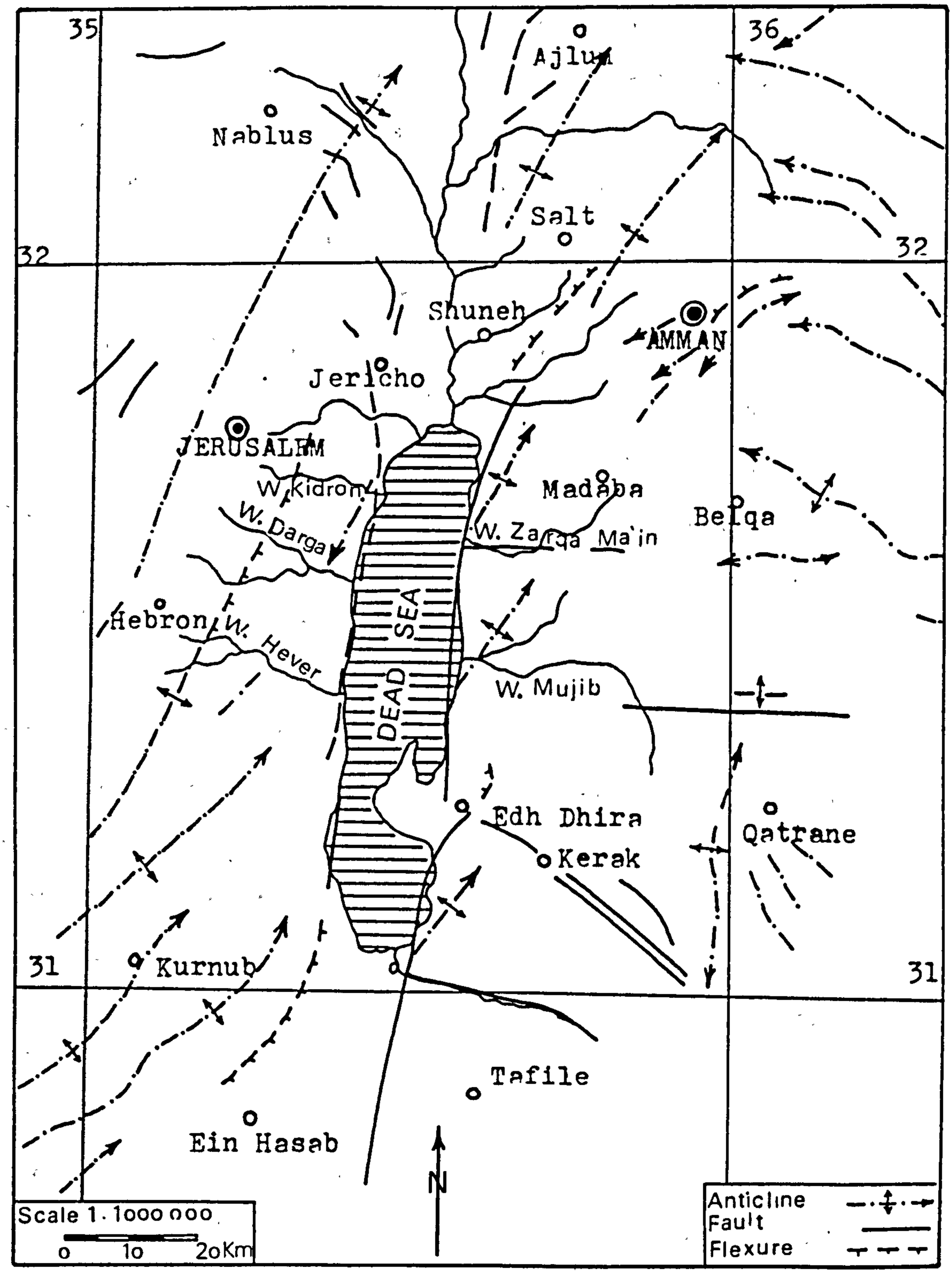

Fig. 1. 3. Structural sketch of the Dead Sea basin in Jordan (Wetzel and Morton, 1959).

a year of fresh water and an equal amount of water was evaporated from its surface. Thus, the area of the sea (1000 km^2) remained fairly constant. This situation has changed since the occupation of Palestine and the establishment of the state of Israel. More than 500 mll / m^3 / year of fresh water was and still is pumped from Lake Tiberias by the Israelis. Smaller amounts of water are also utilized by Jordan. Thus, the Dead Sea started shrinking and by 1982 the Dead Sea level was -402 m and its area was 800 km^2 (Abed, 1983). The Dead Sea is a hypersaline lake with a salinity of about 32%. The major components are $MgCl_2$, NaCl, $CaCl_2$, KCl, $MgBr_2$ and $CaSO_4$.

1.3.2 ORIGIN OF THE DEAD SEA RIFT

Since early last century the evolution of the Dead Sea Rift attracted the attention of many geologists. Several papers have been published on the subject and geologists are divided between those who support horizontal movement along the Rift (Lartet, 1869; Quennell, 1958, 1983; Freund et al., 1970, 1981; Bandel, 1981; Abed, 1984) and those who advocate graben tectonics (Picard, 1943; Wetzel and Morton, 1959; Bender, 1974, 1983).

Quennell (1983) indicated that those who favoured the graben model have mostly worked in local areas, as for example on the Dead Sea itself. On a more regional basis the graben mechanism is unsatisfactory because of the absence of a second fault, and a rift situation

seems more likely. Quennell (1959) lists ten geological features which come into juxtaposition when Arabia is restored with respect to Sinai by a total movement of 107 km.

Bender (1974) stated that Wadi Araba - Jordan Graben extends for some 360 km, and that it forms part of the East African - North Syrian fault system which can be traced for about 6000km. It strikes 15° northeast from the Gulf of Aqaba to the Dead Sea ("southgraben", approx. 200 km), where it changes direction and strikes at 5° northeast towards Lake Tiberias ("Northgraben" approx. 160 km) (Fig. 1. 4). It separates the "Palestine Block" in the west from the "Transjordan Block" in the east. The width of the graben floor which is occupied chiefly by Neogene and Quaternary deposits ranges from 5 to 25 km.

Wagner (1924) was particularly impressed by the coastline fits of the Red Sea and Gulf of Aden which led him to propose the drift of Arabia from Africa. In modern terminology, Arabia has rotated anti-clockwise with respect to Africa with the opening of the Red Sea and Gulf of Aden to the west and south, and the formation of the Toros - Zagros mountains to the north and northeast (Girdler, 1983) (Fig. 1. 4).

Since the pioneering work of Lartet (1869) and Quennell (1958, 1959), the Jordanian Rift has been recognised as a major shear zone with left lateral movement. Quennell estimates the total displacement as 107 km and attributes this to a rotation of Arabia by 6° with respect

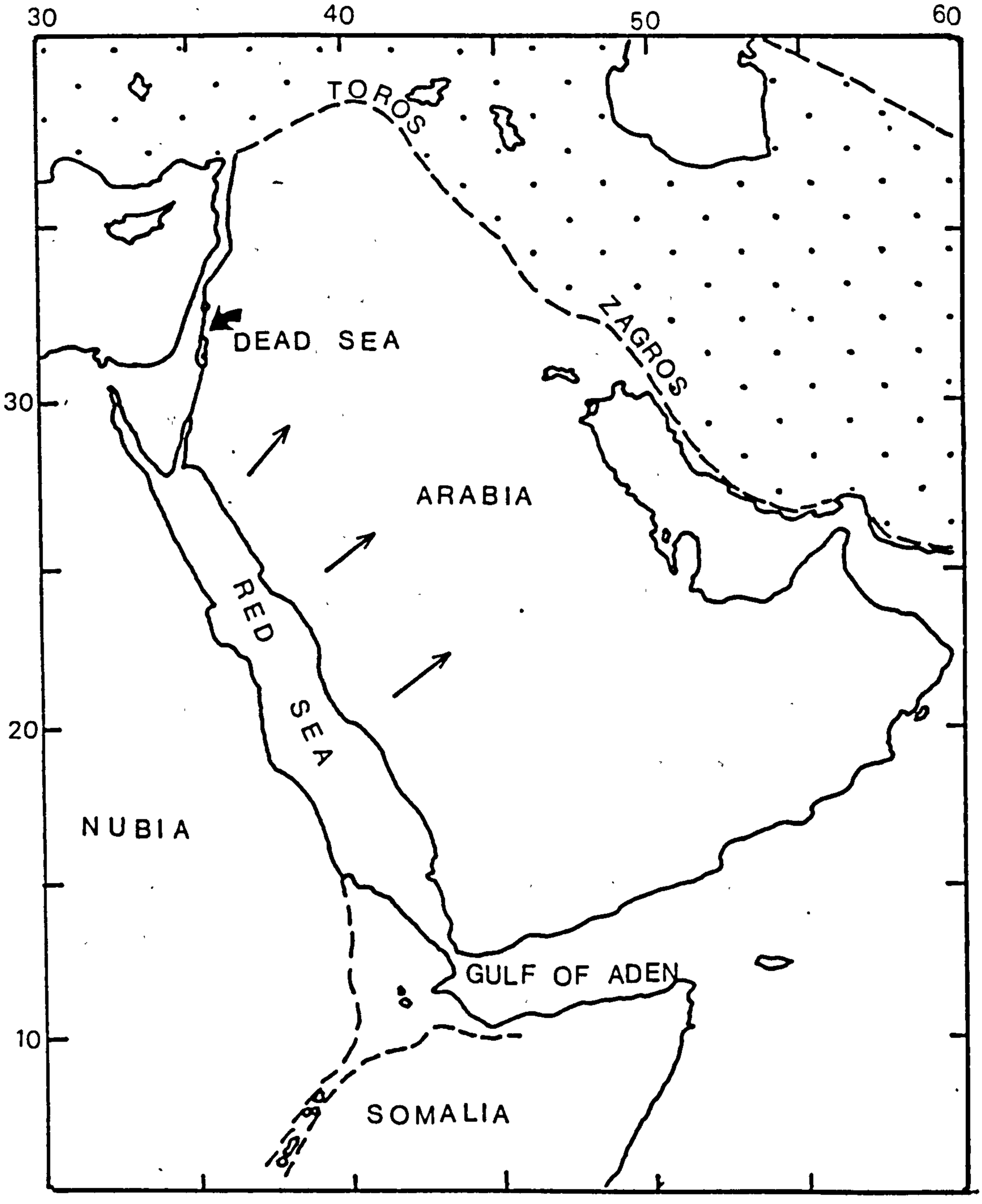

Fig. 1. 4. Generalised plate tectonic setting of the Middle East. The Jordan Dead Sea Rift is a left lateral transform fault system connecting the Red Sea to the Toros - Zagros mountains (Girdler, 1983).

to Sinai about a centre of rotation at approximately 33°N, 24° E. Quennell (1958) also notes that the movement of Arabia in relation to Sinai - Palestine is believed to have taken place intermittently during two principal phases. During the first, the horizontal movement was 62 km and the rotation more than 3° which is considered to be early Miocene and / or latest Oligocene. During the second phase the displacement was 45 km and the rotation more than 2·5°. This is considered to have taken place in the Plio - Pleistocene and is still continuing today. The Lower Miocene is considered by Picard (1943) to have seen the begining of fault movement resulting in the modern rift.

Bandel (1981) has strongly supported the ideas put forward by Quennell (1959) and Burdon (1959) that a sinistral movement of more than 100 km (Quennell) and 107 km (Burdon) has taken place. Recently Salameh (1980) came to a similar conclusion and suggested a shift of 105 to 110 km when he correlated the structural highs of Suweilih, Amman, Es salt - Ajlun as extensions of the Hebron - Ramallah structural highs on the west side of the Rift valley.

1.3.3 THE NUBIAN SANDSTONE

The term "Nubian Sandstone" has been applied to outcrops in Algeria, Libya, Egypt, Sudan, Palestine, Jordan, Saudi Arabia, Niger and Chad. The term was first introduced by Joseph Russegger in 1837. He used the term to designate the thick clastic sequence overlying the

Precambrian crystalline basement and underlying the Upper Cretaceous series which is exposed in Nubia, the region on both sides of the Nile Valley, along the border of southern Egypt and northern Sudan.

On his map Russegger extended the name to the entire, predominantly clastic sequence lying above the crystalline basement in Egypt, Sinai Palestine, Jordan and Saudi Arabia. In the type area where the Nubian sandstone is entirely of Cretaceous age it rests upon a peneplaned Precambrian surface and consists of a series of largely unfossiliferous brown, yellow or buff sandstones. The sandstones are conspicuously cross - stratified on a small to medium - scale and contain much fine-grained gravel, occuring in lenses or scattered randomly across foreset bedding planes. Quartz grains within individual sandstone units are mainly moderate to well sorted and mostly fine - to - medium - grained. The sandstone is thought to have been deposited in aeolian, fluviatile lacustrine, estuarine, beach and near shore marine environments (McKee, 1962).

The main characteristics common to the Nubian sandstones as a whole are their general lithologic uniformity, red - bed type appearance, similar stratigraphic position, continuous deposition over a vast time span and their geographical location (margins of the Arabian and African massifs) (Sneh and Weissbrod, 1978).

Undoubtedly the Nubian sandstone represents a complex of depositional environments in both lateral and a vertical sense, and petrogenetic

studies of this formation have long suffered from too much generalisation based on too few and often unsatisfactory sample data. These sandstones are mostly recycled orthoquartzites whose detrital grains were initially derived from weathering of the ancient Precambrian to Mesozoic Arabo - African craton (Gindy et al., 1982).

Since Russegger, the use of the term "Nubian Sandstone" has spread widely, both in a geographic as well as a stratigraphic sense. The term has been used differently by various authors for similar clastic sequences all over North Africa and the Middle East, and has been applied to rocks ranging in age from Precambrian to Holocene. An excellent review on the stratigraphic terminology and other problems of the Nubian Sandstones is given by Pomeyrol (1968) and subsequent discussions by several authors in the Bulletin of the American Association of Petroleum Geologists (Vols. 53, 54 and 55).

In Egypt the Nubian Sandstones were considered to be Early Cretaceous by Russegger (1837). Figari Bey (1864) assigned the entire sanstone series to the Triassic, while Tate (1871) considered the Nubian Sandstones to be of undoubted Carboniferous age. In the Geology of Egypt (1962) Said concluded that the true Nubian sandstone is Late Cretaceous and that the term should be retained as a formational name and resticted to rocks having facies similar to those found in Nubia and which are known to be of Late Cretaceous age.

Whiteman (1969) has defined the Nubian group for Sudan, as those conglomerates, grits, sandstones, sandy and calcareous mudstones and ironstones which are overlain unconformably by the Hudi Chert Formation (Lower Tertiary) and volcanics (Early Tertiary) and which rest uncon - formably on the predominantly crystalline and metamorphic Precambrian Basement Complex.

Lapparent (1952) compared the Nubian sandstones of the Central Sahara with the continental Wealden sandstones of Algeria and the continental Red Sandstone Series of Hammada Guir in south Morocco. Proceeding with his comparisons, he also indicated the existence of the Nubian Sandstone in Chad, Cameroun and Equatorial Africa. He also equated the Nubian Sandstone with the continental Karoo Series and Kalahari Formation which covers large areas on both sides of the equator.

Termier and Termier (1952) stated " From Tunisia to Egypt and continuing through Arabia and Lebanon, Lower Cretaceous deposits consist of a deltaic facies complex which was sourced by large rivers flowing over the bordering continents, these sediments also contain rare oyster banks. They are the Nubian sandstones, the substratum of which goes back sometimes to the Palaeozoic...".

Desio (1935) used the name "Arenarie della Nubia" to describe the quartz sandstone beds which comprise the most widespread formation of

the Libyan desert, and range in age from Devonian to Late Cretaceous.

The term was also used in a nonstratigraphic sense by Picard (1938) and Quennell (1951), who regarded the Nubian sandstone as a sedimentary facies which could be applied even to Holocene sand dunes.

In a synopsis of Palestinian stratigraphic terminology Picard (1938) mentioned a "Nubian Facies" in the continental deposits of the Arabian shield. These deposits range in age from Precambrian to Recent. Quennell (1951) believed that the term "Nubian Sandstone" should be used as a facies name for sediments produced under arid conditions, with rare marine intercalations from Cambrian to Mesozoic time "preceding the rift movements".

Weissbrod and Sneh (1978) indicated that the Nubian sandstone in Palestine comprises a variable sequence which was deposited during a span of time ranging from Precambrian (in the subsurface only) to Cambrian, Triassic, Jurassic and Lower Cretaceous. Cambrian and Lower Cretaceous Nubian sandstone rock units are exposed in the central and northern Neqab. There are substantial differences between the Nubian sandstone successions occuring in these areas: in the southern exposures which are located closer to the basement massif, the terrestrial influence is greater, and other than the shale, siltstone and dolostone, which represents a Cambrian ingression, most of the sediments are sandstones of continental origin. In northern exposures, however, the influence of the Tethys Ocean is more pronounced and continental

(sandstone) and marine (carbonates and evaporites) sequences alternate.

Wetzel and Morton (1959) published an important contribution to the geology of Transjordan. They described from above the granitic basement the "Petra Sandstone Series" as follows (from top to bottom):

4) Ram and Um Sahm sanstones (Triassic ?),

3) Qunaya sandstones with Cruziana (Silurian?)

2) Burj Formation - Limestone and marly sanstone with trilobites (Cambrian), and

1) Queira Formation (sandstone and conglomerate).

They indicated that this series is Palaeozoic - Mesozoic in age and that it is called "Nubian Sandstone" locally, and was dated as ~~Lower Cretaceous and~~ Precambrian to Cenomanian.

Bender (1974) discussed in detail the "Nubian Sandstones" of South Jordan. He wrote that the term is used for the entire sequence of clastic sediments (about 1500 m thick) above the crystalline base - ment and below the Cenomanian limestones. He revised and completed a subdivision of the Cambrian - Devonian sandy section of southern Jordan, once regarded as Nubian sandstone, into ten mappable lithostratigraphic units. The five following units were dated by fossils (from top to bottom) :

5) "Nautiloidea Sandstone" of the Silurian.

4) "Conularia Sandstone" of the Silurian.

3) "Sabellarifex Sandstone" of the Lower Silurian.

2) "Graptolite Sanstone" of the Ordovician (Graptolites).

1) "Massive, whitish weathered sandstone" of the Lower Ordovician (Cruziana).

Bandel and Khoury (1981) described the lithostratigraphy of the Triassic sediments on the northeastern side of the Dead Sea which consists of a 1000 m thick sequence of mixed clastic and carbonate sedimentary rocks. They were able to subdivide them into nine formations using local names for the units they had differentiated (Fig. 1. 6). Bandel (1981) also described and subdivided the 450 m thick Jurassic rock column of Jordan into six formations using local names.

In his comprehensive and informative paper, Pomeyrol (1968) discussed at length the history of the term "Nubian Sandstone" in terms of its meaning and the way it has been applied. He suggested deleting it completely from the modern stratigraphic nomenclature of North Africa and the Middle East. Pomeyrol's reasons are : (1) the term is assigned to stratal units with a wide range of ages, and (2) the term is used to describe units of different lateral and vertical lithofacies. This conclusion recalls to mind the ideas of Zittel (1883) who proposed either abolishing the name Nubian, or retaining it only for sandstones of Late Cretaceous in age in Nubia, Aswan and the Libyan desert.

Since Pomeyrol's suggestion there has been controversy among several scientists concerning the term Nubian Sandstone. Some are

in favour of keeping the term (Shawa, 1969, 1970; Rigassi, 1969; Whiteman, 1970; Hassan, 1971), whereas others prefer its abandonment (Pomeyrol, 1968; Weissbrod, 1970).

In a discussion of Pomeyrol's paper, Shawa (1969) expressed his opinion that the usage of the term "Nubian Sandstone" can be continued for typical rocks in Nubia (where it was defined originally by Russegger, 1847) and surrounding areas. For the description of similar rocks in the larger area of North Africa and the Middle East, he advocated the use of "Nubian - type sandstone" which has been used by McKee (1962).

Rigassi (1969) suggested that the name "Nubian Sandstone" should be retained for the rock unit which ranges in age from Cambrian to Quarternary, and which occupies the central part of the Arabian - Sudanese shield, because it has a petrologic, mineralogic, and palaeo-environmental connotation remaining uniform in time and space. In other partly marine areas, terrestrial - coastal clastics having lithologic characteristics similar to that of the "Nubian" should be given local rock - unit names accompanied by the term "Nubian Sandstone".

Whiteman (1969) indicated that the term "Nubian Sandstone" cannot be struck off the list of African formations without internal agreement. He did not agree with Shawa's (1969) suggestion that the term "Nubian" should be restricted to Nubia, because the Nubian sandstone is plotted on many useful maps, and its deletion would affect many other well -

known names in African stratigraphy. As an interim solution to the Nubian problem, pending international agreement, Whiteman (1969) suggested the designation of Nubian as a group, in order to provide flexibilty and avoid abandoning a well known and useful stratigraphic term.

Weissbrod (1970) has strongly supported Pomeyrol's suggestion to delete the historic and too general term "Nubian Sandstone" which serves merely to oversimplify the real situation. The Nubian sequence is lithologically variable and fossils are found in almost all formations, contrary to the earlier beliefs that the Nubian sandstone was generally unfossiliferous with a monotonous lithology, mineralogic content and rock fabric.

More detailed stratigraphic study of the "Nubian Sandstone", however, led to its subdivision into definite stratigraphic units. This is well illustrated by Issawi (1971) for several localities in Egypt north of Aswan, by Weissbrod (1970) for southeastern Sinai and southern Palestine, and by Bender (1963) for southern Jordan.

In Jordan, the term "Nubian Sandstone" has been replaced by the new stratigraphically more valid names given by Quennell (1951), Burdon (1959), Wetzel and Morton (1959), Bender (1974), Bandel and Khoury (1981), and Bandel (1981).

1.4 PREVIOUS WORK

1.4.1 GENERAL GEOLOGY

The geology of Jordan is controlled by two factors. The first is its' position between the Arabo - Nubian Shield to the southeast and the Mediterranean Sea (Tethys Ocean) to the northwest. The second factor is the Dead Sea Rift formed by the northward movement of the Arabian plate during the Tertiary.

The Arabo - Nubian Shield,which is a part of the Precambrian basement complex, is exposed in the extreme southwestern part of Jordan, around the Gulf of Aqaba and along the eastern shoulder of Wadi Araba (Fig. 1.2). The constituents of the basement complex are: aplite - granites, granodiorites, quartzporphyries, porphyrites, alaskites, quartzdiorites, hornblende gneiss and paragneiss (Bender, 1974). The basement slopes gently towards the north and east - northeast. It is overlain mainly by clastic sediments which are generally poor in fossils, and which were considered previously as Nubian sandstones (Table 1.1).

1.4.2 CAMBRIAN SEDIMENTS

Bender (1974) indicated that Cambrian sedimentation started with "Basal conglomerates" in the northern Wadi Araba which unconformably overly a distinct Precambrian peneplaned surface of low relief. In the

southern desert of Jordan, Bender informally divided the Cambro - Ordovician sandstones (Table 1.02) into the following four units (from top to bottom):

4) Bedded Brownish Weathered Sandstones;

3) Massive Whitish Weathered Sandstones;

2) Massive Brownish Weathered Sandstones; and

1) Bedded Arkose Sandstones.

Lloyd (1968) renamed these the (1) Saleb, (2) Ishrin, (3) Disi, and (4) Um Sahm Formations respectively which together comprise the Disi Group (Selley, 1972).

Bender also indicated that the "Bedded Arkose Sandstones" are followed by "Massive Brownish Weathered Sandstones" in the southern desert of Jordan, "White Fine Sandstones" in the central Wadi Araba, and a "Dolomite - Limestone - Shale Formation" in northern Wadi Araba and the Dead Sea.

Schneider et al.(1984) divided the Cambrian sediments along the northeastern margin of the Dead Sea into three lithostratigraphic units (from top to bottom) (Fig. 1.05):

C) "Upper Cambrian". This consists of about 110 m of medium - grained, cross - bedded, well sorted yellowish quartzitic locally conglomeratic sandstones, interbedded with thin violet siltstones.

B) "Middle / Upper Cambrian". This comprises some 40 m of inter- bedded fine to medium - grained, multicoloured, cross - bedded, friable

sandstones, containing thin layers of laminated and flaser bedded quartzitic sandstones, as well as intercalated deltaic and lacustrine shales.

A) "Lower / Middle Cambrian". This is about 40 m thick and composed of well bedded, dark - grey limestones, overlain by cross - bedded grey - greenish, fine to medium - grained sandstones. This unit represents shallow water and intertidal to deltaic environments.

Table 1.1 Relative dating of geologic events of the Jordanian Basement (after Abed, 1985).

Burj Formation	Middle Cambrian
Quartz porphyry dykes	Middle Cambrian
Basal conglomerates and Arkoses	Lower Cambrian
Peneplanation and gravels	
Dykes	
Alkali granite (pink granite)	
Extensive dykes	
Aplite, calc - alkali and (grey granites)	
Plagioclase granites	Precambrian
Dykes	
Granodiorites	
High grade metamorphic rocks	

Table 1.02. Previous subdivisons of the palaeozoic and mesozoic sandstones in South Jordan.

Subdivision by LLOYD (1968)		New lithostratigraphic subdivision by BENDER (1974)	Age	Subdivision by QUENNELL (1951, p. 89) and BURDON (1959, p. 26-34, tab. 1)		Subdivision by WETZEL & MORTON (1959, p. 97)		
		Vary-coloured sandstone Massive white sandstone and brown coarse sandstone	In SE-Jordan partly UPPER CRETACEOUS, otherwise LOWER CRETACEOUS	Kurnub sandstone	LOWER CRETACEOUS-UPPER JURASSIC	Hathira sandstone	LOWER CRETACEOUS-UPPER CRETACEOUS	
		- - angular unconformity, erosional hiatus - -				- - - - unconformity, erosion - - - -		
		Worm burrows sandstone	UPPER SILURIAN	not known		not known		
		Red-brown, argillaceous sandstone	SILURIAN	not known		not known		
		Nautiloid sandstone	LOWER SILURIAN	not known		not known		
		Conularia sandstone	LOWER SILURIAN-UPPER ORDOVICIAN	not known		not known		
		Sabellarifex sandstone	MIDDLE ORDOVICIAN	not known		not known		
		Graptolite sandstone	LOWER ORDOVICIAN (LLANVIRN)	not known		not known		
Disi Group	Um Sahm F.	Bedded, brownish weathered sandstone	LOWER ORDOVICIAN	Um Sahm sandstone	JURASSIC-TRIASSIC ?PALEOZOIC	Uhm Sahm sandstone	TRIASSIC, PERMIAN-SILURIAN	Sandy Series of Petra
	Disi F.	Massive whitish weathered sandstone	LOWER ORDOVICIAN	Ram sandstone	PERMIAN-ORDOVICIAN ?CAMBRIAN	Ram sandstone	PERMIAN-SILURIAN CAMBRIAN	
	Ishrin F.	Massive brownish weathered sandstone	CAMBRIAN	Upper Quweira sandstone	?JURASSIC-ORDOVICIAN UPPER CAMBRIAN	Qunaya sandstone	PERMIAN-SILURIAN CAMBRIAN	
		in its lower portions time-equivalent with the white fine-sandstone and with the dolomite-limestone-shale formation	early MIDDLE CAMBRIAN to late LOWER CAMBRIAN early MIDDLE CAMBRIAN to late LOWER CAMBRIAN	not known		not known		
	Saleb F.	Bedded arkose sandstone Basal conglomerate	LOWER CAMBRIAN	Burj limestone group	LOWEST MIDDLE CAMBRIAN	limestones and sandy marls of Burj	MIDDLE and LOWER CAMBRIAN	
				Lower Quweira sandstone	LOWER CAMBRIAN	sandstones and conglomerates of Quweira	LOWER CAMBRIAN	
		- - - extensive peneplanation, locally - - - (Rift zone) distinct relief		- - - - peneplanation, unconformity - - - -		- - peneplanation, unconformity - -		
		Igneous rocks	UPPER PROTEROZOIC	PRE-CAMBRIAN		PRE-CAMBRIAN		

Kata-rocks

Age	Formation	Unit	Thickness	Lithology	Environment
TRIASSIC	Dardur	F	350	Alternating beds of massive sandstones and thinly bedded siltstones and sandstones, cemented by carbonates	
	Ma'in	E	300	Nimra Member: massive, cross - bedded, white, yellowish, fine to medium - grained sandstones, dolomitic cement Himra Member: alternating layers of marls, thinly bedded violet siltstones / sandstones, which are carbonaceous laminated, cross - bedded, rippled, bioturbated and contain shale pebbles and bivalve shells.	Intertidal and Subtidal
ORD-PERMO-TRIAS	Um Irna	D	250 200	Fine to coarse - grained sandstones; multicoloured, friable in the lower portion; contains intraformational conglomerate layers; cross - bedded; poorly sorting, with kaolinite cement, manganese patches and interbedded shales.	Fluvial / Lacustrine
CAMBRIAN	U	C	150 100	Medium - grained, cross - bedded, well sorted, yellowish quartzitic sandstones, with conglomerate layers and thin violet siltstones intercalated with the sandstones.	Continental Fluvial / to Deltaic
	M/U	B	50	Interbedded, fine to medium - grained multicoloured, cross - bedded, friable sandstones.	Deltaic to Lacustrine
	L/M	A	0	Well bedded, dark grey limestones. Trilobite hash, algal mats and strong bioturbation. The upper portion comprises calcareous sandstones.	Shallow water and Intertidal

Limestone/calc.sst. Dolomite/dol.sst. Marl

Sandst.quartzitic Sandst.friable Shale,Siltst.

Conglomerate Paleosol ,pisolit Black shale

Glauconite layer Basaltic sill

Fig. 1.5. Generalised vertical section of the Cambrian, Permo - Triassic and Lower Triassic sediments (after Schneider et al., slightly modified).

The dolomite - limestone - shale unit which was considered by Bender (1974) as early Middle to Late Lower Cambrian, was described as unit (A) of Lower / Middle Cambrian age by Schneider et al.(1984). This occurs at the northeastern side of the Dead Sea and has been known for a long time. It was named and described by Hull (1886) as "Wadi Nasb Limestone", by Wetzel (19 47) as the "Burj Limestone Formation", by Quennell (1951) as the "Burj Limestone Group" with the "Hasa Shale", and by Wetzel and Morton (1959) as the "Formation Calcaire et marnogreseuse de Burj". A Middle Cambrian age was assigned to a crystalline limestone bed on the eastern shore of the Dead Sea by King (1923) on the basis of trilobites. Bender (1974) indicated that the strata overlying the Dolomite - Limestone - Shale Formation, are mainly clastic sediments that indicate an oscillating, but generally retrograde transition from marine to continental depositional environments. The continental environment was fully developed at the time of the deposition of the brown, coarse sandstone, which was reffered to by Schneider et al. (1984) as unit (C). This part of the Cambrian succession has received very little attention. As a result the palaeoenvironments are poorly known. The Burj Formation was given a late Early Cambrian age by Cooper (1976).

1.4.3 PERMO - TRIASSIC SEDIMENTS

In (1974) Bender stated that Permian rocks have not been found in exposures or in subsurface sections in Jordan. Bender, however predicted their presence in the subsurface in the northern and western parts of

Jordan from regional stratigraphical considerations (Permian in Syria, Weber, 1963; Permian - Lower Triassic in Palestine, Gerry, 1967; and Permo - Carboniferous in Saudi Arabia, Helal, 1964).

Bender (1974) noticed the change in colour and lithology, and the presence of iron oxides and plant remains at the base of the Triassic at Wadi Zarqa Ma'in. It seems that these are the sediments considered later in (1981) by Bandel and Khoury as the Permo - Triassic (Um Irna Formation) which is about 85 m thick. They are exposed for about 8 km between Wadi Zarqa Ma'in and Humrat Ma'in. Their base consists of hard, brown Cambrian sandstones, and their top is formed by the first beds with abundant bioturbation (Ma'in Formation).

Bandel and Khoury (1981) divided the Um Irna Formation into six members, reflecting six sedimentary cycles of terrestrial origin derived from the nearby Precambrian basement. Each cycle shows gradation in grain size and composition. The base of each member, except the lowermost, consists of coarse - grained cross - bedded sandstone usually with a conglomeratic base, overlain by laminated silt and clay beds. They also observed rippling, mudcracks, angular clay intraclasts, rounded mud balls and channeling structures. They also reported the presence of iron - oxide pisoliths (up to 20 mm in diameter) in four members. An Upper Permian age was given to the lowermost member on the basis of limited pollen data (Fig. 1. 6) .

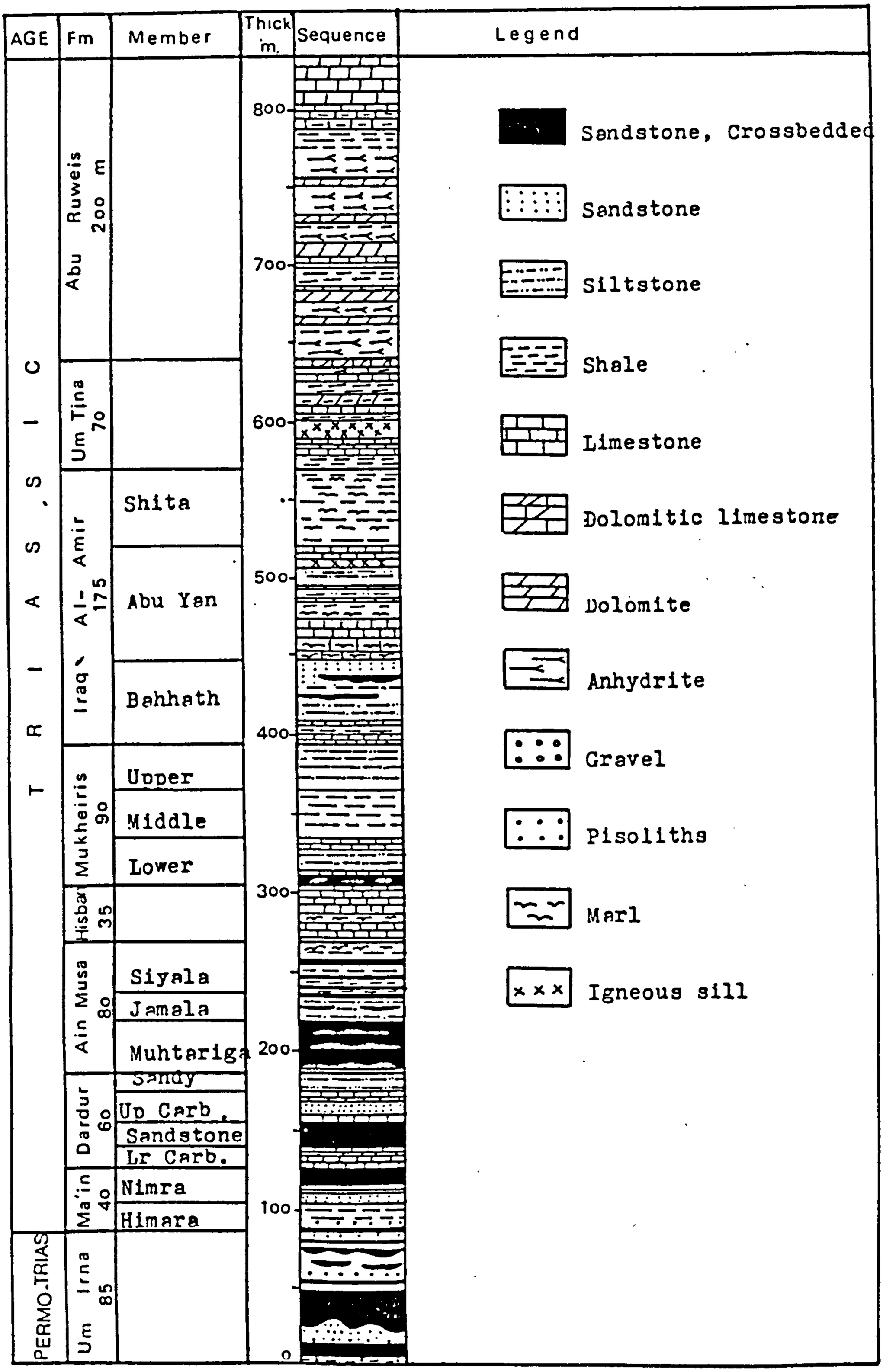

Fig. 1. 6. Triassic lithostratigraphy according to Bandel and Khoury (1981) (slightly modified).

Recently, in the lithostratigraphic subdivison proposed by Schneider et al (1984), the Um Irna Formation was designated as unit (D) of Ordovician ? / Permo - Triassic age (about 80 m thick). Lacustrine and continental environments were documented on the basis of the presence of several decimetre - thick layers of black shales, Fe - pisoliths and Mn / Fe encrustations (Fig. 1.06).

1.4.4 TRIASSIC SEDIMENTS

Cox (1924, 1932) was the first to report Triassic sediments in Jordan. He described the lithology and the fossil content in the northeast corner of the Dead Sea and near Wadi Hisban. In this area, Cox (1932) and Wagner (1934) identified Muschelkalk, which is here almost identical in facies and faunal content to the German Middle Triassic. Blake (1936) and Blake and Ionides (1939) described the Triassic rocks on the northern slope of Wadi Zarqa Ma'in and in the lower River Zarqa near the mouth of Wadi Huni.

Wetzel and Morton (1959) differentiated between the Triassic littoral beds of the River Zarqa and Wadi Hisban, and the deltaic deposits in the Wadi Zarqa Ma'in area. According to Parker (1970) Wetzel (1947) introduced, in an unpublished report the term Zarqa Group for the Triassic and Jurassic rocks exposed in Jordan. This group was subdivided by Parker into the Ma'in Formation (Triassic) and the Azab Formation (Jurassic).

The name Hisban Limestone which is applied to the calcareous unit of the Triassic rock sequence in Jordan was introduced by Daniel (1959, 1963). Lillich (1964) traced the Triassic strata along the mountainous, eastern rim of the Dead Sea, and found that they thin out from the north towards the east and southeast until they wedge out completely in the area of the lower Wadi Mujib, where they overlie transgressively the Middle - ? Upper Cambrian sandstones. Lillich (1964) recognized three different environments of deposition for the Triassic sequence: (1) a continental depositional environment for the lower third of the succession, (2) a marine, near shore and shallow - water environment for the middle third, and (3) a lagoonal environment for the upper third.

Recently, Bandel and Khoury (1981) described the lithostratigraphy of the Triassic sequence east of the rift valley, and subdivided the 1000 m thick sequence of sedimentary rocks into nine formations, each formation being defined by a type section, and assigned a local name. (Fig. 1. 6). The name Ma'in Formation was assigned to a unit up to 45 m thick above the Um Irna Formation. It is exposed in Wadi Zarqa Ma'in and other wadis up to Wadi Mukheiris 13 km to the north. Two members were distinguished, the Himara and Nimra. The Himara Member, about 15 m thick, forms the base of the formation. It is characterised by the first occurence of bioturbation, and dark purplish beds, which consist of alternating thinly bedded sandstone, siltstone and clay, with thin dolomitic limestone beds. Mudcracks, ripple marks, burrowing

and bivalve shells are abundant. The Nimra Member is up to 25 m thick and it forms the upper part of the formation. In the lower portion flaser structures, red and green silt and clay partings and carbonate rich beds are developed. The upper portion is composed of white, fine cross - bedded sandstone, with some pure limestone units, and intraclast horizons composed of reworked burrows. Bioturbation is developed throughout. A tidal or very shallow water marine environ - ment for the deposition of Ma'in formation was suggested by Bandel and Khoury (1981), who considered it to be Scythian in age.

According to the fossil content, Cox (1932) dated the Triassic of Wadi Hisban as Anisian. Wagner (1934) and Wetzel and Morton (1959) confirmed this conclusion. Stoppel (1966) collected fossils from the upper part of the Triassic succession at Wadi Zarqa Ma'in, between 5 - 30 m below the Lower Cretaceous unconformity, and placed these beds in the Scythian. The oldest biostratigraphically dated beds in the Triassic of Jordan belong to the upper carbonate member of the Dardur Fromation from Zarqa Ma'in which overlie the Ma'in Formation. From these Bender (1974) reports conodonts of Scythian age. Hirsch (1975) described similar conodonts from the Lower Zafir Formation and the uppermost Yamin Formation of the Neqab, and assigns them to a late lower to early Upper Scythian age.

1.5 PRESENT WORK

The study area lies on the northeastern edge of the Dead Sea in

central Jordan, between Wadi Mukheiris in the north and Wadi Abu Khusheiba in the south (Fig. 1. 7). It covers an area of about 40 km^2 and geologically consists of Upper Cambrian sediments resting conformably on Middle Cambrian "Burj Formation". The Upper Cambrian is unconformably overlain by Permo - Triassic sediments of the Um Irna Formation, which are in turn conformably overlain by the Lower Triassic "Ma'in Formation". The "Dardur Formation" also of Lower Triassic age, conformably overlies the "Ma'in Formation" (Bandel and Khoury, 1981) but within the study area only the Upper Cambrian sediments, the Permo - Triassic Um Irna Formation and the Ma'in Formation were studied in detail.

The sediments are extensively faulted, folded and jointed, and intruded by several diabase and gabbro dykes and sills. Some parts are extensively covered by travertine and Quaternary debris. In spite of this, exposure is generally good, especially along the Wadis where the measured and sampled sections on which this study is based, were located (Fig. 1.07). Previous work on the depositional environments of the sediments is of a very general nature and generally serves to augment the stratigraphic data. Environments recognised to date have generally been categorised as marine and non - marine without further qualification. As a result the present environmentally based facies study was undertaken in order to try and interpret the depositional sedimentary environments in detail and the way that they evolved in space and time. Comparisons can then be made with the regional palaeogeo-

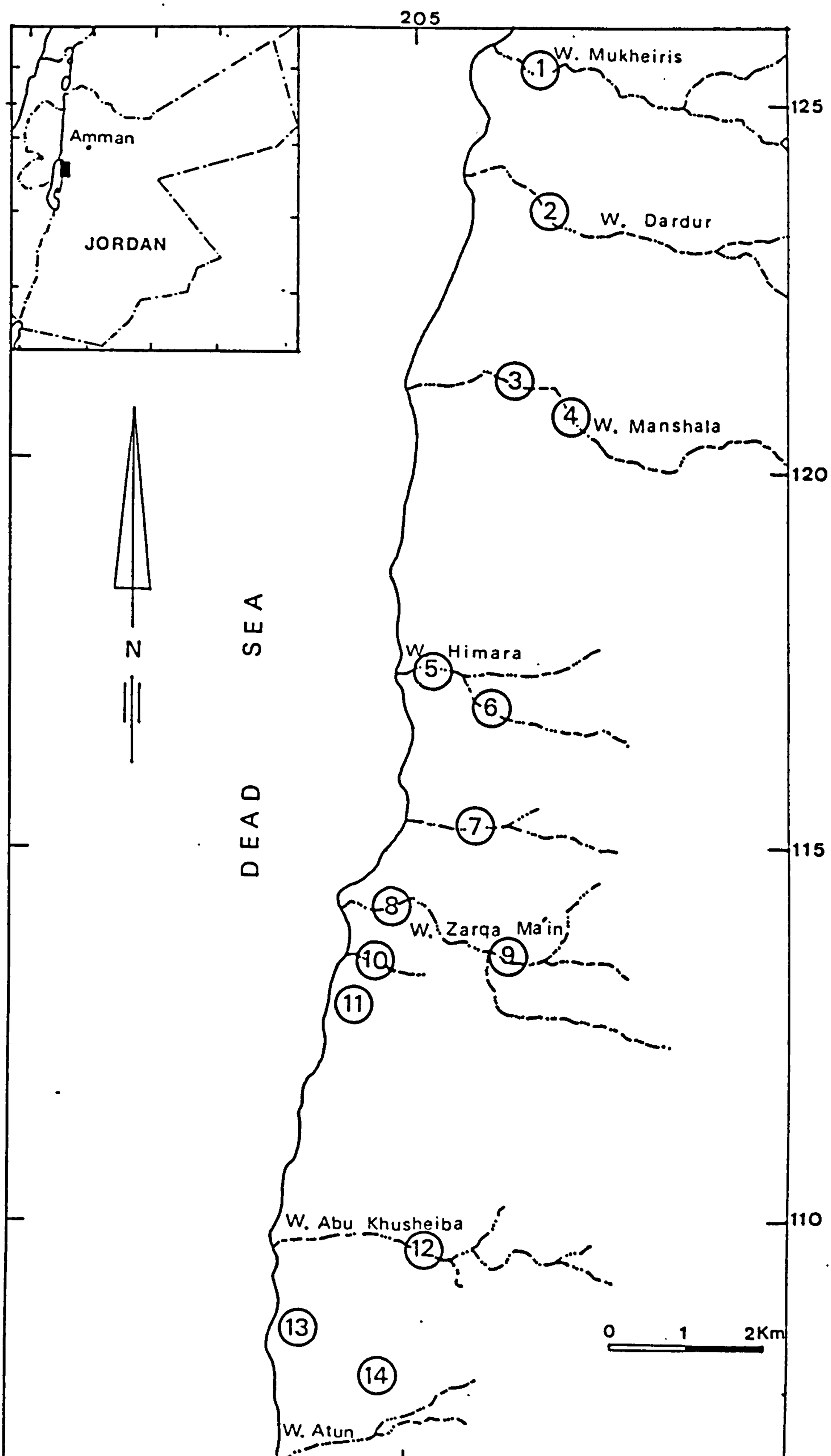

Fig. 1. 7. Locality map showing measured stratigraphic sections labelled 1 - 14.

graphic evolution of the Dead Sea and the surrounding areas.

Fourteen outcrop sections were measured, sampled and described in terms of sedimentary facies and facies sequences. Comparison of these sequences with modern and ancient analogues, enabled them to be interpreted in terms of specific depositional environments. Sedimentary structures, mainly cross - bedding and ripple marks were studied, measured and plotted as rose diagrams, from which the palaeocurrent directions were inferred. Deformed and convoluted cross - beds in the Upper Cambrian sandstones were given detailed attention because of their variable and often unusual features (Chapter 3). In addition, petrographic studies were carried out on forty thin sections from the various stratigraphic units in the succession. Modal analyses provided the basis for classifying the sandstones, and for determining their maturity and provenance (Chapter 6).

Seventeen samples from the Um Irna Formation including sandstones, siltstones, clay and ferruginous pisoliths were examined by X - ray diffraction, to determine their major mineral components (Appendix F). Eight thin sections were prepared from individual ferruginous pisoliths to examine their internal composition and chemical analysis was carried out on 4 pisoliths (Appendix D). The origin of these pisoliths is briefly discussed in Chapter 4. Uranium measurements on the Um Irna Formation and adjacent travertine rocks were also carried out during section measurement and sampling (Appendix E).

Palynological studies on six samples from the carbonaceous shales of the Um Irna Formation confirmed the Permo - Triassic age as had been previously found by Bandel and Khoury (1981).

A geological map (scale 1 : 50,000) showing the detailed distribution of the rocks under study was compiled (Fig. 1.08). This map first map of this kind to be compiled for these rocks in Jordan and it shows a number of differences from the more generalised maps available at present (Quennell, 1959; Bender, 1968) : (1) the boundaries between the Cambrian, Permo - Triassic and Triassic rocks are shown on the map, (2) the boundary between the Middle and Upper Cambrian is shown on the map, (3) a new Permo - Triassic unit was established, (4) the Triassic Ma'in and Dardur Formations have been separated, and (5) the Ma'in Formation has been divided into a lower Himara and upper Nimra Members.

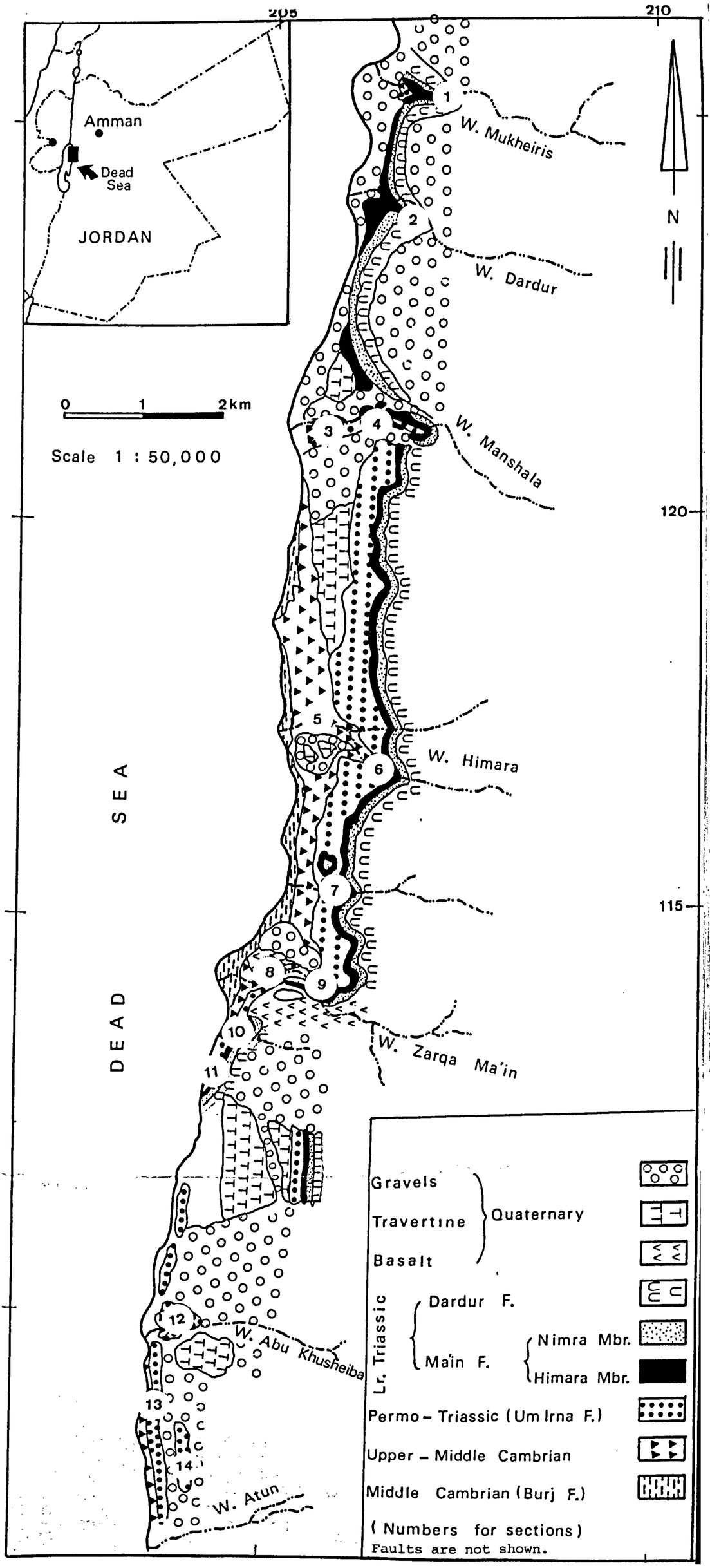

Fig. 1.8. Generalised geological sketch map; structural information not shown showing position of localities in text.

CHAPTER TWO

SEDIMENTOLOGICAL BACKGROUND

CHAPTER TWO

SEDIMENTOLOGICAL BACKGROUND

2.1 FACIES CONCEPT

Reading (1978) defined a facies as a body of rock with specified characteristics, including colour, bedding, composition, texture, fossils and sedimentary structures. Lithofacies refer to an objectively defined rock unit. The concept of facies is used to describe and interpret the depositional environments of ancient rock sequences, in many different senses: (1) the observational sense of a rock product e.g. sandstone facies, (2) the genetic sense for the product of certain processes, e.g. turbidite facies, (3), the environmental sense, e.g. fluvial facies, and (4) the tectonic sense e.g. molasse facies.

The facies should ideally be a distinctive rock that forms under certain conditions of sedimentation, reflecting a particular process or environment. Walther's Law of Facies (1894) states: " a conformable vertical sequence of facies was generated by a lateral sequence of environments (Selley 1976).

Facies may be subdivided into sub - facies or grouped into facies associations. Facies associations are groups of facies that occur together, and are considered to be genetically or environmentally related, while, a facies sequence is a series of facies which pass

gradually from one into the other. In clastic environments, two important kinds of sequence occur: a coarsening - upward sequence which indicates an increase in flow power, and a fining - upward sequence which indicates a decrease in flow power (Reading, 1978).

Facies distribution and changes in distribution are dependent on a number of interrelated controls: (1) sedimentary processes, (2) sediment supply, (3) climate, (4) tectonics (5) sea level changes, (6) biological activity, (7) water chemistry, and (8) volcanism (Reading, 1978).

2.1.1 FACIES MODELS

The concept of the facies model has been the most powerful and successful tool devised by sedimentologists for classifying and explaining ancient sediments (Miall, 1985). The models were developed from studies of modern depositional environments. The use of sedimentary models in geology goes back to the earliest appreciation that the present can be a key to the past. Models are used both to interpret facies distributions and also to predict where, as yet, undiscovered facies may be found (Reading 1978).

At present there are at least a dozen formal fluvial facies models, and many variants of these have been erected to explain specific ancient units (Miall, 1985). Two interpretive features are usually

emphasised: the characteristic vertical profile and the morphology of the channels.

2.1.2 LITHOFACIES NOTATION

The lithofacies notation used in this thesis is that of Miall (1978) who gives a list of lithofacies and their common sedimentary structures known to occur in stream deposits. Each lithofacies is assigned a facies code as shown in Table 2.1. In 1985 Miall proposed a new method of facies analysis of fluvial rocks using architectural element analysis. This approach to facies modelling of fluvial deposits involves analysis of eight basic architectural elements that include: (1) element CH; channels, (2) element GB; gravelly bars and bedforms, (3) element SB; sandy bedforms, (4) element FM, foreset macroforms, (5) element LA; lateral accretion deposits, (6) element SG; sediment gravity flow deposits, (7) element LS; laminated sand sheets, and (8) element OF; overbank fines (Fig. 2.1).

2.2 FLUVIAL SYSTEMS

Because of the importance of fluvial sediments in the Upper Cambrian and Permo - Triassic rock record, it is necessary to discuss the types of river systems, and the sediments that they deposit (with special emphasis on their diagnostic features), prior to describing and interpreting Cambrian fluvial depositional environments.

Table 2.1. Lithofacies classification (from Miall, 1978).

Facies Code	Lithofacies	Sedimentary structures	Interpretation
Gms	massive, matrix supported gravel	none	debris flow deposits
Gm	massive or crudely bedded gravel	horizontal bedding, imbrication	longitudinal bars, lag deposits, sieve deposits
Gt	gravel, stratified	trough crossbeds	minor channel fills
Gp	gravel, stratified	planar crossbeds	linguoid bars or deltaic growths from older bar remnants
St	sand, medium to v. coarse, may be pebbly	solitary (theta) or grouped (pi) trough crossbeds	dunes (lower flow regime)
Sp	sand, medium to v. coarse, may be pebbly	solitary (alpha) or grouped (omikron) planar crossbeds	linguoid, transverse bars, sand waves (lower flow regime)
Sr	sand, very fine to coarse	ripple marks of all types	ripples (lower flow regime)
Sh	sand, very fine to very coarse, may be pebbly	horizontal lamination, parting or streaming lineation	planar bed flow (l. and u. flow regime)
Sl	sand, fine	low angle (<10°) crossbeds	scour fills, crevasse splays, antidunes
Se	erosional scours with intraclasts	crude crossbedding	scour fills
Ss	sand, fine to coarse, may be pebbly	broad, shallow scours including eta cross-stratification	scour fills

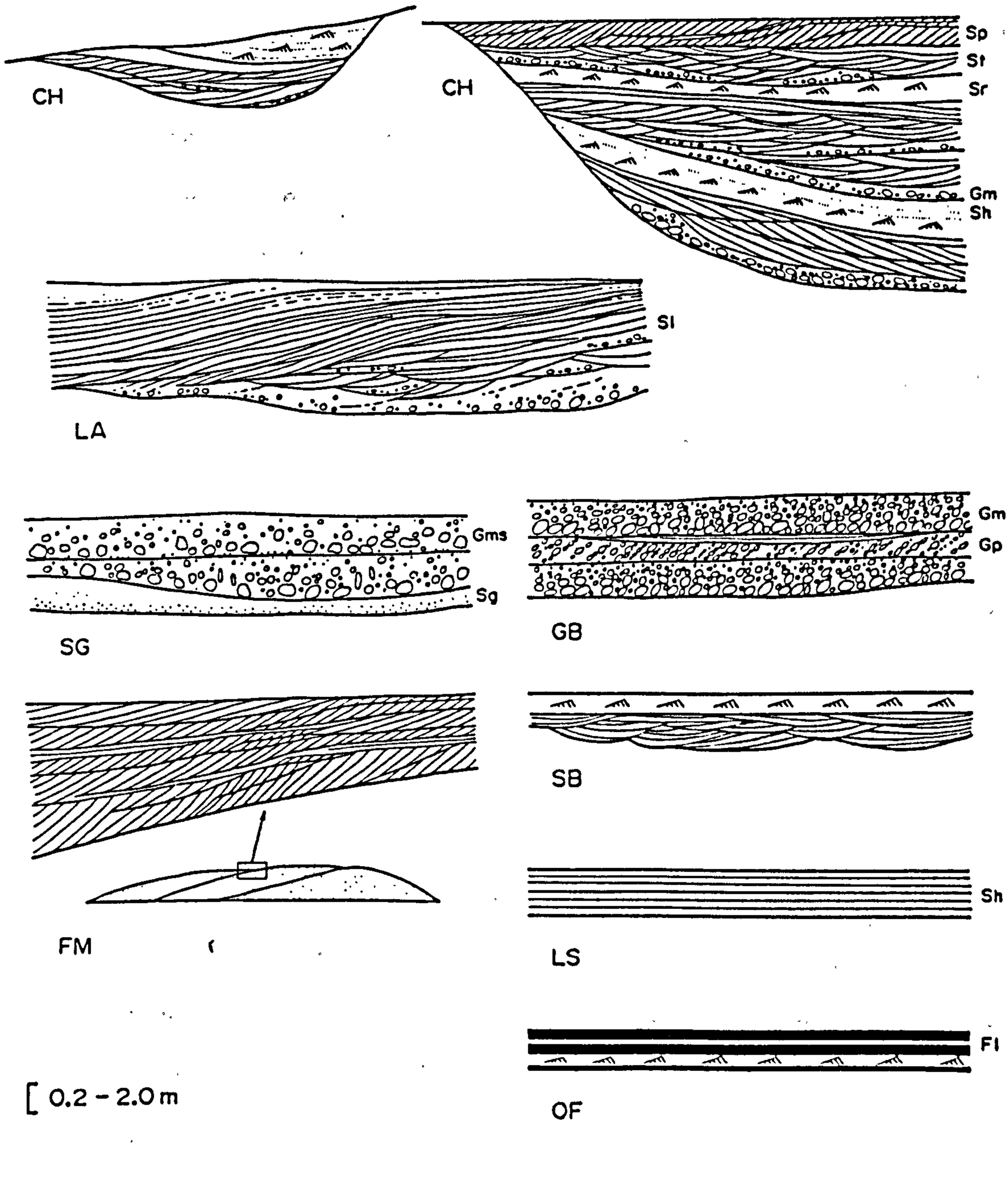

Fig. 2.1. The major architectural elements (from Miall, 1985).

Factors that control the development of a specific type of fluvial system include tectonic, climatic, hydraulic and geomorphic conditions. Processes and products of a fluvial system are influenced by these factors (Flores, 1985). As shown by Leopold and Wolman (1957), at least nine variables interact to determine the nature of the resulting stream channel. They include discharge (amount and variability), sediment load (amount and grain size), width, depth, velocity, slope and bed roughness. Schumm (1968) showed that the amount and type of vegetation growth also will affect stream type and, therefore, climatic and geological factors must also be considered.

Generally the most important feature of a fluvial system is the channel. The majority of channel classifications are based on their plan view morphology (Fig. 2.2). Single channel systems form a continuum from straight to highly sinuous (meandering) (Ethridge, 1985). Rivers can alternate between the meandering and braided (or even straight) condition depending on local river slope, sediment load and flow velocity. Rust (1978) proposed a classification into four basic channel types: braided, meandering, anastomosing and straight, using quantitative sinuosity and braiding parameters. Braided systems are characterised by a low sinuosity channel in which flow weaves around multiple, mobile channel bars at low water stage. An anastomosing system is characterised by contemporaneous high - to low-sinuosity channels that weave around permanent, commonly vegetated islands or floodplain segments. Factors that favour the development of one

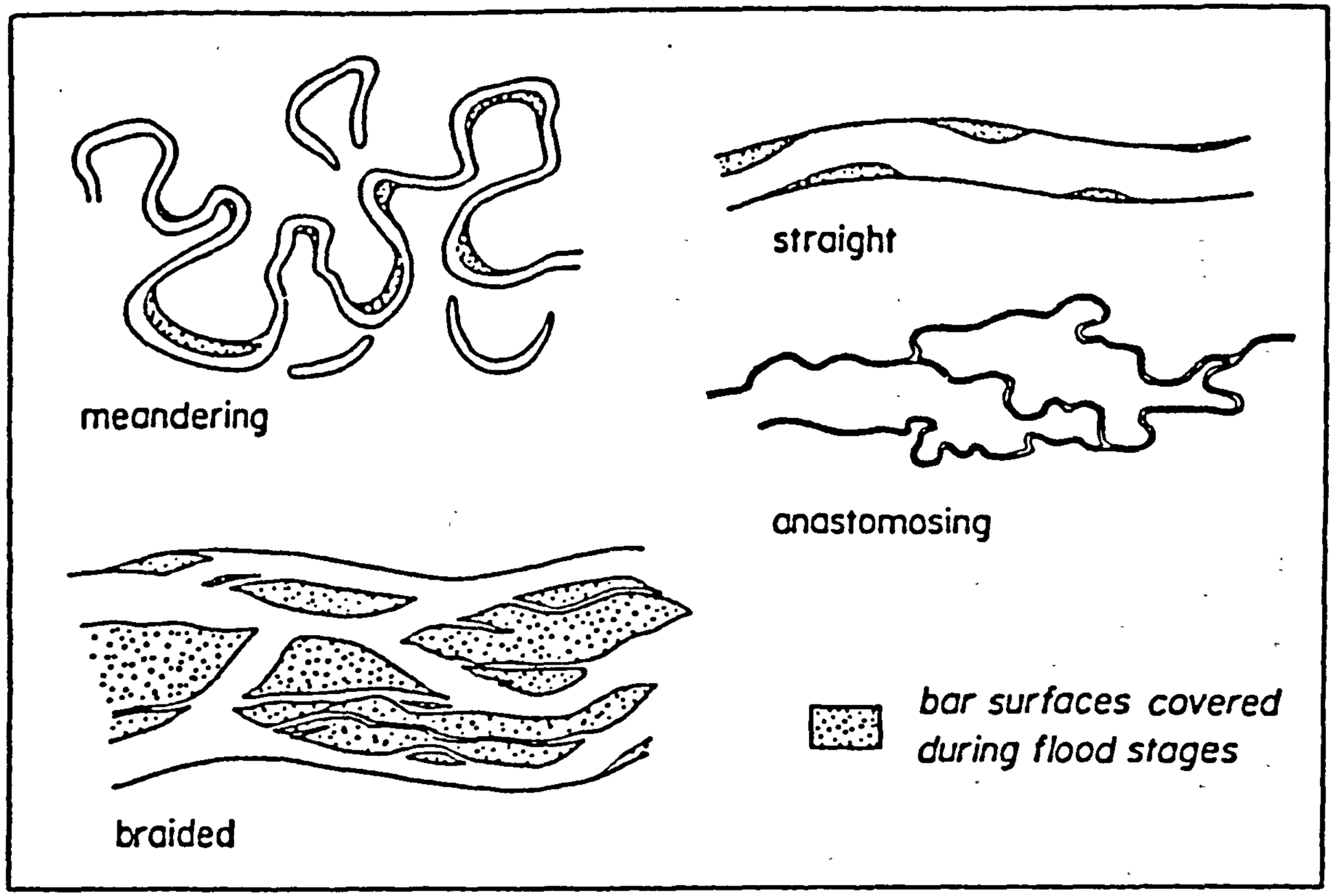

Fig. 2.2. Plan view configuration of principal river types (after Miall, 1977).

channel type over another are the hydraulic and sedimentologic processes (Ethridge, 1985). Schumm (1981) presented a different classification of fluvial channels based on sediment load. This classification scheme (Fig. 2.3) yields bedload, mixed-load, and suspended - load types of fluvial channels. Bedload channels represent braided and coarse - grained meandering streams. Mixed - load channels reflect meandering streams with channel plug deposits. Suspended load channels represent anastomosed streams encased in fine - grained flood-basin deposits. Identification of the variations in properties of various types of fluvial sediment defines facies characteristics that are used to develop facies models for ancient deposits (Fig. 2.4) (Galloway, 1977).

On the basis of width / depth ratios channels were classified into: (1) fixed channels (ribbon - shaped geometry), which are narrow, with width / depth ratios less than 15, (2) mobile channels (broad and shallow with complex fill geometry), which are filled by a process of channel migration or switching within a single major channel scour, with width / depth ratios greater than 15, and (3) sheet - like (essentially unchannelised), where the width / depth ratio exceeds 100 (Friend et al., 1979; Friend, 1983; and Blakey and Gubitosa, 1984).

Cotter (1978) indicated that out of more than one hundred published interpretations, virtually all pre - Silurian rivers were braided, whereas Silurian and younger rivers were either meandering or braided, as a result of tectonic, geomorphic, and climatic settings of the

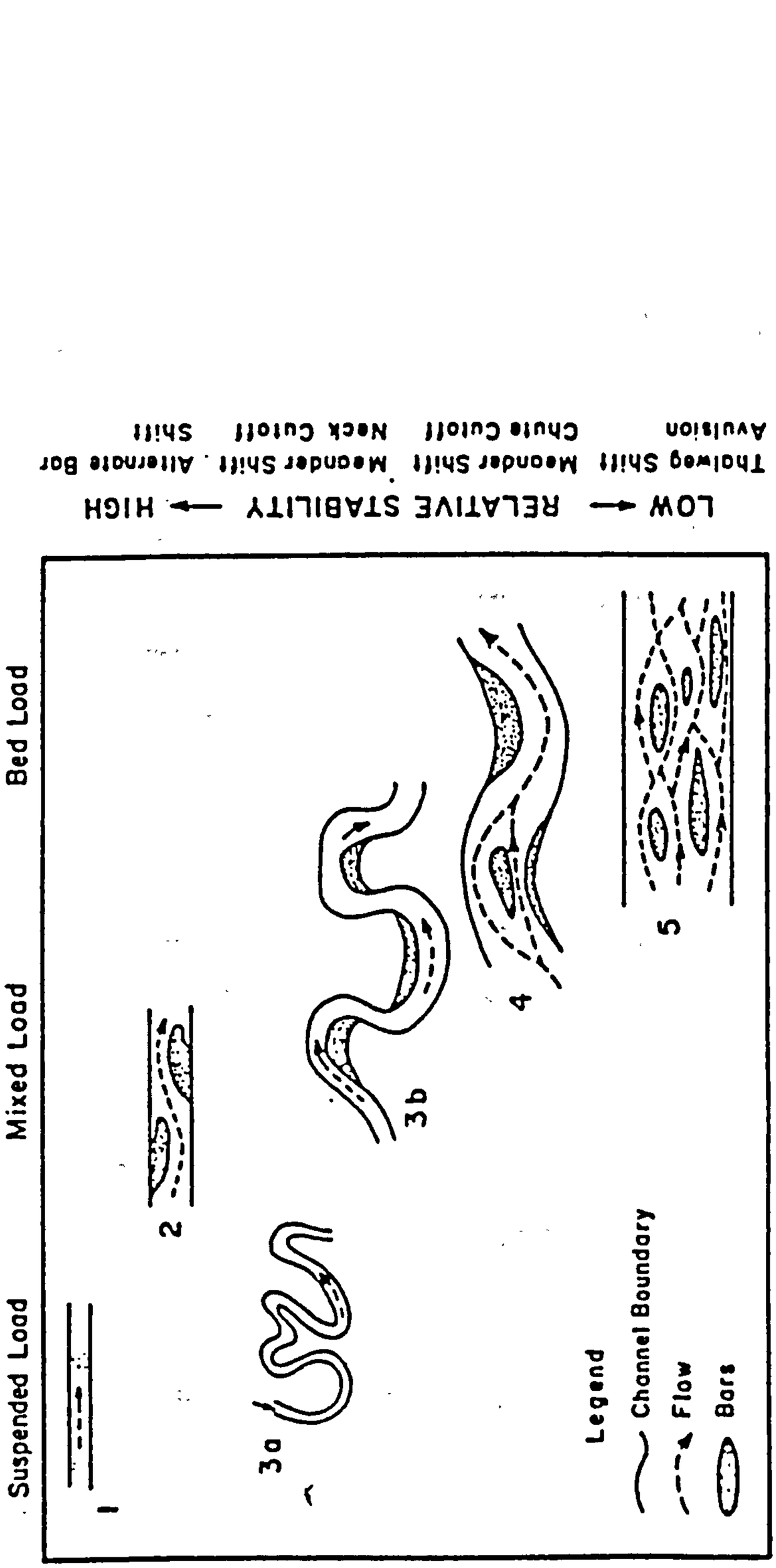

Fig. 2.3. Channel classification based on pattern and type of sediment load with associated variables and relative stability indicated (after Schumm, 1981).

CHANNEL TYPE	COMPOSITION OF CHANNEL FILL	CHANNEL GEOMETRY			INTERNAL STRUCTURE		LATERAL RELATIONS
		CROSS SECTION	MAP VIEW	SAND ISOLITH	SEDIMENTARY FABRIC	VERTICAL SEQUENCE	
BEDLOAD CHANNEL	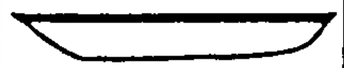 Dominantly sand	 High width / depth ratio Low to moderate relief on basal scour surface	 Straight to slightly sinuous	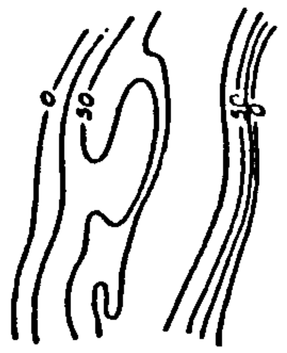 Broad continuous bell	 Bed accretion dominates sediment infill	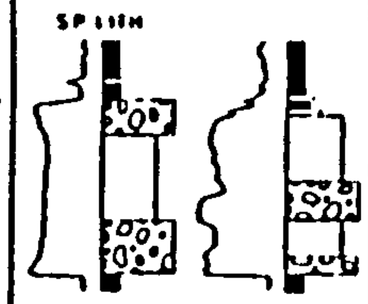 Irregular, fining-up poorly developed	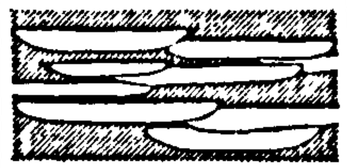 Multilateral channel fills commonly volumetrically exceed overbank deposits
MIXED LOAD CHANNEL	 Mixed sand, silt, and mud	 Moderate width / depth ratio High relief on basal scour surface	 Sinuous	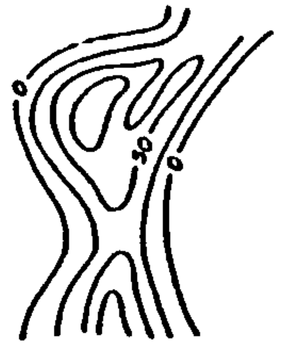 Complex, typically "beaded" bell	 Bank and bed accretion both preserved in sediment infill	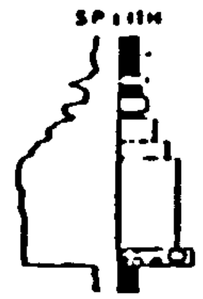 Variety of fining-up profiles well developed	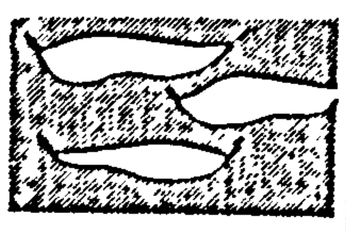 Multistory channel fills generally subordinate to surrounding overbank deposits
SUSPENDED LOAD CHANNEL	 Dominantly silt and mud	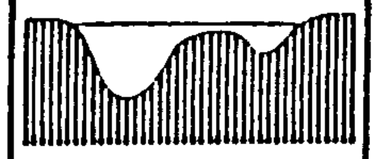 Low to very low width / depth ratio High-relief scour with steep banks, some segments with multiple thalwegs	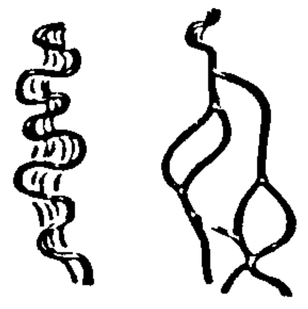 Highly sinuous to anastomosing	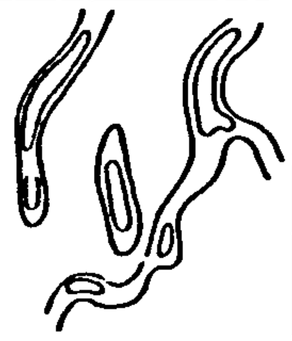 Shoestring or pod	 Bank accretion (either symmetrical or asymmetrical) dominates sediment infill	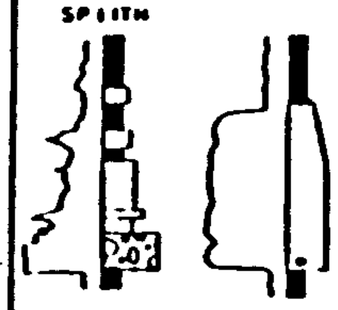 Sequence dominated by fine material, thus vertical trends may be obscure	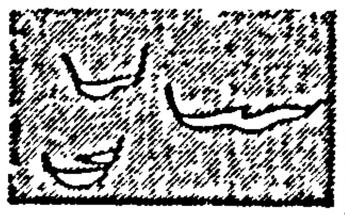 Multistory channel fills encased in abundant overbank mud and clay

Fig. 2.4. Geomorphic and sedimentary characteristics of bed load, mixed load, and suspended load channel segments (from Galloway, 1977).

various depositional sites. This indicates that there was a mid - Palaeozoic change of fluvial style from nearly all braided to a mixture of both braided and meandering, and it is likely that the cause of this change was the advent of land vegetation. Schumm (1967, 1968) speculated that the evolution of land vegetation caused a change in the characteristic pattern of rivers. Vegetation has a significant effect on streams by retarding erosion, decreasing sediment yield, decreasing total runoff, discharge and flood peaks for a given precipitation (Schumm, 1967; Gregory and Walling, 1973; Pearce, 1976), by decreasing bedload grain size and enhancing fine sediment production (Schumm, 1968; Douglas, 1976), and by increasing bank stability (Schumm, 1968; Smith, 1976). The direction of all these indicates that evolving land vegetation would enhance the tendency of streams to meander (Cotter, 1978). Schumm (1967, 1968) thought that before land vegetation appeared in the middle of the Palaeozoic Era, precipitation / sediment yield relations everywhere would have been much like those of arid regions today. Streams would transport great quantities of bedload, and river patterns characteristically would be braided.

Jackson (1978) showed that channel morphology indicates that one can expect a diversity of lithofacies types preserved in many fluvial environments. The variation in facies styles must consist of a continuum including those diagnostic of each of the four recognised channel patterns (such as point bars and accretion bridges in meandering streams, and features most usually associated with braided streams such as longitudinal and transverse bars, and a lack of mud

units). Criteria to distinguish meandering streams from non-meandering streams can be categorised as geomorphological (Table 2.2) or as sedimentological (Table 2.3). The only geomorphological criteria (Table 2.2) of possible broad validity involve gradient and bank stability.

Jackson's discussion of several Holocene meandering streams (1978) revealed the existance of great variability in lithofacies of modern meandering streams including (1) muddy fine -grained streams, (2) sand-bed streams with modest thickness of fine member, (3) sand - bed streams lacking mud and rock gravel, (4) graveliferous sand - bed streams, (5) streams with coarse gravel and little sand. It appears both likely and reasonable to suppose a complete continuum exists between adjacent pairs of the five classes. A meandering stream can show a downstream gradation among these facies types just as some streams display a downstream transition in channel pattern. Most of these facies classes incorporate sedimentary features usually deemed typical of braided streams (Tables 2.2, 2.3): thin to absent fine member, abundance of gravel, presence of coarse gravel, vertical sequences which do not always fine upwards and which show great spatial variabilty, absence of epsilon cross - stratification (ECS) and natural levees, large width / depth ratio of channel, and lack of sedimentary structures.

Jackson (1978) indicated that the few facies criteria which may be braodly reliable are the following: (1) low palaeocurrent variance

Table 2.2. Commonly cited geomorphological criteria for alluvial streams (after Jackson, 1978).

	Braided	Coarse-grained meander belt	Fine-grained meander belt	Straight distributary
Gradient	High			Low
Channel flow	Unconfined			Confined
*Discharge rate	Flashy			Continuous
*Bedload/suspended load	High			Low
*Sand/mud (deposit)	High			Low
*Sand body (deposit)	Wide	Multilateral	Multistoried	Narrow
*Natural levees	Slight			Prominent
Bank stability	Slight			Great

* Criterion is not generally valid.

Table 2.3. Commonly cited sedimentological criteria for fluvial deposits (after Jackson, 1978).

	Meandering	Non-meandering
Vertical sequence of lithofacies	Fining-upward cycles (of grain size and sed. structures)	No consistent sequence
Fine member	Normally common and appreciably thick	Uncommon and thin
Rock gravel in coarse member	Small amounts; few large clasts	Can be abundant, with large clasts
Scroll bars	Common	Absent
Epsilon-cross stratification	Common	Absent
Scouring surfaces in coarse member	Uncommon	Abundant
Channel-fill mud deposits	Common, esp. in muddy streams; long and arcuate	Minor; short
Chute-fill and chute bars	Expected in "coarse-grained" streams	Uncommon
Natural levees	Often prominent	Minor
Dispersion of current indicators	Large, often $>180^{o}$	Small, often $<90^{o}$
Exhumed meander belt	Can be expected in proper sections	Absent
Continuity of sand and gravel beds (in coarse member)	Often great, with little lateral change in texture	Beds often lenticular and discontinuous

of imbricated large pebbles and cobbles is expected in low sinuosity streams, (2) exceedingly coarse gravel (of mean intermediate axes length greater than 0·5 m) is diagnostic of a very proximal non - meandering stream, and (3) asymmetric channel fills with much mud are strongly indicative of meandering streams.

For fluvial deposits of all kinds Jackson (1975) classified bed - forms into microforms, mesoforms and macroforms. Microforms are structures generated by turbulent variations in the inner part of the turbulent boundary layer; small scale ripple marks and current lineations are the result. Mesoforms are the structures generated mainly by dynamic events, particularly flood events occuring during storm - induced run -off or seasonal snow thaw; these include the larger scale flow regime bedforms, such as dunes and sandwaves, minor channels and unit bars such as linguoid, transverse, longitudinal and diagonal bars. Macroforms reflect the cummulative effect of many dynamic events over periods of tens or thousands of years; they include major channels and the larger , compound bar forms such as point bars, side bars, sand flats and islands.

Miall (1985) suggested that all fluvial deposits are composed of varying proportions of eight basic architectural elements. Descriptions and definitions of architectural elements should include the following: (1) nature of lower and upper bounding surfaces; erosional or gradational, planar, irregular, curved, (2) external

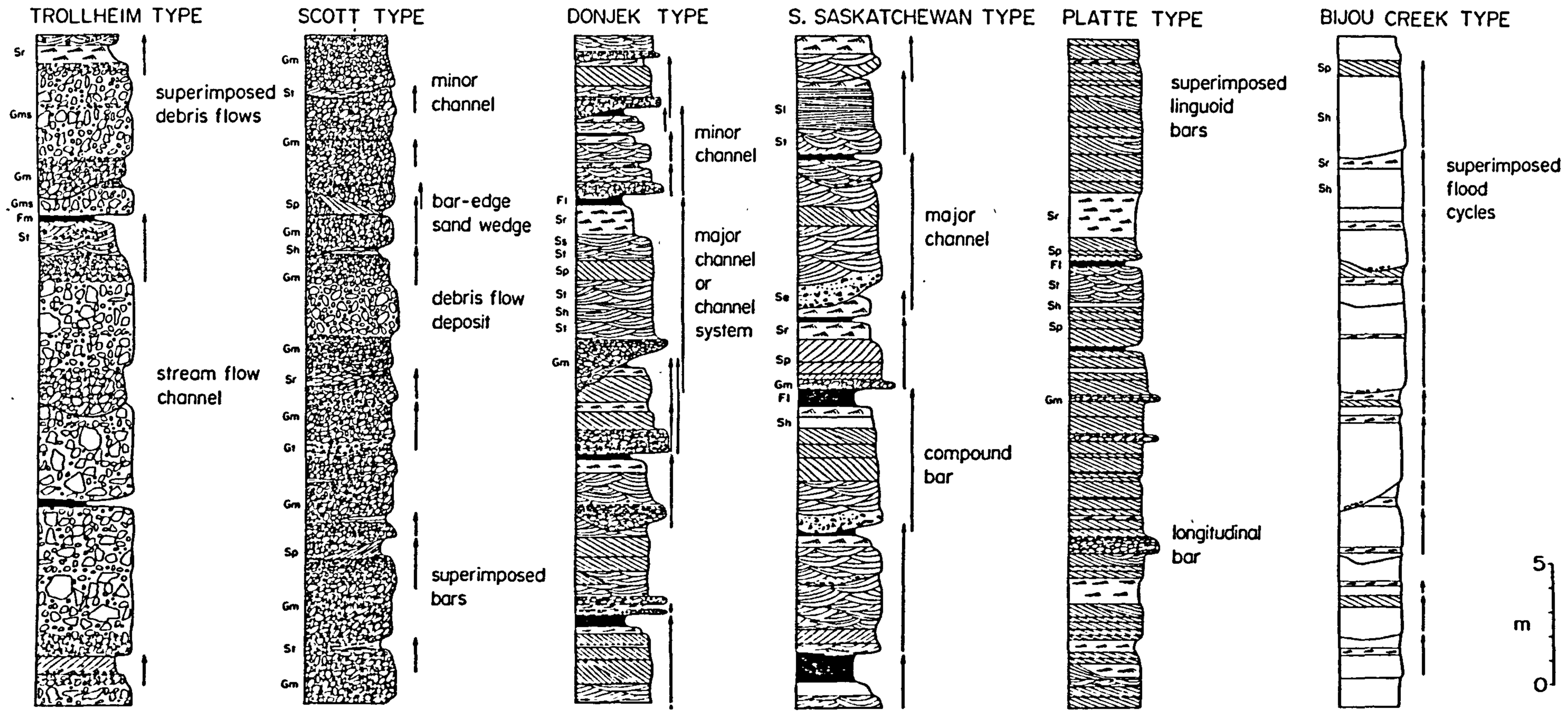

Fig. 2.5. Vertical profile models for braided stream deposits (from Miall, 1978).

Table 2.4. Lithofacies assemblages and facies models for multiple-channel bed - load rivers (from Miall, 1978).

Name	Environmental setting	Main facies	Minor facies
Trollheim type (G_I)	proximal rivers (predominantly alluvial fans) subject to debris flows	*Gms, Gm*	*St, Sp, Fl, Fm*
Scott type (G_{II})	proximal rivers (including alluvial fans) with stream flows	*Gm*	*Gp, Gt, Sp, St, Sr, Fl, Fm*
Donjek type (G_{III})	distal gravelly rivers (cyclic deposits)	*Gm, Gt, St*	*Gp, Sh, Sr, Sp, Fl, Fm*
South Saskatchewan type (S_{II})	sandy braided rivers (cyclic deposits)	*St*	*Sp, Se, Sr, Sh, Ss, Sl, Gm, Fl, Fm*
Platte type (S_{II})	sandy braided rivers (virtually non cyclic)	*St, Sp*	*Sh, Sr, Ss, Gm, Fl, Fm*
Bijou Creek type (S_I)	Ephemeral or perennial rivers subject to flash floods	*Sh, Sl*	*Sp, Sr*

goemetry; sheet, lens, wedge, scoop, U - shaped fill, (3) scale; thickness, lateral extent parallel and perpendicular to flow direction and (4) internal geometry; lithofacies assemblage, vertical sequence, presence of secondary erosion surfaces and their orientation, bedform palaeoflow directions, relationship of internal bedding to bounding surfaces.

Twelve fluvial models can be developed based on the sinuosity, braiding parameter, sediment type and the eight characteristic elements (Fig. 2.5, Table 2.4).

2.3 TIDAL SYSTEMS

Tidal flats are marginal marine environments located along low relief coastal plains and gently dipping continental shelves marked tidal rhythms, provided there is an abundant sediment supply and absence of strong wave action. A scheme which is currently gaining acceptance as a sedimentological classification of shorelines stresses the importance of tidal range and proposes three divisons: microtidal, $<$ 2m; mesotidal, 2 - 4 m; and macrotidal, $>$ 4 m (Davies, 1964; Hayes, 1976; Hayes and Kana, 1976).

Tidal flats occur in low wave energy, mesotidal and macrotidal settings where they dominate extensive streches of shorelines, or form within coastal embayments, lagoons, estuaries and tidally influenced

deltas. In general, tidal flats comprise almost featureless plains dissected by a network of tidal channels. During flood period, tidal waters enter the channels, overtop the channel banks and inundate the adjacent flats. Following a period of still - stand the tidal waters drain seawards via the channels and re-expose the flats (Reading, 1978).

Barrier islands are more prevalent in coastal settings which have the following characteristics: (1) a low gradient continental shelf adjacent to a low - relief coastal plain, (2) an abundant sediment supply, and (3) moderate to low tidal ranges (Glaeser, 1978). Barrier islands occur in microtidal and mesotidal settings but tend to be most common in the latter where they are generally dissected by numerous tidal inlets (Hayes, 1975, 1979). Both the shelf and the coastal plain are composed of unconsolidated sediments which are the material source for the building of barrier islands by nearshore processes.

The overall sediment distribution across a tidal flat is seaward-coarsening and three tidal flat zones are recognised. These zones are (from high to low tide), the high tidal flat, the mid tidal flat and the low tidal flat. Landward of the high tidal flat are supratidal salt marshes, and seaward of the low tidal flat is the shallow, tide - dominated subtidal zone (Klein, 1977). The grain size distribution of each of the tidal flat sub - zones is also distinctive. The high tidal flat is dominated by mud deposition, the mid tidal flat consists of coarser sediments of nearly equal volumes of mud and sand, the low

tidal flat consists dominantly of sand - sized sediment (Klein, 1977). Reineck (1975) differentiated the tidal flat deposits into supratidal (marsh), intertidal (mud flat, mixed flat and sand flat), and subtidal (channels and sand bars) (Table 2.5).

2.3.1 SUPRATIDAL ZONE

This lies above mean high tide level. It may be covered by salt marshes, interlaminated clays and silts in which the laminae are extensively disrupted by bioturbation, rootlets and nodules . Evaporite development depending on the climate (Reineck, 1967). In warm and temperate climatic zones it is vegetated by halophytic plants, and in arid regions it may be devoid of any vegetation.

2.3.2 INTERTIDAL ZONE

This comprises smooth, seaward - dipping flats dissected by large- and small - scale tidal channels. In general, intertidal flats range from mud dominated near the high water mark to sand - dominated near the low water mark (Van Straaten, 1954, 1961). Relatively weak tidal currents and waves interact on sand - dominated intertidal flats to produce extensive areas of asymmetrical and symmetrical ripples, often with complex interference patterns. Intertidal flat facies are dominated by interlaminated clays, silts and sands exhibiting prolific flaser, wavy and lenticular bedding. These facies reflect constantly

Table 2. 5 Tidal Flat Subdivisions Mentioned by Reineck (1975) and Klein (1977)

Reineck (1975)	Subtidal zone	Intertidal zone			Supratidal zone
		sand flat	mixed flat	mud flat	
Klein	Subtidal	low tide	mid tide	high tide	Supratidal

fluctuating but relatively low energy conditions, with brief periods of sand and coarse silt bedload transport by tidal currents and waves alternating with fine sediment deposition from suspension (Reineck and Wunderlich, 1968).

Tidal currents can be inferred from the: (1) bidirectional current-formed sedimentary structures and bimodal palaeocurrent patterns with the two modes approximately 180° apart, reflecting flow reversals. These are the most diagnostic features of tidal currents and may be found in the form of herringbone cross - bedding in which superimposed sets of oppositely dipping cross - strata are thought to preserve both ebb and flood tidal flows; (2) multimodal palaeocurrent patterns reflecting either temporal fluctuations in direction or the rotary nature of tidal currents, possibly with superimposed storm activity, and (3) the abundance of cross - bedding reflecting dunes and sandwaves which today are mainly found in tidal seas.

2.3.3 SUBTIDAL ZONE

This zone is mostly occupied by channels and subtidal sand bars and shoals, usually dominated by winnowed sandstones.

Progradation of tidal flats tends to produce a fining - upward sequence which reflects a transition from low tide level sand flats upward into high tide level mudflats, and eventually into supratidal flats.

CHAPTER THREE

UPPER CAMBRIAN SEDIMENTARY SUCCESSION AND FACIES

CHAPTER THREE

UPPER CAMBRIAN SEDIMENTARY SUCCESSION AND FACIES

3.1 INTRODUCTION

Schneider et al., (1984) divided the Cambrian sediments of Jordan into three major categories; (A) Lower / Middle Cambrian, (B) Middle/ Upper Cambrian, and (C) Upper Cambrian (Fig. 1. 5), based on lithostratigraphy, mineral content and palaeogeography. This study is confined to the upper half of the unit (C) (Plate 3.1, 3.2). Cooper's (1976) work shows Burj Formation to be late Early Cambrian.

The Upper Cambrian succession consists of medium to coarse - grained, well to moderately sorted, mature quartz arenites, interbedded with minor amounts of siltstone and mudstone. These sediments are poorly fossiliferous and are poorly known. The succession maintains a uniform thickness of 110 m, and on the basis of measured sections (Fig. 3. 2) two facies were recognised: an arenite facies and a heterolithic facies (Plates 3. 3, 3. 4). These facies are described below.

3.2 ARENITE FACIES

3.2.1 DESCRIPTION

This is a composite facies consisting of cream coloured (weathering

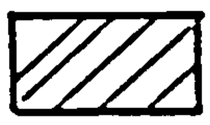

Planar cross-bedding

Trough cross-bedding

Lenticular bedding

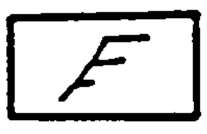

Rippled

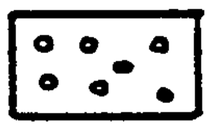

Pebbly sandstones

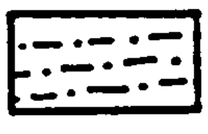

Sandy-shales

Sand clasts and mud clasts

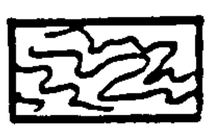

Deformed cross-bedding

Overturned cross-bedding

Fossiliferous

Silty-shales

Erosional surface

Rippled surface

Notations

S = Silty-shale

F = Fine sandstone

M = Medium sandstone

C = Coarse sandstone

P = Pebbly sandstone

M = Thickness in metres

Fig. 3. 1. Key showing lithology, sedimentary structures and other notations used in Fig. 3. 2.

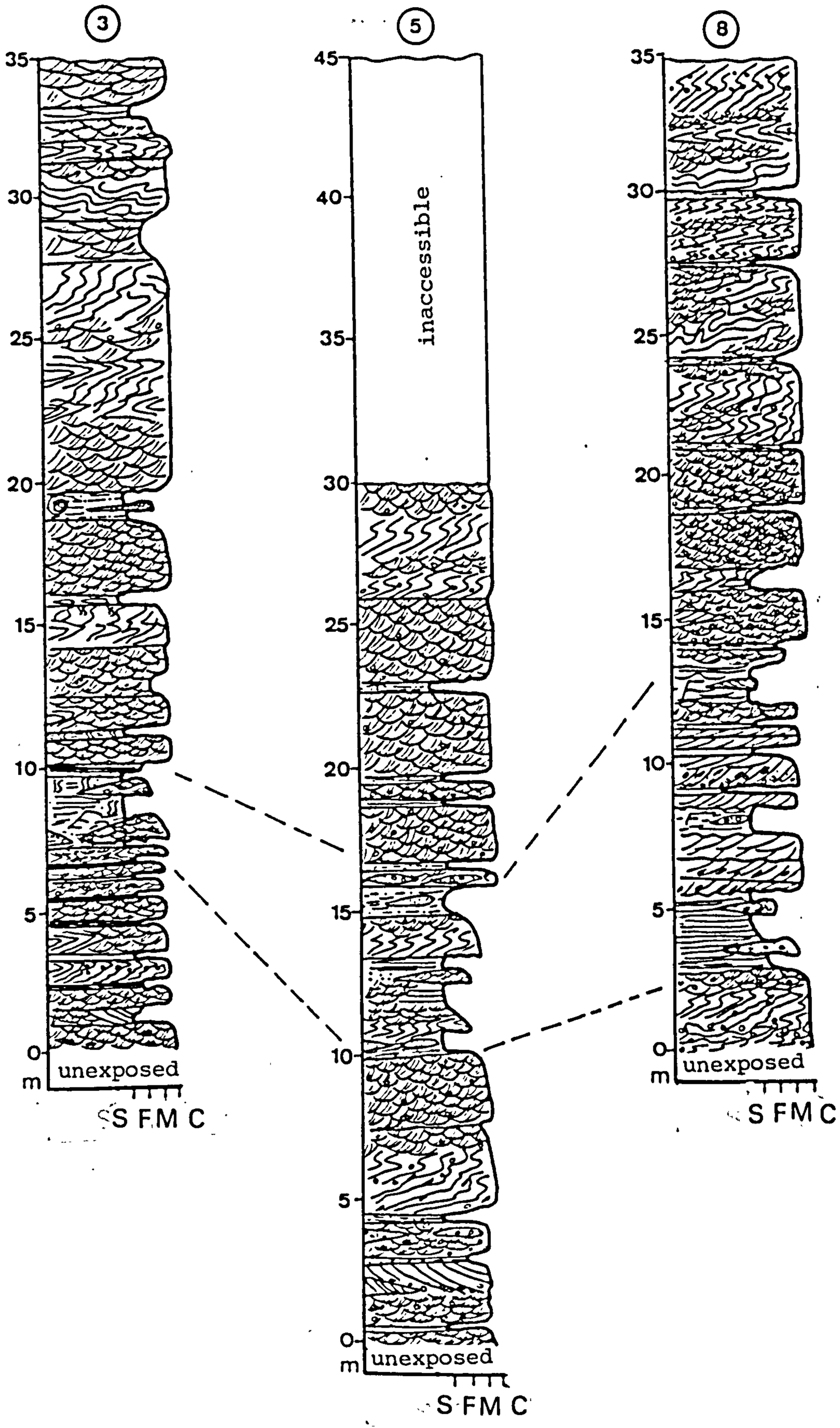

Fig. 3. 2. Measured sections of the Upper Cambrian at different localities (see Fig. 1. 7 for locations and Fig. 3. 1 for legend and notations). The dashed lines represent the lower fine interval. The upper datum is the contact with Um Irna.

brown), medium to coarse - grained quartzitic sandstones with scattered granules and small pebbles locally concentrated into conglomeratic lenses. Pebbly sandstones containing both intraformational and extraformational clasts set in a small pebble to granule - rich coarse quartz arenite. Intraformational clasts consist of subangular to subrounded fragments of siltstone and mudstone. Extraformational clasts comprise well rounded to subrounded pebbles composed predominantly of vein quartz (smokey, milky, and rose coloured varieties), chert and rock fragments up to 1 cm in diameter. Where they overlie beds of mudstone or siltstone, the basal sands may contain scoured clay or silt rip - up clasts. Such clasts vary from pebble size to cobble size (up to 12 cm in diameter). Most clasts appear to have a well developed long axis orientation (fabric) which is consistant with the cross - bedding directions.

Quantitatively the quartzitic sandstones are the most important lithology (element SB : sandy bedforms) in the Upper Cambrian succession. In thin section the grains are generally cemented by silica. They are moderate to well sorted and typically angular and elongate locally. A thin section of a conglomeratic lens shows pebbles, 2 - 6 mm in diameter, of highly fractured subrounded quartz cemented by iron oxide. Feldspar and muscovite are other common constituents (see Chapter 5).

The individual sandstones are medium - grained and generally arranged as compact, medium to thick bedded tabular units and less

commonly lenticular units with thin intercalated beds of siltstone, shale and fine sandstone (heterolithic facies). The sandstones show a tendency to increase in thickness and abundance upwards. The upper surface of each sandstone bed is always erosional (Plate 3.18), whilst the base of the bed is sharp and locally displays irregular erosional surfaces of low relief (<20 cm). Locally the upper and lower erosional surfaces are smooth and planar or gently undulating. The internal sedimentary structures consist of trough cross - bedding (lithofacies St) with subordinate low- angle cross - bedding (lithofacies Sl) and flat bedding (lithofacies Sh) showing parting lineation. Planar cross-bedding (lithofacies Sp) is less common. Trough cross - bedding occurs as solitary sets, usually 20 - 50 cm thick (maximum thickness 80 cm and minimum thickness 7 cm), and cosets up to several meters thick (Plate 3.15). Locally, individual foreset laminae show marked grain - size alternation from fine sand to small pebbles and mudclasts, and the foresets show a tangential relationship to the lower bounding surface.

Sedimentary deformation structures are common and contorted laminations are locally present in this facies (Plates 3.18 - 3.26 and Figs. 3.9 - 3.15). Most of the trough cross - bedding is overturned usually in the downcurrent direction. Because of its peculiar characteristics the overturned trough cross - bedding is dealt with separately (see section 3.4).

Palaeocurrent measurements were made mainly on the foreset azimuths

of trough cross - bedding exposed in plan on sandstone bedding surfaces. Measurement was made as close as possible to the trough axes, that is, the bisectrix of the angle of foreset curvature since this gives the most reliable results (Dott, 1973). A minimum of 20 readings was taken whenever possible at each sample locality for statistical accuracy (Pettijohn and Potter, 1963; Selley, 1983), and the results plotted on current roses at ten degree class intervals. Additional directional data was obtained from clast imbrication in the pebbly sandstones, and from ripple marks in the sandstones and siltstones of the heterolithic facies.

Foreset azimuths show a unimodal distribution to the northwest with about 120 degrees of dispersion both westward and eastward. Readings obtained from various localities indicate that palaeocurrents moved predominantly from the southeast to the northwest, but there is slight variation among the different outcrops (Figs. 3.13 - 3.16).

3.2.2 INTERPRETATION

The sedimentary structures and textures, the unidirectional palaeocurrent trend, and the non - fossiliferous and non - calcareous quartzarenites indicate that this facies may be of fluvial origin (Allen, 1970; Miall, 1976). The sandstones form sheet - like bodies unlike the fluvial sandbodies of meandering stream origin which are typically elongate and enclosed in floodplain mudstone. The fairly

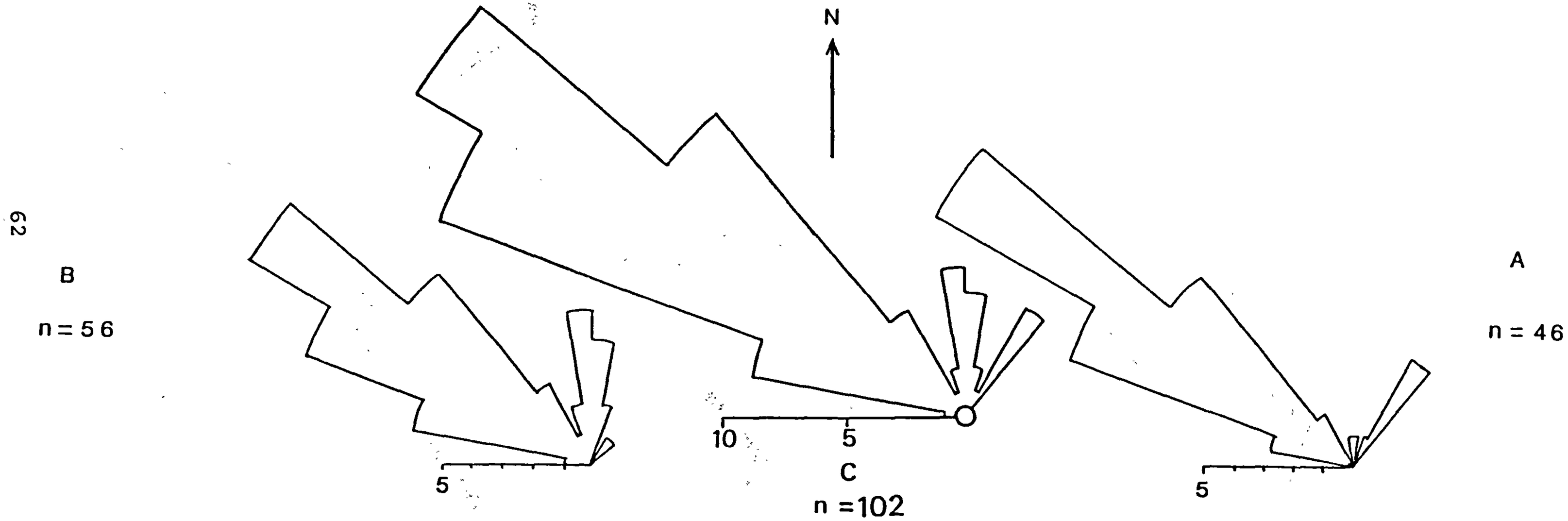

Fig. 3. 3. Palaeocurrent rose diagrams of the Upper Cambrian.(A) overturned cross - beds (31 measurements at section 5 and 15 measure - ments at section 8, (B) trough cross - beds at section 5, and (C) combined palaeocurrent rose, note predominance of palaeoflow towards the northwest (see Fig. 1. 7 for location).

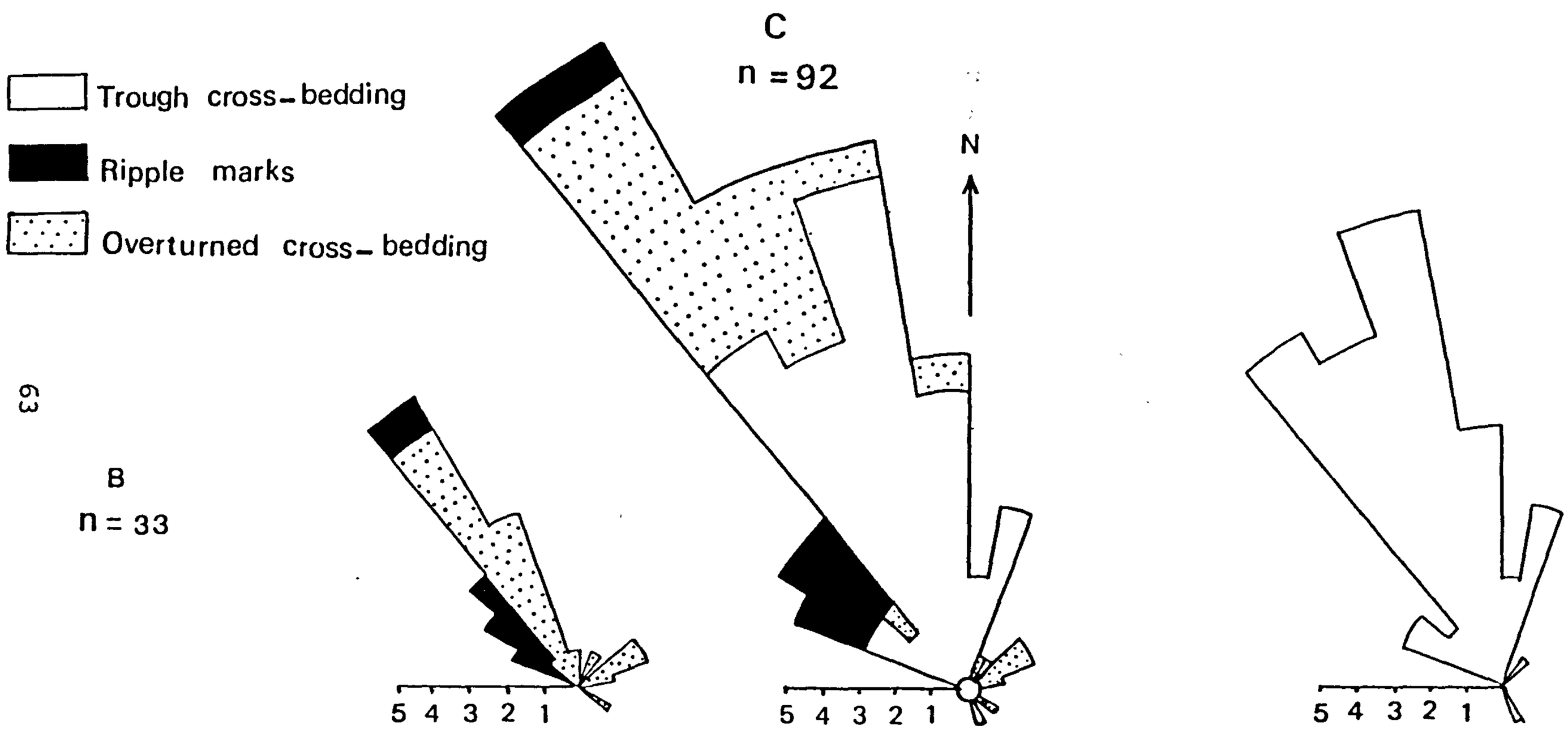

Fig. 3.14. Palaeocurrent rose diagrams of the Upper Cambrian at section 3 (see Fig. 1.17 for location. (A) trough cross - bedding, (B) overturned cross - bedding and ripple marks, and (C) combined rose diagram, note predominance of palaeoflow towards the north - northwest.

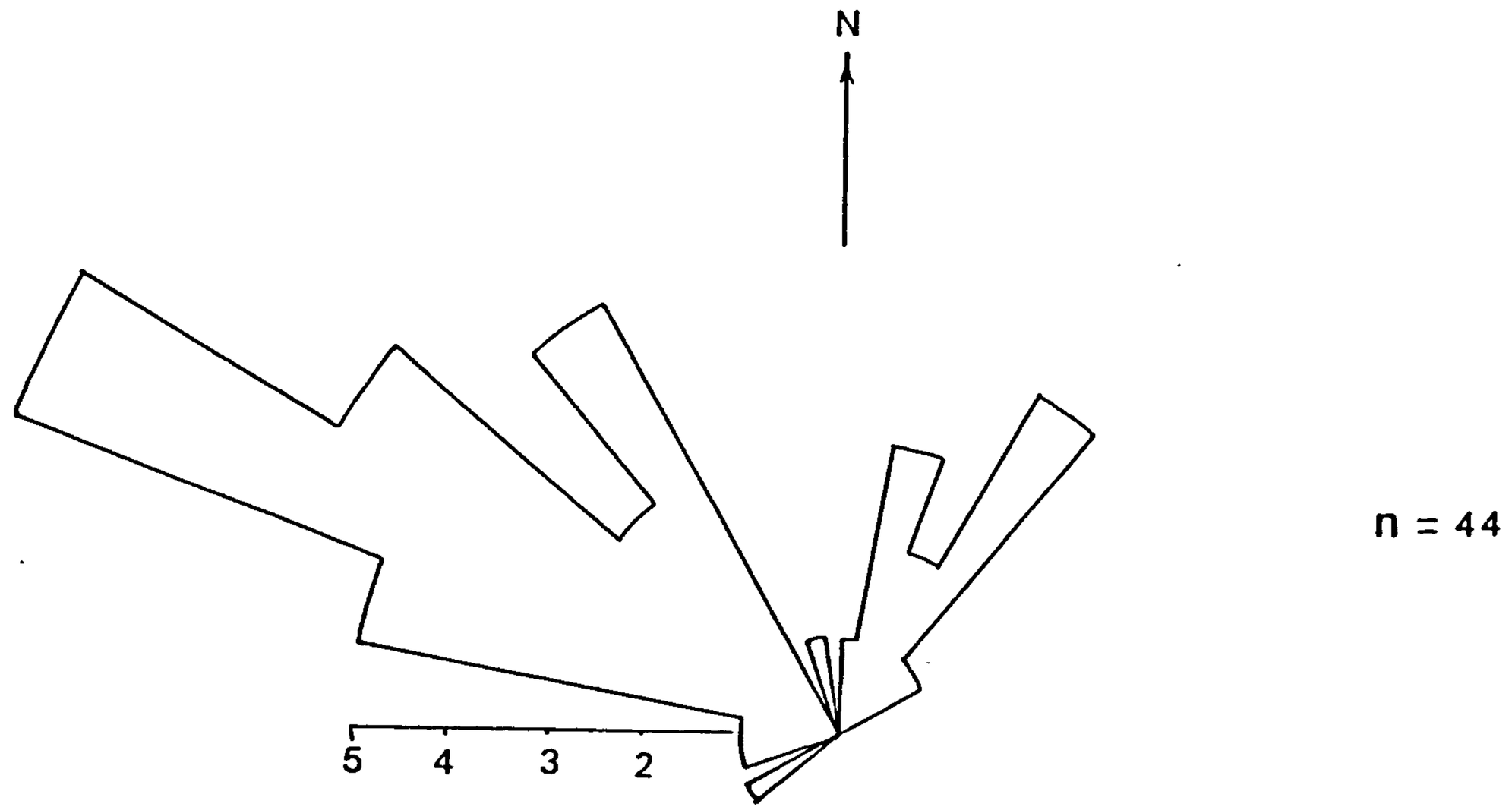

Fig. 3. 5. Palaeocurrent rose of cross - beds at section 8. Note the predominance of the palaeoflow towards the northwest and the sub - ordinate trend to the northeast (see Fig. 1. 7 for location).

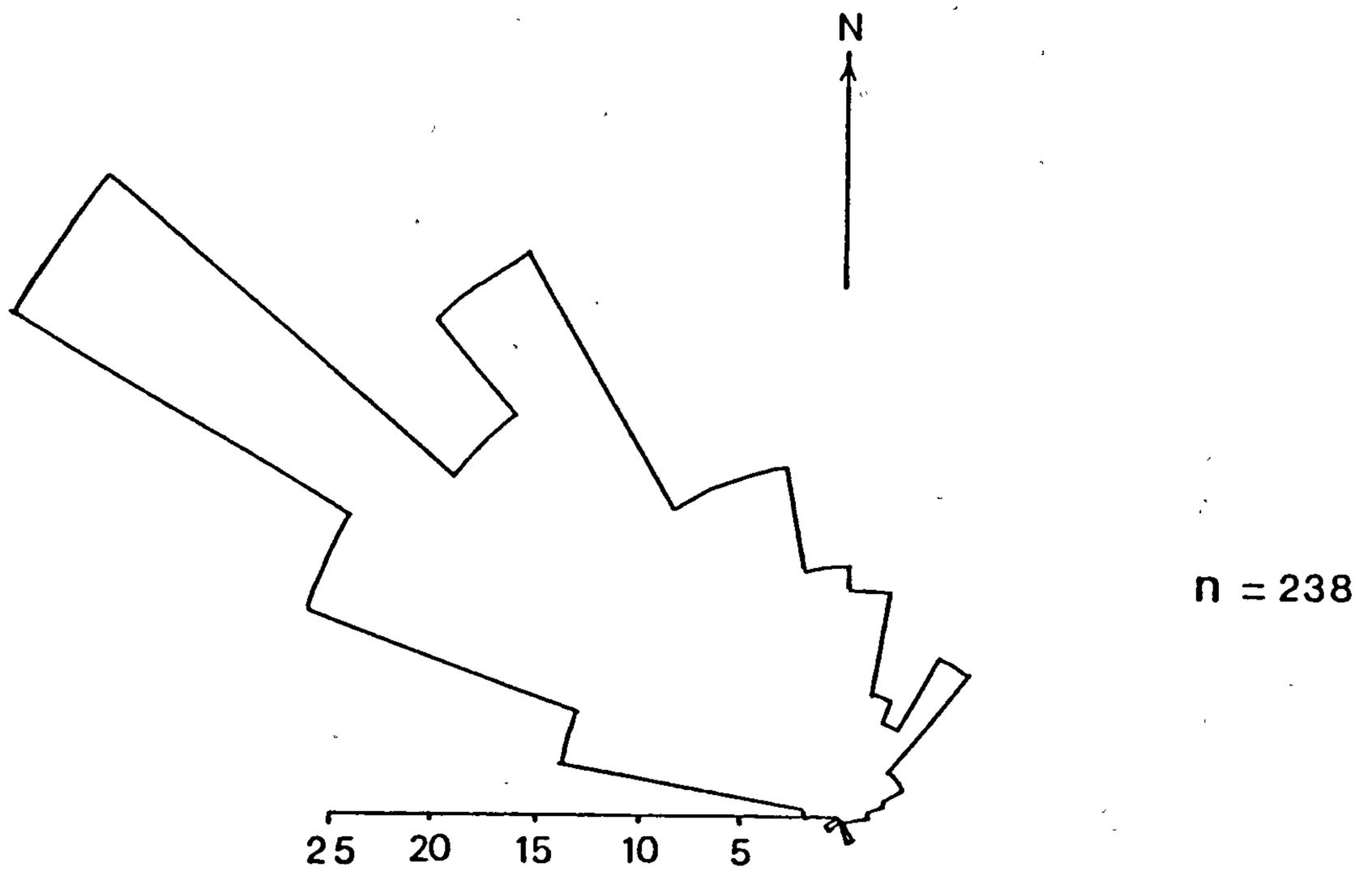

Fig. 3.6. Combined palaeocurrent rose diagram of Upper Cambrian showing palaeoflow at sections 3,5 and 8 (see Fig. 1. 7 for location). Note the predominance of the palaeoflow towards the northwest.

constant unidirectional palaeocurrent trend and the lack of any obvious sedimentary sequences (fining upward or coarsening upward), the high ratio of sand to mud, the rarity of floodplain and channel - fill mudstones, and the sheet - like geometry suggest that the stream channels were of low sinuosity. Sandstone geometry (sheet - like) and the dominance of sand and traction current structures suggest deposition within high gradient, bedload dominated, low sinuosity channels (Schumm, 1972). Similar thin, laterally extensive sandbodies indicative of a sheet - braided fluvial style occur in the Central Appalachian Paleozoic sequence (the three older Palaeozoic units; Bald Eagle, Juniata and Tuscarora) (Cotter, 1978). These were attributed to flow that was flashy, possibly ephemeral, and virtually unconfined by banks due to the lack of bank - stabilizing vegetation in the earlier Palaeozoic.

In braided channels, the finer material (silt and clay) tends to be transported through the system without accumulation. Vertical accretion deposits are rarely preserved, and deposition in flood basins is not such an important process as it is in meandering systems (Cant and Walker, 1978). Successive floods and lateral migration of the depositional system result in channel stacking, in addition to erosion of the siltstones and their incorporation as clasts along the base of the overlying channel sandbodies (Turner, 1986). The record of ancient braided - stream deposits shows that channel deposits rest on scour surfaces and commonly contain a basal lag of gravel (Miall, 1970;

Smith, 1970; Cant and Walker 1976). The presence of the intraformational mudclasts is interpreted as a channel lag formed in response to scouring of the floor and sides of the channels as they constantly shifted across the alluvial plain (Turner, 1983). This may indicate episodes of renewed high - energy flow producing mudstone rip - up clasts which occur abundantly throughout most of the sandstone units, especially in the lower part of the succession. They vary in size from flakes of a few millimeters up to about 12 cm in diameter.

Most large-scale troughs in sandy braided streams result from megaripple migration within the channels and are seldom related to bar formation (Williams, 1971; Bootheroyd and Ashley, 1975; Miall, 1977). At the same time erosion by subsequent floods and constant shifting of the channels would produce overlapping and scoured trough cross - bedded sandstones. Shifting is a function of slope and sediment input, which is in turn controlled by gradient changes, providing that climate and run - off are constant (Blatt et al., 1980).

The relative abundance of trough cosets (lithofacies St) suggests that sedimentation was dominated by the unidirectional migration of three dimensional curve - crested dunes (Harms et al., 1975). Few planar cross - bedded units (lithofacies Sp) were recorded, and these are thought to have formed by migrating straight - crested dunes or by small transverse bars (Harms et al., 1975). In these channels, curve crested bedforms predominate over straight - crested types, thus troughs

are the most prevalent kind of cross - bedding. Cosets of trough cross - beds indicate unidirectional flows of relatively high flow velocities appropriate to the formation of three - dimensional dunes (Ethridge, 1985). Cant (1978) describes major channel deposition and aggradation, common to most sandy braided rivers and attributes it to downstream migration and aggradation of dunes across the channel floor; dune dimensions increasing with increasing flow stage. The development of sinuous - crested dune bedforms (trough sets) is attributed to high stage discharge (Turner, 1986), although they can occur at all stages of flow (Cant, 1978). Walker and Cant (1984) indicated that during average discharge, the typical bedform of the channel floor consists of sinuous - crested dunes ranging in height from about 30cm to one meter. Preservation of these dunes results in trough cross - bedding.

These observations suggest a dominance of unidirectional currents in a depth - velocity range suitable for the development of dunes in medium to coarse sand. The orientation of the trough axes shows a remarkably uniform trend to the northwest, indicating a source area to the southeast (Figs. 3.3 - 3.6).

Harms et al., (1975) indicated that the depth of the flow must exceed the maximum thickness of a cross - bed set. This is at least twice the height of sand waves and several times the height for sand dunes. Assuming that only 50% of the original bedform is preserved (Allen, 1968; Turner, in press), the present trough cross - beds which

range in thickness from 20 - 50 cm, and have a grain size of about 0·5 mm, must have had an original bedform height of between 40 - 100 cm. Using the mean height of large - scale ripples (dunes) plotted as a function of mean water depth (Allen, 1968, Fig. 6.4, p.139), suggests a range of channel depth from 3.8 - 8 m. The depth can then be used to estimate velocity of flow from the depth / velocity plots of Harms et al., (1975, Fig. 2.6, p.22). This indicates a velocity range of 35 - 50 cm / sec.

Low - angle trough cosets (lithofacies Sl) and solitary planar sets (lithofacies Sh) imply fluctuations in flow strengths. Low - angle solitary trough cross - beds are attributed to the filling of channel floor scours and depressions, the contact with the overlying zone of low - angle trough cosets is fairly abrupt (Harms et al., 1982). The development of a plane bed (without ripples or dunes) is favoured by higher velocities and shallower flow depths, and deposition on the plane beds results in horizontal lamination (Haszeldine, 1983). Planar lamination is produced by aggradation during upper - stage plane bed transport. This is supported by the coarse grain size of the deposits (medium to coarse sandstone), which needs a stronger depositing flow. Under upper flow regime conditions sand is moulded into a flat bed with current lineations on the surface which become preserved as parting lineations on bedding plane surfaces (Miall, 1977). Overbank fines are lacking possibly because of erosion and rapid channel shifting (Turner, 1986).

The abundant deformed and overturned cross - bedding throughout the succession suggest frictional current drag on a sand bed liquefied, prior to deformation, by some external mechanism such as seismic shocks (Allen and Banks, 1972) (see section 3.4)

3.3 HETEROLITHIC FACIES

This comprises interbedded mudstones, siltstones and sandstones. Mudstones and siltstones make up over 60% of the heterolithic facies, and alternate with fine to coarse - grained sandstone which occurs as lenticular, wavy or ball - and - pillow units (Plates 3. 3, 3. 4, 3.10 - 3.17; Figs. 3. 7, 3. 8). This facies comprises six fine -grained intervals which occur within the arenite facies, in a repetitive manner, throughout the Upper Cambrian succession. The following description deals with the upper three fine - grained intervals, which are present within the upper half of the Upper Cambrian succession, and which are most easily accessible. They are referred to as lower, middle and upper intervals.

3.3.1 THE LOWER FINE - GRAINED INTERVAL

This unit consists of alternating sandstone, siltstone and mudstone units from > 2 mm to 4 m thick. The beds tend to be consistent in their thickness over several meters laterally. The base of the sandstone units in this interval is always erosional but it may be flat or wavy.

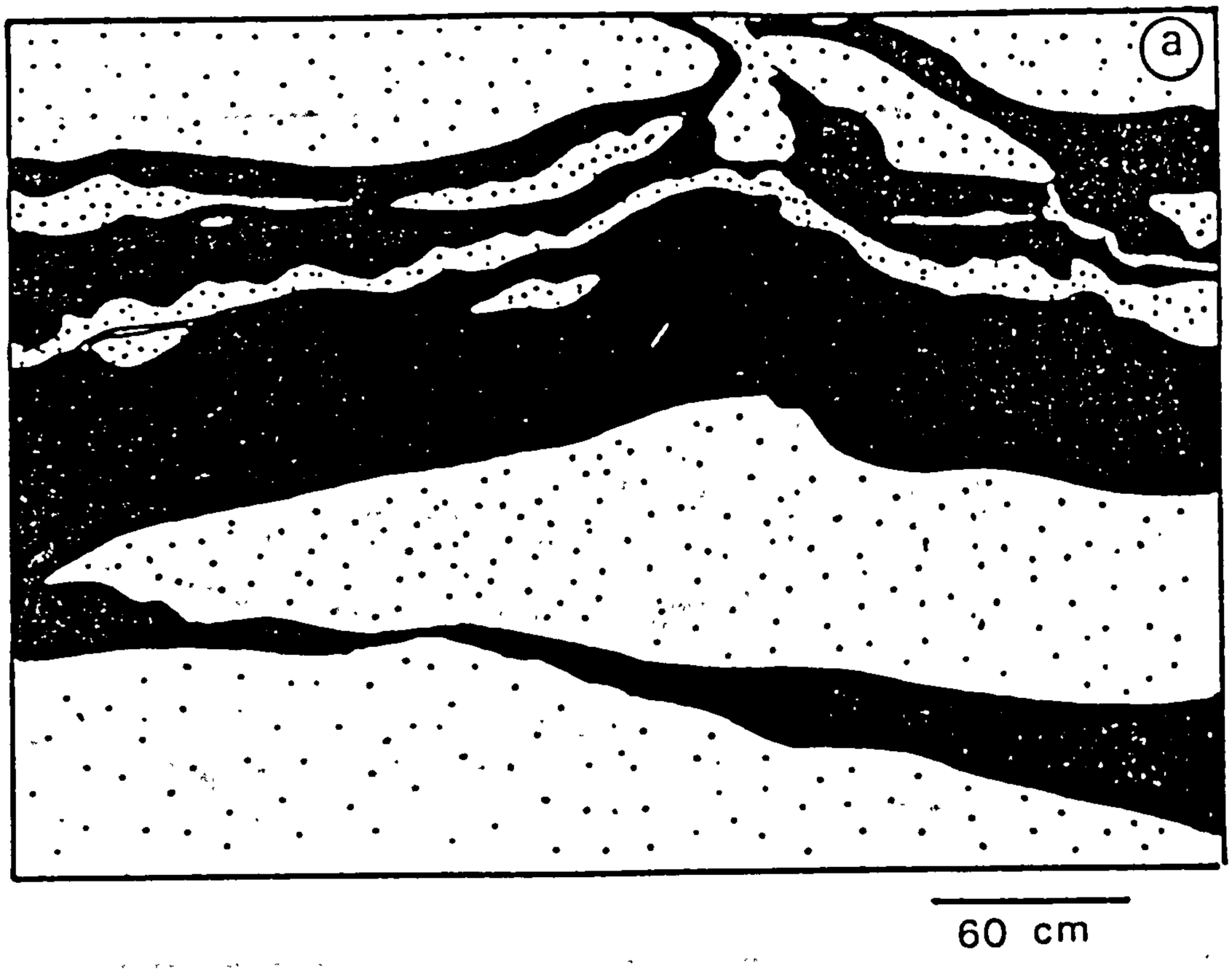

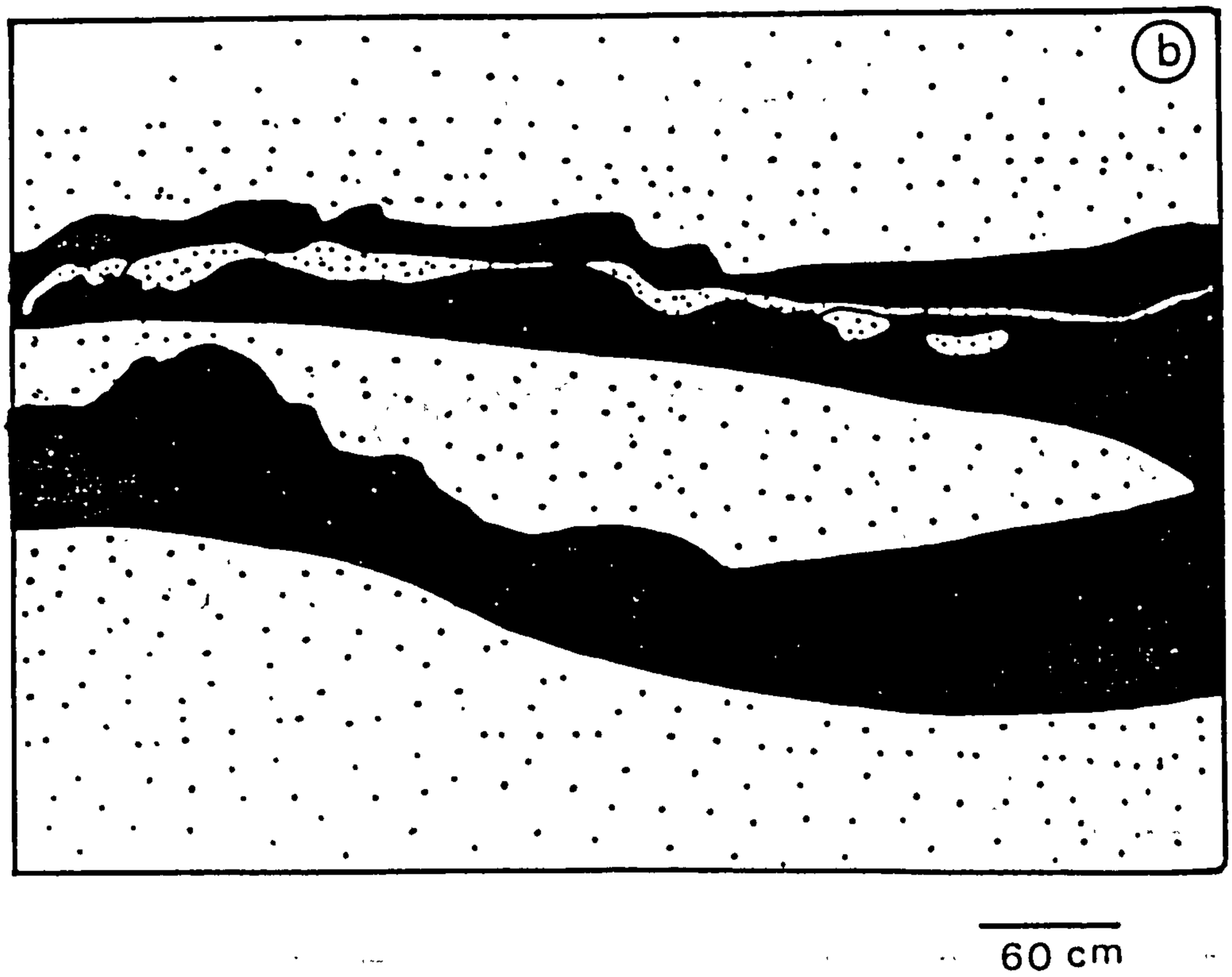

Fig. 3.7. Heterolithic facies of the Upper Cambrian at section 3 showing ball - and - pillow and wedge shaped structures, intercalated within muds. These may be due to differential loading (drawn from photographs).

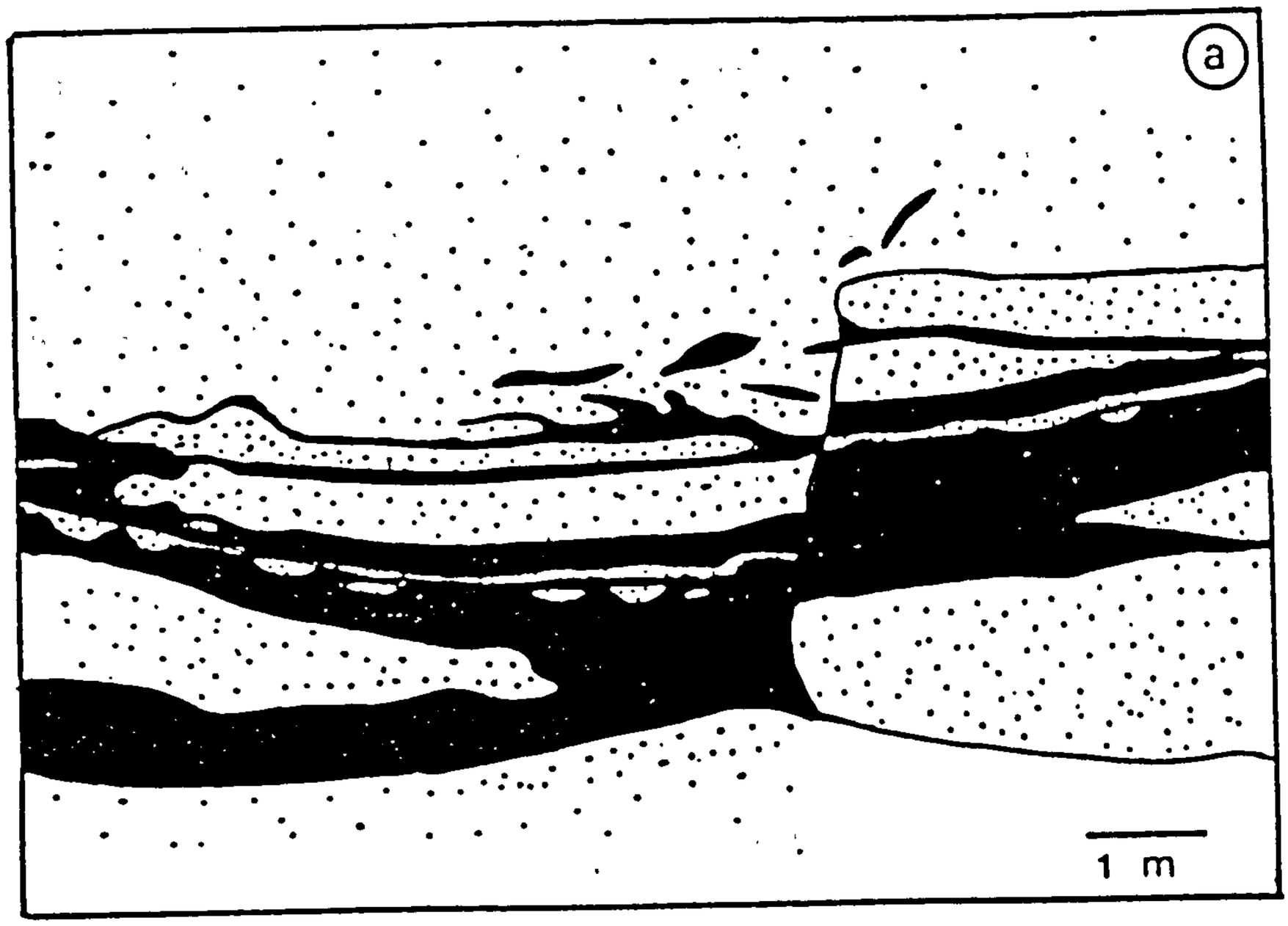

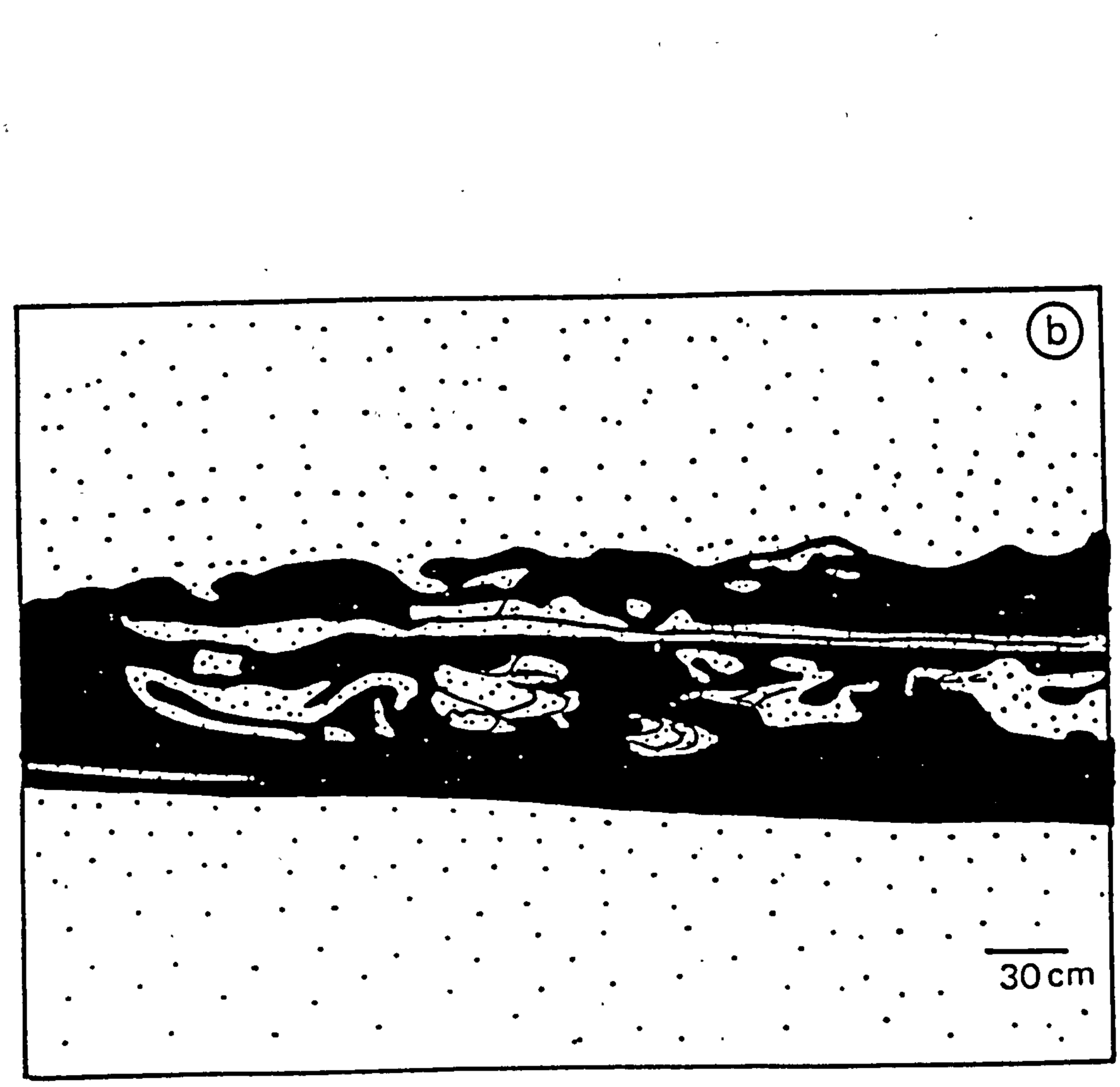

Fig. 3.18. Heterolithic facies of the Upper Cambrian at section 3 showing ball - and - pillow structures. Sandstone masses have sunk down within the mud (drawn from photographs).

The upper bounding surfaces are generally sharp. The sandstone facies alternates with the siltstone and mudstone in an apparently random manner. This interval can be further subdivided into two subfacies; sandstone and silty - shale.

DESCRIPTION

i) Sandstone subfacies

These quartz arenites are of fine to medium - grained texture, with frequent intraclasts. They are pale yellow to cream in colour. Maroon to grey fine - grained sandstones are also common. The sandstone beds are usually less than 30 cm thick. They consist of a chaotic assemblage of structures (eg. medium - scale trough cross - beds, cross - lamination and ripple marks) which merge laterally and vertically into each other. They are characterised by numerous thin shale flakes dispersed throughout the beds, and aligned parallel to the foresets. Both symmetrical and asymmetrical, sinuous to linguoid ripple marks are common. Megaripple marks (wavelength 70 cm and amplitude 15 cm) are also common. The crest of these ripple marks is commonly reworked and removed by currents locally (Plate 3.16). The steep face of the ripple marks dips towards the northwest, whereas, the sinuous crestline generally shows a northeast - southwest orientation.

ii) Silty - shale Subfacies

This comprises micaceous silty shales, ranging in colour from maroon to grey, with subordinate greyish green fine sandstone; the latter occurring as flaser and lenticular rippled beds. This sub - facies makes up over 60% of the heterolithic facies. It occurs inter - bedded with sand laminae or with lenticular, wavy or parallel thin sandstone beds. Small - scale lenticular laminations of lighter coloured siltstone or fine sandstone are common in the silty shale as well as flaser bedding (Plate 3.17).

Interference ripples with sinuous and discontinuous crests are seen on bedding surfaces. The ripples are commonly of small - scale (wavelength 5 cm, amplitude 1 cm). Cross - laminations are clear and show slight deformation. Isolated ripples with mud draped crests were observed and deformed ripples are also present (Plate 3.17). The shales are strongly bioturbated (Plate 3.15) and contain bivalves? and possible faint trilobite traces. Vertical to sub - vertical burrows are also common.

Interpretation of the lower fine - grained interval

Because layers of two different lithologies alternate repeatedly, they resemble rhythmites (Reineck and Singh, 1973). The preferred environments of such rhythmites are (1) areas where change takes place

between slack water and turbulent water and (2) where the required kind of sediments exist. Thus it occurs mainly in subtidal zones (Reineck, 1963 a; Reineck et al., 1968). In tidal environments the genesis of flaser and lenticular bedding is related to the tidal rhythm, i.e., to the periods of tidal currents alternating with periods of slack water (Reineck and Singh, 1973).

In the sandy subfacies , the presence of two distinct groups of ripples; small ripples with wavelength 5.5 to 20 cm, and megaripples with wavelength 70 cm, and the obvious overlapping of the two classes of ripples indicate that the superimposed small ripples are produced at relatively low energy. Reineck and Singh (1973) show that two distinct groups of ripples are present in tidal environments; (1) small ripples almost always less than 30 cm in wavelength, and (2) megaripples always more than 60 cm in wavelength, ranging up to 30 m.

Very little palaeocurrent data have been collected from the sandy subfacies However, the steep face of asymmetrical linguoid ripple marks was measured in the rippled fine sandstones, and the axial azimuths of the scarce medium - scale trough cross - beds (in the medium - grained sandstone), These show northwest palaeocurrent pattern similar to that of the arenite facies. The thin sandstones which occur locally interbedded with the siltstones are interpreted as having been deposited in an intertidal flat environment by incursions of alluvial

sands dispersed by wave and tidal activity.

In the silty - shale subfacies , the lamination is one of the most common features; with the darker laminae relatively rich in clay ~~or carbonaceous material~~. Ripple crests tend to sink down into the underlying soft muddy layer due to overloading, while other ripples show that they have been piled up and completely rotated (Plate 3.17).

This muddy unit is interpreted to be of nearshore marginal marine origin. This is suggested by the fossil bivalves?and by the strong bioturbation and its association with rippled and deformed silty shale. Most of the sediments accumulated in a low - energy coastal mixed flat environment.

3.3.2 THE MIDDLE FINE - GRAINED INTERVAL

This is dominated by deep maroon mudstones and silty - shales with subordinate sandstones. They are of laterally variable thickness with a maximum observed thickness of 2·5 m in the north, thinning rapidly within a short distance (30 m approximately) to the south to only 15cm. The thinning is usually accompanied by a loss of sandy interbeds. Two sub - facies can be recognised.

DESCRIPTION

i) Sandy Subfacies

These sediments are usually cream coloured, medium - grained

sandstones, with subordinate fine and coarse varieties. They contain mud flakes and commonly occur as shaped lenticular to wedge - shape masses, 15 cm to 6 m wide and 10 cm to 90 cm thick. The thickest parts of the lense shaped masses show faint medium - scale trough cross - bedding. This trough cross - bedding when traced laterally merges into massive beds.

The sandstone beds decrease in grain size and thickness upwards. They are predominantly fine - grained, and are characterised by numerous thin mudstone and siltstone intraclasts; quartz granules are also present. They form ball - and pillow masses at certain horizons, while in others they are in the form of thin (about 8 cm thick) continuous beds. The upper surface shows small - scale symmetrical ripples (wavelength 12 cm, amplitude 2 cm). The uppermost sandy unit is fine - to medium - grained and forms conspicuous isolated pillows (1 to 5 m wide, up to 43 cm thick). The upper and lower surfaces are erosional with 10 to 14 cm relief (Figs. 3. 7, 3. 8; Plates 3.12, 3.13).

ii) Silty - shale Subfacies

This subfacies consists of silty - shales and mudstones. The colour ranges from deep maroon to subordinate dark grey, depending upon the content of clay and carbonaceous matter. They can be divided into two parts, lower and upper. The lower part is predominantly wavy laminated and contains small - scale linguoid ripples (wavelength 6 cm,

amplitude 1 cm). In the upper part parallel lamination prevails. This fine subfacies is bioturbated. ~~and contains abundant comminuted plant fragments~~. Bivalves also occur but are less common.

Interpretation of the middle fine - grained interval

The most prominent features of the present heterolithic facies are load and ball - and - pillow structures. They are attributed to deposition of sand over a hydroplastic muddy layer, whence a reverse density gradient is established, due to the different porosities of the newly deposited sand and clay. According to Mills (1983) "sand porosity is approximately 45%, and clay porosity is 70 - 90%". These textural relations produce a metastable arrangement. Depending on the influences of other factors such as the degree of cohesion and viscosity of the sediments, deformation structures known as load structures may occur (Mills, 1983).

Potter and Pettijohn (1977) relate ball - and - pillow structures to abrupt thixotropic transformation of the underlying clays. According to Blatt et al., (1980) structures produced by the sinking of heavier sediments into lighter sediments are generally called load structures. In ball - and - pillow structure, a bed of fine sand is broken up at the base into "pillows" with rounded bottoms, but the upper part of the bed may be relatively undisturbed and display an almost flat top.

3.3.3 THE UPPER FINE - GRAINED INTERVAL

DESCRIPTION

The heterolithic facies at this level is up to 83 cm in thickness. It consists of sandstone and siltstone alternations intercalated with conglomerate.

The lowest part of this unit is a maroon, ripple laminated to massive siltstone up to 20 cm thick. This sandstone grades upward into a cream coloured, medium - grained sandstone up to 15 cm thick with mudclasts. It is overlain by 23 cm of maroon siltstone, slightly rippled, bioturbated and fossiliferous (Brachiopods?). It is overlain by lenticular bodies of pebbly conglomerate which are locally present in this heterolithic facies (Plate 3.11). These pebbly conglomerates are fossiliferous (Lingula), and are bounded at the top and the bottom by sandstone. The lenses are mostly less than 15 cm thick and several meters long. They are composed of subrounded granules and pebbles of grey quartz, ranging between 2 to 6mm in diameter. Microscopic study shows that these granules are highly fractured, and cemented by iron oxide.

Interpretation of the upper fine - grained interval

The interpretation here is devoted to the conglomerates which

represent a new element in the heterolithic facies. The conglomerates comprise second cycle or multicycle quartz pebbles and granules and are interpreted to be lag deposits of either the backshore or foreshore. Most likely the pebbles were derived from stream mouth gravels. After reaching the shoreline, they were further dispersed by local waves and currents to their present strand line position. Some of these pebbles can be seen in plan view (on the bedding surface), which clearly shows that they have formed as gravel deposits in local topographic lows (Plate 3.11). The presence of Lingula within the conglomerates emphasises the marine influence in their formation.

3.4 DEFORMED CROSS - BEDDING

3.4.1 INTRODUCTION

Penecontemporaneous deformation of cross - bedded units is the dominant feature in the arenite facies. The deformation ranges from simple recumbent folds, through complex folds and diapiric - like structures, to severly convoluted forms. Based on the nature of deformation two distinct types of contorted structure are apparent; overturned, buckled and convoluted foresets (cf. Allen and Banks, 1972; Hendry and Stauffer, 1975, 1977).

3.4.2 OVERTURNED CROSS -BEDDING

These comprise simple and complex recumbent folds:

1) Simple Recumbent Folds

These result from the oversteepening of cross - laminae to form a single recumbent fold, whose axial plane is parallel or nearly so with the base and top of the deformed unit. Here the original upper part of a cross - bed forms the overturned limb. Apical angles are as high as 120 degrees but most folds are between 25 and 70 degrees (Plate 3.18 - 3.20). Several kinds of recumbent folds are found at different outcrops, the differentation being based on the following characteristics:

i) The intensity of deformation;

a) Slight steepening of the upper part of the cross - bedded unit (Figs. 3. 9 c, 3.11 a);

b) Moderate steepening of the upper part of the cross - bedded unit, to form asymmetrical recumbent folds (Figs. 3. 9 d, 3.11 c);

c) Complete overturning of the upper part, forming an upper limb that is roughly parallel to the top, with the lower limb parallel to the bottom of the cross - bed. In this case the upper and lower limbs of the fold are almost parallel (Figs. 3. 9 a, b; 3.10 a - d; 3.11 d).

ii) The position of the fold nose

The fold nose in a cross - bedded unit may be at almost any level, although commonly it occurs in the central portion. In the observed recumbent folds, the hinge zone is located in the upper part (Figs. 3. 9 c, d; 3.11 c), in the middle part (Figs. 3. 9 a,b; 3.11 c), and in the lower part, close to or at the base of the cross - bedded unit

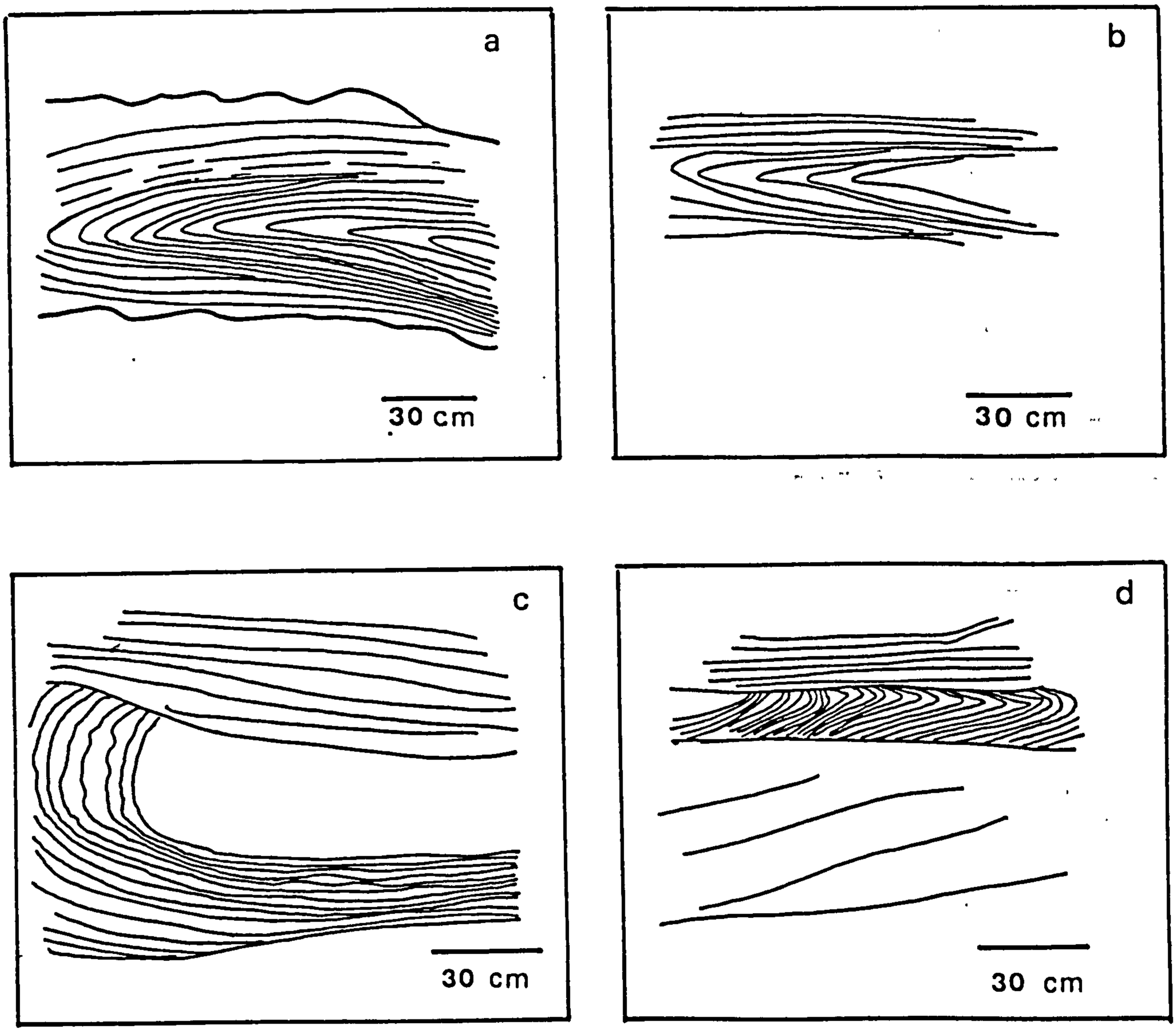

Fig. 3. 9. Overturned cross - beds. (a) and (b) are simple recumbent folds with smooth, completely overturned limbs, and fold nose in the middle portion. (c) Slight steepening of the upper part of the cross - bed with the hinge zone located in the upper part which shows slight undulations. (d) The upper part is moderately steepened to form an asymmetrical recumbent fold (right side). The hinge zone is located in the upper part and slightly undulated. (b) and (d) at section 5, (a) and (c) at section 3, (drawn from photographs).

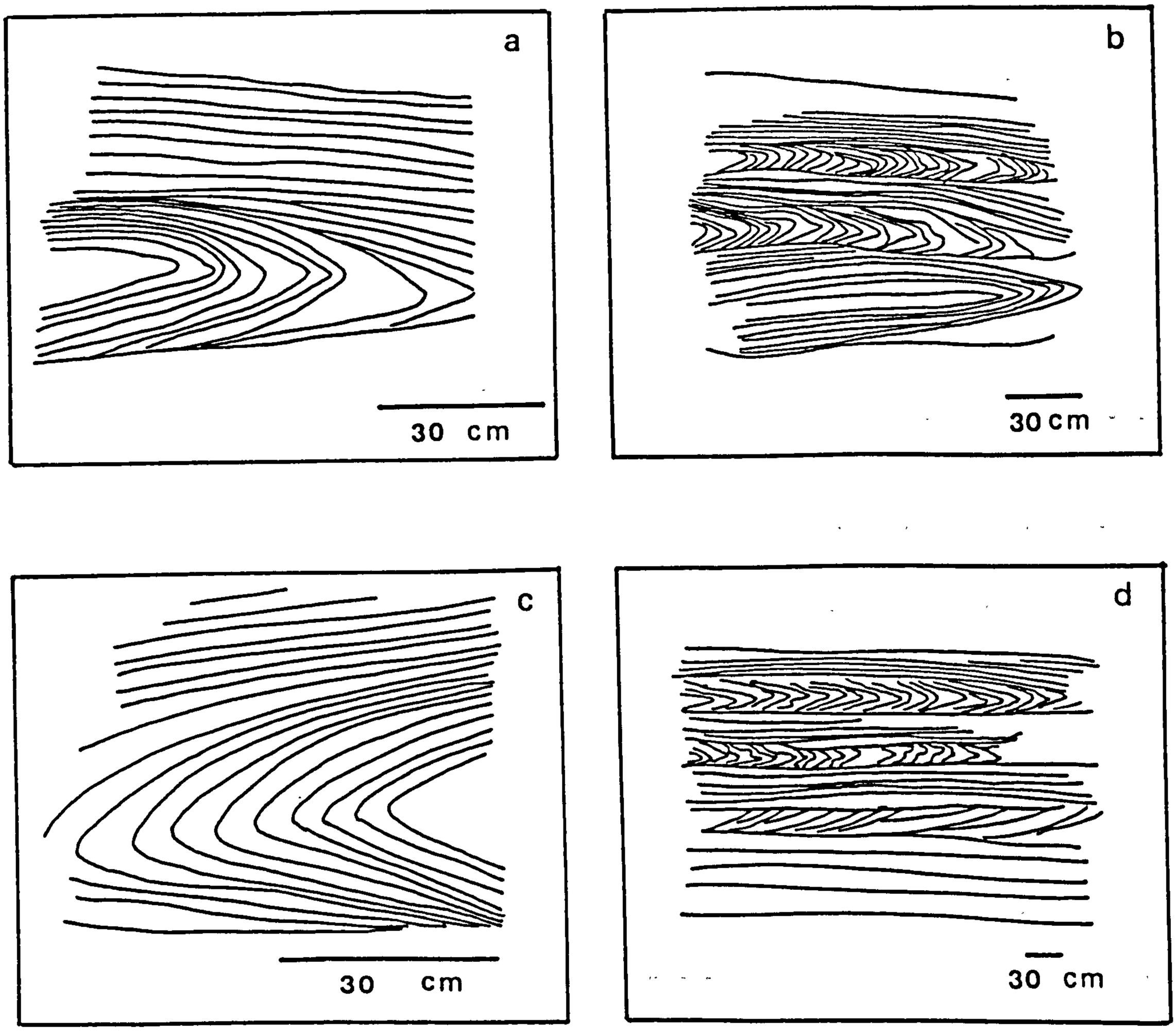

Fig. 3.10. Overturned cross - beds. (a) and (c) are simple recumbent folds (completely overturned limbs) with fold nose near to the lower surface. The lower and upper limbs are almost parallel. (b) and (d) show overturned cosets in which the hinge zone is undulatory. (a) and (d) at section 8, (b) and (c) at section 3, (drawn from photographs).

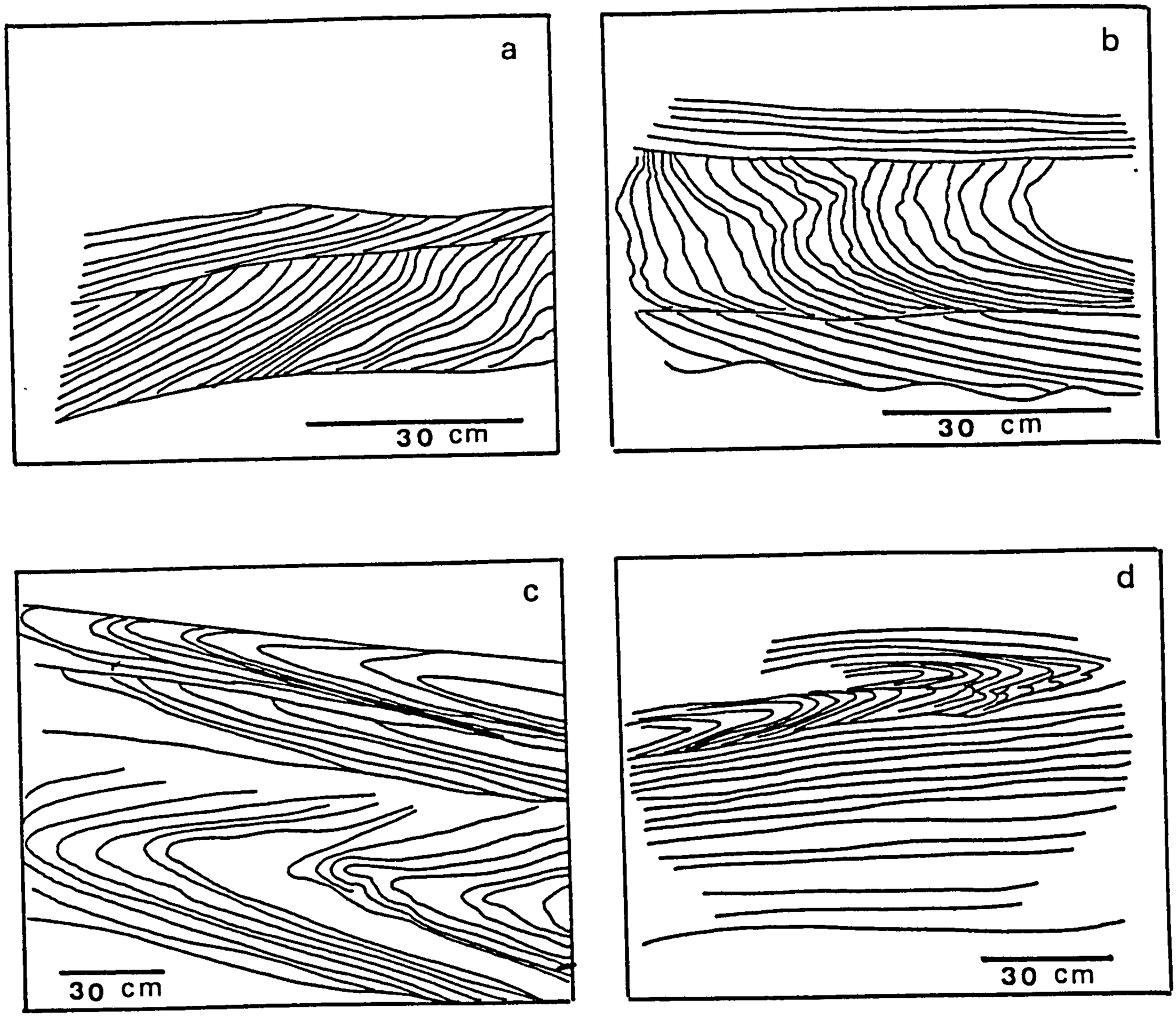

Fig. 3.11. Overturned cross - bedding. (a) slight steepening of the upper part. (b) Moderate overturning with an undulated hinge zone. (c) Moderate steepening of the upper part of the cross - bed to form asymmetrical recumbent folds. In the upper recumbent fold the hinge zone is located in the upper part. In the lower recumbent fold the hinge zone is located in the middle part. (d) The upper and lower limbs are almost parallel. (a,b, and d) at section 3, (c) at section 5, (drawn from photographs).

(Figs. 3.10 a - d).

iii) The development of minor folds.

The original recumbent fold may be smooth (Figs. 3. 9 a, b; 3.10 a - c), or undulating. Minor folding might take place at the hinge zone (Figs. 3. 9 c,d; 3.10 d; 3.11 a - c; 3.12 a - c; 3.15 a), or at the fold limbs, either the upper limb (Fig. 3.12 b,d) or the lower limb (Fig. 3.12 b,c).

2) Complex Recumbent Folds

Some deformed cross - beds have more than one recumbent fold within a single set. In fact, three types can be observed; S - shaped, trifold and multifold.

i) S - shaped folds (backfold or bifold) : In this type double overturning occurs in a single cross - bedded set to form two recumbent folds with one recumbent anticline above a recumbent syncline (Fig. 3.13 a,b; Plates 3.21).

ii) Trifold : In this type triple overturning occurs in the cross - bedded set to form three recumbent folds, with one recumbent anticline overlain and underlain by recumbent synclines. The upper part of the cross - bedded set is truncated while the lower part is tangential (Fig. 3.14 c; Plate 3.23).

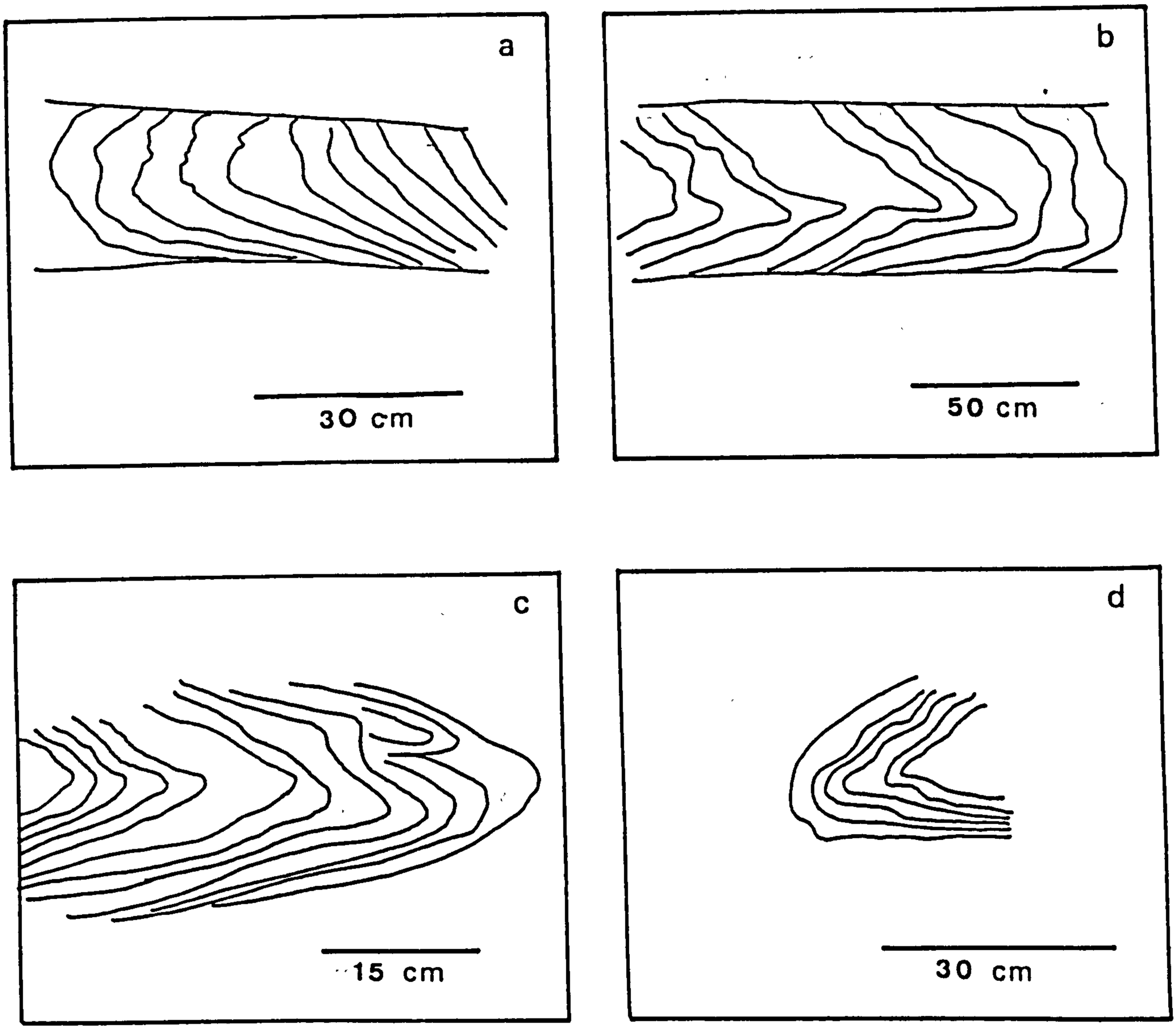

Fig. 3.12. Overturned cross - beds, with minor folds developed at the hinge zone on either limbs, (a) at section 8,(b,c and d) at section 3, (drawn from photographs).

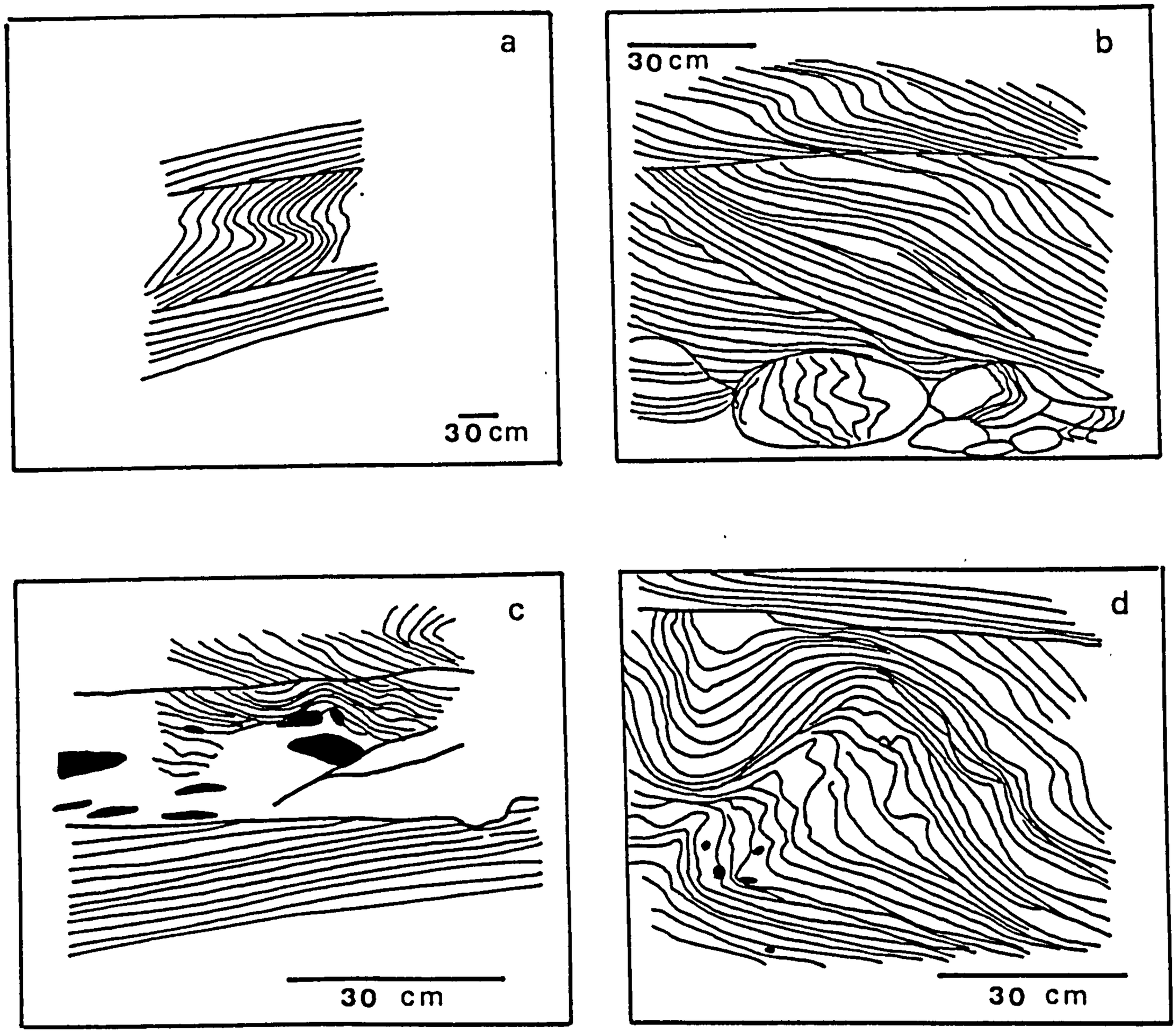

Fig. 3.13. Complex recumbent folds. (a) and (b) form S - shaped recumbent folds, in which double overturning took place in the cross - sets, to form a recumbent anticline above a recumbent syncline (at section 3). (c and d) show multifolded and buckled cross - sets, with a diapiric like structures. (c) at section 3, (d) at section 5, (drawn from photographs).

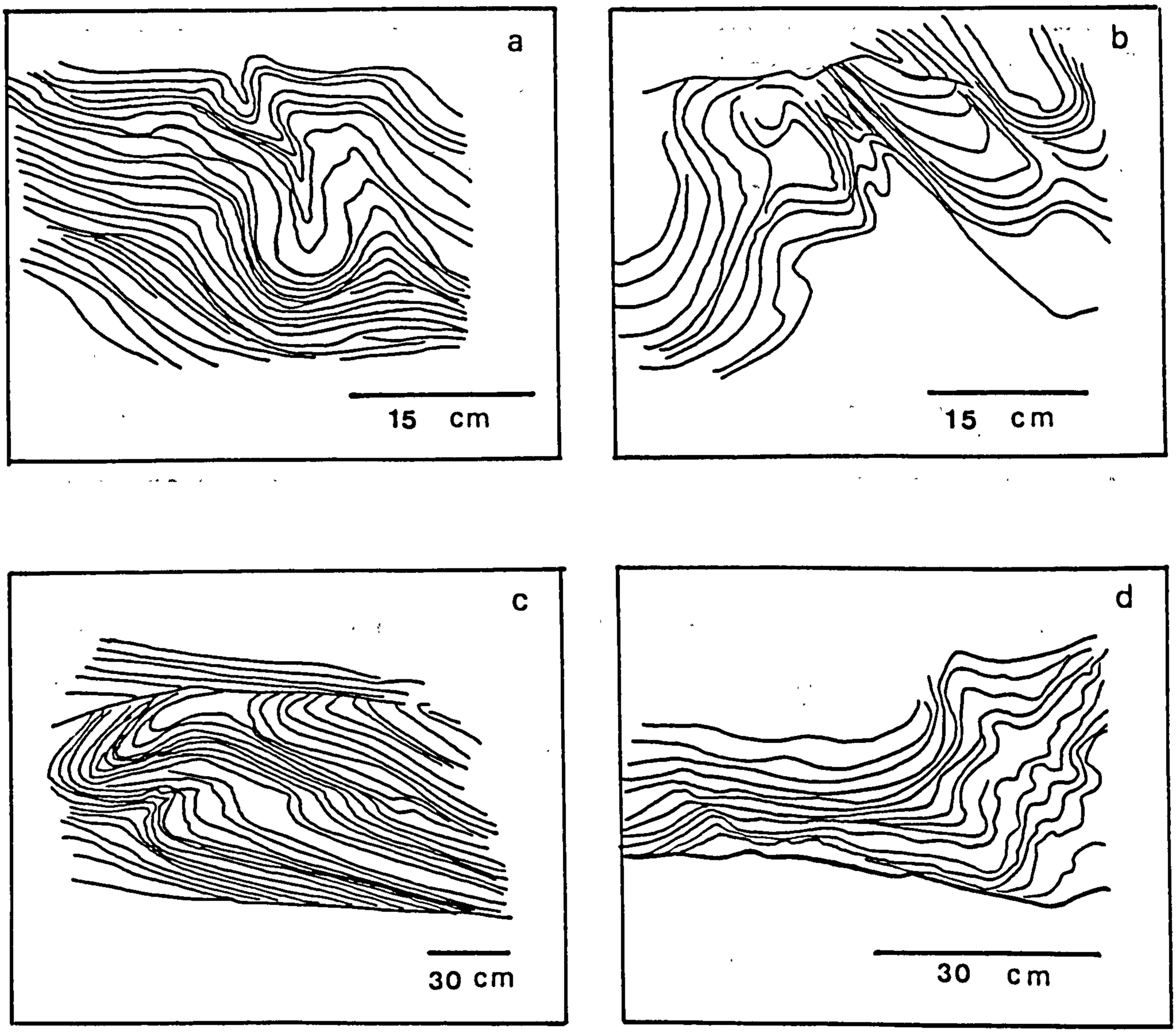

Fig. 3.14. Complex recumbent folding and deformation: (a) multi - folded cross - set forming a series of synclinal and anticlinal folds, with a diapiric - like structure. (B) Buckled cross - set with diapiric - like structure. (C) Trifold in which the upper part of the cross - set is truncated while the lower part is tangential. (d) Highly contorted cross - set, at section 8, (a, b and c) at section 3, (drawn from photographs).

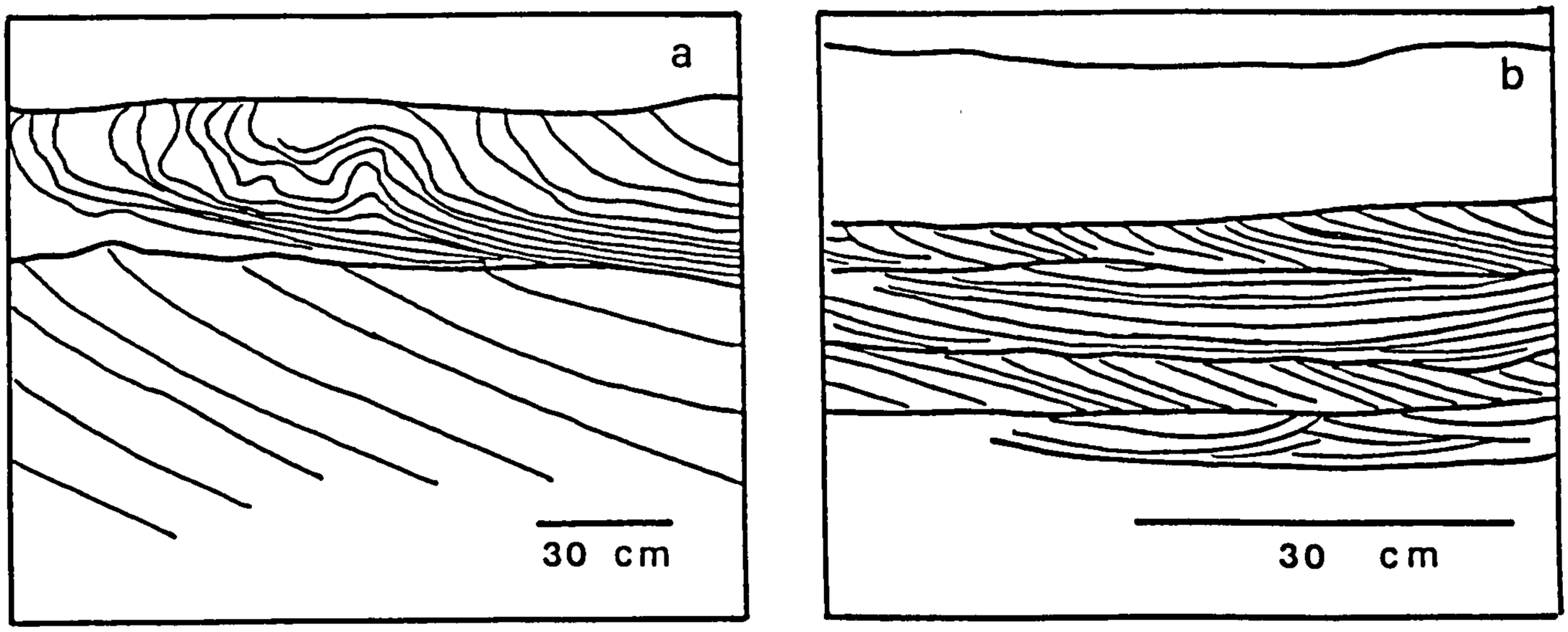

Fig. 3.15. (a) Overturned cross - bed with a clear diapiric like structure, penetrating upward, at section 5. (b) Truncated cross - beds, at section 5, (drawn from photographs).

iii) Multifold : In this type a cross - bedded set is highly deformed to produce a series of synclinal and anticlinal folds, usually starting with a synclinal fold (Figs. 3.13 c, d; 3.14 a) while a major part of the anticlinal crest is eroded (Figs. 3.13 c,d; 3.14 a).

3.4.3 BUCKLED AND CONVOLUTED CROSS - BEDDING

This type is restricted to the severely deformed cross - beds, and is marked by the presence of numerous folds, usually differing in shape, size and attitude of the axial plane. The bottomsets are usually wrinkled but still tangential in most cases whilst the topsets are usually truncated. The lamination in the upper part of the bed may be blurred. A clear diapiric intrusion penetrating upward from a contorted zone can be seen in Figs. 3.13 c,d; 3.14 a,b; 3.15 a. The deformed unit is usually bounded by an upper and lower horizontal surface (Fig. 3.14 b,d; Plates 3.24, 3.25).

3.4.4 INTERPRETATION OF THE DEFORMED CROSS - BEDS

Deformation of sediments occurs either contemporaneous with or closely following deposition, while the sediments remain water saturated (Mills, 1983). Deformation structures occur generally in coarse - silt to fine - sand size ranges. The determination of optimum grain size condition does not exclude deformation of deposits of other

grain sizes (Mills, 1983).

The primary mechanisms responsible for soft - sediment deformation include (1) liquefaction or fluidisation, (2) reverse density gradation, (3) slope failure or slumping, and (4) shear stress (Blatt et al.,1980). Other mechanisms capable of inducing liquefaction in a subaqueous cross - bedded sand are tidal stage changes (Bjerrum, 1971), compaction of underlying sediments, slumping and cyclic loading from waves and currents (Lowe, 1976; Turner, 1981). Williams (1971) considered the high water table as an extra condition necessary for the production of bedding disturbances by current drag, preferably when the water table (local or regional) is combined with upward or laterally seeping ground - water. With such conditions, quicksands may occur and bed stability is reduced. The cause of "spontaneous" rapid water loss was attributed primarily to cyclic, concentrated earthquake shocks (Seed, 1968), but may also occur as the result of rapid rates of deposition (Lowe and LoPiccolo, 1974) or altered groundwater movement (Selley, 1969).

Liquefaction and fluidisation are related processes that account for several deformation features. The primary force is vertical gravitational compaction expressed on low cohesive, metastable sands with excess pore - pressure. Both liquefaction and fluidisation represent the breakdown of the grain supported framework of under consolidated sands (Allen and Banks, 1972). Liquefaction occurs when metastable, loosely packed grains are shaken apart from one another by

a generated stress. The excess pore pressure establishes a fluid - supported matrix (Terzaghi, 1956; Seed, 1968). During liquefaction, there is a net movement of sediment particles downward and pore fluid upward until grain stability and hydrostatic pressure are in equilibrium. Fluidisation occurs when there is rapid dewatering. The upward rush of escaping water produces a fluid drag on the sediment particles equal to or greater than the downward gravitational force resulting in a temporary state of equilibrium or upward movement of sediment particles (Selley and Shearman, 1962). In liquefaction the fluid source generally is considered to be within the sand body, whereas the source of fluids in fluidisation may be intraformational or from underlying sediments. Both processes produce slurries, but liquefaction occurs homogeneously throughout the bed, whereas fluidisation is more brief and local, with fluid movement restricted to vertical pipes or conduits (Brenchley and Newall, 1977).

Within this sandy facies, the deformation sructures range from simple recumbent folds, through complex multifolds to buckled and diapiric - like structures. Recumbent - folded deformed cross - bedding has been reported from sediments and rocks of many different ages and geographical localities. A comprehensive list of reports is given by Allen and Banks (1972). The type marked by recumbent folds is interpreted as due to the deformation of a liquefied sand by current drag. The cause of liquefaction is generally thought to be an earth - quake shock (Allen and Banks, 1972).

Penencontemporaneous deformation of cross - bedded units into recumbent folds generally has been attributed to current drag on top of the cross - bedded unit. It has been proposed that a sand - laden current would be required to produce a frictional force, strong enough to deform the bedding (Robson, 1956; McKee, 1962 a, 1962 b; Selley 1963; Stewart, 1964; Rust, 1978; Selley 1969; Banks et al., 1971; Allen and Banks, 1972; Hendry and Stauffer, 1975, 1977; Doe and Dott, 1980, and Turner, 1981).

Allen and Banks (1972) have argued that liquefaction of sediment is required for the deformation of cross - bedding, and as liquefaction of sands is common as a result of seismic shocks during earthquakes (Seed, 1968) they suggest that the distribution of recumbent - folded deformed cross - bedding in time and space could indicate earthquake activity in the past. Hendry and Stauffer (1975) have described the same structures from the Pleistocene Floral Formation near Saskatoon, where earthquake - induced liquefaction was not common as the Saskatoon area is relatively inactive seismically. They have argued that the folding was caused by frictional drag as a result of the passage of a mass of saturated sand over the surface of the cross - bedded sand.

In a series of experiments McKee et al. (1962)concluded that the dominant mechanism for the development of recumbent folding involved lateral drag of a flowing sediment - rich fluid mass over water - saturated sand. They also concluded that the form of the recumbent

shear folds produced were related to the speed and duration of the overriding shearing sediment flow. Rapid flows that were of longer duration produced V - shaped fold axes, while slow flows of short duration produced rounded fold axes.

Evidence from associated current structures indicates that for many beds, the orientation of the fold axes is normal to the palaeocurrents with folds overturned predominantly in the downcurrent direction. This situation suggests strongly that the deformation was caused by the shear stress exerted on the bed by the current itself (Blatt et al., 1980).

Allen and Banks (1972) also suggested that deformed cross - bedding is chiefly a fluvial phenomenon. But Doe and Dott (1966), and Hendry and Stauffer (1975, 1977) have reported deformed cross - bedded sediments representing a variety of environments. Mills (1983) indicated that the development of deformed cross - beds in a range of environments reduces their diagnostic value as indicators of specific environments of deposition.

The amount of the deformation produced should be proportional to the amount of time that the sand remains liquefied, therefore, the greatest deformation is to be expected near the centre of the liquefied zone and the least deformation at its margins (Doe and Dott, 1980). Typically, the amplitude of the contortions decreases from mid - unit upward, until the upper surface is laminated and planar. Kuenen (1953) attributed the

parallel surface feature to waning currents, with return to normal depositional conditions. Deformational depressions are filled and parallel cross - lamination reestablished. Sanders (1960) accounted for the planar surface by suggesting a fluctating velocity regime. The transition from contorted laminae to parallel laminae reflects an abrupt jump from lower flow regime to upper flow regime conditions. With upper flow regime conditions bed shear is increased, contemporaneously eroding the depositional surfaces. The overlying normally cross - laminated sediments indicate return to lower flow regime.

On the basis of the different types of recumbent folds present in these rocks, and their relative downcurrent orientation, it could be suggested that these overturned structures were formed in liquefied sand units, by the action of sediment - laden current drag on the top of the cross - beds. The liquefaction state could be produced seismically as a result of the Caledonian movement which had a profound affect on the Cambrian and other Lower Palaeozoic sediments.

Plate 3. 1. General view showing a vertical sequence of the different rocks under study. Upper Cambrian, Permo - Triassic (Um Irna Formation) and Lower Triassic (Ma'in Formation). The total vertical section in the picture is more than 115 m. Section 6.

Plate 3. 2. General view showing the contact (arrow) between the Middle Cambrian (fine sediments) and the Upper Cambrian (compact sandstones), in the area between Wadi Himara and Wadi Zarqa Ma'in.

Plate. 3. 3. General view showing a vertical section of the Upper Cambrian succession at section 5. The sandy facies is brownish and the heterolithic facies is maroon coloured. The total thickness within the picture is nearly 30 metres. Section 5.

Plate 3. 4. Sharp planar contact separating the heterolithic facies below from the sandy facies above. Upper Cambrian, section 5 (hammer is 30 cm long).

Plate 3.07. Small - scale trough cross - bedding resting on and overlain by massive sandstones in the quartzarenite facies of the Upper Cambrian at section 5. View parallel to the direction of current (hammer is 30 cm long).

Plate 3. 8. Thick bedded quartzarenites of the Upper Cambrian. Beds are separated by erosional surface (at hammer), section 5, (hammer is 30 cm long).

Plate 3. 9. Sandy unit of the Upper Cambrian, in which the lower part is composed of friable parallel laminated sandy, silty shale. The upper part is composed of compact, trough cross - bedded locally overturned sandstone, current direction is to the left. Section 3, (hammer is 30 cm long).

Plate 3.10. Planar tabular cross - bedded set (at hammer) interbedded within heterolithic facies of the Upper Cambrian. View is parallel to the current direction (left to right) section 8, (hammer is 30 cm long).

Plate 3.11. The uppermost interval of the heterolithic facies of the Upper Cambrian, composed of siltstone, conglomerate lenses and sand - stone. Section 3, (hammer is 30 cm long).

Plate .3.12. Large sandstone pillows within a deep maroon mudstone. The sand layer is broken up into isolated pillows, some of them showing deformation structures. Note that the structure is confined to a specific bed, and it is laterally persistent. Heterolithic facies, Upper Cambrian, section 3, (hammer is 30 cm long).

Plate 3.13. Ball - and - pillow structure and bottom irregularities in sandstone bed ascribed to load casting in interbedded sandstone and shale. Note the predominance of down - facing convexities and the lateral persistence of the deformed layer. Heterolithic facies, Upper Cambrian, section 3, (hammer is 30 cm long).

Plate 3.14. Bedding surface showing sinuous crested - ripples. Note silty shale lamination (to the left) in the heterolithic facies of the Upper Cambrian at section 3, (hammer is 30 cm long).

Plate 3.15. Bedding surface showing bivalve?fossils and bioturbation in a silty shale unit of the heterolithic facies, Upper Cambrian, section 5, (pen is 15 cm long).

Plate 3.16. Thin sandy and silty shale beds of the heterolithic facies, Upper Cambrian, showing the following sedimentary structures; small -,medium - and large - scale ripple marks, cross - lamination, wavy bedding surfaces and load structures. Section 5, (hammer is 30 cm long).

Plate 3.17. Thin rippled beds and laminations of sandy, silty and clayey components comprising part of the heterolithic facies. Note the clay draped ripples and the dissected behaviour of lenses and ripples. Some ripples suggest that they have been piled up and completely rotated (below the pen). Upper Cambrian, section 5, (pen is 15 cm long).

Plate 3.18. Overturned cross - bed forming simple recumbent fold with completely overturned limbs. The fold nose is near to the upper surface. Quartzarenite facies, Upper Cambrian, section 5, (hammer is 30 cm long).

Plate 3.19. Overturned cross - beds forming simple recumbent folds with completely overturned limbs and fold nose near the lower surface. Quartzarenite facies, Upper Cambrian, section 3, (hammer is 30 cm long).

Plate 3.20. Overturned cross - bedding, with a moderate steepening of the upper set to form asymmetrical recumbent fold in which the hinge zone is located in the upper part. In the lower set (at hammer) the hinge zone is located in the middle part. Quartzarenite facies, Upper Cambrian, section 5, (hammer is 30 cm long).

Plate 3.21. S - shaped folds in which double overturning took place in a cross - set, to form a recumbent anticline above a recumbent syncline. Quartzarenite facies, Upper Cambrian, section 3, (hammer is 30 cm long).

Plate 3.22. Vertical section showing the contact (arrow) between the Upper Cambrian and the Permo - Triassic (Um Irna Formation). Note the differenc in colour, cross - bedding and weathering surface. Section 3, (hammer is 30 cm long).

Plate 3.23. Close up of plate 3.22 showing the deformed cross - bedding of the Upper Cambrian, section 3, (hammer is 30 cm long).

Plate 3.24. Contorted lamination in medium - grained sandstone indicating hydroplasticity during deformation. In the lower part the foresets are tangential, but truncated sharply at top by a planar surface. Quartzarenite facies, Upper Cambrian, section 5, (hammer is 30 cm long).

Plate 3.25. Contorted and crumpled cross - set with tangential base and truncated top. Note the undisturbed layers above and below. Quartzarenite facies, Upper Cambrian, section 5, (hammer is 30 cm long).

CHAPTER FOUR

THE PERMO - TRIASSIC (UM IRNA FORMATION)

SEDIMENTARY SUCCESSION AND FACIES

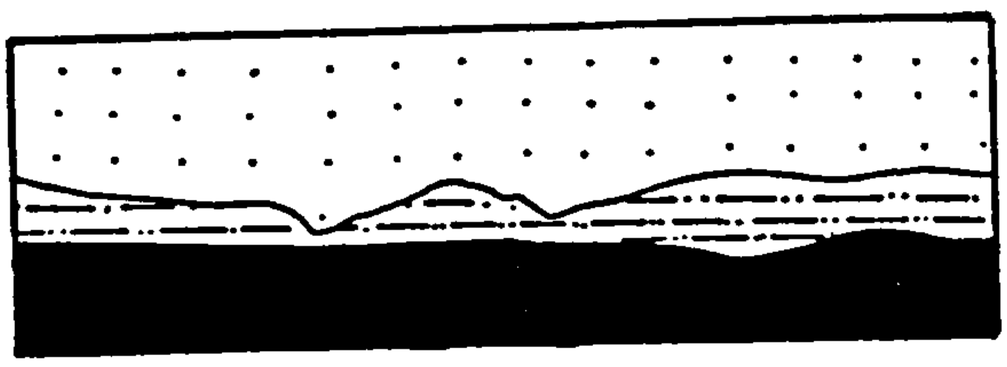

Section 6

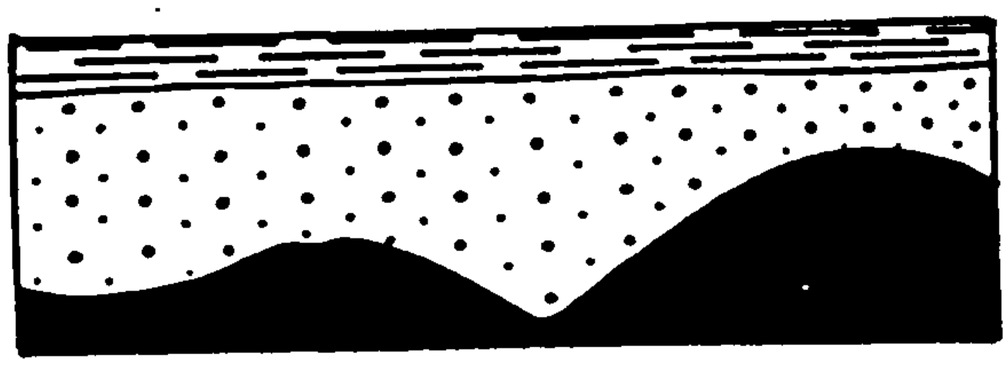

Section 12

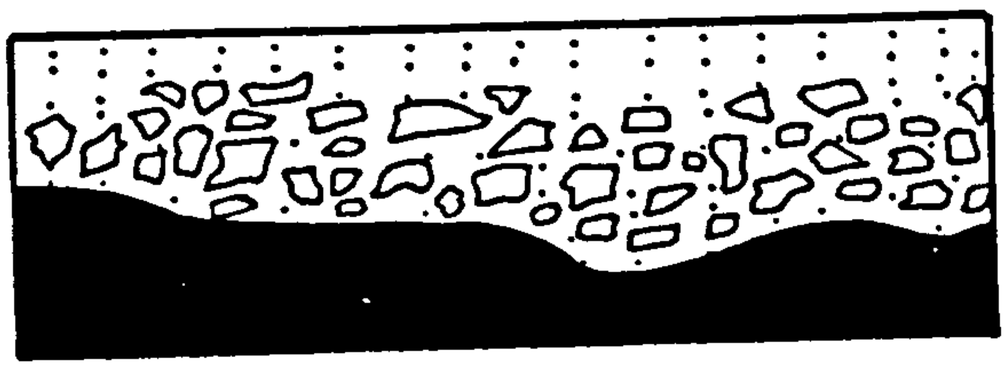

Section 13

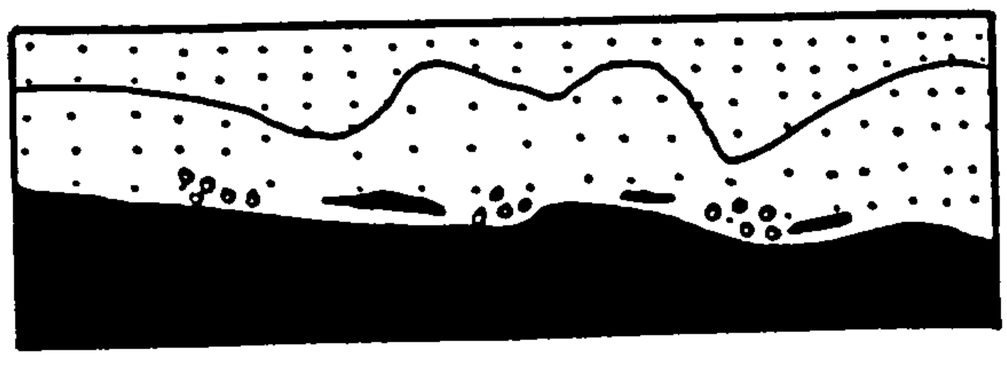

Section 9

Sandstone

Pebbles&Mudclasts

Sandclasts

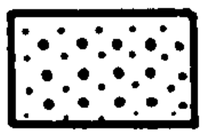

Pisolitic Sandstone

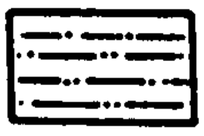

Silty shale

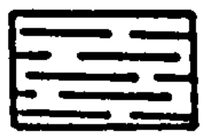

Carbonaceous shale

Cambrian sandstone

Fig. 4. 1. Contact types between the Upper Cambrian and the Permo - Triassic sandstones at different sections.

pebbles locally concentrated into scour pockets. This sandy bed is cut into another erosional surface with high relief of up to 1 m, overlain by similar material.

The sandstones differ from those in the underlying Cambrian in their finer grain size, darker chocolate - brown colour, more thinly bedded nature and less abundant cross - bedding (Table 4. 1, 4. 2).

Lithostratigraphically the Um Irna Formation can be devided into a lower and upper member according to grain size and the ratio of sandstone to siltstone and shale (Figs. 4. 2, 4. 3).

4.2 SEDIMENTARY FACIES

The Um Irna Formation can be divided into two sedimentary facies, each facies being characterised by a particular association of rock types and sedimentary structures. These facies, which correspond to the informally designated lower and upper members of the formation,are shown in Fig. 4. 3.

4.2.1 Facies (1) - Lower Member

I Description

This facies occurs in the lower part of the Um Irna Formation where it consists of about 10 m of interbedded sandstone and subordinate

	Upper Member of the Um Irna	Upper Cambrian
1	Sandstone with high pebble content.	Less pebble content.
2	Fining-upwards sequences are well defined.	Fining-upward sequences are not well defined.
3	Pebbly sandstones are very thick bedded.	Sandstones are medium to thick bedded.
4	Lenticular forms are well developed.	Sheet - like forms are well developed.
5	Trough cross - beds are undeformed.	Trough cross - beds are highly deformed.
6	The ratio of fine sediments to coarse sediments is higher.	The ratio of coarse sediments to fine sediments is higher.
7	Pisolitic iron oxides are abundant.	Pisolites are lacking.
8	Lag deposits are common.	Lag deposits are rare.
9	Fine material is unfossiliferous and structureless.	Fine material is fossiliferous and rippled.

Table 4. 2. Differences between the Upper Member of Um Irna Formation and the Upper Cambrian.

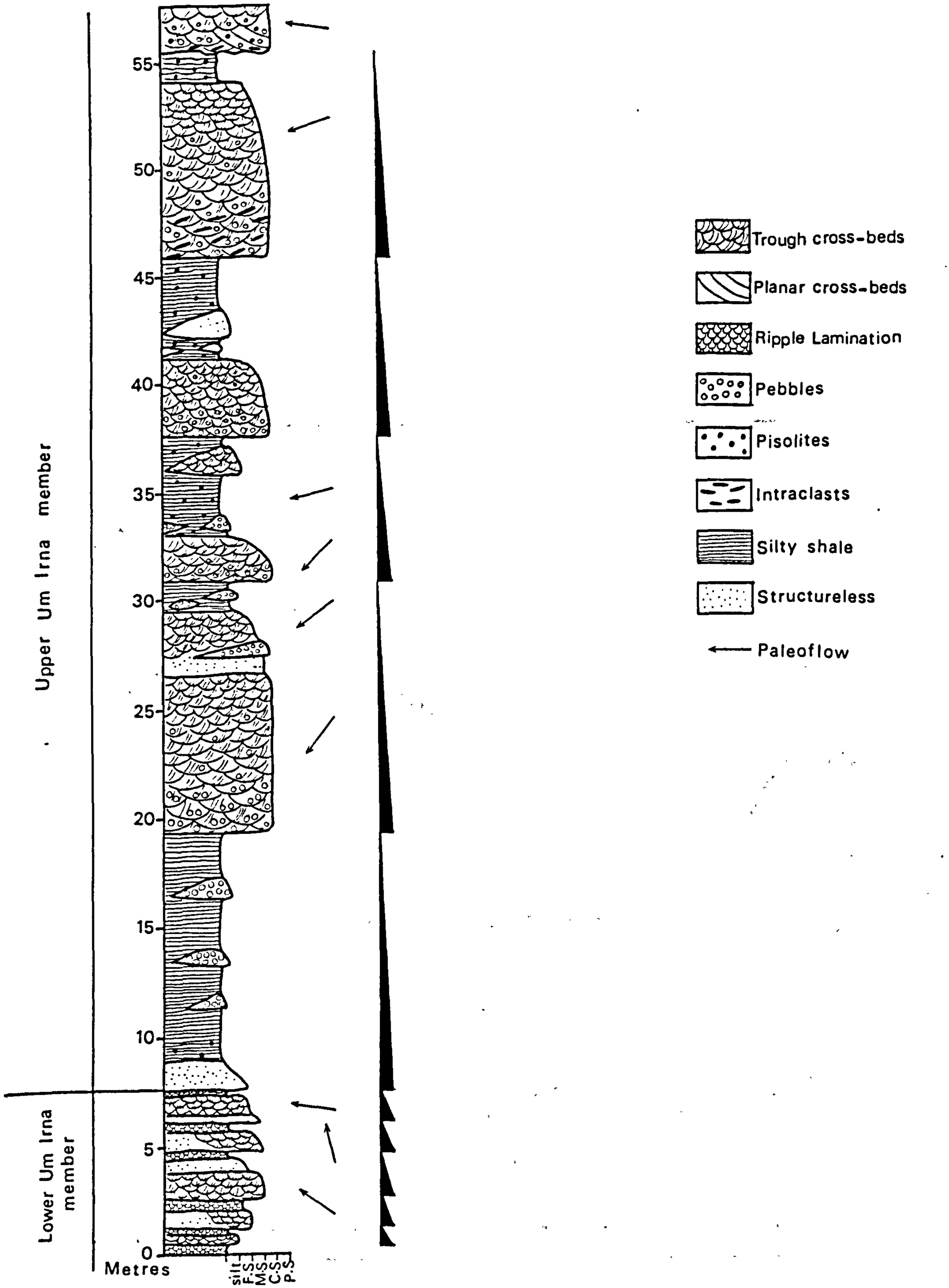

Fig. 4. 2. Vertical section through the Um Irna Formation at section 6.

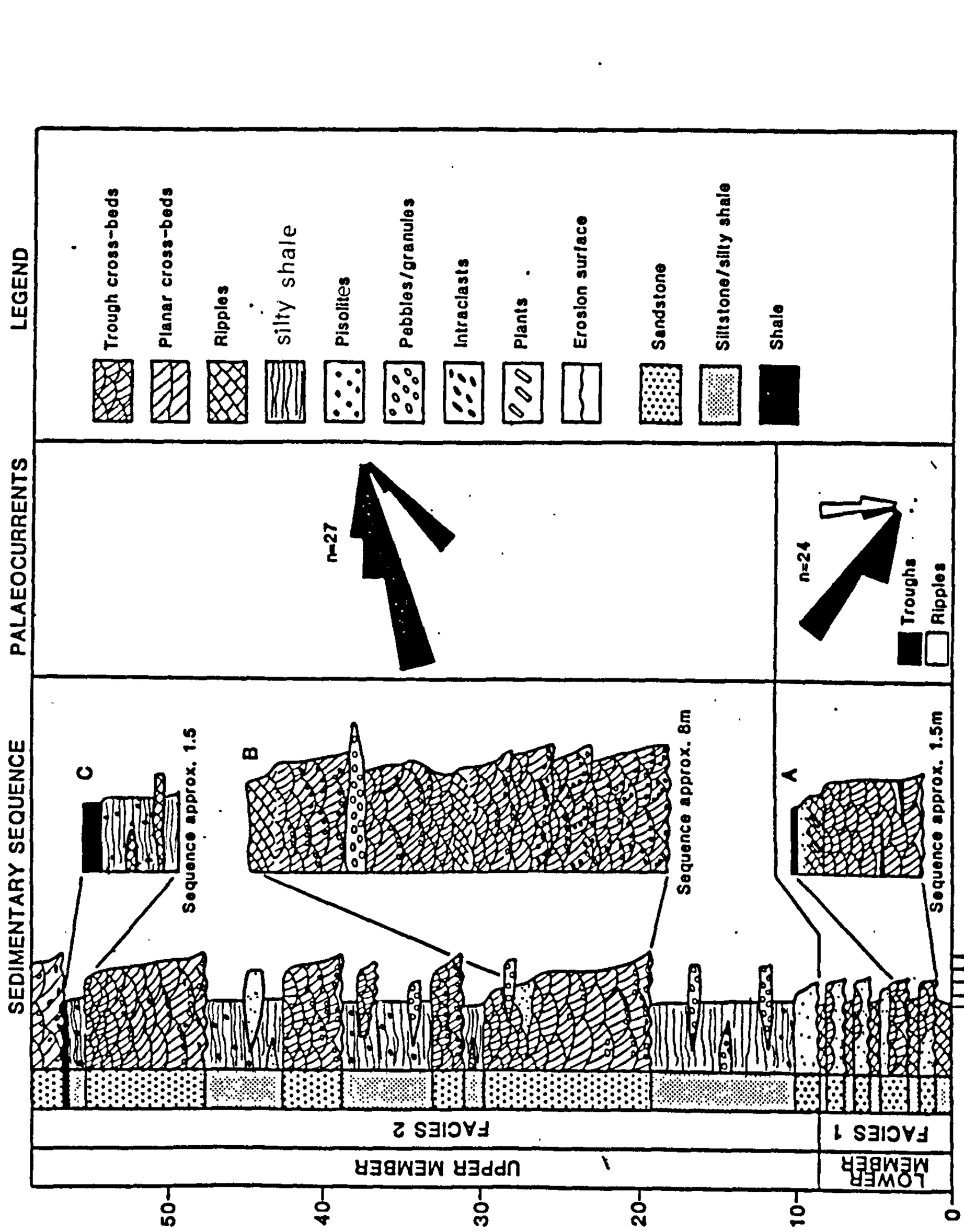

Fig. 4.3. Measured section through the Um Irna Formation at section 6 showing fining upward sequences and palaeocurrent roses (see Fig. 1.07 for location).

siltstone and silty - shale arranged in up to five fining-upward sequences (Fig. 4. 3, 4. 4). Each sequence comprises a lower erosion surface overlain by tabular to lenticular sandstone units from 0·75 to 2·15 m thick, passing vertically and laterally into siltstone and silty - shale (Plates 4. 2, 4. 3). The sandstones are moderately well sorted quartzarenites, which weather from a white and pale yellow colour to a distinctive chocolate - brown. Individual units exhibit a fining - upward grain size trend from coarse - grained at the base with rare subrounded quartz granules, to medium and fine - grained at the top. A few local shaly lenses occur in some sandstones, but intraclasts are generally lacking.

Sedimentary structures in the arenites in the lowermost part of the facies are poorly developed and consist of a few small (<10 cm thick) trough cross - beds with occasional ripple cross - lamination. Higher up sedimentary structures become more abundant and comprise mainly trough cross - bedding, which shows an upward decrease in set thickness from about 20 cm to 5 cm, concomitant with a similar decrease in grain , size. Ripple cross - lamination occurs in the upper, finer grained part of the sandstone units, with the steeper lee face inclined towards the north - northwest. Azimuths of trough foresets indicate transport direction towards the west - northwest, with a spread of about 50° (Fig. 4. 3).

The fine - grained sandstones pass gradationally upwards into

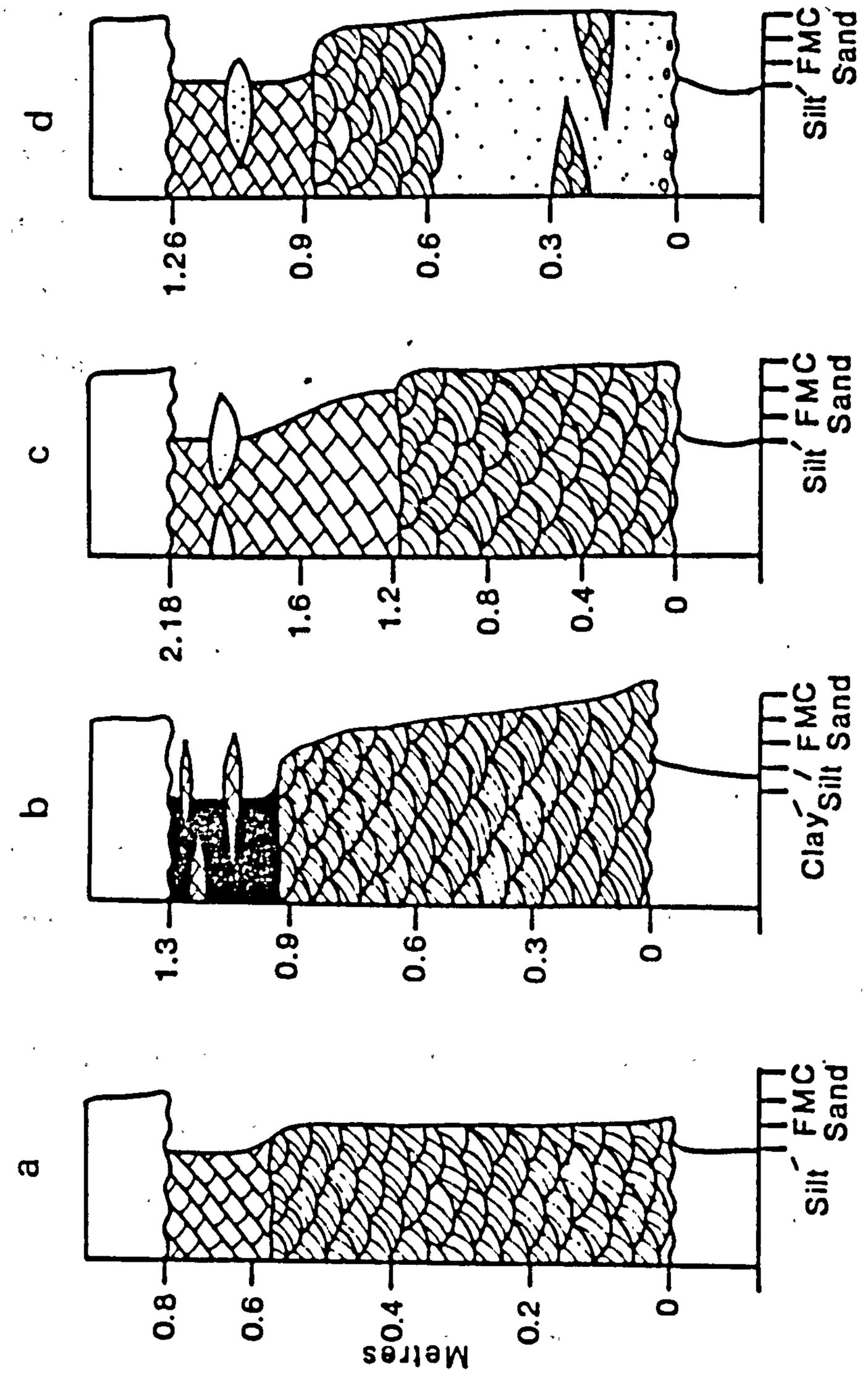

Fig. 4. 4. Vertical sequences of the Lower Member of the Um Irna Formation at section 6 (see Fig. 4. 3 for location and Fig. 4. 7 for legend).

maroon to grey rippled siltstone and silty - shale, with subordinate green mudstone, forming laterally impersistant beds up to 35 cm thick, truncated by erosively - based sandstones. The siltstones and silty - shales are darker and more carbonaceous in character in the lower part of the facies. They contain small carbonaceous plant fragments, commonly surrounded by greenish grey reduction haloes. Fine - grained sandstone lenses occur within the siltstone and silty - shale (Plate 4. 9), which also contain iron oxide concretions (pisoliths) at one locality (Wadi Abu Khusheiba) where they directly overlie paler coloured Cambrian sediments.

II Interpretation

The general characteristics of the erosively - based fining - upward sequences are consistent with the scouring and filling of fluvial channels (Allen, 1965; Miall, 1977). The consistently simple internal structure of the sand bodies and their fining - upward grain size trend suggests that they were deposited under steadily decelerating flow conditions during a single flood event (Fig. 4. 4). There is no evidence such as rapid variations in texture, sedimentary structures and the presence of internal scour features to indicate any significant fluctuations in discharge as deposition proceeded. The lack of intraclasts above erosion surfaces may be attributed to two factors; the sandy incoherent nature of the channel bed and banks and the low bed shear stress conditions prevailing during deposition. These

conditions favour the development of dune and ripple bedforms rather than upper phase plane beds (horizontal lamination), despite the shallow flow depths and fine grain size of the sands (Allen, 1982). The dominance of trough cross - bedding reflects the widespread development of curved, discontinuously - crested three dimensional dune bedforms at nearly all stages of flow, migrating down the floor of the channels. These were followed by ripple bedforms at lower stage flow.

The siltstones, silty - shale and mudstones probably represent low stage accretion processes and overbank sedimentation (Miall, 1977). Bandel and Khoury (1981) report the presence of desiccation cracks in the finer lithologies indicating periodic exposure and drying out of the depositional surface, following these short - lived flood events. Judging by the thickness of the preserved sediment fill, the channels were at least 3 m deep, and probably a few tens of metres wide. The scale of the channels and lateral persistence of the sandy-fill compare closely with many low sinuosity channel deposits, which may form internally graded sheet sands, in response to shifting of the channel complex across the alluvial plain (Kessler, 1971; Campbell,1976). The vertical and lateral relationship between the sandstone and the siltstone and silty - shale in the sequences show the effect of this multilateral and multistorey channeling.

The facies is interpreted to be a result of deposition by shallow, low sinuosity sand bed channels draining the distal reaches of a low

gradient alluvial plain, which probably extended northwards into a shallow marginal marine environment (Bandel and Khoury, 1981). Because of the lack of any significant suspension fines, deep channeling and the development of extensive areas of overbank sedimentation more typical of perennial , meandering streams were precluded. The presence of some carbonaceous plant material and locally developed ferruginous concretions interpreted as pedogenically produced pisoliths, together with the absence of calcrete argues for a warm, but seasonally wet climate (Blatt et al., 1980; Bown and Kraus, 1981).

4.2.2 Facies (2) - Upper Member

I Description

This facies corresponds to the upper member of the Um Irna Formation, and consists of a 50 m thick sequence of sandstone, siltstone and silty - shale (Fig. 4..5). The boundary between these sediments and those of the underlying facies is conformable and defined by the presence of abundant ferruginous concretions (pisoliths) (Plate 4. 2). The upper contact of the facies (Plate 4.)1) is marked by extensive bioturbation typical of the overlying Ma'in Formation (Bandel and Khoury, 1981).

The succession is composed of five, well defined fining - upward sequences from 4 to 14·5 m thick (Fig. 4. 2, 4. 3). Individual

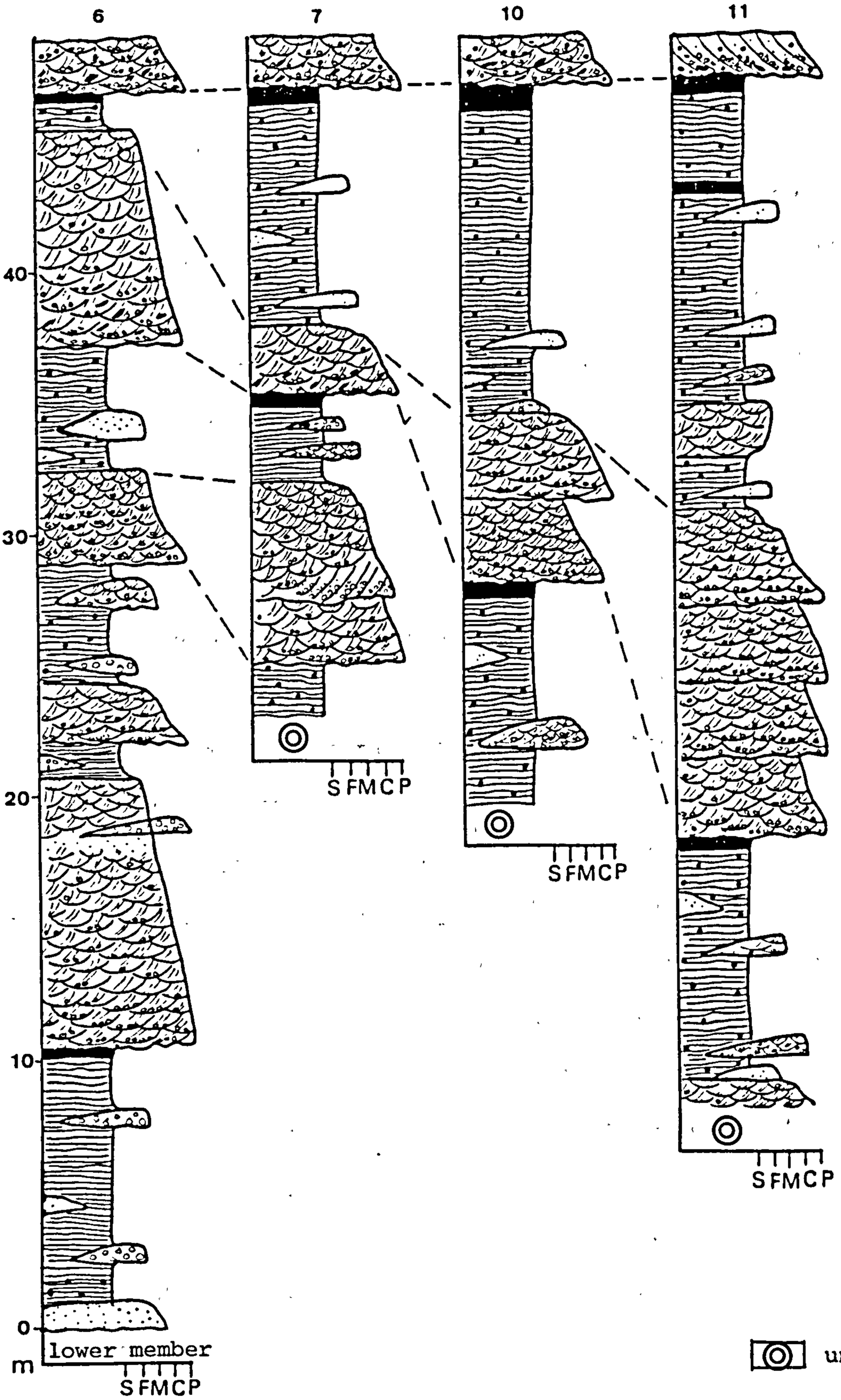

Fig. 4.15. Measured sections of the Upper Member (Um Irna Formation) at four localities. Correlation of the sections between localities illustrates lateral changes in facies and thickness. The datum used is the uppermost pebbly bed recognisable in all sections (see Fig. 1. 7 for locations and Fig. 4. 2 for legend), dashed lines represent the uppermost fining upward sequence.

sequences comprise an erosionally based coarse pebbly sandstone grading up through medium and fine - grained sandstone into siltstone and silty - shale (Fig. 4.6). Within these sequences the coarse pebbly sandstones show a discernable increase in the size and abundance of pebbles towards the top of the succession (Plate 4.14). The pebbles are generally less than 3 cm in diameter, and composed mainly of subrounded to subangular vein quartz with minor amounts of jasper and chert.

The sandstones are similar in colour to those in Facies I. However, they are more poorly sorted and locally feldspathic, cont - aining subangular grains and granules of pale pink feldspar. Individual sandstones are tabular and laterally persistent, internally complex units up to 6 m thick, composed of lenticular interbeds of pebble conglomerate, coarse pebbly or granular sandstone and medium to fine grained sandstones. The lenticular interbeds have sharp, irregular boundaries and frequently exhibit fining - upward grain size trends (Fig. 4.12). The coarser grained sandstones contain trough cross - bedding arranged in erosively - bounded cosets (Plates 4.15, 4. 6). Within cosets individual sets show an upward decrease in set thickness from about 70 cm to 10 cm, concomitant with a similar decrease in grain size. Rare coarsening - upward trends from coarse sandstone to coarse pebbly sandstone, accompanied by a similar increase in cross-bedding set thickness (from 6 cm to 20 cm), have been recognised in some cosets. Intercalated with the smaller troughs near the base of

	Upper Member	Lower Member
1	Thick to very thick bedded, with major variation in thickness laterally.	Thin bedded, lenticular, shows pinch and swell structure.
2	Pebbly sandstones with large - scale trough cross - beds, decreasing in size and thickness upward.	Medium to coarse - grained sandstones with small - scale trough cross beds.
3	Five very thick sequences fining-upwards.	Five thin sequences fining-upwards.
4	Several sequences fining-upwards within a major fining-upward sequence.	Absence of such features.
5	Silty shales are structureless and pisolitic.	Silty shales are rippled and locally pisolitic.
6	Much lower ratio of coarse to fine material	Much higher ratio of coarse to fine material.
7	Several carbonaceous horizons.	Only one carbonaceous horizon.
8	Pebbles and mudclasts are abundant within the coarse material.	Pebbles and mudclasts are very rare and quartz granules are sparse.

Table 4. 3. Comparison of petrographiccharacteristics of Upper Member and Lower Member of Um Irna Formation (see Fig. 4.11).

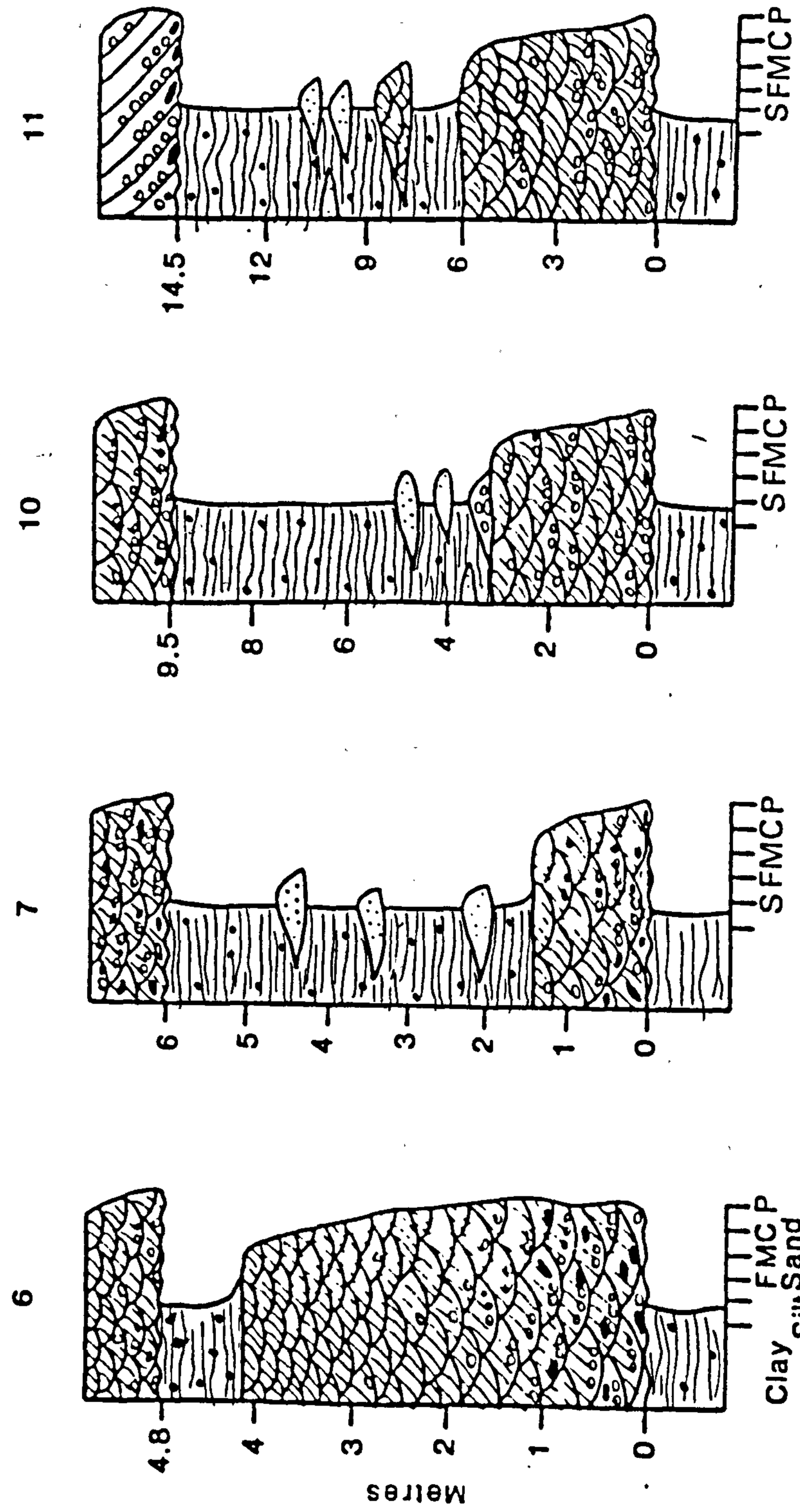

Fig. 4.6. Vertical sequences of the Upper Member of the Um Irna Formation at different localities (see Fig. 1. 7 for location and Fig. 4. 2 for legend).

these coarsening - upward cosets are thin (< 15 cm) rippled horizons. Trough foresets are internally graded and sharply defined with small pebbles and granules commonly concentrated along the base of foresets and trough sets (Plates 4. 7, 4. 8). They are also scattered throughout the coarser sandstones and concentrated into thin pebbly lenses and stringers. The finer grained sandstone interbeds are normally rippled, and commonly wedge out along strike due to truncation by the erosive base of the coarser sandstone above. Foreset azimuths are uniformly directed towards the west - southwest (Figs. 4..3, 4..7).

The uppermost sandstone unit terminating the succession south of Wadi Zarqa Ma'in (section 11) pinches and swells laterally. It attains a maximum thickness of about 1·9 m with the lower erosion surface showing deep scour pits strewn with intraformational clasts. Internally the sandstone is structured by planar cross - bedding, arranged in cosets. Large mud clasts up to 20 cm in diameter, small quartz pebbles and ferruginous concretions are commonly associated with these cosets (Plate 4. 7).

The finer grained sandstones grade up into 1·3 to 11 m thick sequences of maroon and greenish - grey to black mottled siltstone and silty - shale containing occasional thin (<15 cm thick) shale beds. The siltstone and silty - shale units are laterally persistent and contain lenticular interbeds of coarse to fine-grained sandstone from 0·1 to 2 m thick. The sandstones have erosive bases overlain by

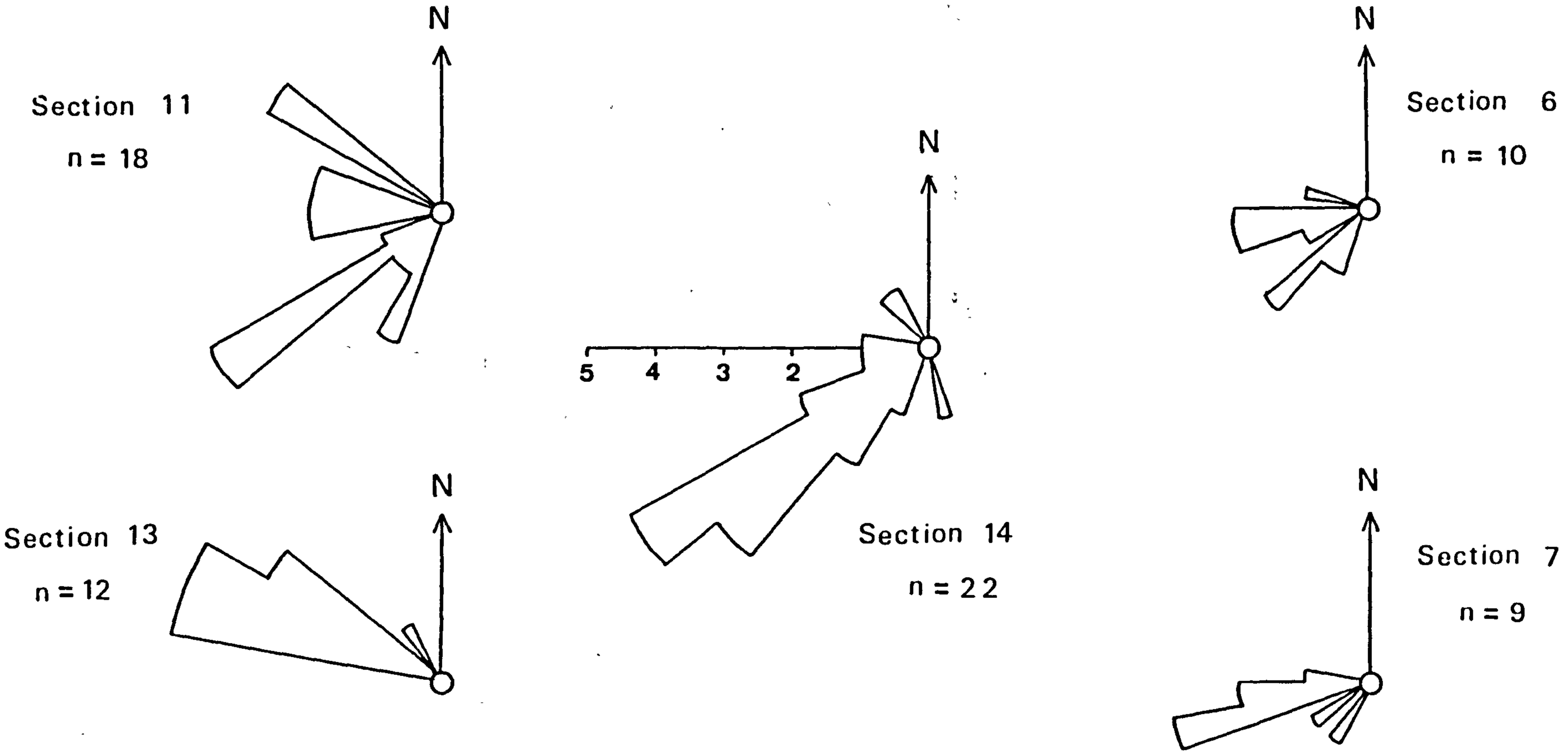

Fig. 4. 7. Cross - bedding rose diagrams for the Um Irna Formation at different localities. (See Fig. 1. 7 for location).

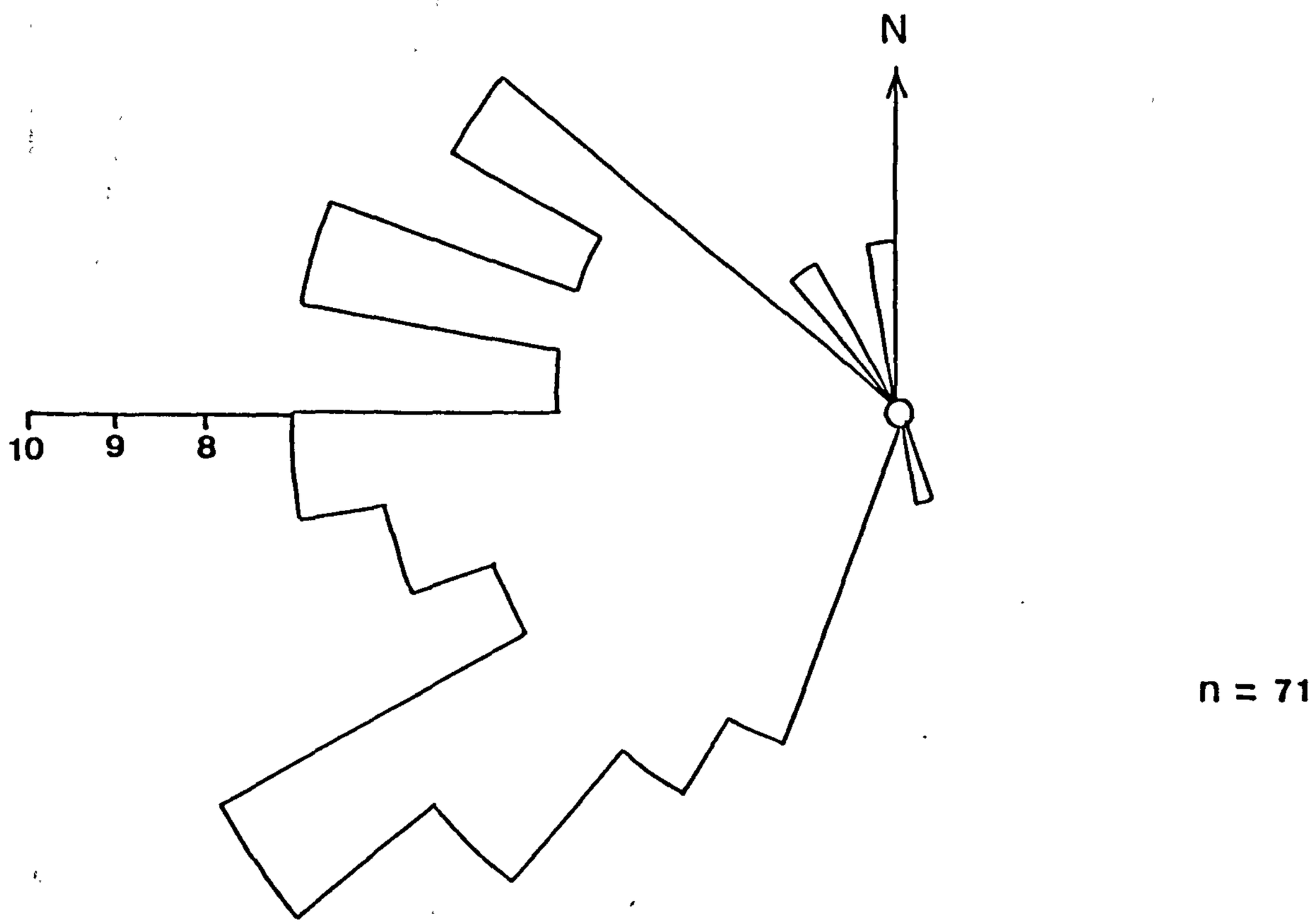

Fig. 4. 8. Cross - bedding rose diagram for the Um Irna Formation. The uppermost unit (Fig. 4g) is not included.

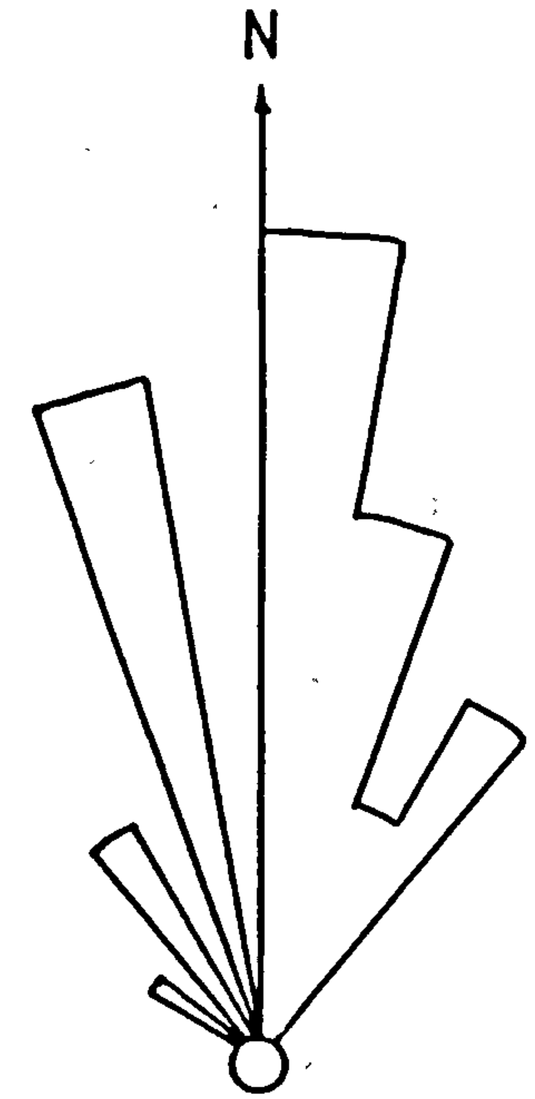

Intraclasts
n = 23

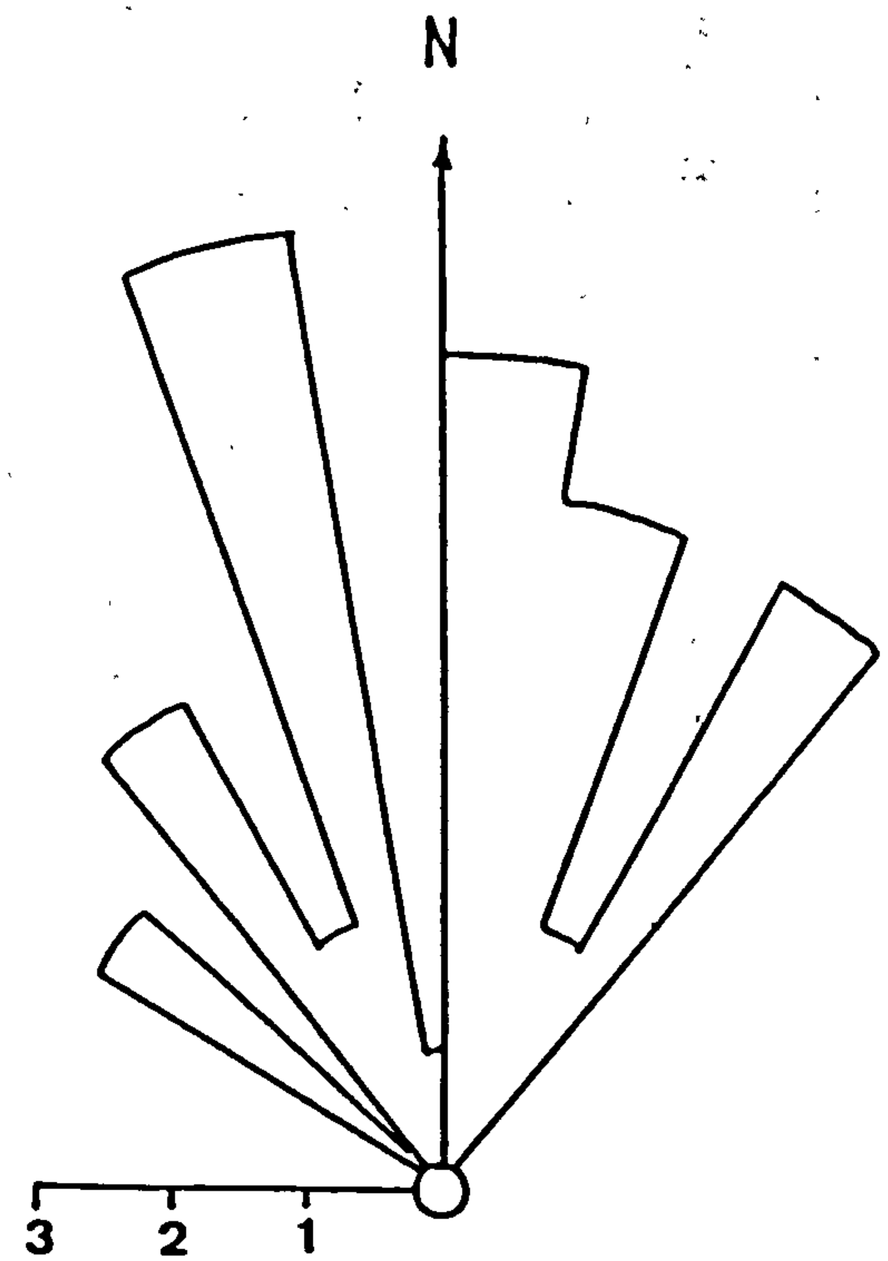

Composite
n = 37

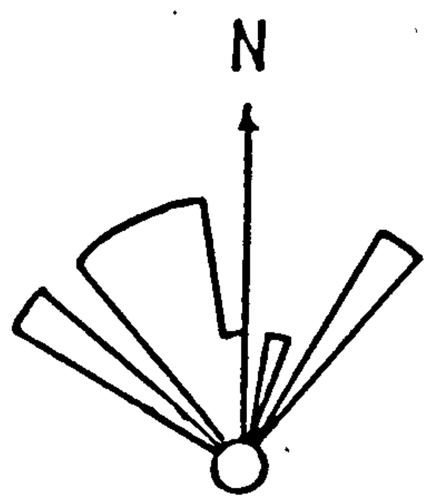

Cross – bedding
n = 12

Fig. 4.9. Palaeocurrent directions in the uppermost unit of the Um Irna Formation at section 7. (See Fig. 1.7 for location).

small (< 1 cm) intraclasts of siltstone and silty - shale, and are internally structured by small to medium - scale (15 to 30 cm in set thickness) trough cross - bedding and ripple cross - lamination. Some of the rippled - marked tops of these beds are draped with maroon mudstone. Up to four closely spaced sandstones were seen to thicken and merge proximally into a single, much thicker sandstone.

Sedimentary structures are generally lacking in the siltstone - silty shale units, except for a few ripples in the coarser siltstones. Near the top of section 11 south of Wadi Zarqa Ma'in a silty - shale unit is capped by a black, carbonaceous - rich fissile shale, containing small carbonaceous plant fragments and coaly stringers. This shale is overlain by up to three, stacked fining - upward sequences about 1.5 m thick, comprising an erosively - based coarse to medium - grained structureless sandstone grading up through siltstone and mottled maroon and greenish - grey silty - mudstone into mudstone at the top. These sequences are succeeded by the transitional sandstone at the base of the overlying Ma'in Formation (Bandel and Khoury, 1981).

A characteristic feature of the siltstone - silty shale unit is the presence of abundant ferruginous concretions (Plates 4. 7, 4. 9, 4.10). These tend to concentrate towards the top of the siltstone - silty shale units in the succession, and were referred to by Bandel and Khoury (1981) as iron oxide pisoliths. The concretions occur mainly as rounded to subrounded particles ranging from 2 to 25 mm in diameter

with a smooth outer surface. Some particles have fused together into larger concretionary aggregates up to 10 cm in diameter. In thin section two types of concretion can be recognised: those showing a well developed concentric structure (Plate 4.13), sometimes disrupted by micro - faulting, and those which lack any internal structure (Plate 4.14). X - ray diffraction analysis shows the concentric texture to be preserved by submicroscopic hematite and goethite crystallites (Appendix H.6). Fine to very coarse angular to subrounded quartz grains are enclosed within the concretions (Plate 4.17) with some of the grains fractured into a number of fragments (2 to 5) and then coated by iron oxide (Plate 4.18). Other pisoliths show lopsided inclusions (Plate 4.16). The concretions increase in overall abundance upwards through facies, together with a corresponding increase in bed thickness. The chemical analysis of four pisolith samples show a range of iron oxide content from 54·9 - 67·8% (Appendices D.1, E.1).

II Interpretation

The fining - upward sequences in this facies show characteristics of both meandering and braided stream deposits (Allen, 1965; Cant and Walker, 1976; Miall, 1977). The thickness of sandstone, dominance of trough cross - bedding and the high proportion of siltstone and silty-shale compare closely with the meandering stream model of Allen (1970) Fig. 4.10. In contrast to this the lateral persistence and variation in thickness of the sandstone, its coarse grain size and internally

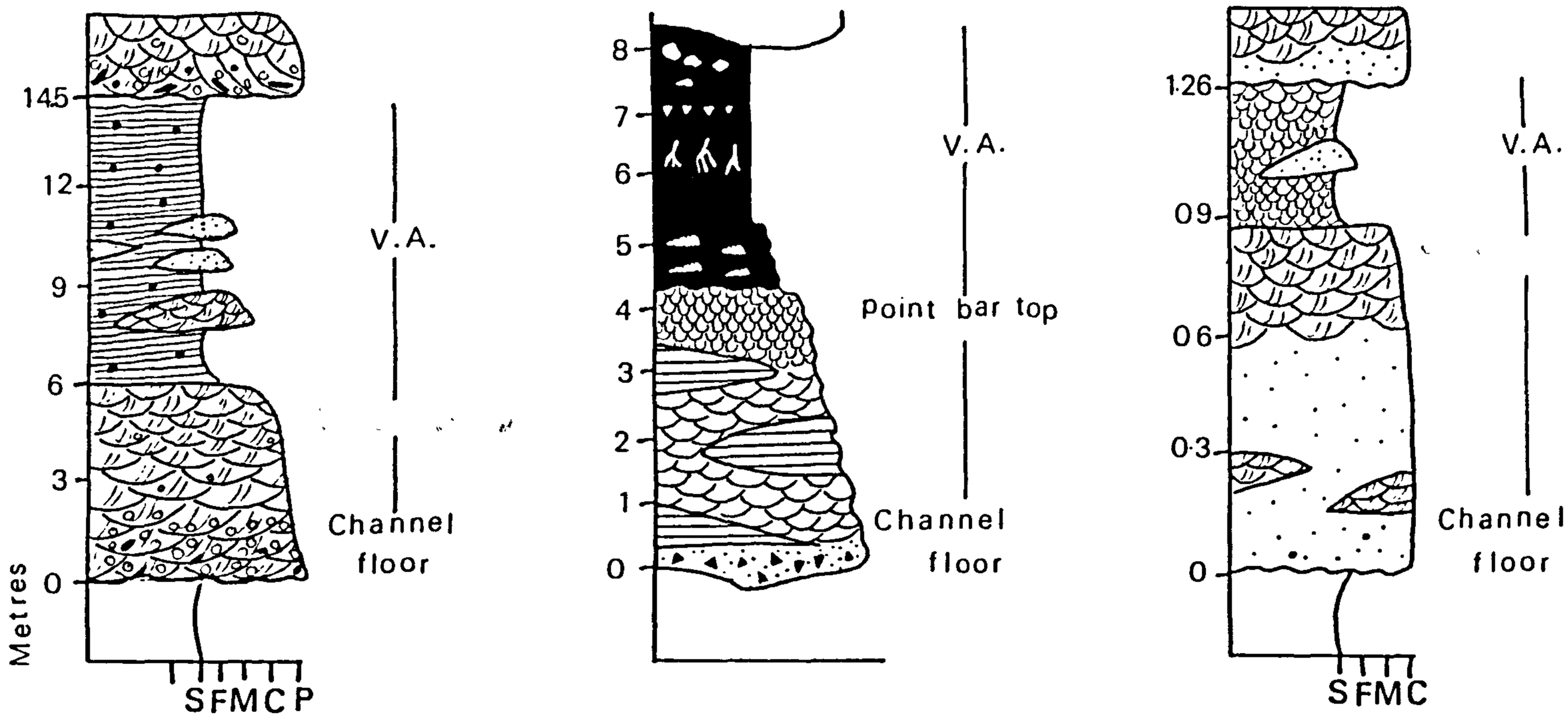

Fig. 4.10. Comparison of a summary sequence of facies for the Upper and Lower Um Irna Members with the meandering river model (Allen, 1970).

complex multilateral and multistorey nature are more in keeping with braided stream models (Miall, 1977). This interpretation is further strengthened by the presence of erosively - bounded trough cosets arranged in fining and rare coarsening upward sequences, the absence of abandoned channel - fills and lateral accretion surfaces indicative of migrating point bars, and the consistently west - southwesterly direction and low dispersion of the palaeocurrent measurements throughout the major sandstone units in the facies (Fig. 4. 3).

The internal complexity of the sandstone in the sequences points to deposition under high energy, rapidly fluctuating discharge conditions. Erosion by rising flood waters was locally intense with flood flows capable of moving mudclasts up to 20 cm in diameter. Individual flood events of varying magnitude are recorded in the fining and rare coarsening-upward trough cross - bedded and rippled sandstone lenses which together constitute the deposits of an active channel complex. Lower flow regime conditions prevailed during deposition of most of the complex, favouring the development and preservation of sinuous - crested dune bedforms, and to a lesser extent ripples at lower stages of flow. Channel bars were seldom developed, but their association with large intraclasts suggests that they formed during high stage flow, in contrast to the dune bedforms which formed at all stages of flow. Both vertical and lateral aggradation were important depositional processes during accumulation of this facies. Thus the siltstone - silty shale units can be explained in terms of major shifts in the

locus of active channel sedimentation. As a result fine silt and mud were deposited on the adjacent, temporarily inactive (abandoned) parts of the alluvial plain.

A similar situation was recorded by Williams and Rust (1969) for the braided Donjek River where bedform migration generated mainly sets of trough cross - strata. Channel shifting and aggradation may lead to preservation of such sets in the rock record, in the form of erosively - based fining and thinning upward trough cosets (Rust, 1978) like those in the Um Irna.

Vegetation quickly established itself on these abandoned parts of the Um Irna alluvial plain which were subjected to periodic flooding and subaerial exposure conducive to the formation of pedogenic ferruginous concretions. The presence of thick (<2 m), erosively - based sandstones within the overbank siltstone and silty shale suggests that minor channels were still active during the flood events. The growth of vegetation helped to stabilise the active channel tract, allowing for the accumulation of relatively thick overbank silts and clays prior to channel shifting. Because the depositional system was not confined by valley walls extensive inactive areas were able to develop giving rise to thick laterally persistent fine - grained units and fining - upward channel sequences which resemble those of meandering fluvial deposits.

The sandstones which thin out and separate distally into the overbank sediments are interpreted as crevasse splays, emanating from major distributary channels during floods. The composite, more proximal sandbody adjacent to the main channel sand probably records the crevasse channel or breach through which sediment - laden flood waters were funnelled into the overbank area during several episodes of crevassing (Saxena, 1976). Thus, crevassing and overbank sedimentation were important depositional processed during the accumulation of this facies (Fig. 4.11).

The nature of the concretions suggests that the diagenetic (pedogenic) environment was complex with alternating episodes of leaching, cementation and fracturing during their growth. Such variability is a characteristic feature of the vadose zone, particularly in the subsoil where weathering is generally more effective. Three different types of Guadalupian pisoliths were recognised by Dunham (1965): (1) large marine ooliths; (2) organic (algal?) pisoliths or oncoliths; and (3) pisoliths with nuclei of older pisolitic material showing a concentric internal structure episodes of fracturing and leaching, and lopsided inclusions of quartz and carbonate concentrated on one side. The first two types bear little resemblance to the Um Irna pisoliths. The third type, however, is very similar to those in the Um Irna except for the presence of carbonate. Unlike many pisoliths they were brittle and not deformably soft, as evidenced by the repeated fracturing during growth. As far as the writer is aware no similar

Age	Fm	Mbr	Sequences	Facies	Description	Interpretation
Permo Triassic	Um Irna Formation	Upper member	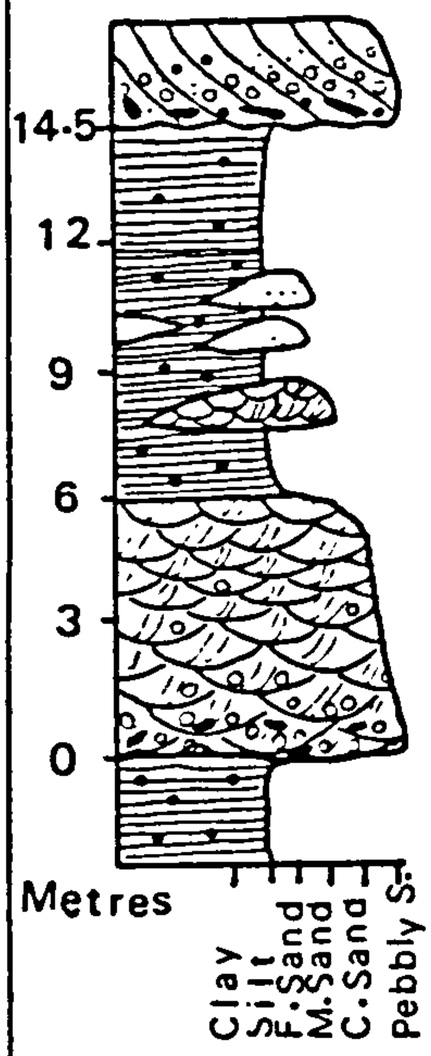	Silty Shale Sandstone pebbly Sand.	Pisolitic; colour maroon ; Lenticular; non pebbly. Medium to Large-scale trough cross beds	FloodPlain Crevasse Splays Channel Floor
		Lower member	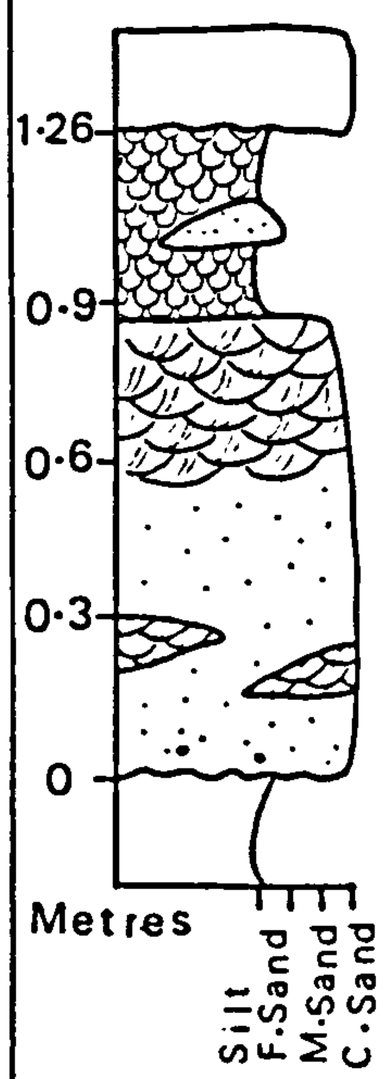	Silty Shale C-M Sand.	Rippled; Small scale troughs, pinch & swell.	Floodplain Channel Floor

Fig. 4.11. Schematic summary of the rock types and their environmental interpretations within an idealized upward - fining sequences in the Lower and Upper Um Irna Members.

pisoliths have been recorded in the geological literature.

4.3 PALAEOCLIMATE

Evidence of the climatic conditions prevailing at this time is provided by the ferruginous concretions (pisoliths) in the siltstone - silty shale units in the succession. The fracturing of the quartz grains and their subsequent coating with iron oxide suggests that the concretions are diagenetic in origin. This interpretation is supported by the lack of well developed primary bedding features and associated current generated structures in these deposits. Similar concretionary structures are a common diagenetic feature in the vadoze zone of humid tropical climates and include aluminous oxide and hydrated iron oxide pisoliths (Blatt et al., 1980). Within humid tropical climates chemical weathering and leaching cause primary iron - rich minerals to alter firstly to clay minerals and then to aluminium and iron oxides. The development of these oxides, which represent the most stable residues of chemical weathering in the soil profile depends mainly on whether rainfall is seasonal or continuous Tropical climates with alternating wet and dry seasons favour the development and stabilisation of iron oxides. During the wet season iron is leached from the mineral grains and maintained in the ferrous state due to the presence of organic matter acting as a reducing agent. The ferrous iron then moves lower in the soil profile where it becomes oxidised and precipitated as insoluble hydrated ferric oxides during the dry season, possibly aided by

bacterial activity (Blatt et al., 1980). The close association of some of the concretions with organic matter (plant material and coaly stringers) suggests that they may have formed in a similar manner. The climate was sufficiently warm and seasonally wet to support the growth and preservation of vegetation and extensive leaching, which effectively removed the base cations from the soil and prevented any carbonate enrichment (caliche). The upward increase in abundance of the pisoliths in the succession suggest that such conditions became more effective during deposition of the upper part of the Um Irna Formation.

Plate 4. 1. General view showing the uppermost fining-upward sequence of the Um Irna Formation at section 11. The contact with the Ma'in Formation is shown by the arrow. Section 11.

Plate 4. 2. Vertical section showing the contact (arrow) between the lower and upper Members of the Um Irna Formation at section 12.

8 m

Plate 4. 3. Lenticular bedded sandstone interbedded with silty - shale (hammer head) typical of the Lower Member of the Um Irna Formation. Note faint low angle trough cross - beds in sandstone. Section 7, (hammer is 30 cm long).

Plate 4. 4. General view showing the upper part of the Um Irna Formation overlain by the Ma'in Formation at section 11.

Plate 4.7. Planar - tabular cross - bedding, composed of Fe - pisoliths, pebbles and large-scale mudclasts, overlying greenish, pisolitic shales (transport to right). This unit marks the top of the Um Irna Formation. Section 11, (pen is 15 cm long).

Plate 4. 8. Trough cross - bedding in the Um Irna Formation (Upper Member) in which the internal laminae are graded and fine - upward. Colour reflects oxidation reduction processes. Section 7, (hammer is 30 cm long).

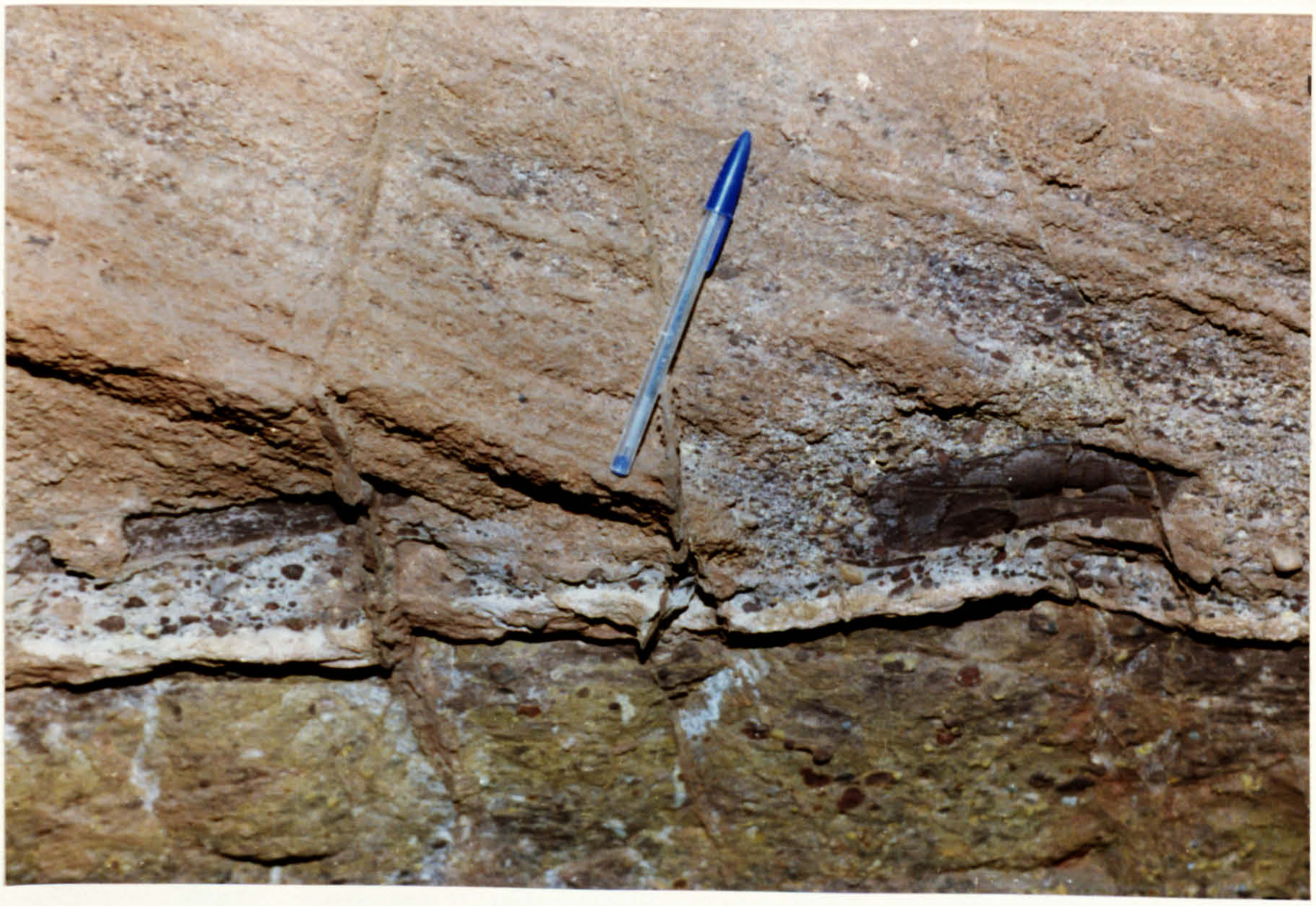

Plate 4..9. Silty shale unit composed of Fe - pisoliths up to 3 cm in diameter in the Um Irna Formation, immediately above the Upper Cambrian rocks, at section 12, (hammer is 30 cm long).

Plate 4.10. Bedding surface showing maroon silty matrix supported oval - shaped pisoliths (iron concretions) with large concentric internal structure (films and nuclei). Some pale reduction haloes are present. Upper Member of the Um Irna Formation at section 12, (coin is 2·5 cm in diameter).

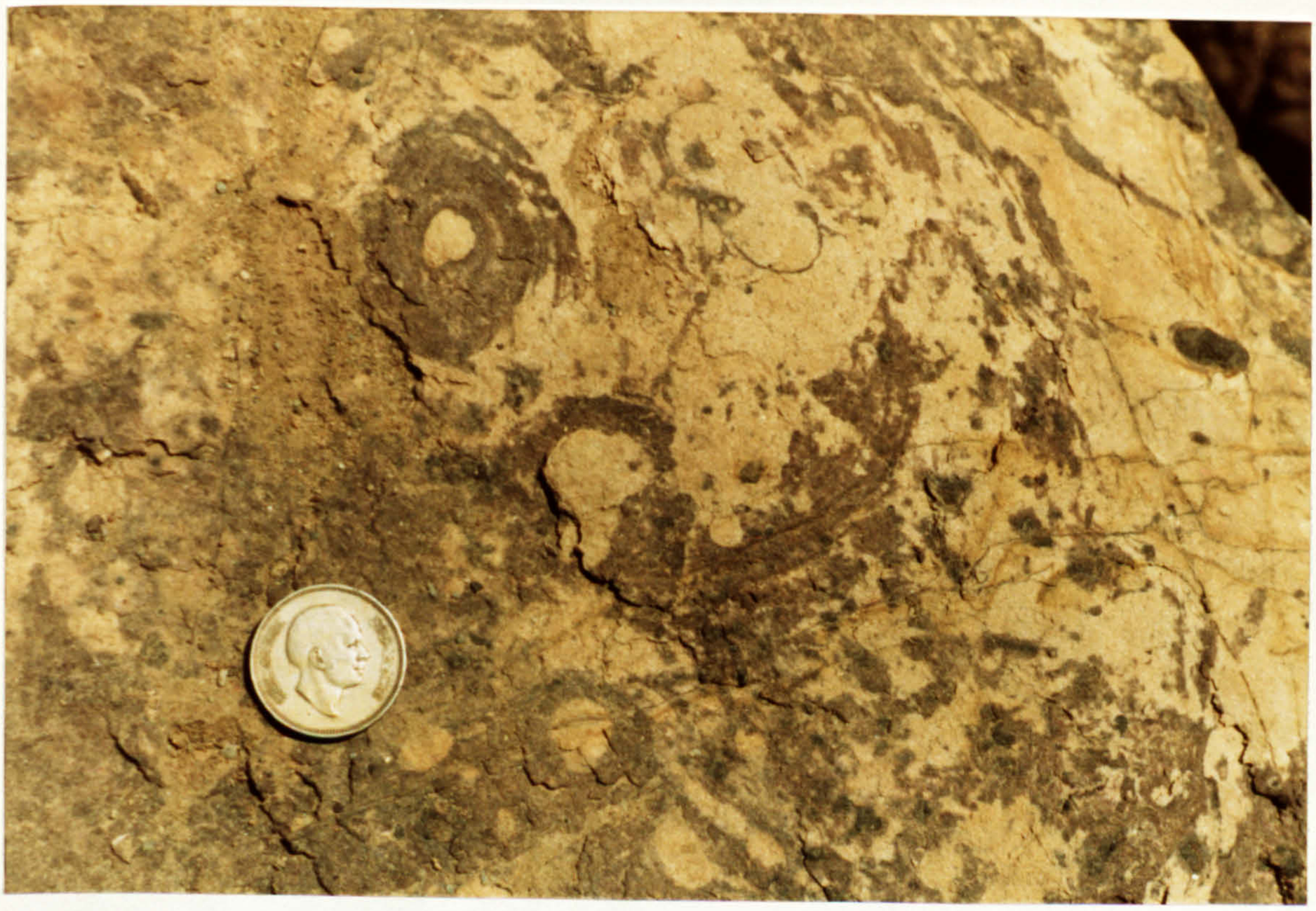

Plate 4.11. Sandstones with carbonaceous material of the Um Irna Formation (Upper Member) at section 6. Note the lower limonitic part, (hammer is 30 cm long).

Plate 4.12. Flaser - bedded, ripple laminated silty - shale. Fe- pisoliths are common, especially in the lower part. Um Irna Formation (Upper Member) at section 13, (hammer is 30 cm long).

Plate 4.13.. Photomicrograph of a ferruginous pisolith showing a well developed concentric structure, silty - shale, Upper Member, Um Irna Formation, section 11, polarised light.

Plate 4.14. Photomicrograph showing a ferruginous pisolith lacking any internal structure. Note dendritic fractures and scattered fine to coarse angular to subrounded quartz grains enclosed within the concretion. Silty - shale, Upper Member, Um Irna Formation, section 11. Polarised light.

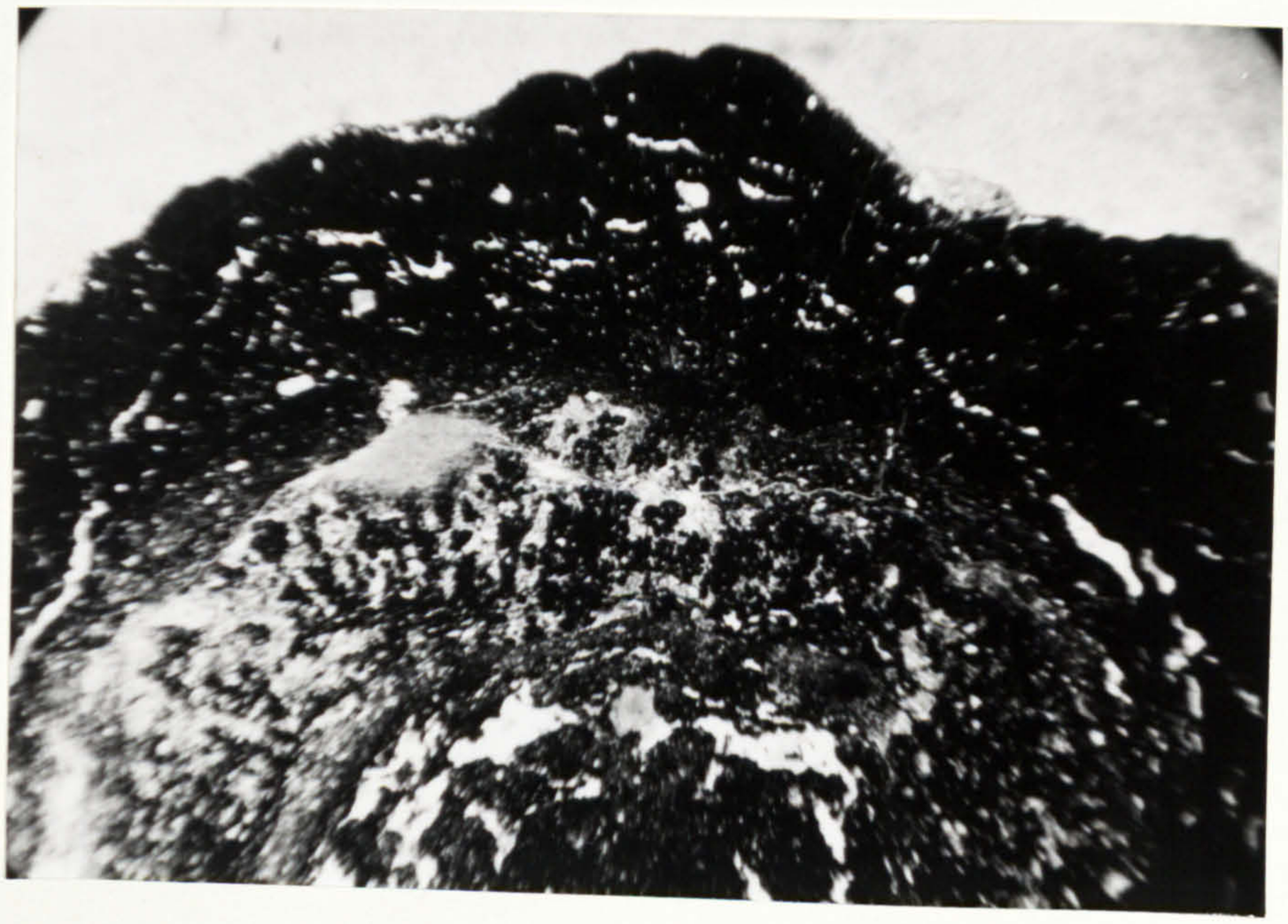

2 mm

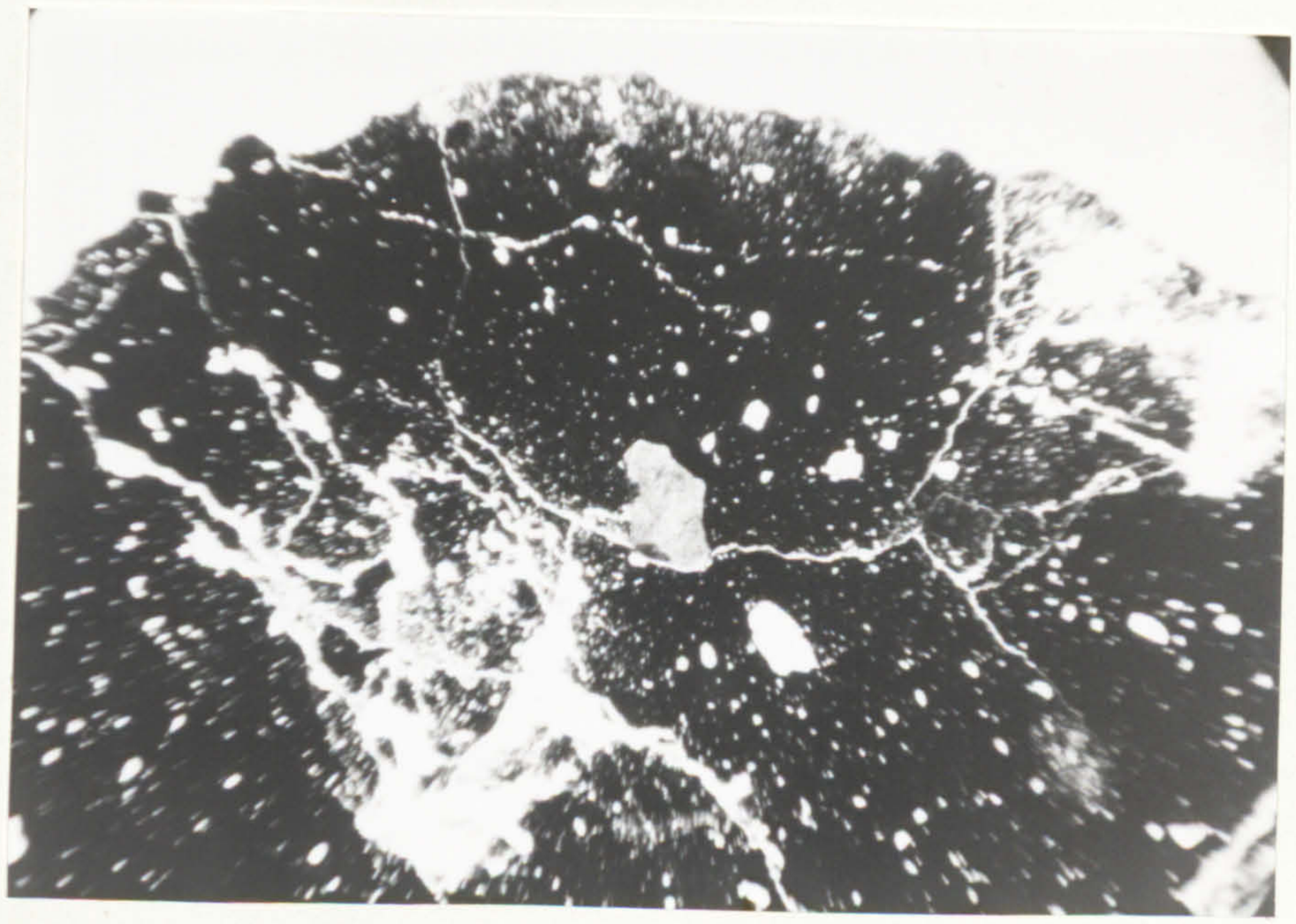

2 mm

Plate 4.15. Photomicrograph of a ferruginous concretion showing a concentric structure. The nucleus is formed by an aggregate of sand-size quartz clastics. Silty - shale, Upper Member, Um Irna Formation, section 11. Polarised light.

Plate 4.16. Photomicrograph of a ferruginous concretion showing lopsided inclusions of fine to coarse angular to subrounded quartz grains. The pisolith has been flattened during diagenesis. Silty - shale, Upper Member, Um Irna Formation. Polarised light.

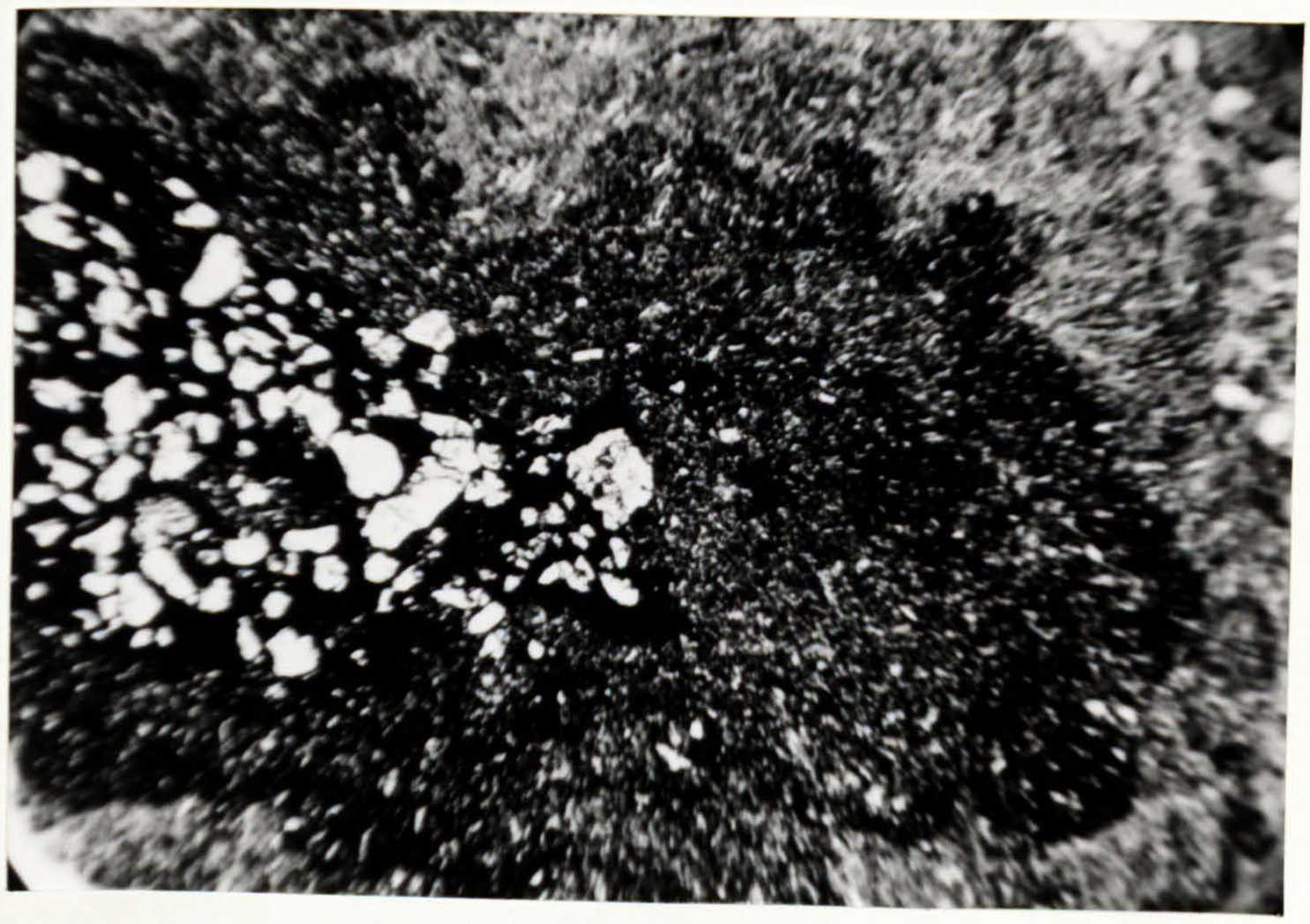

2.2 mm

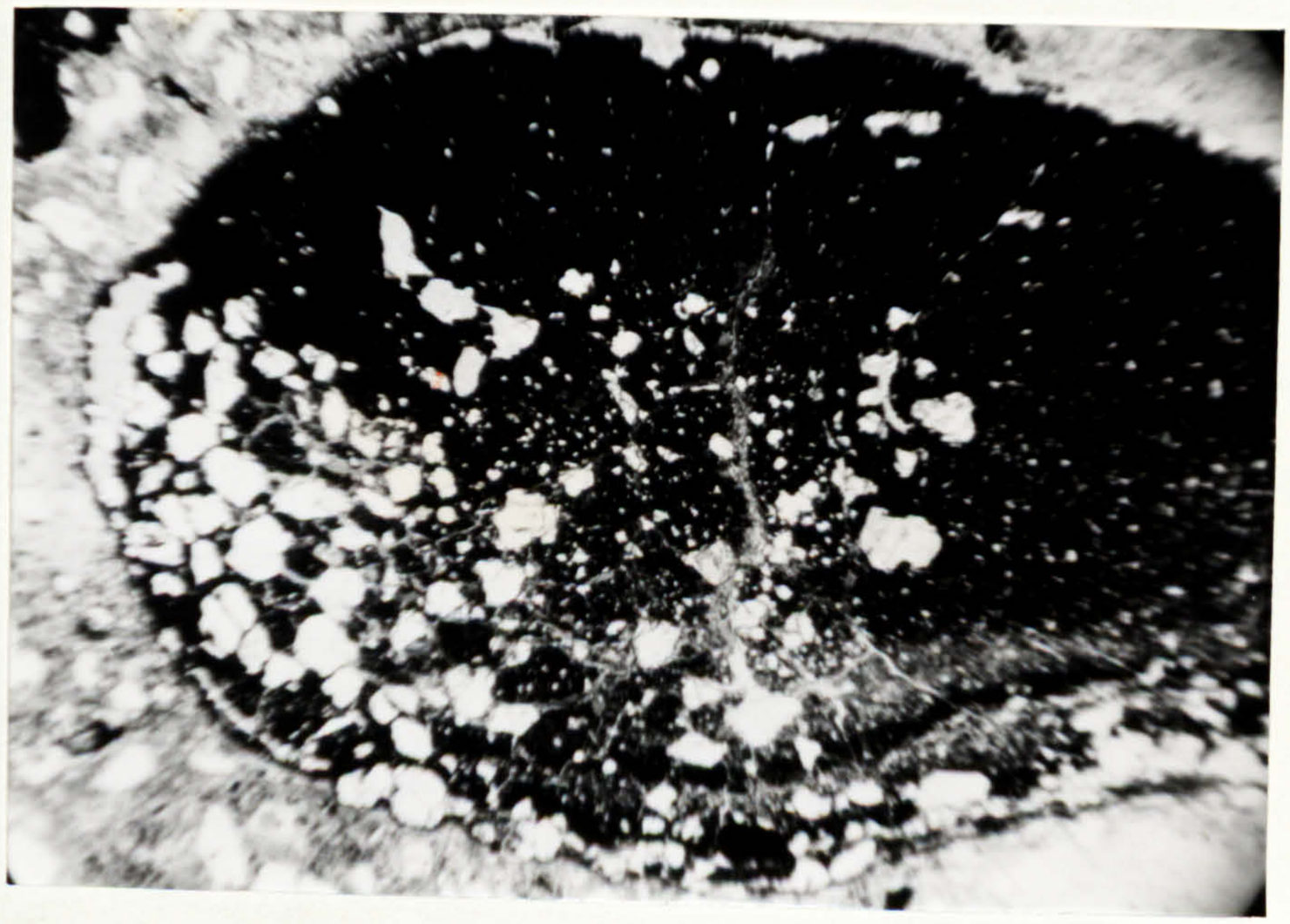

2.2 mm

Plate 4.17. Photomicrograph showing two generations of ferruginous concretions. To the right a concretion formed by the cementation of accumulated angular to subrounded quartz grains. To the left smaller ferruginous pisoliths showing quartz nuclei. Silty - shale, Upper Member, Um Irna Formation, section 13. Polarised light.

Plate 4.18. Photomicrograph showing some of the enclosed quartz grains fractured into a number of fragments (2 - 5) and then coated by iron oxide. Silty - shale, Upper Member, Um Irna Formation, section 11. Polarised light.

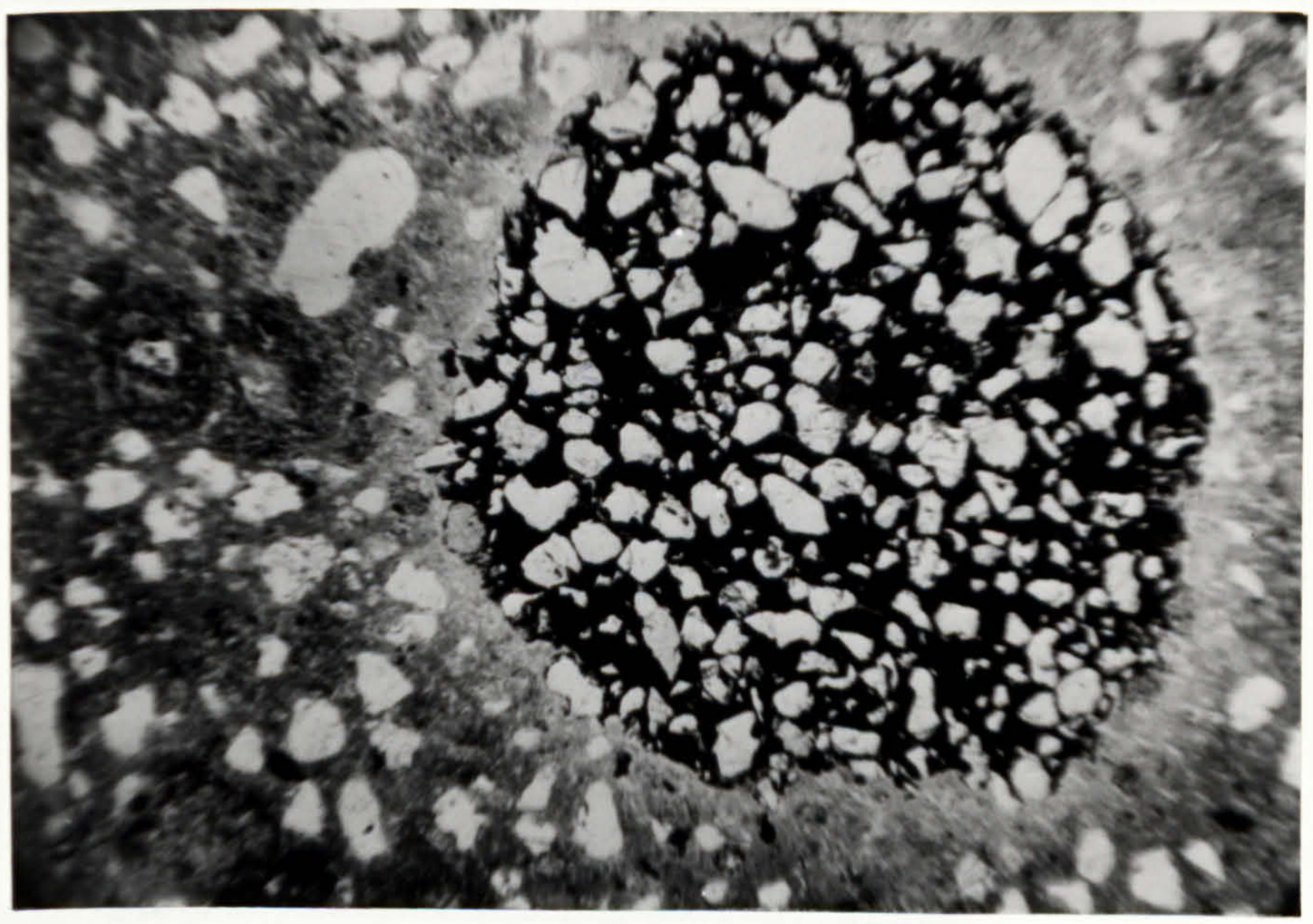

1.1 mm

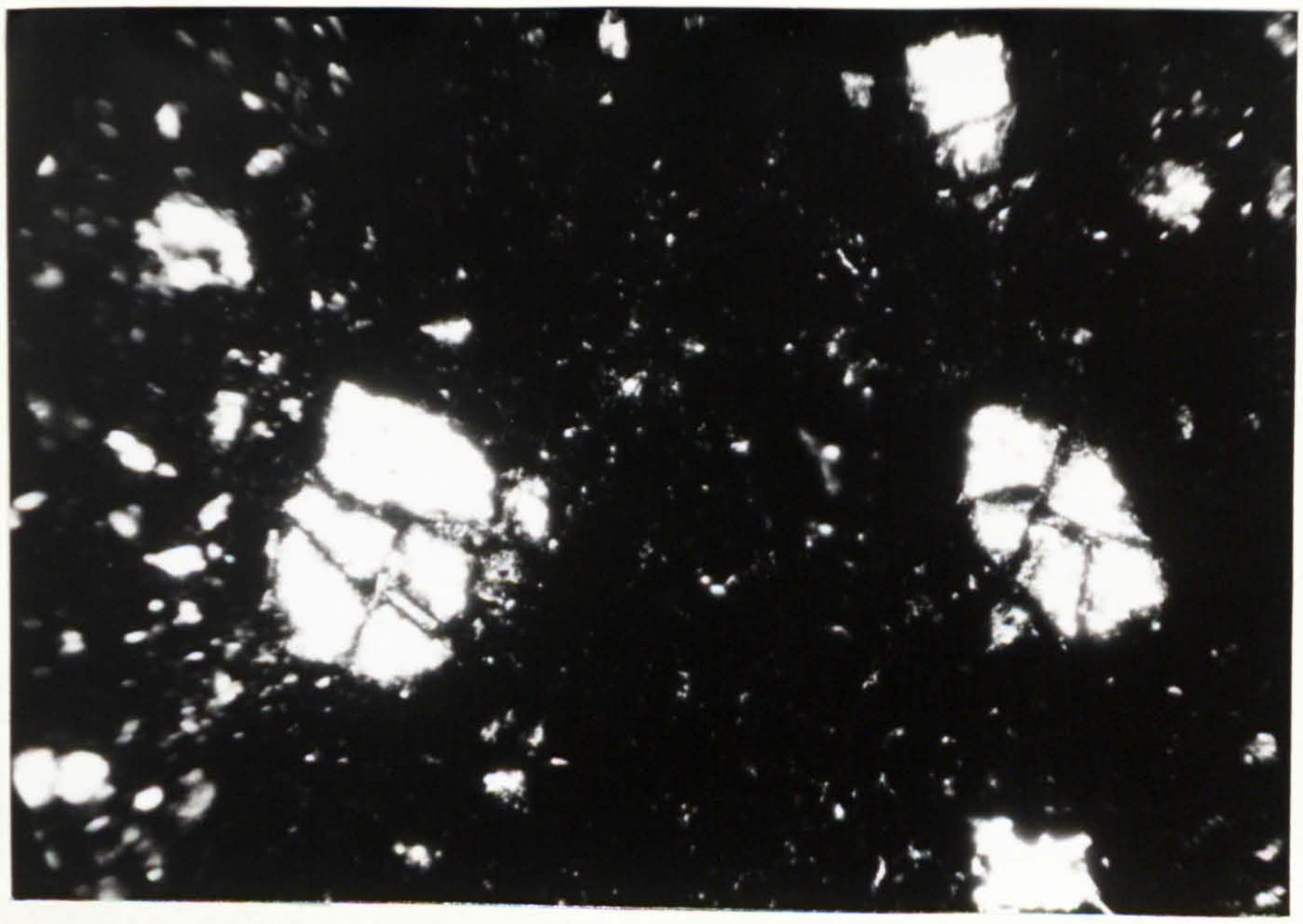

0.5 mm

CHAPTER FIVE

THE LOWER TRIASSIC (MA'IN) FORMATION

SEDIMENTARY SUCCESSION AND FACIES

CHAPTER FIVE

THE LOWER TRIASSIC (MA'IN) FORMATION

SEDIMENTARY SUCCESSION AND FACIES

5.1 INTRODUCTION

In 1981 Bandel and Khoury divided the Ma'in Formation into two formal Members, referred to as the Himara member, and the Nimra member. The Ma'in Formation conformably overlies the Um Irna Formation. The boundary is marked by an erosional surface with local relief of up to 10 cm, first trace of bioturbation and purple colour. The upper contact with the Dardur Formation, a 60 m thick marl - sandstone sequence is sharply defined by the occurrence of yellowish and greenish carbonate cemented sandstone. This in turn is capped by the Ain Musa, Hisban and Mukheiris Formations (Fig. 1. 6). The Dardur Formation was referred to by Bandel and Khoury (1981) as Dardun Formation.

Bandel and Khoury's work was essentially lithostratigraphic and paid little attention to the interpretation of depositional environments. In this study, five outcrop sections along the Dead Sea were measured, and divided into lithofacies according to lithology, sedimentary structures and biogenic features (Figs. 5. 2, 5. 3, 5. 5). The facies were described and interpreted by comparison with ancient and modern analogues. The location of the sections is shown in figure (1. 7).

5.2 Himara Member

The 30 m thick Himara member forms the basal part of the Ma'in


Planar cross-bedding


Trough cross-bedding

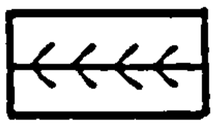
Herringbone cross-bedding


Rippled sandstone


Rippled silty-shales


Bioturbation

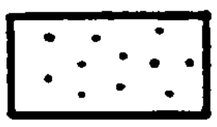
Structureless sandstones


Lenticular bedding


Mudcracks


Deformed bedding


Intraclasts

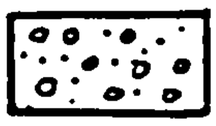
Pebbly sandstone

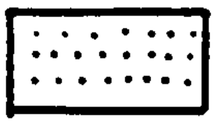
Laminated sandstone


Calcareous sandstones


Flaser bedding


Fossiliferous sandstone


Erosional surface

Rippled surface


Fining-upward


Coarsening-upward

Notations

S = Silty-shale

F = Fine sandstone

M = Medium sandstone

C = Coarse sandstone

P = Pebbly sandstone

M = Thickness in metres

Fig. 5. 1. Key showing lithology, sedimentary structures and other notations used in Figs. 5. 2, 5. 3, 5. 5 and 5. 7.

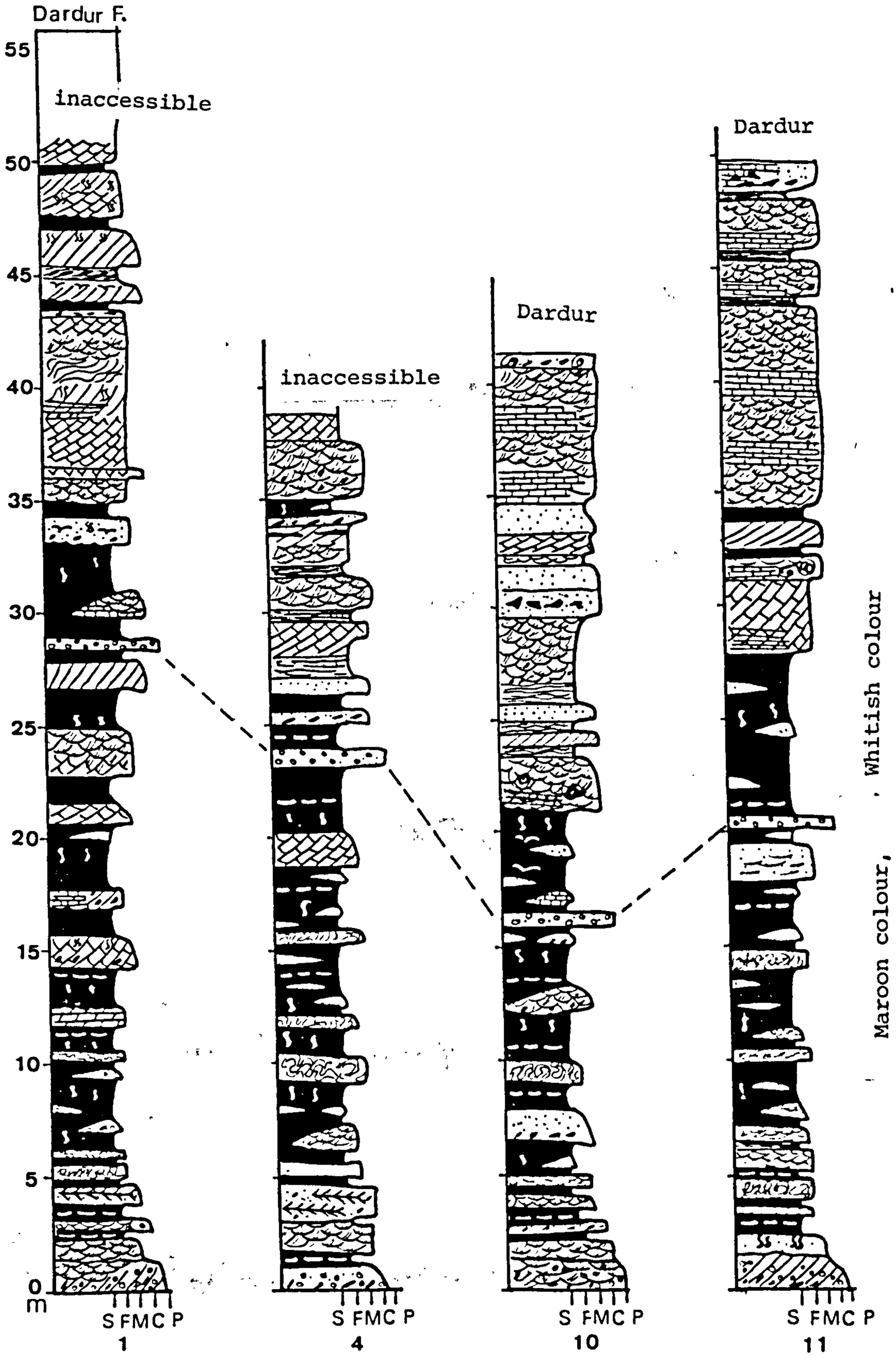

Fig. 5. 2. Generalised stratigraphic columns of the Ma'in Formation, from the north, central and southern parts of the study area. The datum used is the lowermost pebbly bed (top of Um Irna Formation) recognisable in all sections. (See Fig. 1. 7 for locations, Fig. 5. 1 for key, and appendix G for detailed sections).

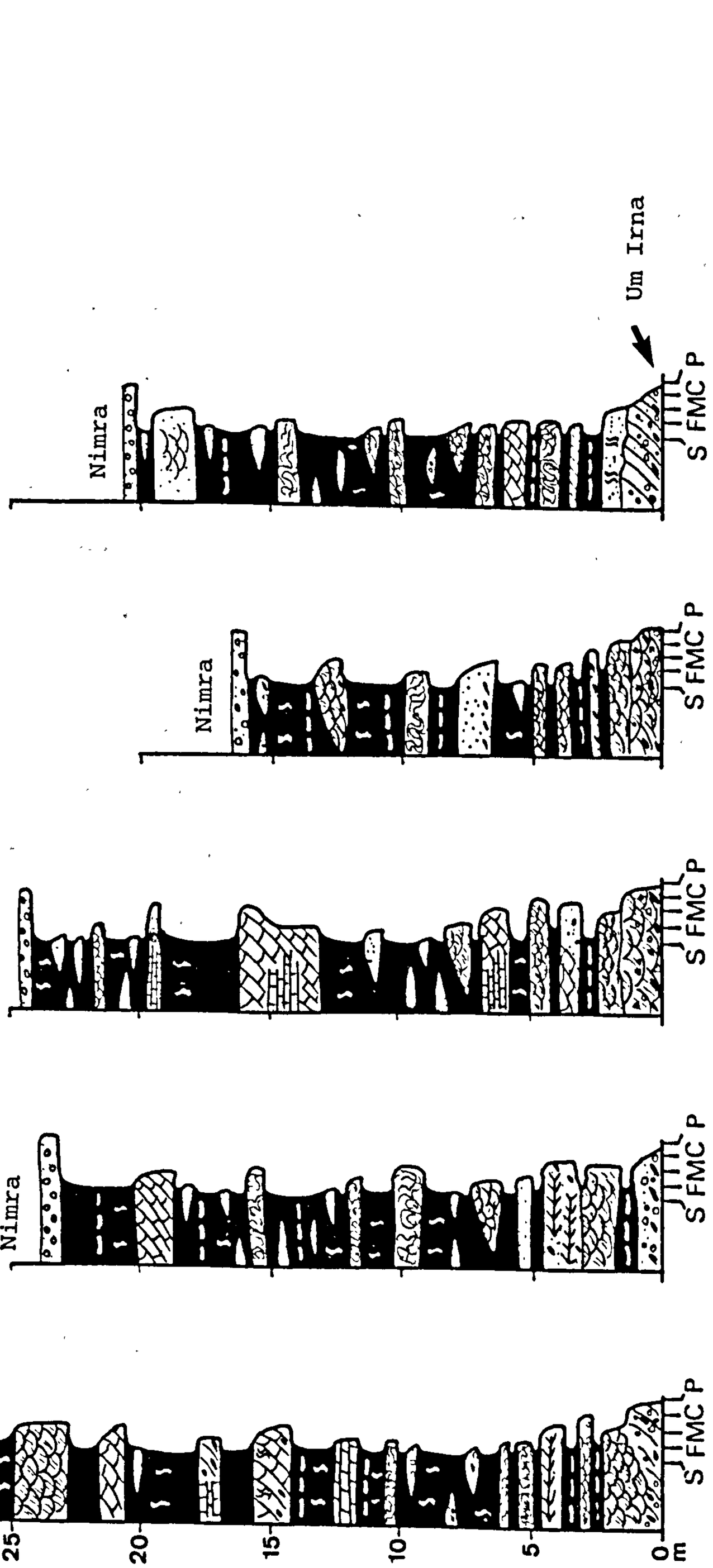

Fig. 5. 3. Representative stratigraphic columns of the Himara Member at different localities. (See Fig. 1. 7 for locations, Fig. for key, and appendix G for detailed sections).

ranges in thickness from 16 to 30 m, Formation in the Dead Sea area, and consists of siliciclastic sediments which are gradationally overlain by calcarenaceous sandstones (Nimra Member) up to 25 m thick (Fig. 5. 2, Plate 5. 1).

The Himara Member consists of quartz arenite with interbedded siltstone and mudstone (rhythmites), with a tendency for the proportion of argillaceous to arenaceous material to increase upward (Plates 5. 2-5. 5). Several fining - upward sequences from 0.4 to 4.2 m thick occur, each sequence comprising a coarse - grained sandstone grading upwards through interlayered siltstone and very well sorted, fine - grained sandstone into very fine - grained silty sandstone and mudstone at the top. A few thin, grey, dolomitic limestone horizons are present especially in the upper part. The Himara Member can be divided into two lithological facies: (1) Quartz arenite facies, and (2) Hetero - lithic facies.

5.2.1 Facies Description

i) Quartz arenite facies

The quartzarenites of this facies are sheet - like, thin to thick bedded (up to 1 m thick, but average 40 cm), and contain abundant flaser, lenticular and wavy beds (Plates 5. 3, 5. 5). Layers of reworked siltstone, mudstone and bivalve clasts up to 2 cm in diameter are present especially within the upper part of the facies

(Plate 5.18).

The sandstones, comprising coarse - to fine - grained maroon quartz arenites, dominate the lower third of the member. The quartz grains are generally subangular to subrounded, well sorted and well packed with little matrix. Mica (biotite and muscovite) and feldspar (plagioclase, microcline and orthoclase) are also common, with silica and iron oxides the most important cementing agents. The iron concretions, referred to by Bandel and Khoury (1981) as pisolites, are proved by thin section study to be merely iron oxide cement concentrations and do not affect the texture.

The dominant sedimentary structures in these sandstones are small to medium - scale trough cross - bedding with planar cross - bedding next in abundance. Azimuths of trough and planar foresets reveal a unimodal distribution directed to the northwest (Fig. 5. 6-1). Two herringbone cross - bedding structures were observed in the lower part of this facies at section 1 (Plate 5.15) and section 4 which were oriented ESE - WNW.

Bedding surfaces display ripples of diverse forms (symmetrical, asymmetrical, linguoid and ladder - back) and orientations, some of which are characterised by wide troughs and narrow crests. The upper surfaces of most of these beds are intensely bioturbated and casts of marine fossils and bivalves occur locally, in addition to a wide

variety of tracks and feeding traces of marine organisms, many of which are concentrated along the ripple troughs (Plates 5.10 - 5.13). Most of the shells are convex upwards.

Stromatolites include crinkle and dome forms and were observed in the mixed tidal flat zone in the lower part of the Himara member at section 4. Some of these structures are isolated while others show linked stromatolite domes (plates 5.22 - 5.24). Internally, stromatolites reveal a diagenetic pattern of laminations which may closely follow the external growth surface. The main types of arrangement that appear to exist in recent stromatolites are; laterally linked hemispheriods (LLH), discrete, vertically stacked hemispheriods (SH) and spheroidal structures (SS) (Logan et al., 1962).

II . Heterolithic Facies

This facies is composed mainly of silty shales and mudstones interbedded with fine - to coarse - grained sandy beds and lenses and occasional dolomitic horizons. The facies is predominantly a deep maroon colour. However, some varicoloured bands (greenish, cream and grey) are common especially in the upper part (Plates 5. 2, 5. 4).

All the transitions from flaser bedding through wavy bedding to lenticular bedding and parallel lamination exist. In lenticular bedding the ripples or sand lenses are discontinuous and isolated not only in a vertical but also in a horizontal direction (Plates 5.19,

5.22). The descriptive term "rhythmic sand / mud bedding" or alter - nating bedding is proposed (Reineck and Singh, 1973) to include all the bedding types composed of alternating layers of sand and mud.

Sand - filled desiccation cracks are abundant in the maroon siltstones and mudstones (Plates 5. 5 - 5. 9). Fracture systems as seen in plan (Plates 5. 7 - 5. 9) are divided between nonorthogonal and orthogonal, on the basis of the angles made where their cracks or their projections intersect (Lachenbruch, 1962, 1963. Fig. 5. 4). Some of these desiccation cracks are complete random orthogonal (Plate 5. 7), with regular crack shape. Generally, 3,4 or 5 sided, complete desiccation cracks occur, with the four - or five-sided cracks the most abundant. The sides of the cracks are not always straight, some are slightly curved and some are sharply bent (Plate 5. 7). The dimensions of the polygons vary from one polygon to another, the smallest and the greatest polygons observed attain a diameter of about 3 cm to 30 cm, with the longer dimensions occuring in the thicker mudstone beds. Cracks are 0.5 cm to 3 cm across, with depth of penetration up to 7 cm. The cracks have a simple infill composed mainly of fine cream sandstone. The surface of the polygons is usually horizontal or slightly concave upward, and they are commonly associated with burrowed surfaces (Plate 5. 9).

Asymmetrical, symmetrical, linguoid and interference ripple marks abound on bedding planes, with associated microtrough cross - laminations

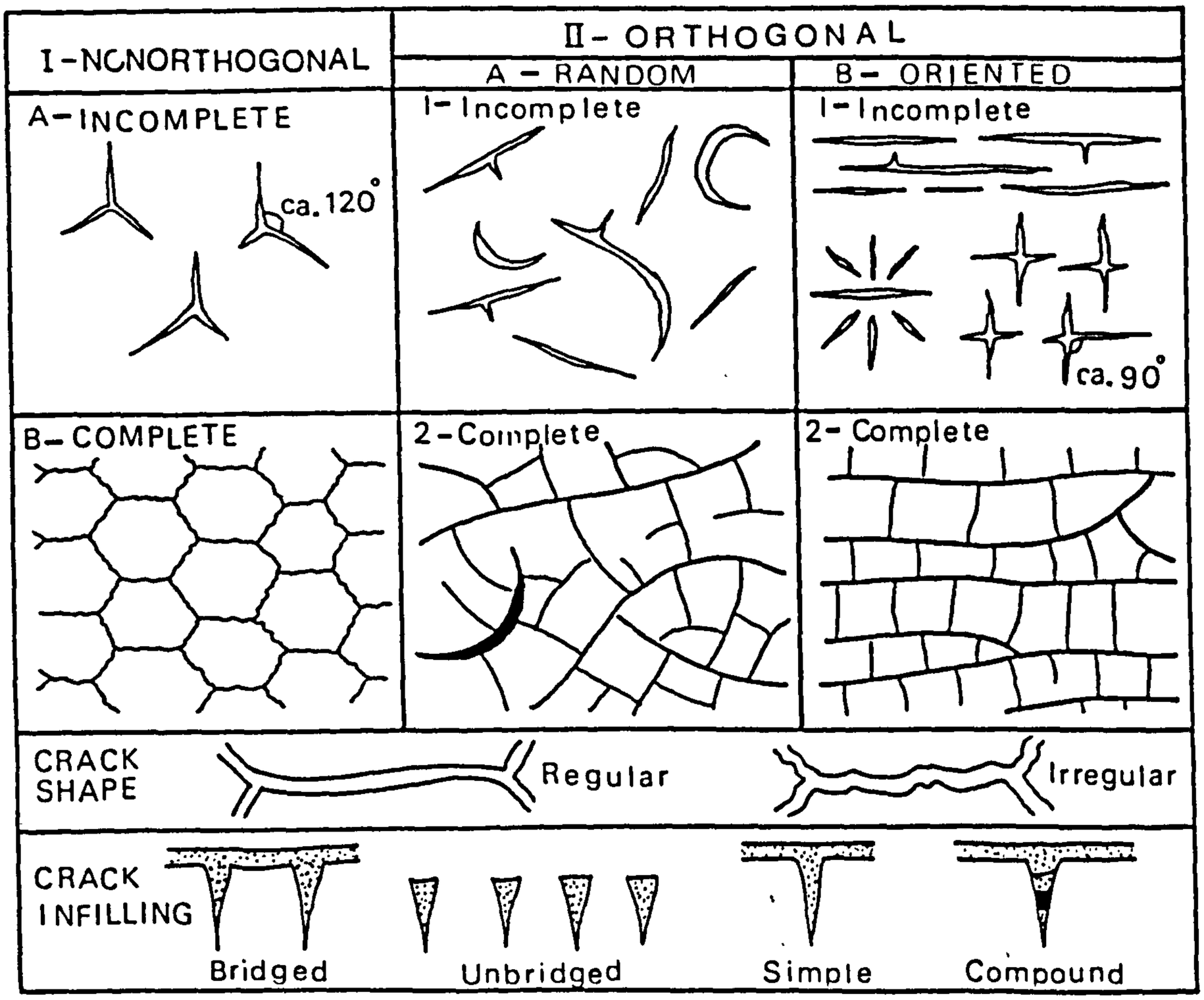

Fig. 5.14. A classification of shrinkage cracks and their infillings. (Lachenbruch, 1962, 1963).

(Plates 5.10 - 5.13, 5.16). Ladder - back ripples (Plate 5.13) and flat - topped ripples with eroded crests are common throughout the facies. Ripple crests are sinuous to straight or disconnected (Plates 5.10, 5.11); clay draped ripples are also common (Plate 5.19). Small - scale asymmetrical ripples with an average wavelength of 3.5 cm (oriented 195°) are superimposed at right angles on larger asymmetric ripples which have an average wavelength of 8 cm (Plate 5.13).

Azimuths of sinuous crested ripple marks reveal a bimodal distribution directed toward the northwest and southwest (Fig. 5. 5). The north - west trend is consistent with the orientation of the cross - bedded sandstones in the lower facies.

Penecontemporaneous deformation structures present in the lower parts of the sequence are of variable form and size and include convolution, ball - and - pillow and pseudonodule structures, ranging in diameter from 2 cm to 30 cm (Plates 5.19 - 5.22). It was observed that the diameter of these structures is proportional to the grain size of the sediments, with the larger structures occuring in the coarser sediment; these structures are either isolated or continous. Other features include small - scale slump structures, rill marks, load casts and rain imprints (Plate 5.14).

5.2.2 Interpretation

The Himara member represents a transitional zone between the

fluvial sediments of the Um Irna Formation below and the marine sediments of the Nimra member above, precisely the stratigraphic position where one would expect to observe signs of tidal influence. A common expectation among stratigraphers is to find tidal deposits where marine strata merge with nonmarine strata either in laterally or vertically exposed sequences (Walker and Harms, 1971).

Quartz arenites and associated siltstones and mudstones of the Himara member are interpreted to be analogs of tidal flats and tidal sandbodies. Combinations of sedimentary structures, vertical sequences, textural attributes and palaeocurrent patterns suggest that they were deposited within a tide dominated depositional environment.

Flaser bedding implies that both sand and mud were available and that periods of current activity alternate with periods of slack water. Conditions were relatively more favourable for the deposition and preservation of sand than for mud. In contrast to flaser bedding the lenticular bedding is produced under conditions more favourable for the deposition and preservation of mud than of sand, whereas, the genesis of wavy bedding requires conditions where the deposition and preservation of both sand and mud are possible (Reineck and Singh, 1973). Flaser and lenticular bedding is suggestive of alternating bedload transport and suspension during tidal reversals (Reineck and Wunderlich, 1968). The preferred environments of

formation are, therefore, areas where a change takes place between slack water and turbulent water, and where the required sediments exists. Thus, the main environments of its occurrence are subtidal zones (Reineck, 1963 a; Reineck et al., 1968) and intertidal zones (Höntzschel, 1963 a; Van Straaten, 1954 a).

Evidence of exposure in the Himara member is abundant, and consists mainly of desiccation cracks and a few rain imprints. Desiccation cracks are completely connected polygonal fractures which result from dewatering. These fissures develop in layers of muddy sediment that lose water through subaerial exposure on drying (Allen, 1982. p. 545). Desiccation cracks in the Himara member muddy sediments in fact are mainly random orthogonal cracks, defining mainly four - sided polygons (Plates 5. 7, 5. 8), having developed from very few points rather slowly (Allen, 1982). Fine examples abound in dried - up tidal mud flats (Kindle, 1923; Van Straaten, 1954 a, among others). Nonorthogonal desiccation cracks are comparatively rare in muddy sediments (Allen, 1982). Complete systems defining predominantly six - sided polygons on the order of 10 cm across occur on playas, tidal mud flats and salt marsh pans (quoted by Allen, 1982. P. 546 - 547). In most systems the polygons are in the order of 10 cm to 1 m across and the cracks seldom more than 5 cm wide and 25 cm deep. Most of the desiccation cracks are small (3 cm to 30 cm in diameter) because mud layers deposited during high tide slackwater were thin and exposed for short intervals (Plates 5. 7, 5. 8).

Small - scale symmetrical ripples with an average wavelength of 4 cm suggest very short period shallow water waves (Harms et al., 1975). Clay drapes on wave ripples indicate high slackwater suspension deposition (Reineck and Wunderlich, 1968). Slightly asymmetric forms are possibly a product of combined wave - current processes or, alternatively, formed by asymmetry of landward and seaward orbital wave velocities in the near-shore zone (Clifton et al., 1971).

Interference ripples, and small - scale ripples on larger ripples (ladder - back) (Plate 5.13) are interpreted to have been produced by late stage emergence runoff phenomena immediately prior to exposure (Klein, 1977). Of particular importance in this process is the development of changes in flow direction as the tide ebbs, thereby producing multimodal orientations in the resulting sedimentary structures. Furthermore, the scale of superimposed structures is always smaller than the structures produced in deeper water, indicating both a change in flow intensity and water depth (Klein, 1977). Evidence of late stage runoff is provided by the ladder - back ripples; the smaller ripple train was probably generated by water flowing laterally along the troughs, possibly due to downslope drainage or wind induced shear (Tankard and Hobday, 1977). Flat - topped ripples are common in the intertidal zone, and Anan et al., (1969) have attributed them to late-stage wave action planning off ripple tops.

	Sedimentary structures	Inferred depositional process
1	Mudcracks, raindrop imprints	Exposure
2	Mud - chips	Tidal scour
3	Load casts, pseudonodules, convolute laminae.	Differential loading and compaction due to rapid sedimentation deposition.
4	Wavy, flaser and tidal bedding (rhythmites) Isolated thin and flat lenticular bedding.	Alternation of tidal current bedload sediment transport with mud suspension deposition during slack water periods either at high or low tide.
5	Herringbone cross - stratification with sharp set boundaries.	Reversing tidal current bedload transport; tidal current phases of nearly equal flow velocity.
6	Micro - cross laminae and parallel fining - upward palestidal range sequences.	High rate of tidal flat progradation.
7	Interference ripples, current ripples superimposed at 90° on current ripples.	Late - stage emergence runoff producing changes in flow direction at shallower depths during ebb tide prior to exposure.
8	Escape burrows, Tracks and trails Burrows	Burrowing, rapid escape by organisms from environment in response to sudden influxes of sediment.

Table 5. 1 Depositional structures and inferred sedimentary processes in the Himara member (after Klein, 1971).

Algal laminated structures termed stromatolites are most prolific at the present day in very shallow waters of both marine and non - marine environments. In the marine environment they are characteristic of the shallow subtidal to supratidal zones of tropical to subtropical carbonate environments, although colonisation of siliciclastic shorelines has been increasingly recognised in recent years (Leeder, 1982). The growth of algal films on sediment surfaces causes characteristic internal laminations and external growth forms to develop according to ecological position, physicochemical and biochemical factors.

Soft sediment deformation is the disruption of unlithified sedimentary strata which occurs contemporaneously with, or closely following, deposition of the water saturated sediment. It typically occurs in coarse silt to fine sand, of terrigenous or marine origin. Ball and pillow structures in the Himara member (Plates 5.20, 5.21) compare closely to those identified by Mills (1983) as fine sand units with relatively undisturbed flat tops and bulbous "pillowed" bases. They often display concave - up laminae within the disturbed lower portions. Potter and Pettijohn (1977) relate ball - and - pillow structures to abrupt thixotropic transformation of the underlying clays. Their formation is attributed to reverse density mechanisms, but they may be genetically distinct from pseudonodules (Plates 5.19, 5.25) in that the latter consists of distorted fragments of sand or silt with a lower convex surface that have become completely enclosed in mud

(Blatt et al., 1980). Convolute bedding is attributed by Coleman (1969) and Wunderlich (1970) to emergence and draining of pore water from rapidly sedimented material, but the deformation may also be a product of differential loading (Blatt et al., 1980; Mills, 1983).

The Himara deposits are characterised by the vertical alternation of bedload traction and suspension deposition sediments. The coarse (sandstone) to fine (siltstone and mudstone) ratio within the succession (Fig. 5..3) is approximately 2 to 1 in the lower part and 1 to 5 in the upper part, the succession is interpreted as mixed intertidal flat accumulations with the lower more sandy facies deposited close to the low - tidal flat, and the upper more argillaceous facies close to the high - tidal flat (Figs. 5. 7, 7..3, 7. 5 A) as evidenced by the alternating bedload and suspension transport, current reversals (herringbone cross - bedding), bioturbation and periods of shallowing and subaerial exposure. Similar deposits are documented from ancient and modern tidal flats (Van Straaten, 1959; Reineck, 1967, 1972; Reineck and Wunderlich, 1968; Vos and Eriksson, 1976; among others). The structures generally considered to be most characteristic of modern tidal flats are the extensive wavy , lenticular and flaser bedded units, herringbone cross - bedding , and the bipolarity of current flow reflecting successive ebb and flood dominated current episodes (Klein, 1970).

A cyclical sequence of arenite transportation and deposition

followed by suspension settling of a muddy fraction, and its subsequent exposure and desiccation, can be inferred. This compares closely with modern mid - tidal flat deposits which are submerged for shorter periods than low tide sand flats. Mid - tidal flats typically show evidence of alternating coarse - grained bedload and high water stage suspension load sediemntation. This evidence of intermittent current activity of variable direction, periodic slack water settling of fines and frequent intervals of subaerial exposure is characteristic of the intertidal environment (Reineck, 1967; Klein, 1977). In contrast to the greenish - grey and whitish argillaceous intercalations in the quartz arenite facies, the maroon mudstones and siltstones in the heterolithic facies reflect a higher oxidation rate.

Hayes (1975) differentiated between three kinds of coasts on the basis of tidal action;

(1) wave dominated coasts (microtidal) with tidal range < 2m.,

(2) tide dominated coasts (macrotidal) with tidal range > 2m., and

(3) mixed energy coasts (mesotidal) with tidal range 2 - 4 m.

The method used for the palaeotidal range determination consists of measuring the thickness of palaeotidal range fining - upward sequences (Klein, 1971). The thickness of the fining - upward cycles at all sections within the Himara member seems to be of 0·48 m to 4 m (mean 2·28 m). If the sequence is interpreted as a succession of prograding tidal flats this value may reflect the maximum palaeotidal range. Klein (1977, Fig. 87) shows that the overall average palaeotidal range

of the past was mesotidal, with accessory macrotidal and minimal microtidal range. The depositional model proposed for the Himara Member based on the palaeotidal range is one of the microtidal to mesotidal coastline. There is no preserved evidence to suggest that the tidal flats were protected from the sea by a barrier.

5.3 NIMRA MEMBER

The Nimra Member comprises the upper part of the Ma'in Formation, and shows major bedding surfaces dipping at angles of between 9 and 20° to the SSW. It gradationally overlies the Himara member and attains a thickness of about 25 m. There is no sharp boundary between the two members, and the only discriminating feature is a change in colour, from mainly maroon in the Himara to mainly whitish in the Nimra. However a single granular quartz bed is present at this level in most of the studied localities, but it pinches and swells and varies in thickness from 5 - 14 cm (Fig. 5. 2).

The Nimra sediments contain variable admixtures of sandstone, siltstone and mudstone, and display a coarsening-upward trend in contrast to the fining-upward trend in the Himara (Fig. 5. 5). The Nimra can be subdivided into two major sedimentary facies:(1) Heterolithic facies (lower part) and (2) Quartz arenite facies (upper part).

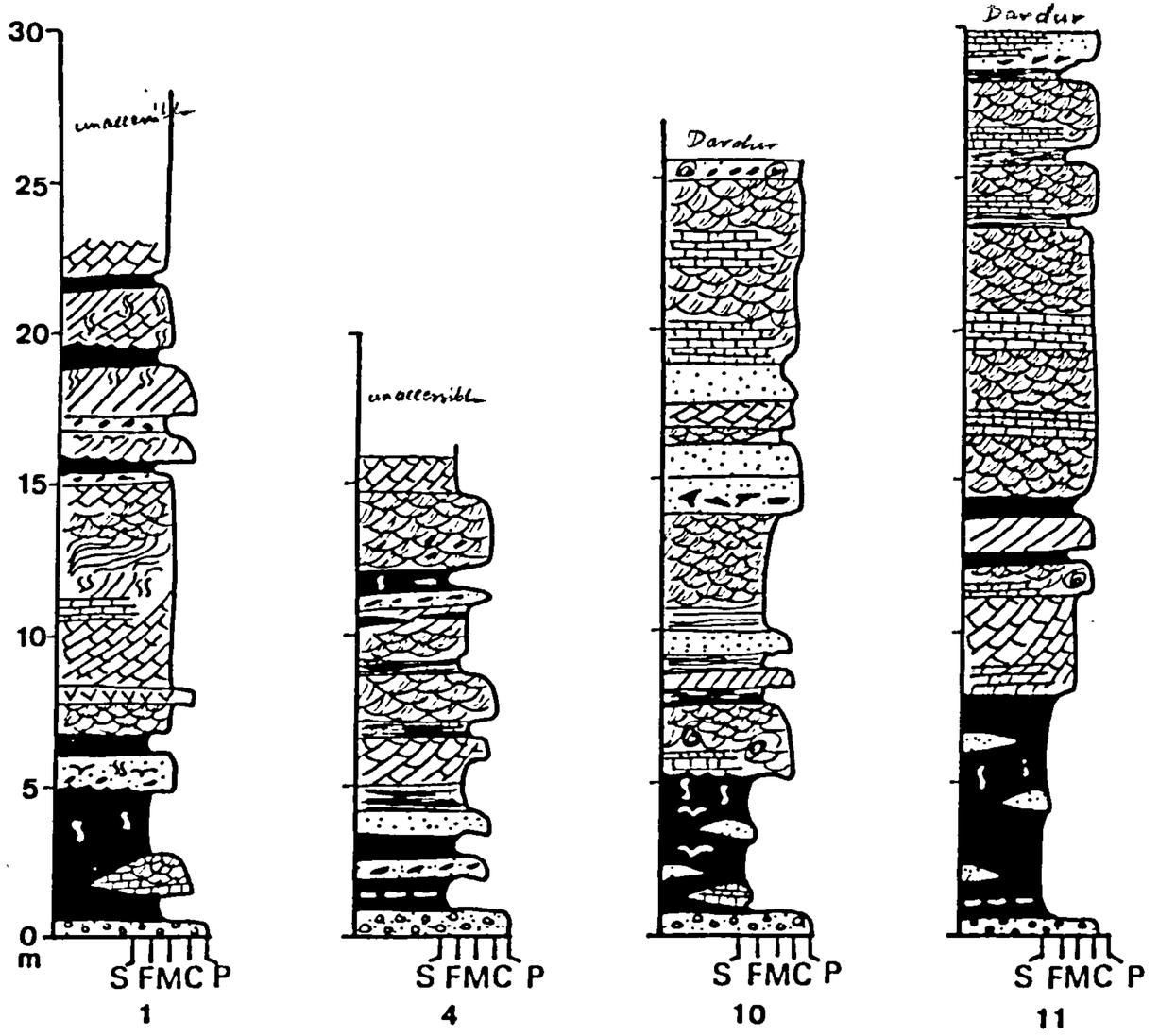

Fig. 5. 5. Representative stratigraphic columns of the Nimra Member at different localities. (See Fig. 1. 7 for locations, Fig. 5. 1 for key, and appendix G for detailed sections).

5.3.1 Facies Description

I Heterolithic Facies

This argillaceous dominated facies is restricted to the lower third of the member (Plate 5.27). It consists of siltstone, mudstone, marl and fine - grained sandstones with sand intraclasts intercalated with the finer lithologies. These rocks are mainly whitish (cream) in colour, although some varicoloured beds (maroon, green and grey) exist, especially in the lower part of the succession.

The sediments are laminated and thinly bedded (< 30 cm) and show wavy, rippled and flaser bedding (PLate 5.27). Lenses of small - scale (10 - 16 cm wide and 1 - 3 cm thick) are interbedded with more continuous lenses which pinch and swell (Plate 5.25)

Bedding surfaces are usually rippled. Most of the ripples are symmetrical types with some asymmetric types. Both ripple types are of small - scale and medium - scale ranging between 3 - 18 cm in wave-length and 1-2 cm in amplitude (Plate 5.25). Asymmetric current produced ripples have lee face azimuths of about 70° which is consistent with the orientation of cross - beds encountered within the sandy units (Fig. 5. 6).

II Quartz Arenite Facies

This facies comprises units of medium - to coarse - grained,

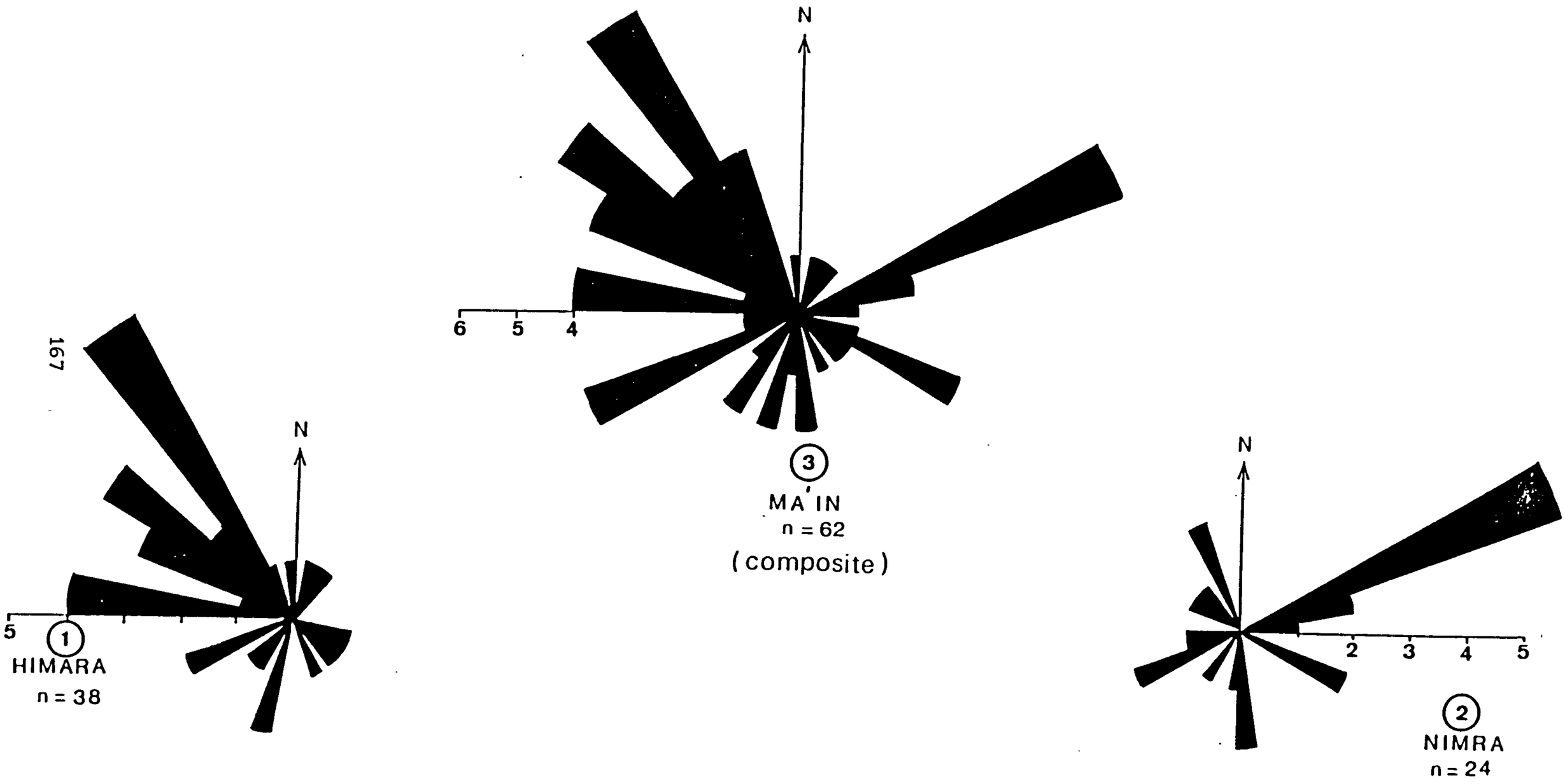

Fig. 5.16. Rose diagrams showing the palaeocurrent pattern of the (1) Himara Member, (2) Nimra Member, and (3) Ma'in formation as a whole.

medium-to thick-bedded (20 - 200 cm) quartz arenites, with basal erosional surfaces. Quartz grains are well sorted and well rounded, with carbonate cement. These sandstones gradationally overly the rhythmically alternating arenaceous - argillaceous units of the lower heterolithic facies.

The sandstones show cyclic alternations. Seven cycles can be recognised, each cycle consisting of yellowish and whitish sandstones (Plate 5.28). The whitish sandstones are friable, soft, trough cross - bedded and non - calcareous, while the yellowish sandstones are comparatively hard, massive, fossiliferous and calcareous. A few beds are composed of fossil bivalve fragments, forming intraformational bioclastic conglomerates (coquinas). The sandstones are highly bioturbated and fossiliferous with burrow casts common along the bedding surfaces. Burrow tracks are also associated with the rippled bedding surfaces (Plate 5.29).

Among the sedimentary structures, planar cross - beds are most abundant, with individual sets between 5 - 20 cm thick; some of them are slightly deformed. Foresets dips show a bimodal trend towards the northeast and northwest, with the northeast trend predominating. Small - scale trough cross - beds are also common ranging in width between 6 - 12 cm, while larger-scale troughs about 46 cm wide and 7 cm thick occasionally develop. Trough cross - bed foresets are directed mainly towards the southwest. However, azimuths of ripples

and planar and trough foresets reveal a unimodal trend directed towards the northeast.

5.3.2 Interpretation

The textures, structures and depositional sequences suggest that the siliciclastic and carbonate sediments of this member were probably deposited in the tide dominated environment of an epeiric sea. The coarsening-upward facies sequence, with associated carbonates and trace fossils, and the arrangement of sedimentary structures, provides evidence of deposition in a tidal flat and shallow subtidal zone (Table 5. 2). Studies of modern tidal flats have demonstrated that bedload traction transport dominates in the shallow subtidal zone and the low - tidal sand flat. Landward lies the mid - tidal flat with mixed suspension and bedload sedimentation. The high tidal mudflat is characterised by suspension sedimentation, and the supra-tidal salt marsh (Tankard and Hobday, 1977).

The Nimra is represented by vertically stacked sediments comprising subtidal sand flat quartz arenite and rhythmically alternating low - tidal mixed arenaceous argillaceous units deposited in the lower distal part of the mixed tidal flat environment (Fig.5. 7). The lithological maturity of these clean sandstones, and rounding of the quartz grains, reflects intense reworking of tidal sand bodies during bedload transport (Balaz and Klein, 1972). These arenites probably developed in an open

	Sedimentary structures	Inferred depositional process
1	Wavy, flaser and tidal bedding, Isolated thin lenticular bedding	Alternation of tidal current bedload sediment transport with mud suspension deposition during slack water periods either at high or low tide.
2	Convolute laminae	Differential loading and compaction due to rapid sediment deposition.
3	Interference ripples, current ripples superimposed at 90° on current ripples	Late - stage emergence runoff producing changes in flow direction at shallower depths during ebb tide prior to exposure.
4	Tracks and trails, Burrows	Burrowing, rapid escape by organisms from environment in response to sudden influxes of sediment.

Table 5. 2 Depositional structures and inferred seimentary processes in the Nimra Member (after Klein, 1971).

	Fm	Mbr	SEQUENCE	FACIES	DESCRIPTION	INTERPRETATIO	
TRIASSIC	FORMATION	NIMRA	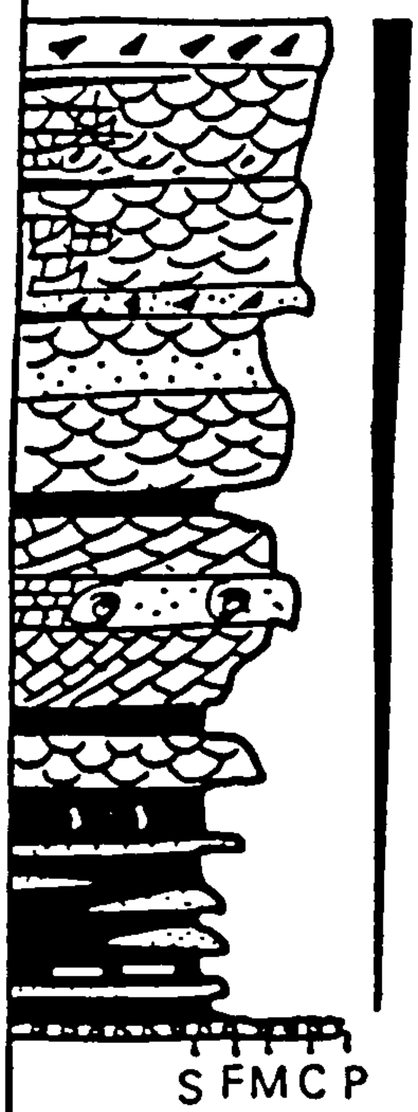	Quartz arenite	Quartz arenite; medium to coarse grained; cream colour; fossiliferous; bioturbated with large intraclast content; coquinas Shale intercalations; trough and planar cross - beds; some deformed; ripples. Some are massive; high carbonate content and wavy beds.	Subtidal	
				Heterolithic	Silty - shales with interbedded sandy lenses (trough cross - bedded); mainly of whitish colour, with varicoloured bands in the lower part (maroon, purplish, grey and green); bioturbated and mudcracked in the lower part.	Low - tide	Flat
LOWER		MAIN	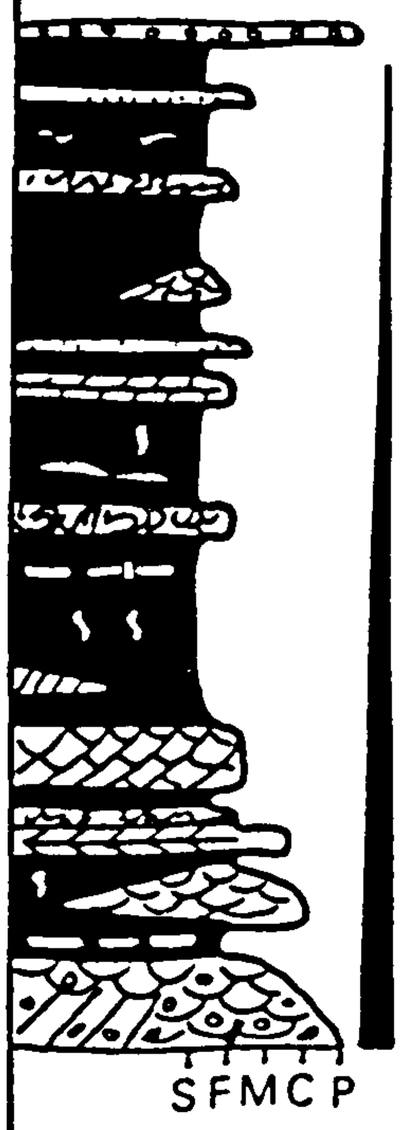	Heterolithic	Silty - shales with sandy interbeds; rhythmic, rippled, flaser and wavy bedding. Deformed sandy horizons; trough cross - beds and cross - laminations; sand - filled desiccation cracks; rainprints; load casts and dolomitic horizons. Sandy lenses with abundant mudclasts. Deep maroon colour, some varicoloured bans especially in the upper part (whitish, grey, yellowish and greenish) and bioturbated.	High - tide	Intertidal
				Quartz arenite	Quartz arenites with sandy interbeds; deep maroon colour. Medium to small trough and planar cross - beds. Herringbone cross-beds; lenticular and flaser bedding ripples, sand - filled desiccation cracks, bioturbation and water - escape structures.	Low to mid-tide	Mixed

Fig. 5. 7. Idealised facies sequences illustrating vertical arrangement of Himara and Nimra members, derived from pooled data.

subtidal shelf environment as evidenced by the presence of an open marine fauna (foraminifera, bryozoa, gastropoda and bivalves). Absence of features indicative of subaerial emergence, suggests a predominantly subtidal depositional environment. The rounded grain, mature sandstones may, in part, be derived from an offshore barrier island complex.

Plate 5. 1. A general view of the Ma'in Formation at section 1, showing the contact (arrow) between the Himara Member (reddish, lower) and the Nimra Member (cream, upper).

Plate 5. 2. Thin rippled beds of silty, very fine-grained sandstone comprising the Himara Member (Ma'in Formation) at section 1. Note the oxidation (red) reduction (cream) colour of sediments (hammer "arrow" is 30 cm long).

Plate 5. 3. Vertical section showing the contact between Um Irna Formation (lower) and Ma'in Formation (upper) see arrow. Below the contact a greenish pisolitic silty shale of the Um Irna Formation is overlain by a bed composed of quartz pebbles, mudclasts and pisoliths. Above the contact the Ma'in Formation begins with rippled silty and sandy laminations which are usually bioturbated, cross - laminated and mudcracked. Alternations of sand, silt and clay are common. Section 6, (hammer is 30 cm long).

Plate 5. 4. Folded, rhythmic bedding composed of thin clayey, silty and sandy beds. Section 2, (arrow shows hammer 30 cm long for scale).

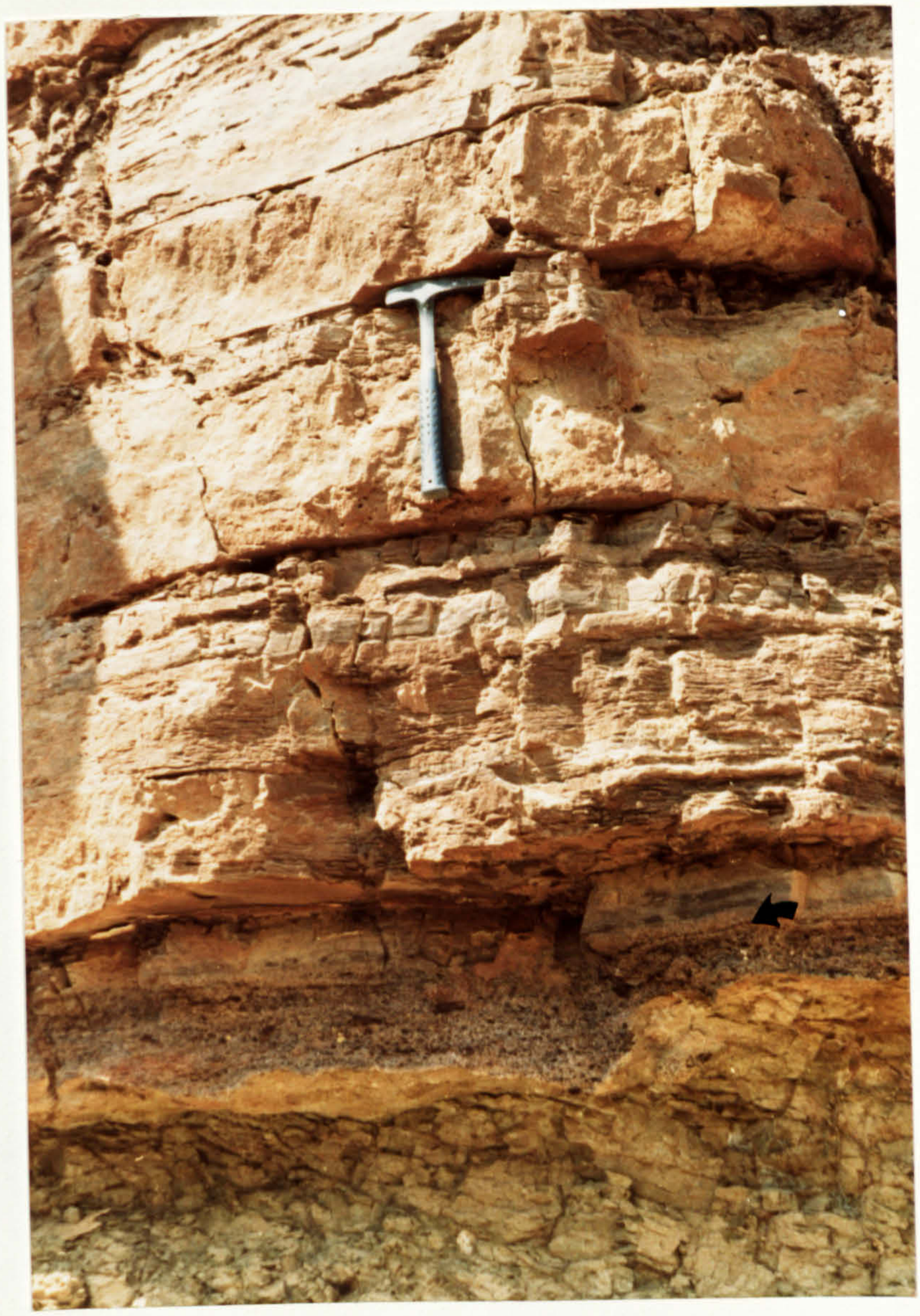

Plate 5. 5. General view showing the lower part of the Himara Member, consisting mainly of sandy facies below hammer, and silty shale facies above. Bedding surfaces are usually rippled and bioturbated. Note mudcracks at the bottom. Section 1, (hammer is 30 cm long).

Plate 5. 6. Vertical section showing sand infilled desiccation cracks at two levels. Note ripple cross - laminations at top of pen. Section 1, (pen is 15 cm long).

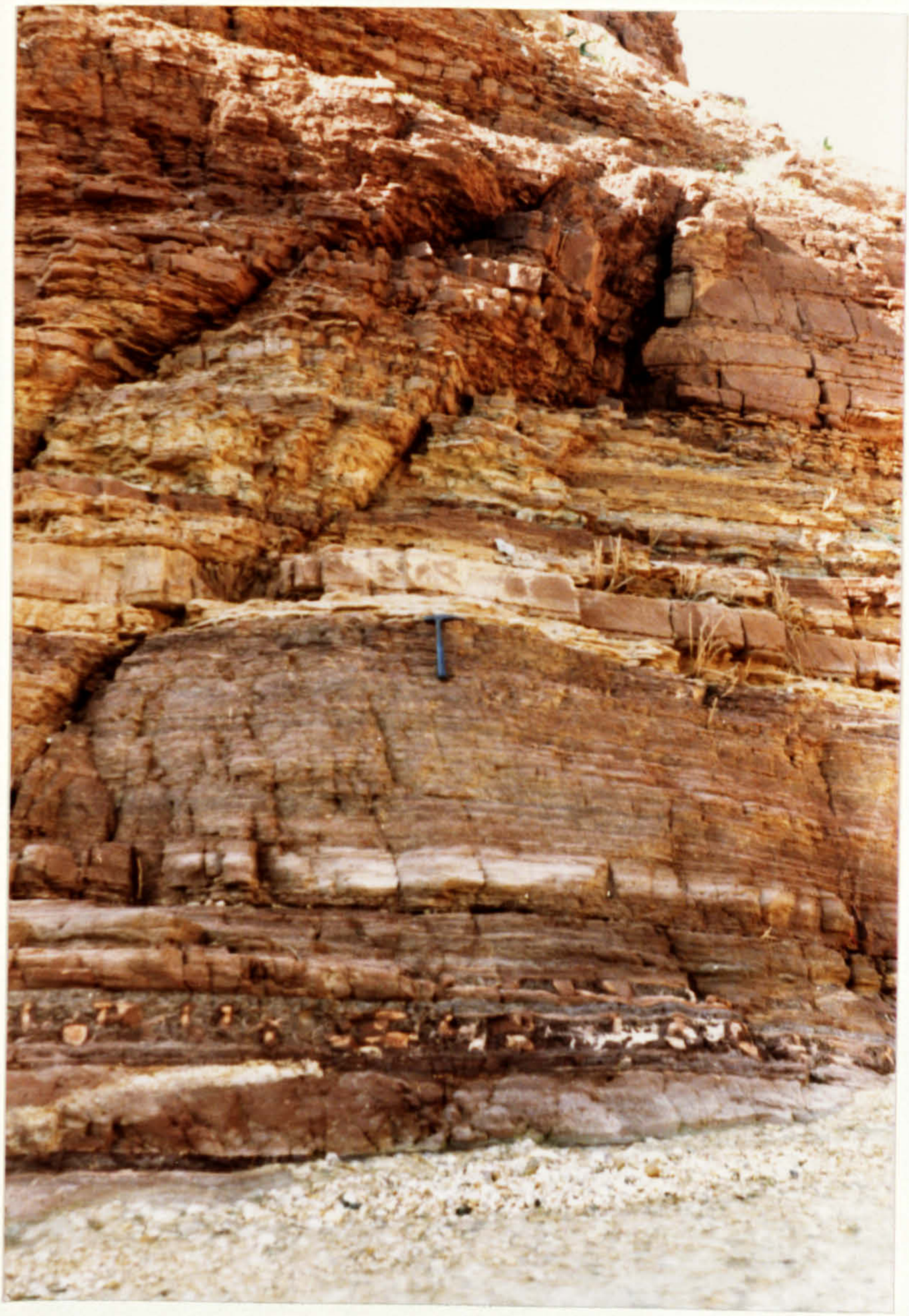

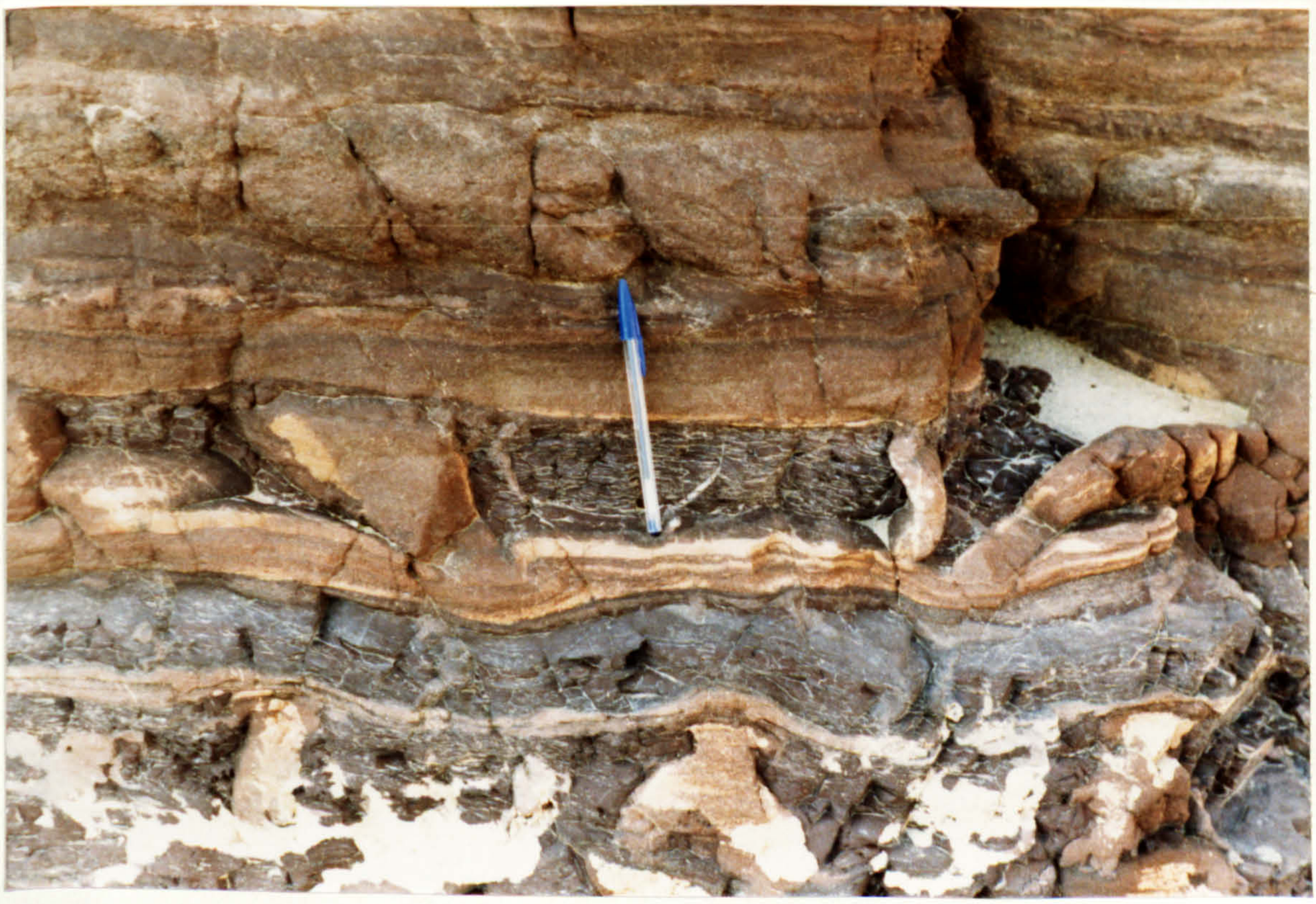

Plate 5. 7. Bedding surface showing mudcrack polygons enhanced by sand infilling. Himara Member, section 1, (pen is 15 cm long).

Plate 5. 8. Underside of thin bedded sandstone showing casts of sand polygons filling eroded mudcracks. Himara Member, section 4.

Plate 5. 9. Bedding surface and vertical section (two dimension) associated with animal trails. Himara Member, section 10, (hammer is 30 cm long).

Plate 5.10. Sinuous ripple marks on bedding surface with abundant horizontal burrows (tracks, trails and smooth - walled meandering tubes) along the troughs. Himara Member, section 10, (hammer is 30 cm long).

Plate 5.11. Sinuous - crested current ripples superimposed obliquely on different bedding surfaces. Note that the ripples having dissimilar crest orientations are on different bedding planes. Himara Member, section 1, (hammer is 30 cm long).

Plate 5.12. Linguoid ripple marks on thin bedded sandstone, current from upper left to lower right. Himara Member, section 4, (hammer is 30 cm long).

Plate 5.13. Interference current ripples on bedding surface, top of picture above hammer head. On the left ladder back ripples comprise a secondary train of very small - scale ripples (2 cm wave - length) oriented at 90° to the troughs of the larger ripples (4 cm wavelength). On the right slightly sinuous - crested ripples are shown. Himara Member, section 6, (hammer is 30 cm long).

Plate 5.14. Bedding surface of a fine - grained sandstone showing rain imprints, wrinkle marks and crawling trails. Himara Member, section 7, (pen is 15 cm long).

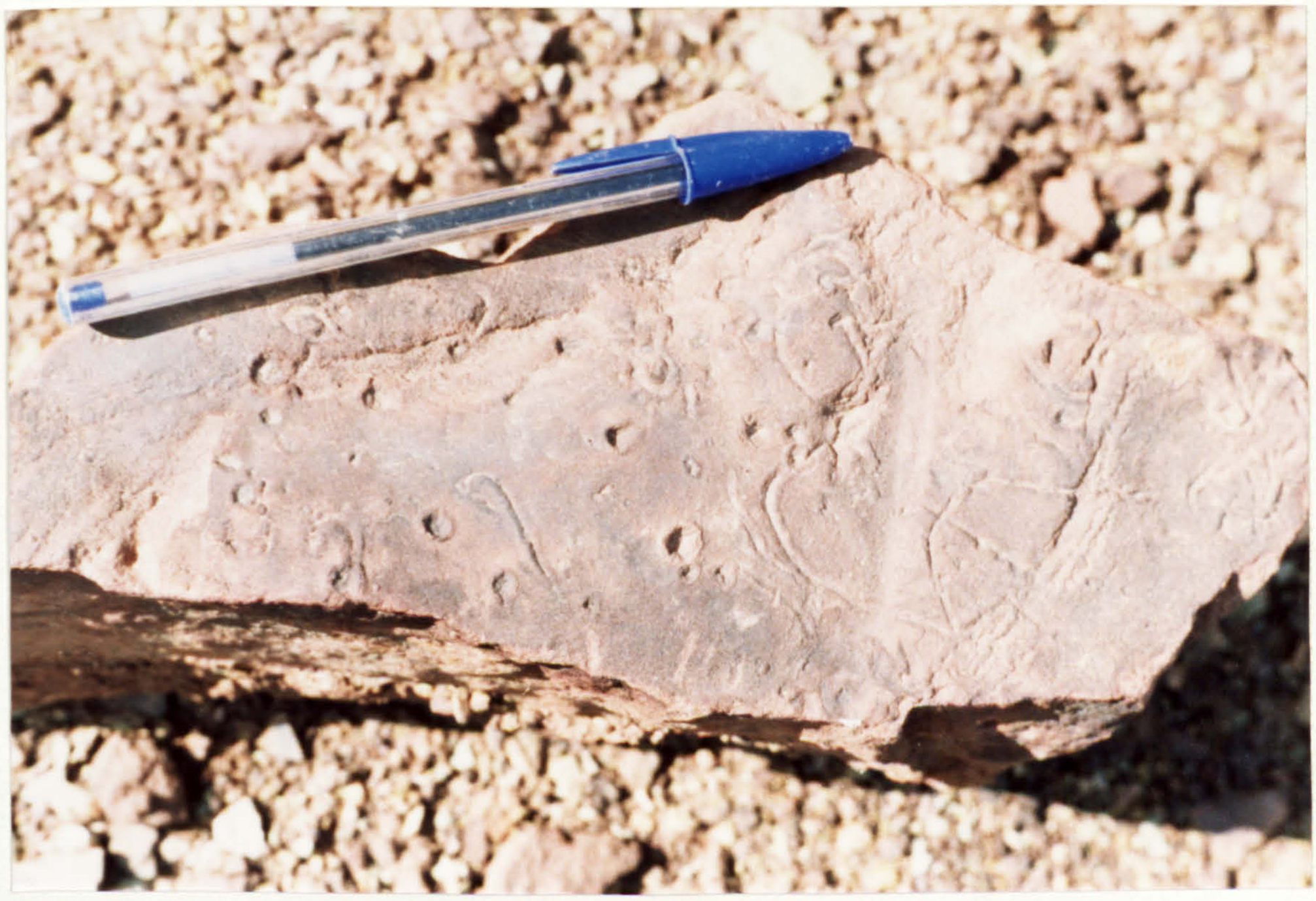

Plate 5.15. Herringbone cross - bedding above sand infilled desiccation cracks, at base of Himara Member. Note rippling and wavy laminations upward, section 1, (pen is 15 cm long).

Plate 5.16. Micro cross - laminations in the lower part of the Himara Member. Below pen is a claystone horizon. Himara Member, section 6, (pen is 15 cm long).

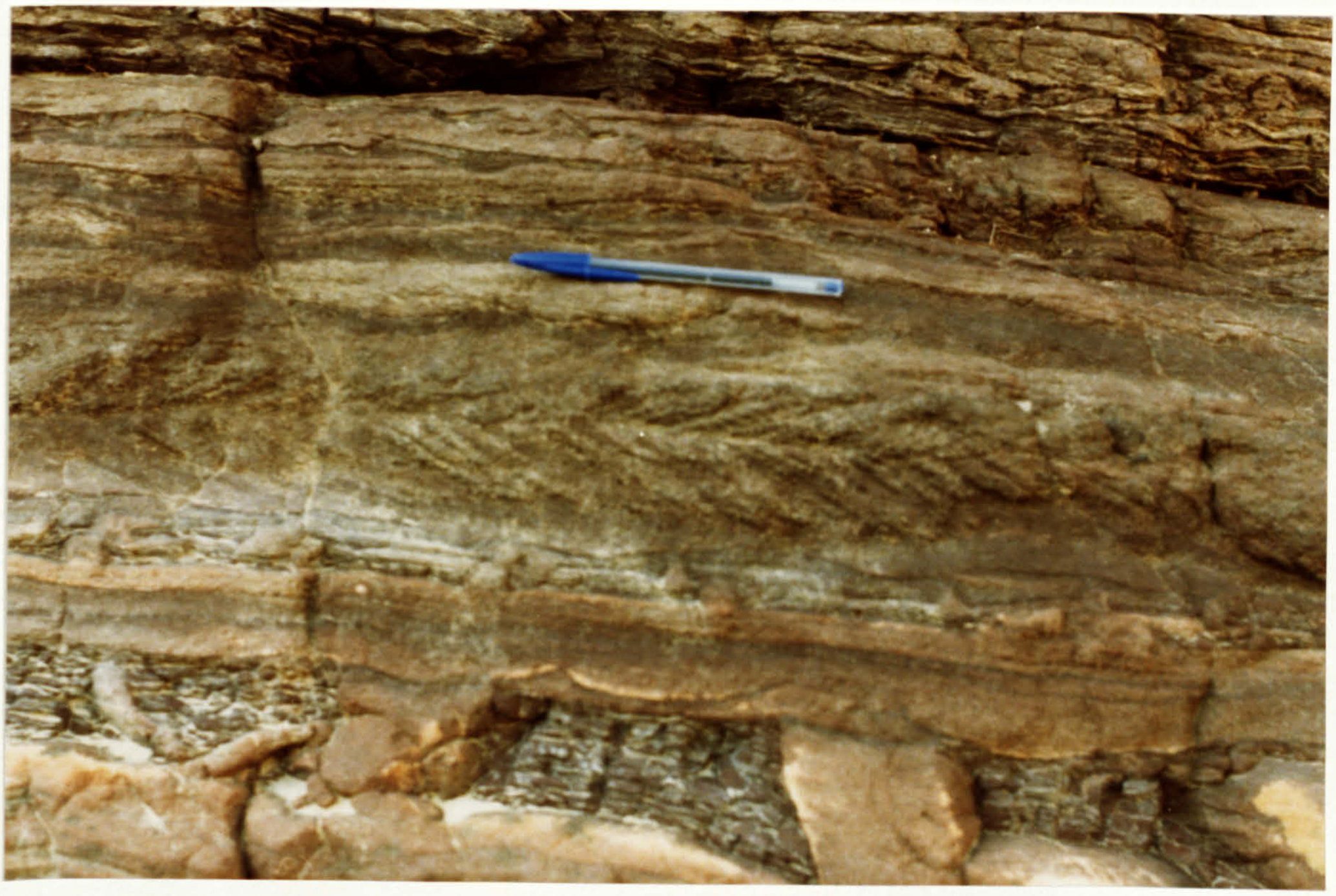

Plate 5.17. Ripple cross - laminations at base passing upward into parallel laminations within a sandstone bed. Himara Member, section 11, (pen is 15 cm long).

Plate 5.18. Bedding surface showing a fossiliferous bed (coquina) composed of bivalves, in the sandy facies of the Himara Member, section 6, (pen is 15 cm long).

Plate 5.19. Silty - shale facies of the Himara Member showing the following sedimentary structures; wavy, rippled, flaser and lent - icular bedding. Note soft sediment deformation features above the pen which may be due to differential compaction (thixotropy) or dewatering processes. Mud draped ripples at the base of pen. Section 1, (pen is 15 cm long).

Plate 5.20. Sequence of interbedded thin sandstone and mudstone exhibiting soft - sediment deformation and balling - up, possibly due to thixotropy. Note rippling and oxidation (red) reduction (cream, greenish) colour of sediments. Himara Member, section 1, (pen is 15 cm long).

Plate 5.21. Interbedded sandstone and shale exhibiting soft - sediment deformation and balling - up, possibly due to thixotropy or a water escape plume. Himara Member, section 4, (hammer is 30 cm long).

Plate 5.22. Bedding surface showing laterally linked and discrete stromatolite structures. Himara Member, section 4. (hammer is 30 cm long).

Plate 5.23. Vertical section showing stacked, linked hemispheroidal stromatolites? Himara Member, section 4, (hammer is 30 cm long).

Plate 5.24. Vertical section showing hemispheroidal stromatolites with clear laminations. Himara Member, section 4, (hammer is 30 cm long).

Plate 5.25. Ripples in alternating sand and silty shale with interbedded deformation structures (balling - up, convolution and pseudonodules) which may be due to thixotropy. Nimra Member, section 11, (pen is 15 cm long).

Plate 5.26. General view showing the upper contact of the Ma'in Formation with the Dardur Formation (arrow). Section 11.

Plate 5.27. Internally rippled rhythmites in the lower part of the Nimra Member, section 11, (hammer is 30 cm long).

Plate 5.28. Alternating calcareous (cream) and non calcareous sandstone (white) comprising the upper part of the Nimra Member. Section 2.

Plate 5.29. Sinuous ripples (symmetrical) on bedding surface, with abundant horizontal burrows, usually along the ripple troughs. Nimra Member, section 1, (pen is 15 cm long).

Plate 5.30. Intrusive igneous sill (at hammer level) embedded between two sandstone layers. Nimra Member, section 1, (hammer is 30 cm long).

CHAPTER SIX

PETROGRAPHY

CHAPTER SIX

PETROGRAPHY

6·1 INTRODUCTION

Thin sections were prepared for petrological analysis from sandstone samples collected from the different stratigraphic levels at the measured section localities. The location of these samples is shown in Fig. 1. 7. Nine samples were collected from the Upper Cambrian, 14 from the Permo-Triassic (Um Irna Formation) and 7 from the Lower Triassic (Ma'in Formation). Samples were labelled with respect to rock formation / member name and locality number. The studied samples are not truly representative of whole lithologies in each stratigraphic unit, and are selected examples from different sections at different levels.

The 30 samples range in size from coarse sandstone to coarse siltstone (Table 6·1). Modal volumetric composition was determined by point counting. Five hundred points were counted from each thin section according to the method of Chayes (1956). Grain size measurements were carried out using the grain size terminology of Wentworth (1922). Grain roundness classes described are based on those of Pettijohn (1972).

6·2 AIM OF THE PETROLOGICAL STUDY

i. To carry out compositional analysis of the rocks under study, using the scheme of McBride (1963) for the classification of

Table 6.1. Texture of rock samples studied, for the different stratigraphic units (Wentworth scale, 1922).

Diameter (mm)	Texture	Cambrian	Permo-Trias. (Um Irna)	Lr. Trias (Ma'in)
1				
	Coarse sand	C 05 14	U 06 05a	
			U 11 00	
			U 13 07	HN 07 23
0.5			U 11 07	
			U 11 04	
	Medium sand		U 06 12	N 07 08
		C 03 16	U 06 04	
		C 00 24	U 06 06	
		C 03 18	U 11 01	N 11 16
0.25		C 03 19	U 06 09	
		C 03 17	U 13 06	N 10 10a/
		C 03 20	U 06 10	
			U 11 05	
	Fine sand			
		C 08 15		H 06 30
		C 03 22		
0.12			U 06 01	
	V. fine sand			H 11 15
				H 07 22
0.06				
				H 07 07
	Coarse silt			

terriginous sandstones. The classification scheme is shown in Fig.6·07.

ii. To make an initial assessment of the mineral compositions of the different stratigraphic units.

iii. To identify the sediment source area and the original pre-exisiting source rocks, and to infer the tectonic conditions of the provenance area at the time of deposition, by the investigation of Q - F - L , Qm - F - Lt , and Q - P - K framework diagrams (Figs. 6· 8 - 6·14, Table 6·3).

iv. To describe the nature of the diagentic process in the different sandstones.

v. To identify any fossil associations present in these rocks.

6·3 COMPOSITION

The composition of framework constituents is described according to the sandstone classification of McBride (1963). Tables A·1 - A·3, 6·2 and Figures 6·,1 - 6· 6 illustrates the modal compositions of the 30 clastic rocks studied, and show the difference in compostions of the rocks at different stratigraphic levels.

6·3·1 UPPER CAMBRIAN SANDSTONES

The Upper Cambrian sandstones show a uniformly high maturity. Their average composition falls in the sublitharenite (45%), litharenite (22%), quartzarenite (11%), subarkose (11%) and feldspathic litharenite (11%), categories of McBride (1963)

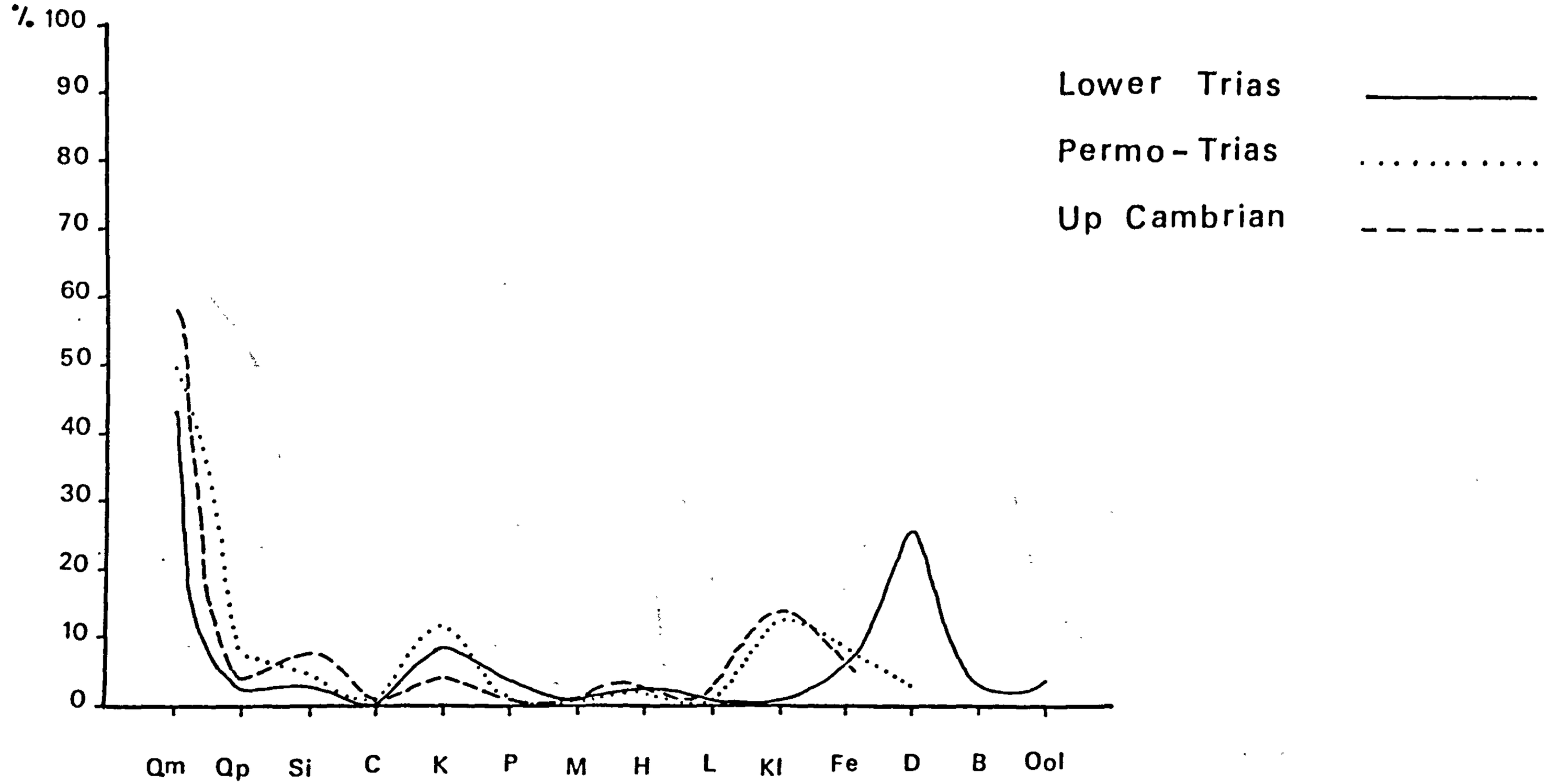

Fig. 6. 1. Frequency curves showing the mineral composition of the Upper Cambrian, Permo - Triassic, and Lower Triassic sandstones (data from Appendix A).

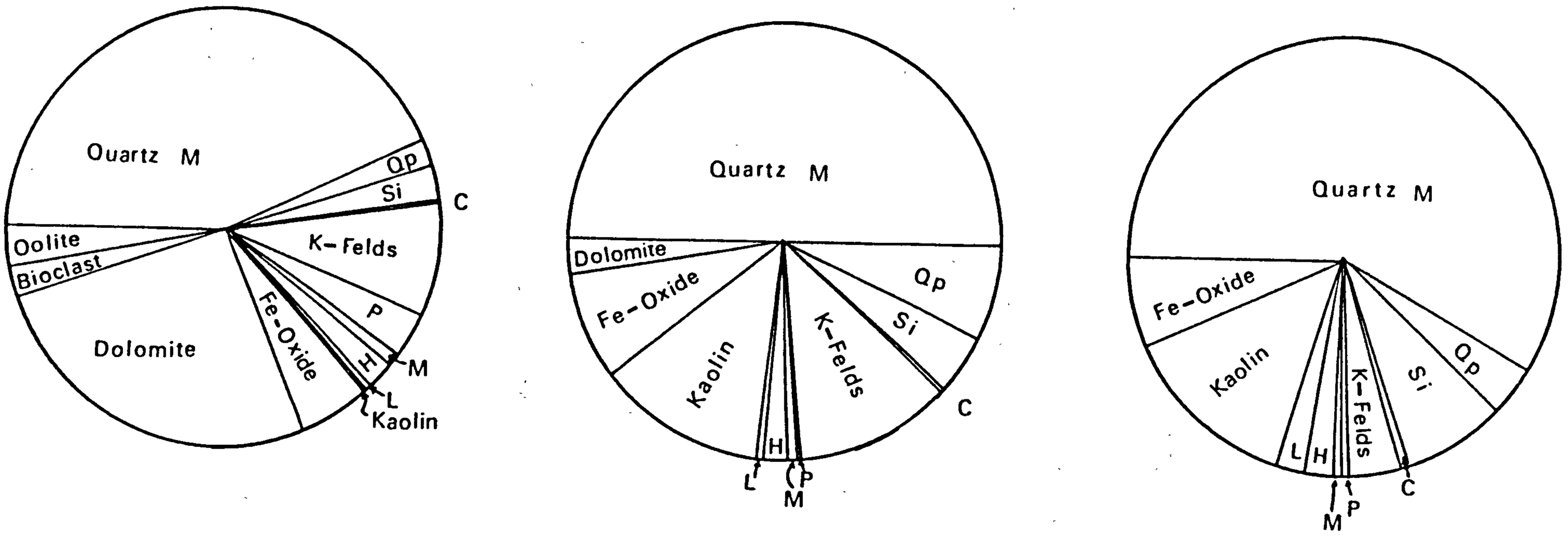

Fig. 6. 2. Pie diagrams showing average composition of the Upper Cambrian, Permo - Triassic, and Lower Triassic sandstones (data from Appendix A).

(Figs. 6· 5 - 1 -, 6· 6 and Table 6·2, Table A·1).

These sandstones are very fine to medium grained (Table 6·1), and well sorted. Individual grains are subangular to subrounded in shape (Plates 6· 1, 6· 2). Quartz is the major component, occuring as primary and secondary, monocrystalline grains usually with syntaxial overgrowth (Plate 6· 1). Quartz grains display uniform and wavy (undulose) extinction. In certain sections (C0317 and C0024) quartz grains show microfractures. Quartz grains with heavy mineral inclusions are frequently met with, others enclose fibrolite. Other forms of silica are present as lithic fragments of polycrystalline quartzite and detrital chert. Chert occurs also as a cement and secondary precipitates of silica. Feldspars are present in some sections in the form of fresh and altered detrital grains, mostly of microcline and orthoclase. Plagioclase is less common. Micaceous flakes are rare, but a few biotite grains are present as inclusions in quartz grains. Among the resistant minerals which can withstand several cycles of transportation zircon and tourmaline are the most abundant, with lesser amounts of rutile, garnet, brookite and opaque minerals. These include ilmenite and iron oxides which occur mainly as magnetite, hematite and limonite. Three coloured varieties of tourmaline are present as detrital (rounded or prismatic) grains or as inclusions in quartz grains: (a) olive green with weak to strong pleochroism; (b) zoned green and blue; and (c) colourless (elbaite).

Zircon grains are common, mostly as well rounded equant elongated grains. Three varieties of zircon are present: (a) elongated grains

Table 6.2

Percentage Of The Sandstone Categories In The Different Rock Units Under Study (Categories Of McBride,1963).

Rock Name	Upper Camb.	Permo Trias.	Lower Triassic H.Mbr	Contact	N.mbr
Quartzarenite	11.0	-	-	100.0	-
Sublitharenite	45.0	28.7	-	-	100.0
Subarkose	11.0	7.1	-	-	-
Litharenite	22.0	7.1	-	-	-
Arkose	-	7.1	100.0	-	-
Lithic Subarkose	-	50.0	-	-	-
Feldspathic Litharenite	11.0	-	-	-	-
Lithic Arkose	-	-	-	-	-
Number Of Samples	9	14	4	1	2

with abnormal high interferance colours, (b) grains with dark boundaries and (c) a very stable variety on which toothed authigenic overgrowths are developed in optical continuity with the detrital zircon.

Cementation is either by the syntaxial overgrowth of quartz which characterizes most of the sections or by iron oxides (mostly hematite) In some sections later diagenetic clay minerals (mostly kaolin) are evident and block the pore spaces (Plate 6· 2).

On the other hand, subarkosic sandstones are well developed in the upper third of the succession at locality 3. These are fine-grained, moderately sorted sandstones with subangular grains. Major components are quartz and feldspars (Table A·1). Quartz is present in primary and secondary forms, with some quartz grains enclosing grains of zircon and tourmaline. Feldspars are very frequent. Both potash and alkali feldspars are common (orthoclase, microcline and plagioclase). Some plagioclase and orthoclase grains are prismatic with parallel sides. Feldspars commonly show alteration; potash feldspars being altered to sericite.

Among the heavy mineral assemblage associated with the feldspathic sandstones zircon, tourmaline, rutile and ilmenite are the most important. Zircon occurs in quartz grains as inclusions or as rounded elongated grains with dark borders. Tourmaline grains are present in prismatic form, as inclusions in quartz grains. Equant and rounded grains of

rutile are present. Opaque minerals are represented in thin section (CO3 16) by some ilmenite grains with later diagenetic leucoxenic overgrowths (Plate 6·3). Cements present consist of silica and subordinate iron oxides. Syntaxial quartz overgrowth is also an important factor in eliminating the intergranular pore space. A clay mineral (kaolin) is mostly fibrous in form and partially fills the pore space (Plate 6· 2).

6·3·2 PERMO - TRIASSIC SANDSTONES (UM IRNA FORMATION)

Permo - Triassic sandstones are mostly lithic subarkoses (50%). Other varieties include sublitharenites (28·7%), arkoses (7%), subarkoses (7%) and litharenites (7%), (Figs. 6· 5-2-, 6· 6 and Table 6·2, Table A·2). In grain size they range from coarse to very fine grained (Table 6·1). They are poorley sorted and comprise subrounded to subangular grains (Plates 6· 5, 6· 6). Intergranular pore spaces are negligible. They contain a slightly higher percentage of feldspars and clay minerals than the Upper Cambrian sandstones. Quartz is still the major component of these sandstones and occurs as mono- and polycrystalline grains usually with syntaxial overgrowths (Plate 6· 5). Detrital chert is also present. The main feldspars present are microcline with minor amounts of plagioclase and orthoclase. They show some alteration. Among the heavy minerals tourmaline, zircon, garnet and opaques are the most frequent, and they usually occur as detrital prismatic or rounded grains, or as inclusions in quartz grains.

Two varieties of tourmaline are present; pleochroic olive green and colourless (elbaite) grains. Biotite is also encountered Chlorite and sericite clay minerals are present after the alteration of ferromagnesian minerals, and kaolin is also present filling the pore spaces and exhibiting fibrous form (Plate 6· 5). The Um Irna sandstones are compact and are usually cemented by syntaxial quartz overgrowths, while secondary ferroan dolomite (rhombic form) and iron oxide cements are also present. Ferroan dolomite rhombs are well developed in a few sections (Plate 6· 7), while in others they are subhedral to anhedral forms. The secondary origin of the dolomite is evidenced by its corrosion of some of the original rock constituents (Plate 6· 7).

6·3·3 LOWER TRIASSIC SANDSTONES (MA'IN FORMATION)

These are represented in the studied thin sections by two members: Himara and Nimra.

1. Himara Member.

The coarse fraction of the Himara Member comprises maroon coloured very fine sandstones to coarse siltstones of arkosic composition (Figs. 6· 3, 6· 4, 6· 5 - 3-, 6· 6, and Tables A·3, 6·2). Individual grains are predominantly subrounded to subangular in shape. The major component of these sections is quartz. The feldspars present are microcline, orthoclase and plagioclase. They generally show signs of alteration but occasional fresh grains are present (Plate 6· 9).

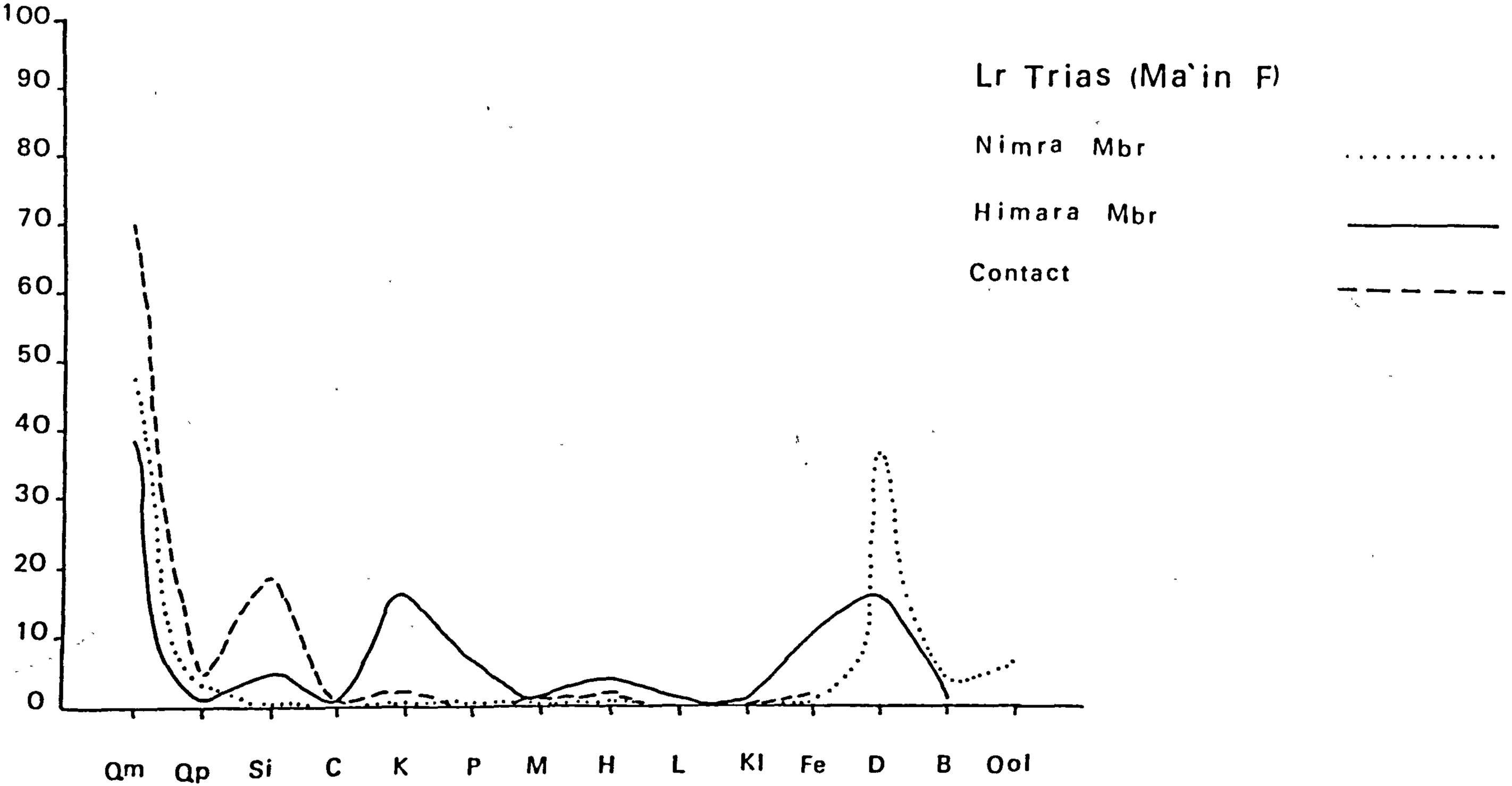

Fig. 6. 3. Frequency curves showing the mineral composition of the Lower Triassic sandstones (Himara Nimra contact). Data from Appendix A.

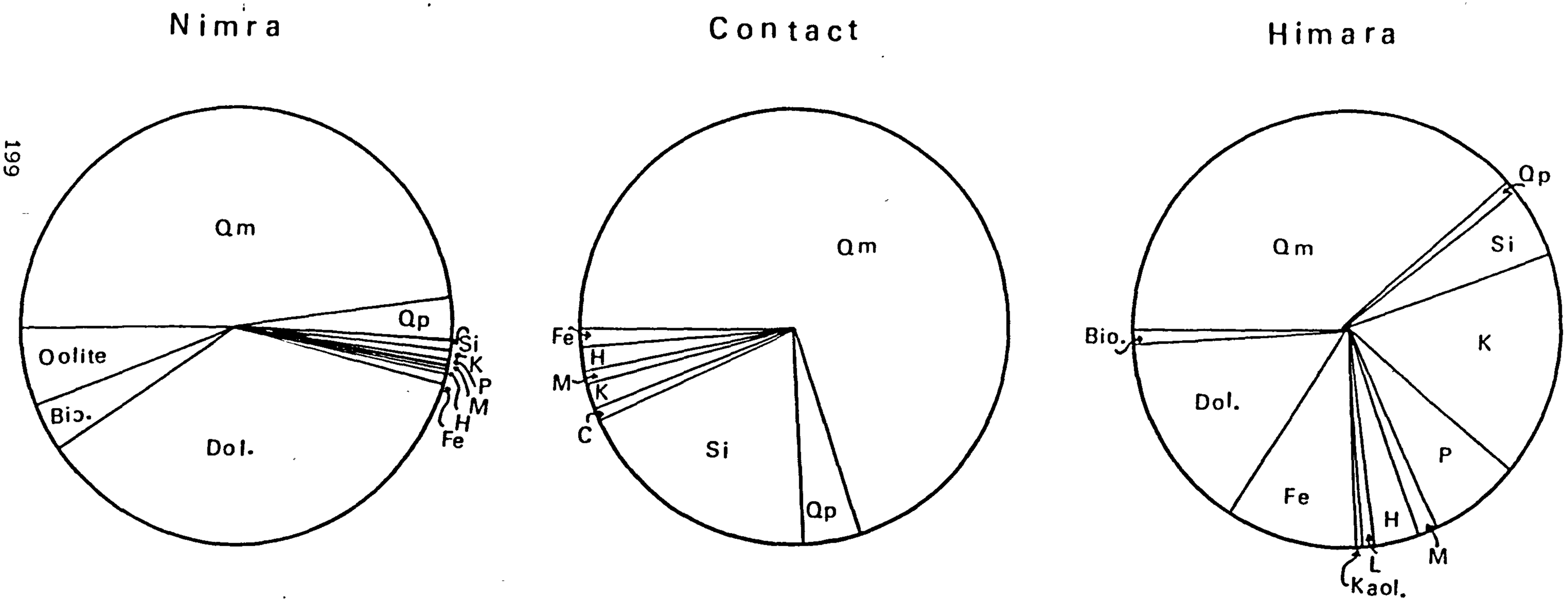

Fig. 6. 4. Pie diagrams showing the average composition of the Ma'in Formation (Himara Nimra contact). Data from Appendix A.

Micas are represented by greenish flakes of biotite and elongated flakes of muscovite usually showing some flexuring and plastic deformation, probably caused by compaction. The heavy minerals present are tourmaline, zircon, rutile, staurolite and opaques. Tourmaline is represented by two varieties possessing different colours: green and yellow. The green coloured tourmaline is strongly pleochroic. Zircon is present as rounded grains. Rutile is present with etched surfaces. A partially altered greenish amphibole grain is also present. Later diagenetic clay minerals occupy pore spaces. They are mostly kaolin, with occasional chlorite grains. Unidentified fossil remains (foraminifera ?) are also present but they are badly preserved. Cementation is due to silica or carbonates (mostly dolomite) or both, with subordinate iron oxides (Table A·3). The carbonate in this member may be derived from the alteration of the fossil material. Two kinds of concretions occur: carbonate concretions (section H 07 22), and iron oxide concretions (section H 11 15).

A thin section (HN 07 23) from a single horizon located approximately at the contact between the two members of the Ma'in Formation consists largely of subrounded quartz grains and is of quartzarenite composition. Quartz occurs as mono - and polycrystalline grains (nearly 95%), which usually display wavy twinning. Detrital chert and cryptocrystalline silica are also present in the intergranular pore space; mostly as cementing material, with subordinate iron oxides. Carbonate material is totally lacking in this single sample. Plagioclase and microcline

are also rarely present, and biotite grains occur as inclusions in the quartz grains. Heavy minerals are represented by tourmaline and epidote? as detrital grains and inclusions in quartz (Figs. 6·3, 6·4 6· 5 - 3 -, and Tables A·3, 6·2).

2. Nimra Member

The proportion of carbonate and fossil remains to terrigenous material increases in this member. As a result these samples fall into the calcarenaceous orthoquartizite class of Pettijohn (1957 p.404). They range in size from coarse siltstones to medium sandstones (Table 6·1) with subangular to subrounded grain shapes (Plates 6·11 - 6·14). The major component is quartz which is generally found as floating grains (slightly exceeding 50%) within the carbonate cement (Plates 6·11 - 6·14). Heavy minerals are negligible except for a few grains of zircon and tourmaline (elbaite). The carbonate components present are: fossils, ooliths, micrite and dolomite. Fossils present include algal remains, zoned and infilled by micrite (Plates 6·13, 6·14). Lamellibranch fragments are present and partially or completely dissolved (Plates 6·11, 6·14). Foraminifera are also present as large fusiforms (Plate 6·11), in addition to echinoid spines. Bryozoan and gastropod fragments are common and usually show some obliteration and recrystallization (Plate 6·12). Calcareous ooliths are present as single or composite forms, usually with quartz or carbonate nuclei. They display an outer concentric structure (Plate 6·13). Carbonates

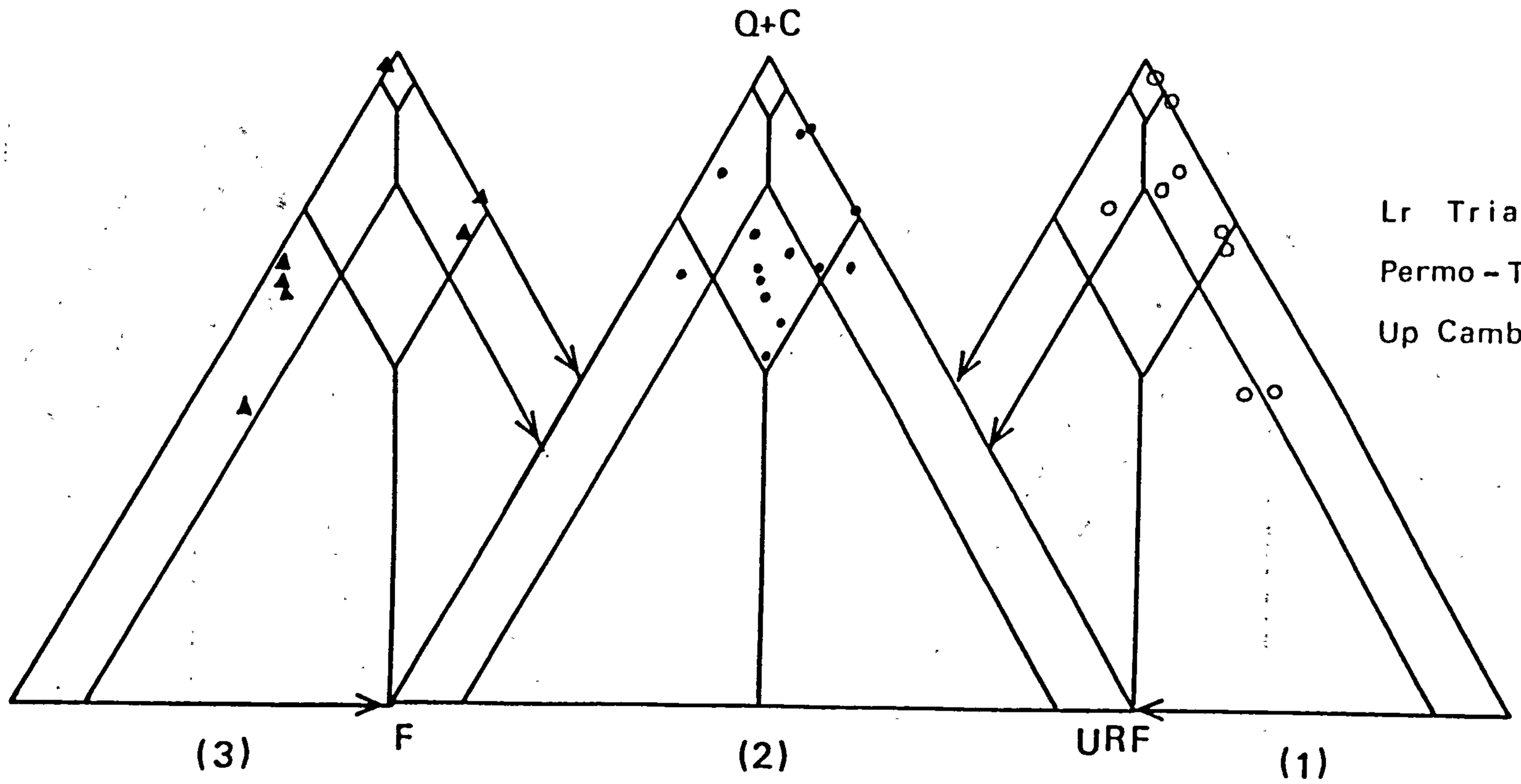

Fig. 6. 5. Triangular diagrams showing the classification of : (1) Upper Cambrian, (2) Permo - Triassic, and (3) Lower Triassic sandstones. Data from Appendix A.

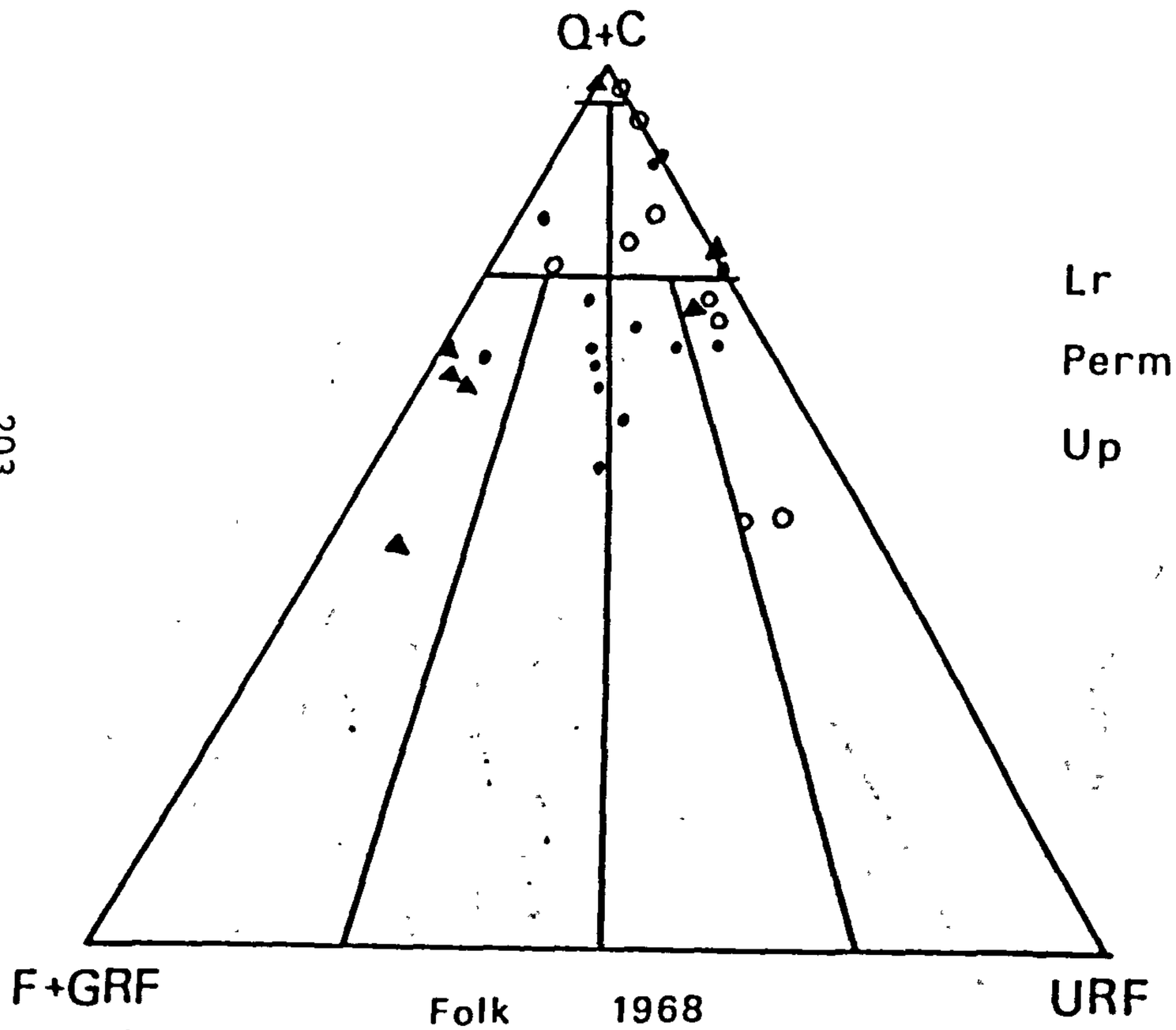

Lr Triassic ▲

Permo - Triassic ●

Up Cambrian o

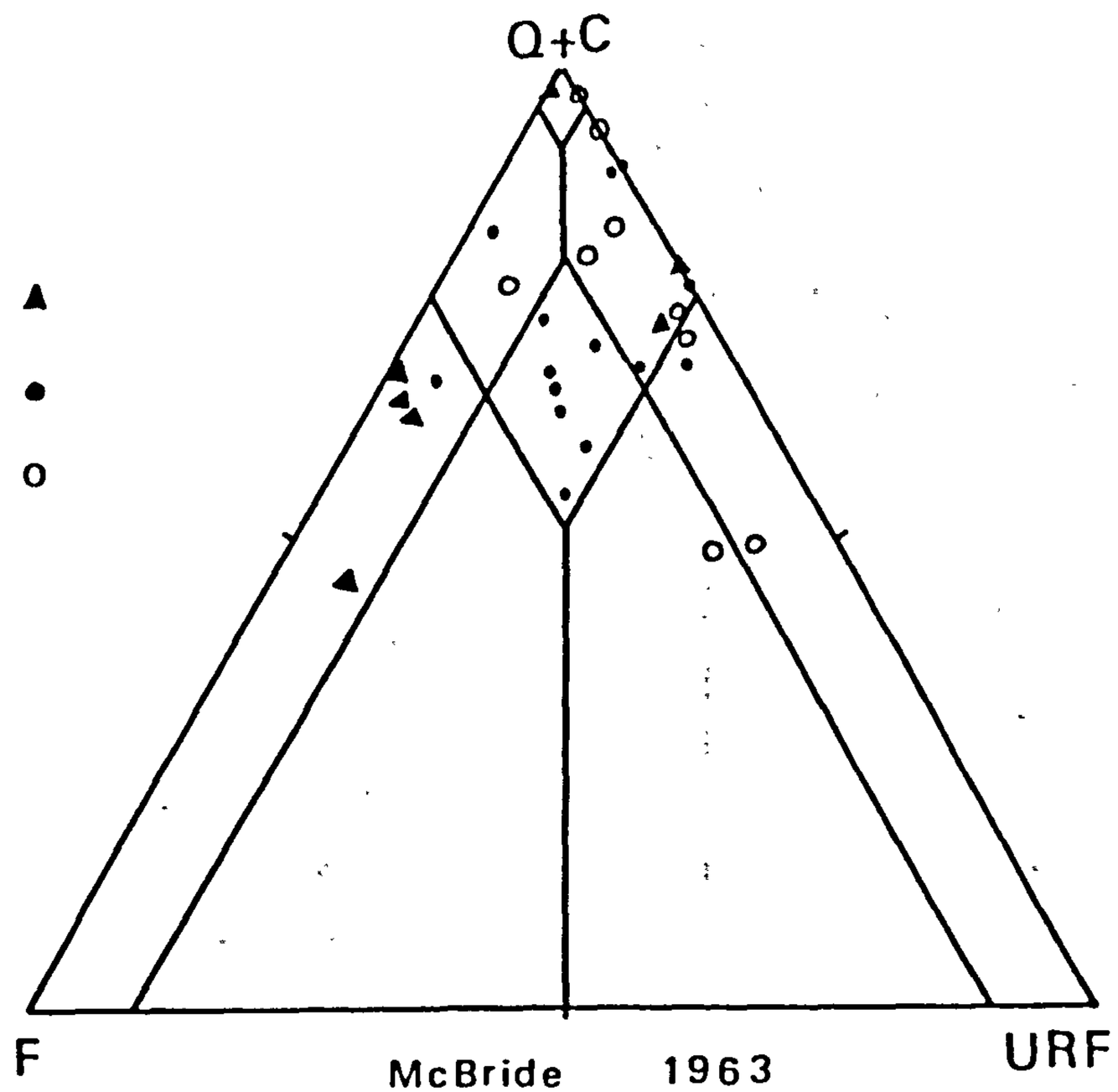

Fig. 6. 6.. Triangular diagrams of McBride (1963) and Folk (1968) showing the distribution of the Upper Cambrian, Permo - Triassic, and Lower Triassic sandstones. Data from Appendix A.

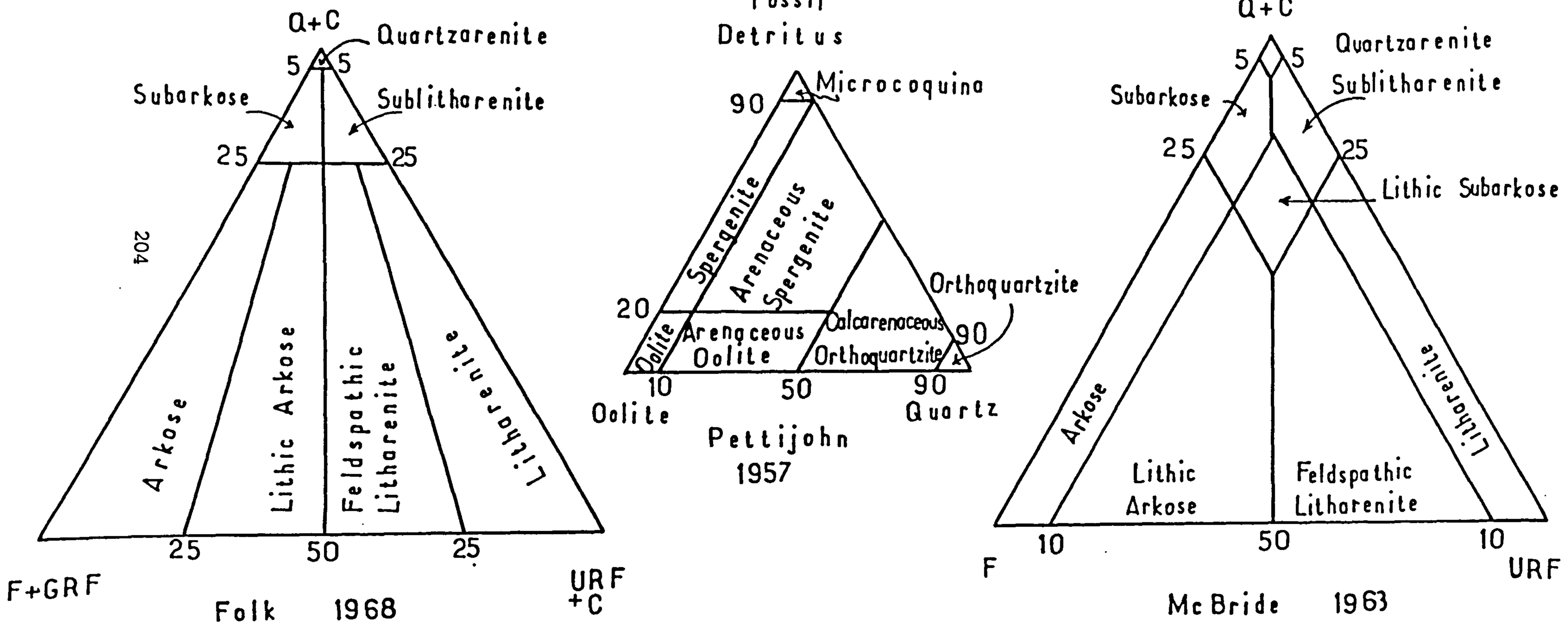

Fig. 6.7. Classification schemes used for the sandstones under study. McBride, 1963; Folk, 1968 and Pettijohn, 1957.

are subjected to further recrystallization. Cementation is usually due to ferroan dolomite. Some dolomite concretions were formed enclosing quartz grains.

6·4 DIAGENESIS

6·4·1 INTRODUCTION

The diagenetic behaviour of sandstones during progressive burial is controlled largely by framework composition and original depositional texture, in addition to a complex set of boundary conditions including the nature of the interbedded strata, the local geothermal gradient, the rate of burial, the chemistry of the pore fluids and the hydrodynamic setting (Dickinson and Suczek, 1979).

Authigenic cementing minerals are abundant in most thin sections, and include quartz overgrowths, several forms of dolomite, clay minerals and leucoxenic overgrowths.

Of all the chemical processes involved the most important one is the interaction between solid mineral grains and pore fluids. Because the bulk and mineral compositon of the solid changes only slowly and slightly during diagenesis, most of the sequence of diagenetic events inferred from petrographic evidence must be related to evolutionary changes in pore water chemistry (Pettijohn et al.,

1972; Blatt et al., 1980).

6·4·2 QUARTZ CEMENT

Cementation of the Upper Cambrian sandstones and the Permo-Triassic sandstones (Um Irna Formation) is mainly by syntaxial quartz overgrowth (ranging from 0·2 - 14 percent in Upper Cambrian sandstones, 0 - 11·6 percent in the Permo - Triassic sandstones, 0·4 - 8·2 percent in the lower part of the Lower Triassic sandstones "Himara Member", and 0 - 1·6 percent in the upper part of the Lower Triassic "Nimra Member"). These overgrowths are usually recognised in thin section by a dust film between the detrital grain and the overgrowth, which shows crystallographic continiuty and occasional euhedral facets.

Silica precipitation may have occured in the subsurface where silica-charged water has been mixed with water of greater salinity. Quartz overgrowth may be precipitated as the product of crystallization from a supersaturated pore solution passing over detrital quartz surfaces. Another possibility is that the quartz may be a precipitate of the excess silica released by the hydrolysis of nearby feldspar grains by water containing carbon dioxide (Pettijohn et al., 1972).

6·4·3 CARBONATE CEMENT

Dolomite is the dominant carbonate cement, mostly with a significant

iron content. It is present as a pore filling sparry, granular and rhombic dolomite, and probably represents recrystallization products of earlier deposited and dissolved skeletal fragments and ooliths. In the Lower Triassic sandstones (Ma'in Formation), dolomite cement ranges from 11·6 - 31·4 percent in the Himara Member, and 30·8 - 42·8 percent in the Nimra Member. Dolomite is also observed in a few samples (28% of the samples studied) of the Permo - Triassic sandstones (Um Irna Formation) and ranges from 0·2 - 21·4 percent. Dolomite cement is totally absent from the Upper Cambrian sandstones.

Carbonate cement apparently replaced much of the original quartz grains in the Nimra sandstones. The most frequently encountered texture in these sandstones is the etching and embayment of detrital grains by carbonates (Plate 6·13). The typical replacement of quartz by calcite implies that the pore waters must be undersaturated with respect to quartz and supersaturated with respect to calcite (Pettijohn et al., 1972).

Calcareous ooliths range from 6·4 to 11·6 percent in the Nimra Member. Dissolution of the interior of ooliths both nucleus and many of the precipitated ring coatings, is a common phenomenon. Sometimes only the outer rings and cement appear to outline the original spherical shape of the particle (Blatt et al., 1980).

6·4·4 AUTHIGENIC CLAYS

Kaolin is the most commonly recognised authigenic clay in the

Upper Cambrian sandstones (0·6 - 34·2 percent), and the Permo - Triassic sandstones (0·2 - 25 percent), while it is negligible in the Lower Triassic sandstones (0 - 1 percent).

The authigenic clays occluding pore spaces have the appearance of radial fibres and booklets in most cases (Plates 6· 2, 6· 5). The kaolin determinations in Permo-Triassic samples have been confirmed by X-ray diffraction analyses. They are referred to in this study as kaolin, but Schneider et al., (1984) using EDAX - analysis interpreted the clay as halloysite.

Authigenic clays occur as pore linings, pore - filling and replacement clays (Wilson and Pittman, 1977) and can partially or completely replace detrital grains or infill voids left by dissolution of detrital grains. Feldspar can be partially to completely replaced by or dissolved and later infilled by kaolin (Wilson and Pittman, 1977).

A minor part of the kaolinite is probably the result of in situ alteration of feldspar. Some feldspar grain surfaces remain undisturbed. Similar phenomena have been described by Dypvik and Vollset (1979). As a result of this transition from feldspar to kaolin , silica was liberated and may have been precipitated as cement in other parts of the sediments (Dypvik and Vollset, 1979). In contrast to this mode of formation, the kaolin in pore spaces has been precipitated from

silica and alumina enriched solutions in the sediments (Dypvik and Vollset, 1979). For such a precipitate to have formed by direct precipitation, the entering solution must have carried both dissolved silica and alumina. Dissolved silica is generally mobilised as monomeric silicic acid H_4SiO_4 (Pettijohn et al., 1972).

6·5 FRAMEWORK CONSTITUENTS

Quartz grains are grouped according to optical properties into monocrystalline grains with undulatory or nonundulatory extinction and polycrystalline grains. The concentration of monocrystalline quartz grains far exceeds that of polycrystalline quartz in all rocks under study. Detrital grains were counted separately.

Total quartz is high and decreases steadily upward from Upper Cambrian to Lower Triassic. Monocrystalline quartz shows the same trend; polycrystalline quartz increases in Permo - Triassic sandstones but with its lowest proportion found in the Ma'in Formation. The proportion of feldspar increases towards the top of the succession. The highest proportion of feldspar occurs in the Himara Member (12·3%), while, in the Um Irna it constitutes 11·8% The lowest proportion of feldspar is found in the Upper ~~Middle~~ Cambrian sandstones (5%). In the samples studied the order of abundance is microcline > orthoclase > plagioclase. Ma'in sandstones tend to be slightly more feldspathic and slightly less lithic than Um Irna sandstones. The content of quartz

grains is generally comparable in both terrains. In general, all sandstones studied are rich in quartz and poor in rock fragments (Tables A·1 - A·3).

6·6 MODAL COMPARISONS

Dickinson and Suczek (1979) classifed all provenance and derivative sandstone suites into three general groups: (1) continental block, for which sediment sources are on shields and platforms or in faulted basement blocks; (2) magmatic arc, for which the sources are within active arc orogens of isolated arcs or active continental margins; and (3) recycled orogen, for which sources are deformed and uplifted stratal sequences in subduction zones, along collision orogens, or within foreland fold thrust belts (Fig. 6· 8)

To display the data resulting from point counting (Tables A·1 - A·3) three triangular compositional diagrams (Figs. 6· 8 - 6·14), each of which involves a different set of grain populations (B·1 - B·3, C·1), were used to differentiate the three sandstone groups; namely, Upper Cambrian, Permo - Triassic and Lower Triassic.

1. In the Q - F - L triangular diagram (Fig. 6· 8 right), where all the quartz grains are plotted together, the emphasis is on grain stability, and thus on weathering, provenance relief, and transport mechanism as well as source rock (Dickinson and Suczek, 1979).

Triangular Diagram	Uppermost Pole	Lower Left Pole	Lower Right Pole
Q-F-L	Q Quartzose grains (=Qm + Qp)	F Feldspar grains (= P + K)	L Lithic fragments
Qm-F-Lt	Qm Monocrystalline quartz grains	F (same as above)	Lt Total lithic frag. (= L + Qp)
Qm-P-K	Qm (same as above)	P Plagioclase grains	K K-Feldspar grains

Table 6.3. Definition of grain populations for triangular compositional diagrams.

In this diagram all three groups plot closest to the Q pole. Cambrian sanstones plot in the field of recycled orogenic provenance, except for one out of the nine samples which plots in the continental block provenance (craton interior). In the case of Permo-Triassic sandstones 86% of the samples plot in the field of recycled orogenic provenance, and 14% plot in the continental block provenance (Transitional zone). The Lower Triassic samples are split into two fields; the samples of the lower part (Himara Member) plot in the field of continental block provenance (uplifted basement zone), while the samples of the upper part (Nimra Member) plot within the recycled orogenic provenance. Only one quartzarenite sample of the Ma'in Formation (HN 07 23) representing the contact between both members plots in the continental block provenance (craton interior).

2. The Qm - F - Lt triangular diagram (6·08, 6·09) shows that where all lithic fragments are plotted together the emphasis has shifted towards the grain size of the source rocks, because finer grained rocks yield more lithic fragments in the sand size range (Dickinson and Suczek, 1979).

In this diagram all three groups plot closest to the Qm pole, but the Upper Cambrian sandstone samples are the most quartzitic. Qm proportions are 58% in the Upper Cambrian samples, 49·8% in the Permo-Triassic samples and 43% in the Lower Triassic samples. This richness in quartz reflects the fact that stable or mature grains in these

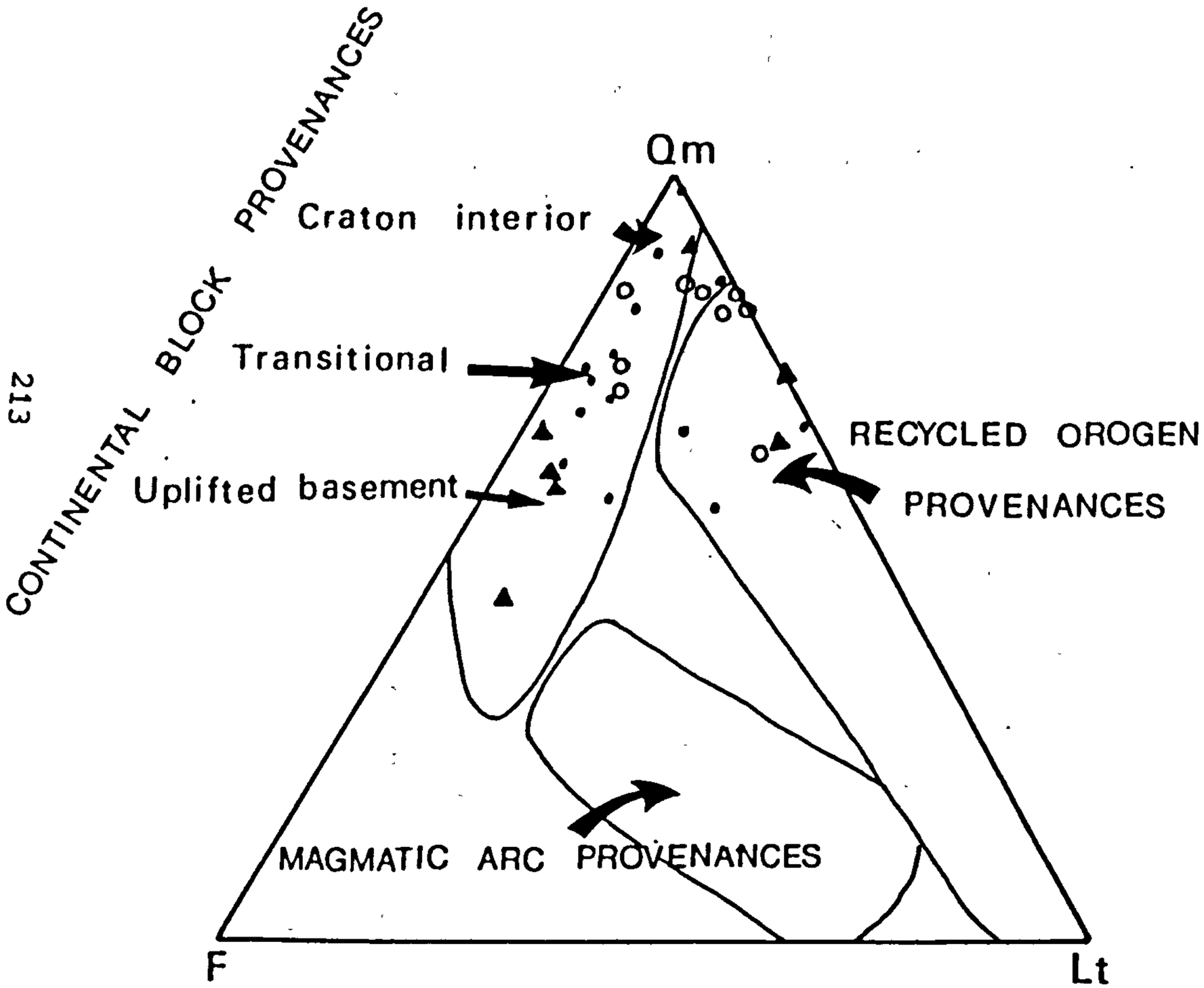

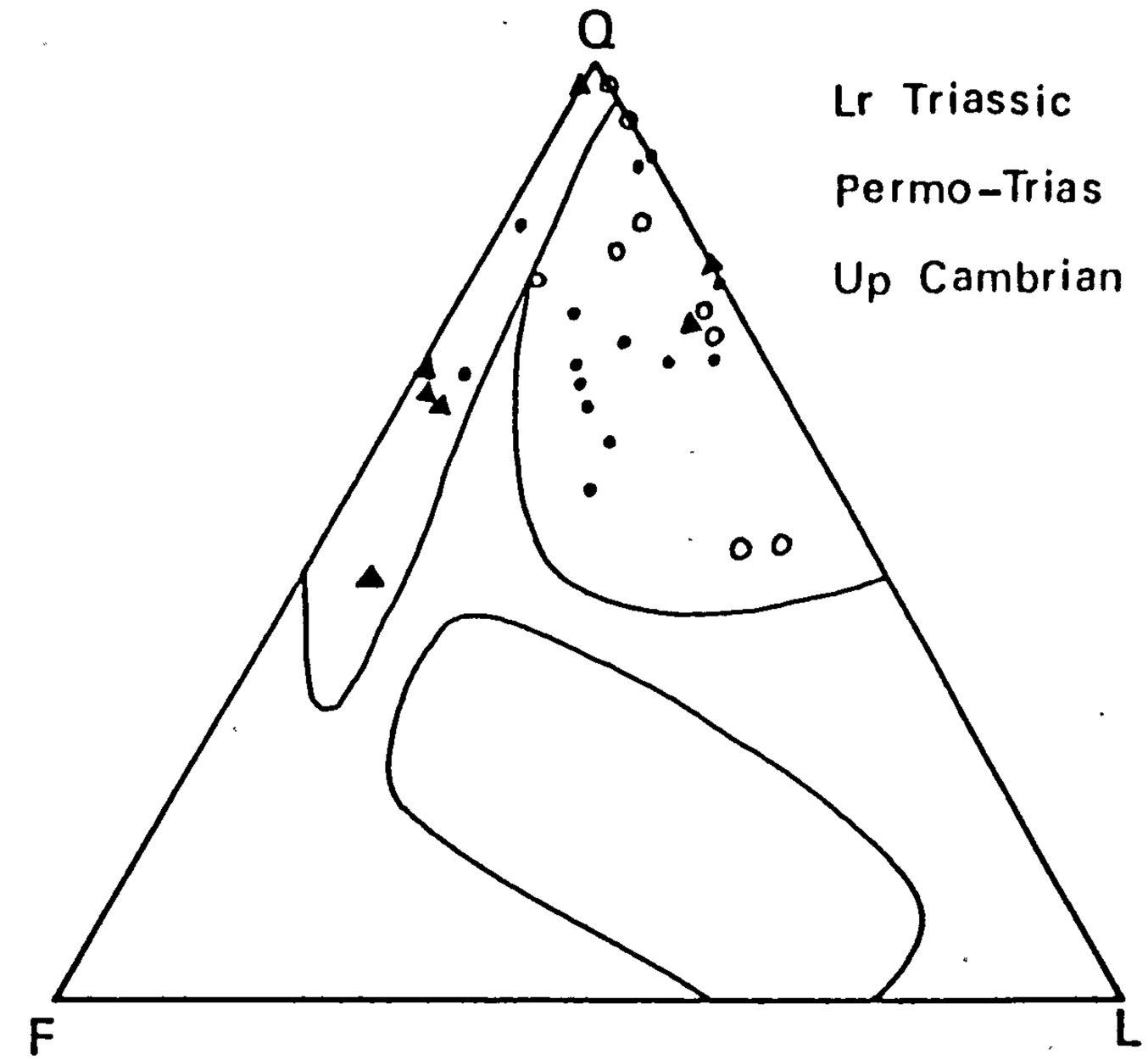

Fig. 6.8. Q - F - L (right) and Qm - F - Lt (left) framework modes of the sandstones from the Upper Cambrian, Permo - Triassic, and Lower Triassic. Data from Appendix B.

rocks are mainly monocrystalline quartz grains. All samples studied plot in the recycled orogenic and continental block fields and probably reflect mature and stable provenances.

3. The Qm - P - K triangular diagram (Figs. 6.10, 6.11), shows only partial grain populations, but reveal the character of the monocrystalline components of the framework. In this diagram, the Permo-Triassic samples plot along or near the Qm - K axis with little or no plagioclase present. The Upper Cambrian group plot closest to the Qm pole along or near the Qm - K axis. The Lower Triassic samples display admixtures of both P - and K - feldspars, although K is more abundant than P, Qm is the most abundant.

Triangular diagrams showing framework proportions of quartz, the two feldspars, polycrystalline quartz, lithics, and unstable lithics of volcanic and sedimentary origin successfully distinguish the key provenance - types. They distinguish quartzose sands from continental cratons, arkosic sands from uplifted basement blocks, volcaniclastic lithic sands and more complex volcano - plutonic sands derived from magmatic arcs. Recycled orogenic sands, rich in quartz or chert plus other lithic fragments derived from subduction complexes, collision orogens, and foreland uplifts (Dickinson and Suczek, 1979). Crook (1974) and Schwab (1975) have shown previously that quartz - rich rocks are associated typically with passive continental margins, that quartz - poor rocks are mostly of volcanogenic derivation from magmatic island

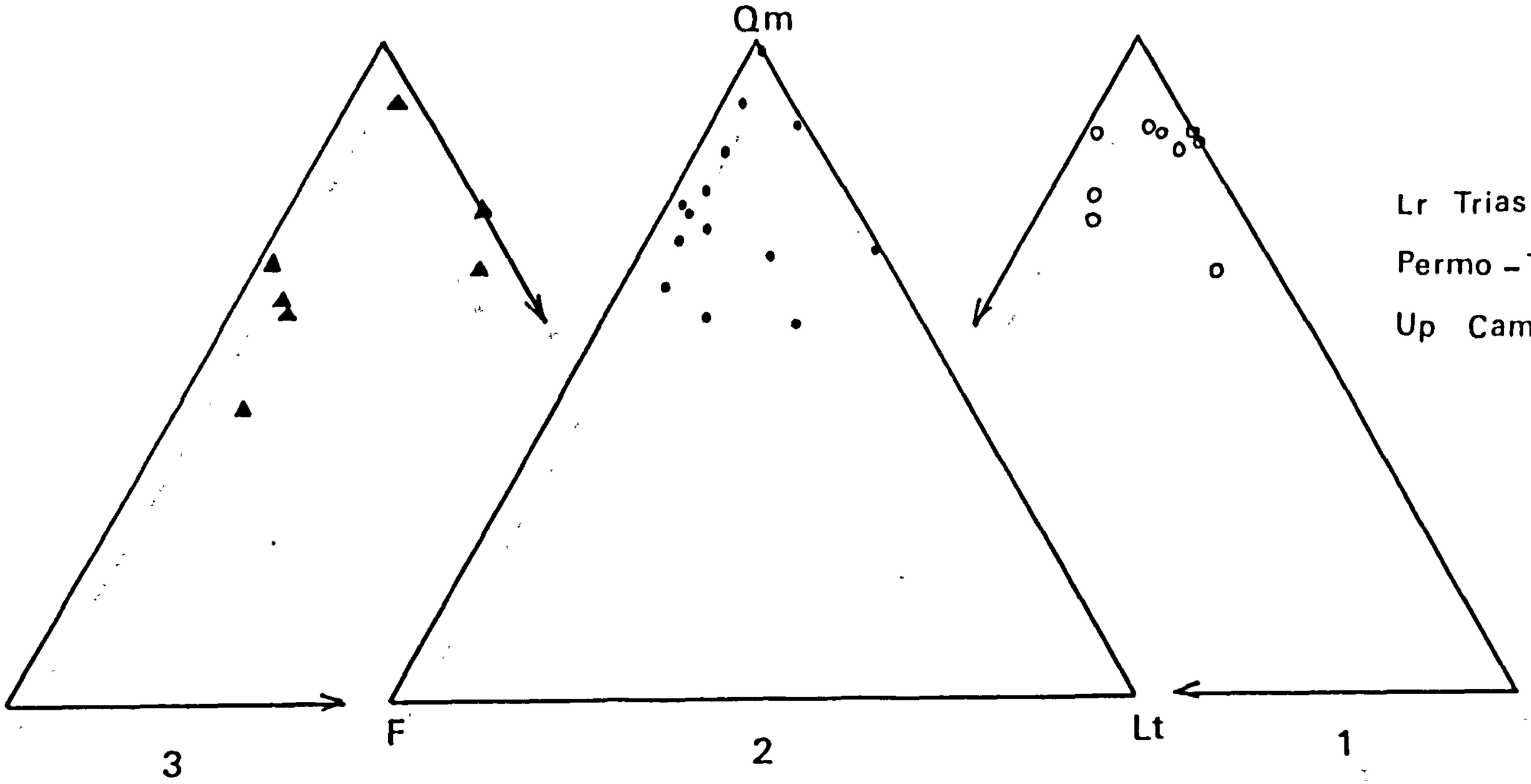

Fig. 6. 9. Qm – F – Lt triangular diagrams showing framework modes of (1) Upper Cambrian, (2) Permo – Triassic, and (3) Lower Triassic. Data from Appendix B.

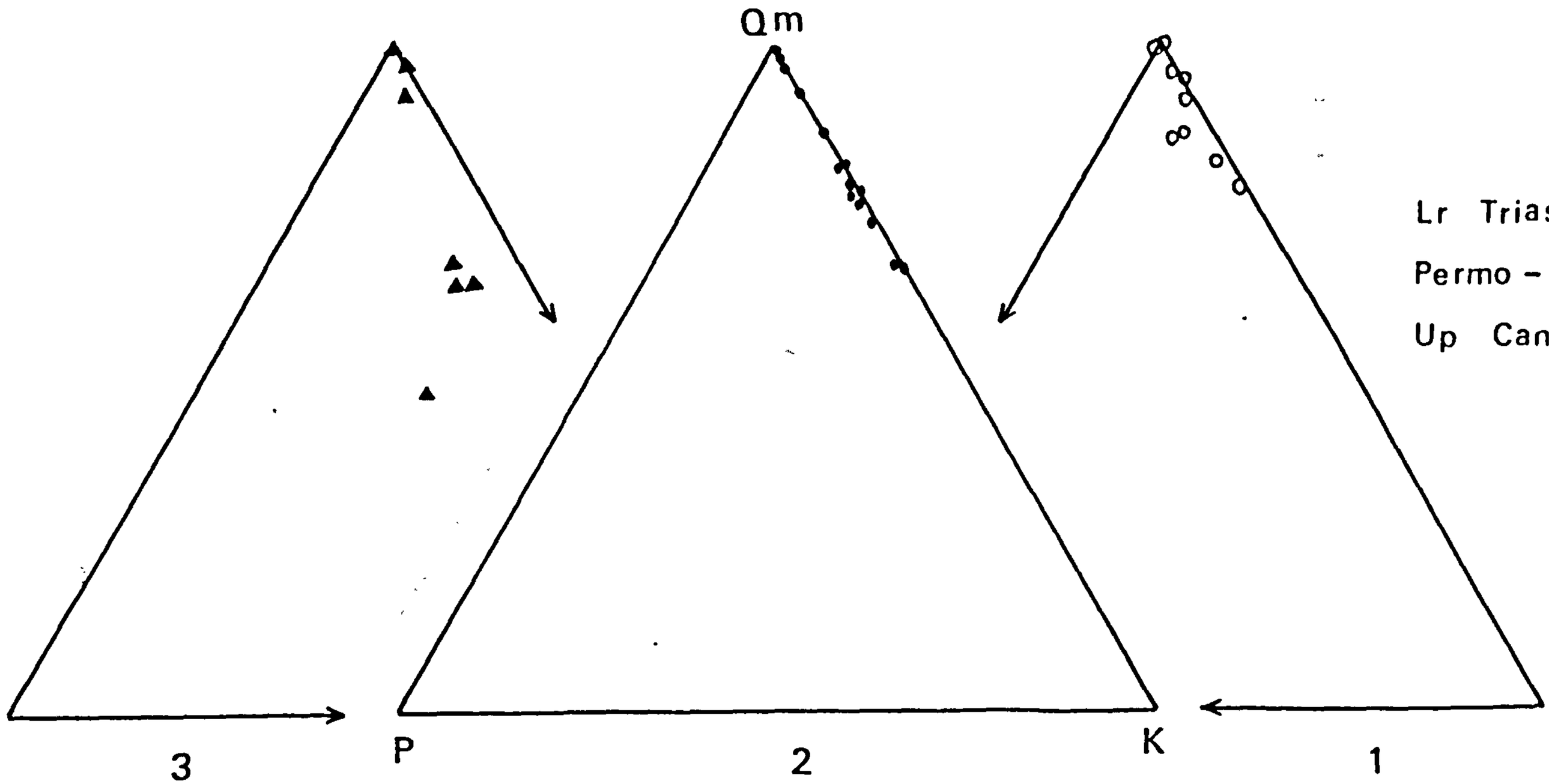

Fig. 6.10. Qm – P – K triangular diagrams showing framework modes of (1) Upper Cambrian, (2) Permo – Triassic, and (3) Lower Triassic sandstones. Data from Appendix B.

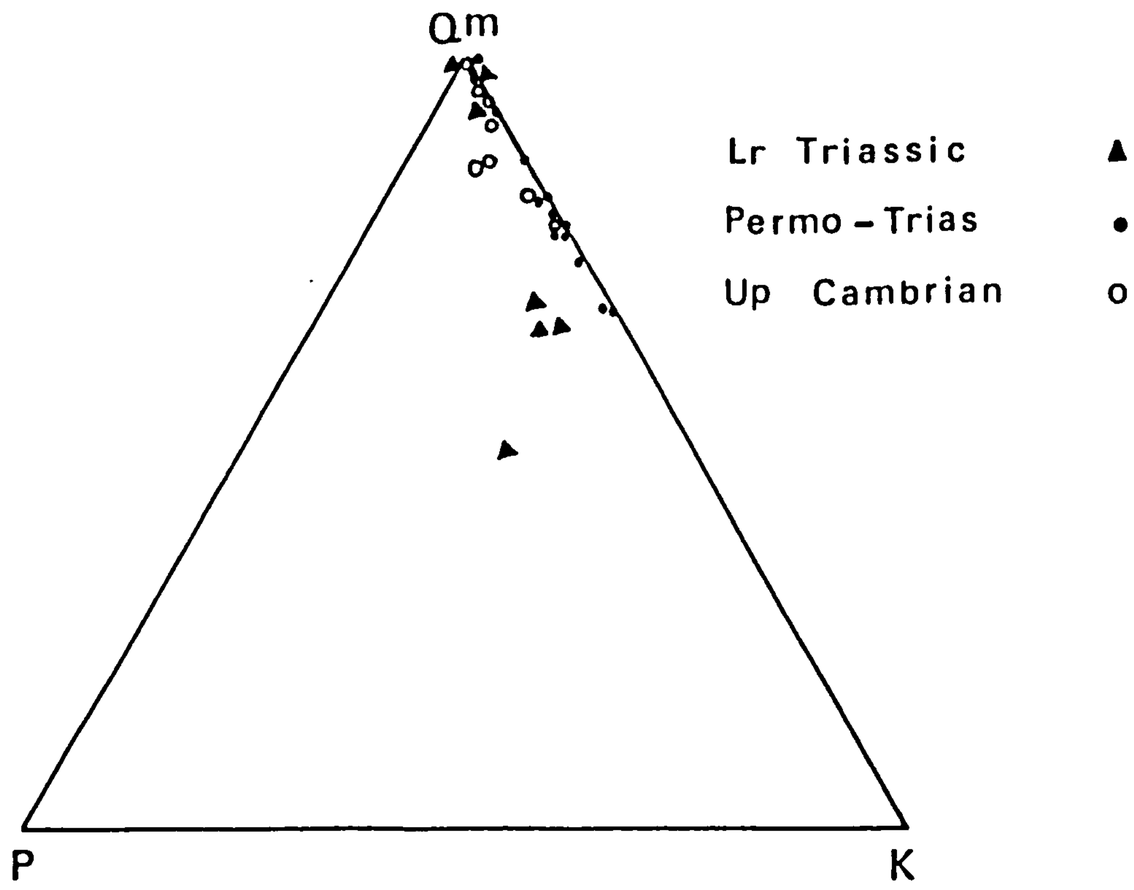

Fig. 6.11. Triangular Qm - P - K plot showing framework modes of the Upper Cambrian, Permo - Triassic, and Lower Triassic sandstones. Data from Appendix B.

arcs, and that rocks of intermediate quartz content are associated mainly wiht active continental margins or other orogenic belts. Dickinson (1982) shows that stable cratons yield quartz-rich sands that typically contain more K - feldspar than plagioclase.

6·7 PROVENANCE

Sandstone composition is influenced by the character of the sedimentary provenance, the nature of the sedimentary process within the depositional basin, and the kind of dispersal paths that link provenance to basin. The key relations between provenance and basin are governed by plate tectonics, which thus ultimately controls the distribution of different types of sandstone (Dickinson and Suczek, 1979).

The mineral constituents in a derived sediment are determined by its rock source. Thus the mineralogy of these sandstones under study provides the best indication of source rock composition, particularly quartz types and the less stable mineral species such as calcic plagioclase and ferromagnesian minerals. The crystallinity of quartz (mono- and polycrystalline types), its extinction, effects of stress and strain and the associated heavy mineral suite provide useful guidelines to provenance location and composition.

The ratio of monocrystalline to polycrystalline quartz grains

is 58 to 3·8 percent in the Upper Cambrian sandstones, 49·8 to 7 percent in the Permo - Triassic sandstones and 43 to 2·1 percent in the Lower Triassic (Tables A·1 - A·3). The ratio of K - feldspar to plagioclase grains is 4 / 0·5 percent in the Upper Cambrian sandstones, 11·6 to 0·2 percent in the Permo - Triassic sandstones, and 8·6 to 3·5 percent in the Lower Triassic sandstones. The relative abundance of quartz and potash feldspar, the maturity of these sandstones with a high ratio of monocrystalline to polycrystalline quartz grain displaying mainly uniform extinction with occasional undulatory extinction, and the noticeable absence of ferromagnesian minerals suggest that the source rocks were crystalline igneous and metamorphic rocks of acidic to intermediate composition, or that they were derived from pre-existing older clastic sedimentary rocks. Krynine (1946) attributed great significance to quartz types. Nonundulatory quartz grains were attributed to plutonic igneous source rocks, and undulatory, strained and polycrystalline quartz grains were thought to represent metamorphic source rocks. Seemingly, undulatory and polycrystalline quartz grains are less stable than nonundulatory quartz and are selectively destroyed during recycling of sediment (Andersen and Picard, 1974).

The overall reduced labile grain content relative to the increased quartz content may suggest the reworking of a first cycle sediment thus indicating a multicyclic origin. Though the composition of the Permo - Triassic and Lower Triassic is less mature than the Upper Cambrian sandstones, it can be assumed that both of them were derived

from the same provenance field during the whole sedimentation period.

The results obtained from the palaeocurrent data (Figs. 7· 6) indicates transport from the southeastern provenance areas, were the crystalline, granitic and metamorphic basement rocks of the Arabian Nubian Shield are located.

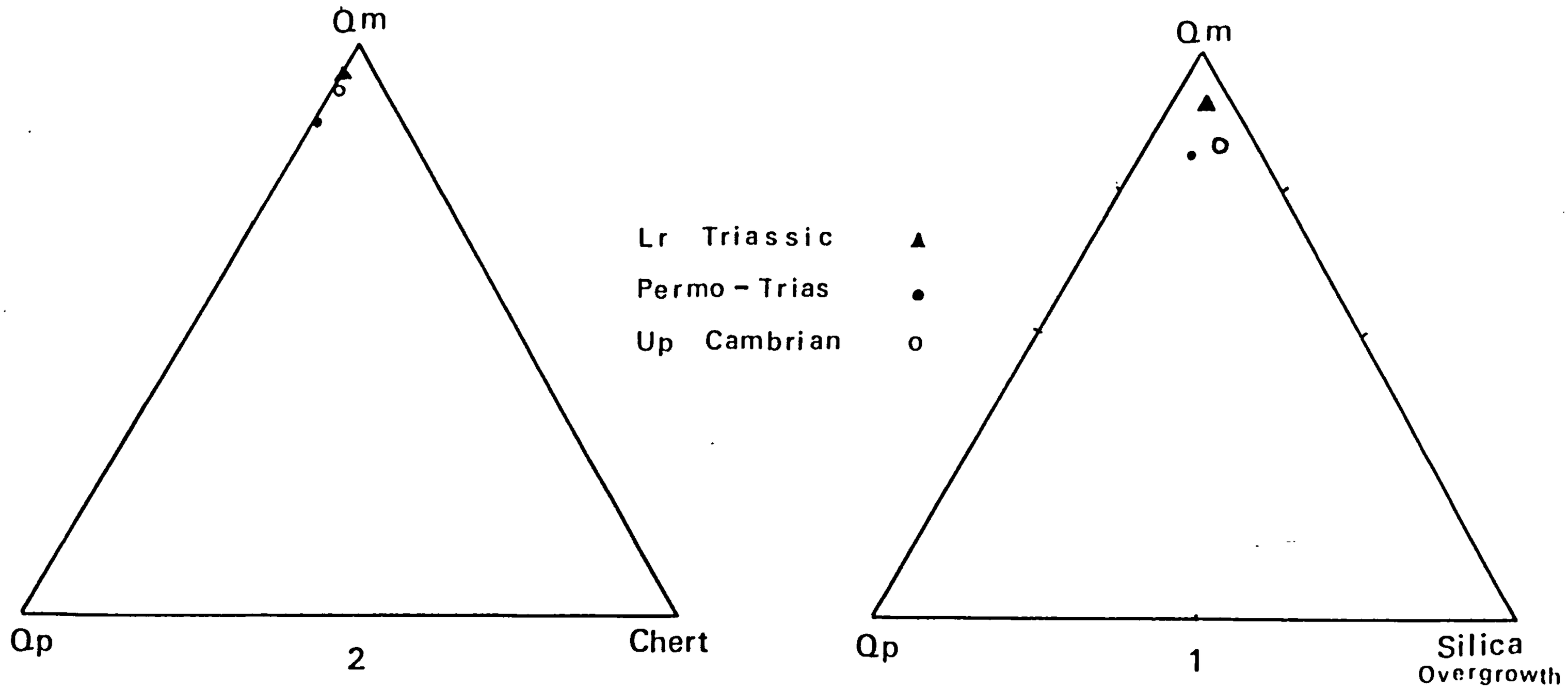

Fig. 6.13. Triangular diagrams showing the relation of: (1) Qm - Qp- Silica overgrowth, and (2) Qm - Qp - Chert, in the Upper Cambrian, Permo - Triassic and Lower Triassic sandstones. Data from Appendix 'C.

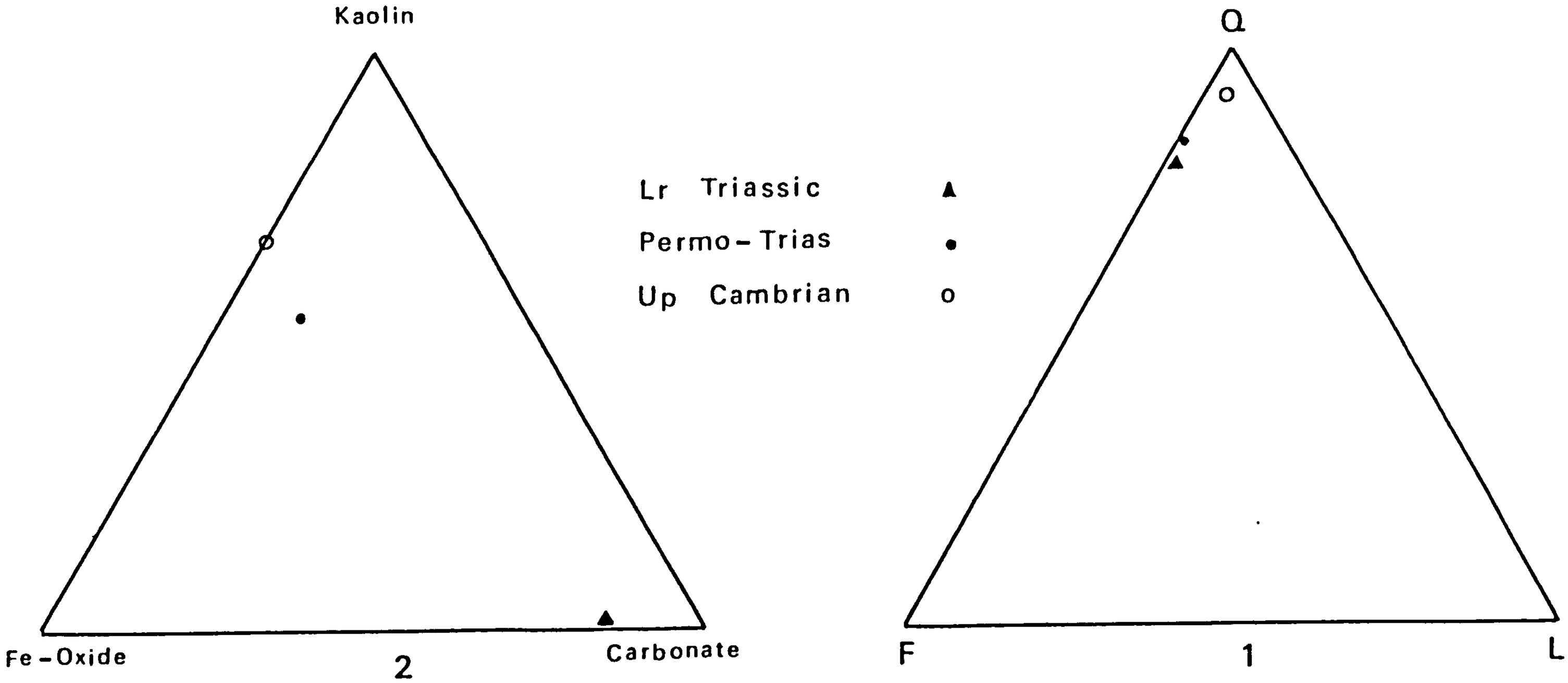

Fig. 6.14. Triangular diagrams showing (1) Q - F - L plot showing mean framework modes of Upper Cambrian, Permo - Triassic, and Lower Triassic sandstones. Data from Appendix B (2) Triangular diagram showing the relation between iron oxide, kaolin, and carbonates in the Upper Cambrian, Permo - Triassic, and Lower Triassic sandstones. Data from Appendix C.

Plate 6. 1. Photomicrograph of a medium - grained well - sorted quartzarenite (nearly 96 percent quartz), with well - rounded to sub - rounded quartz, cemented by quartz overgrowth in optical continuity with the detrital grains. The boundaries between detrital core and overgrowth are made very distinct by a continuous line of "dust" particles (commonly clay minerals). Polarised light, sample No. C 0514.

Plate 6. 2. Photomicrograph of a fine - grained moderately well-sorted sublitharenite. Quartz grains are subangular and highly interlocked fabric due to large amount of quartz overgrowth cements. Intergranular pore space is infilled mainly by iron oxide cement and kaolin (fibrous) matrix (centre). Quartz overgrowths are also visible. Crossed polars, sample No. C 03 20.

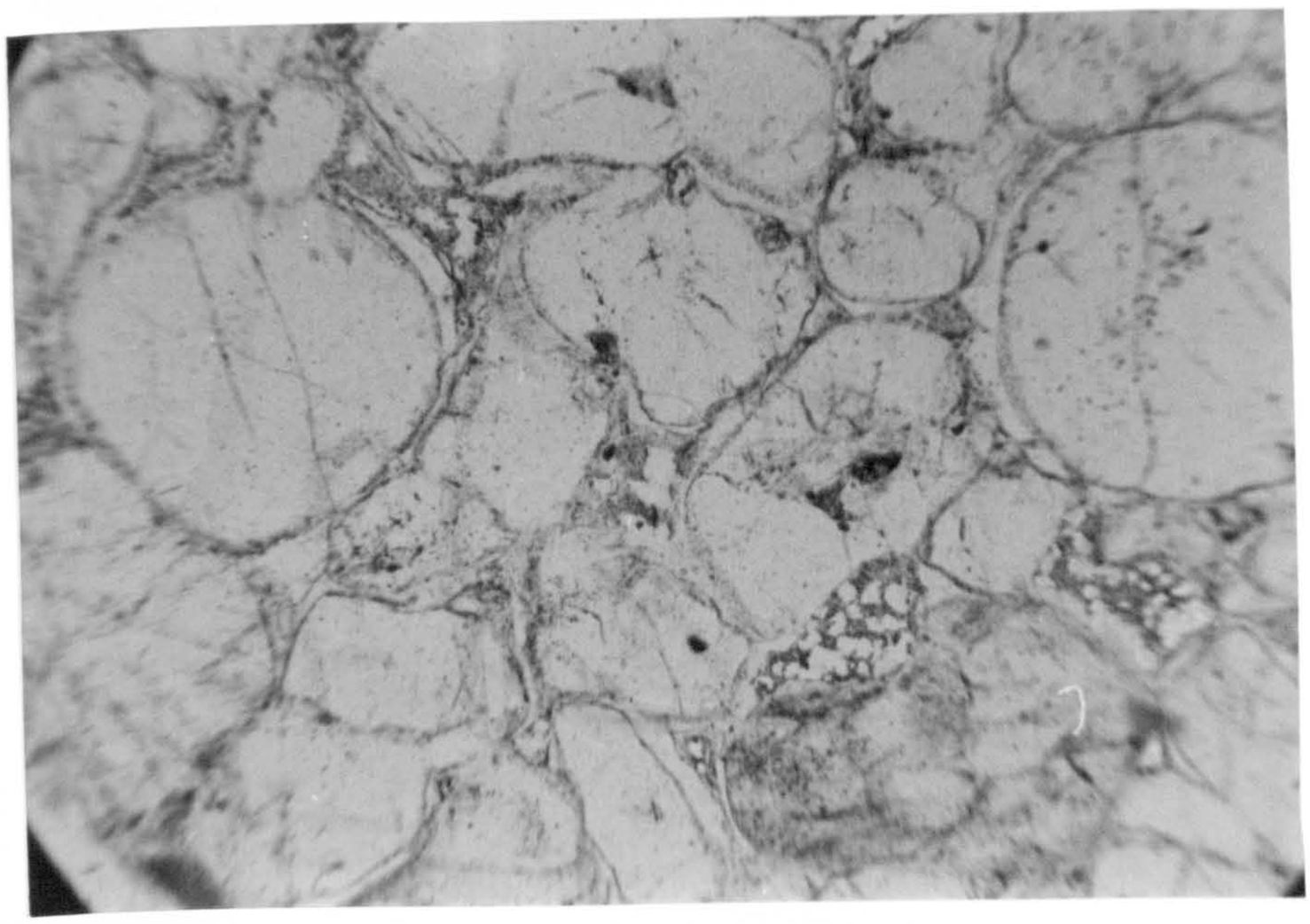

0.7 mm

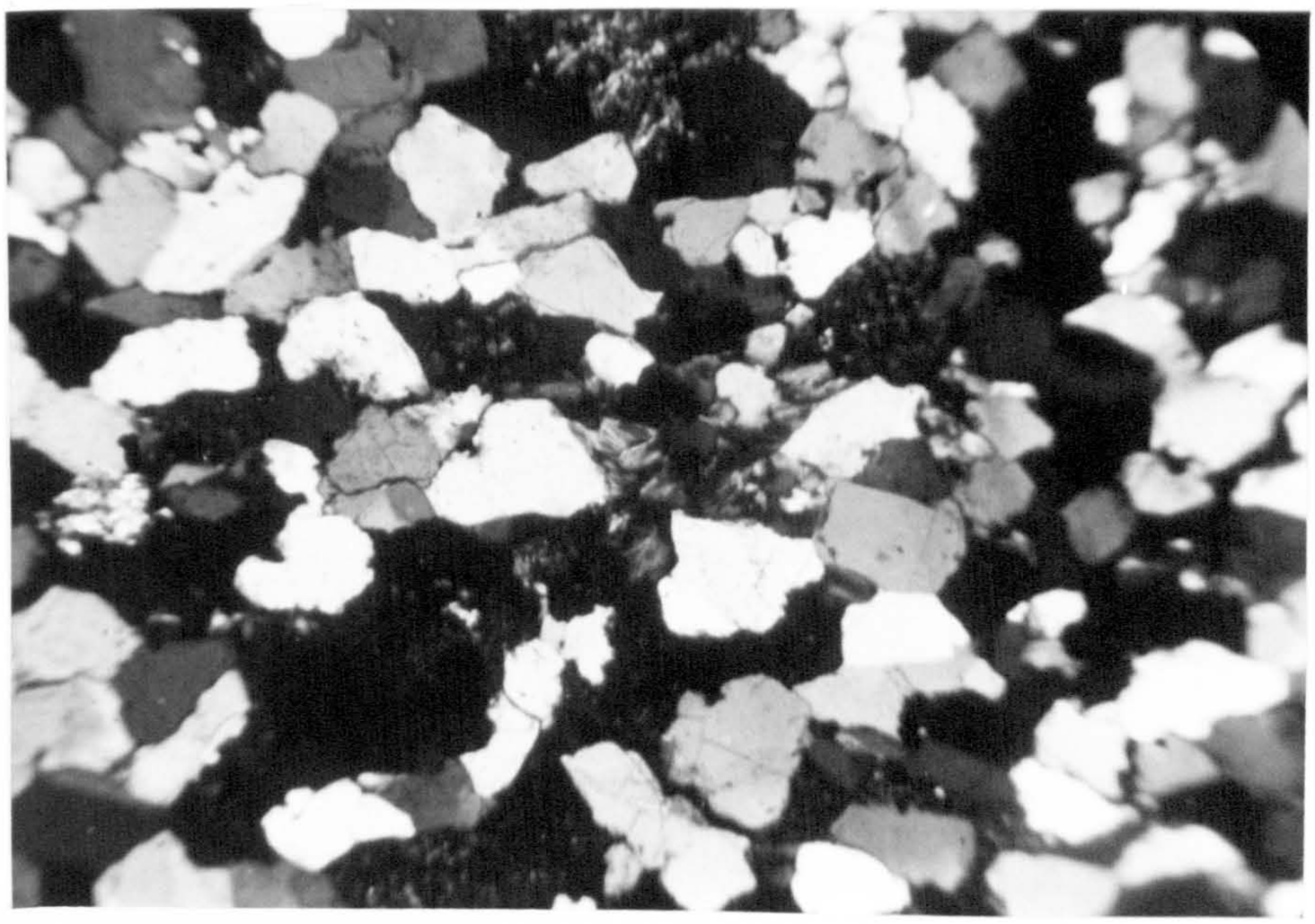

0.2 mm

Plate 6. 3. Photomicrograph showing a grain of ilmenite (black, centre), with secondary overgrowths giving rise to the formation of leucoxene (colourless) with euhedral toothed form. Polarised light sample No. C 03 16.

Plate 6. 4. Photomicrograph of a ferruginous pisolitic siltstone of the Um Irna Formation, showing a ferruginous pisolite with quartz nuclei. The matrix is mostly kaolin (white) and iron oxides (black). Polarised light,sample No. U 12 01.

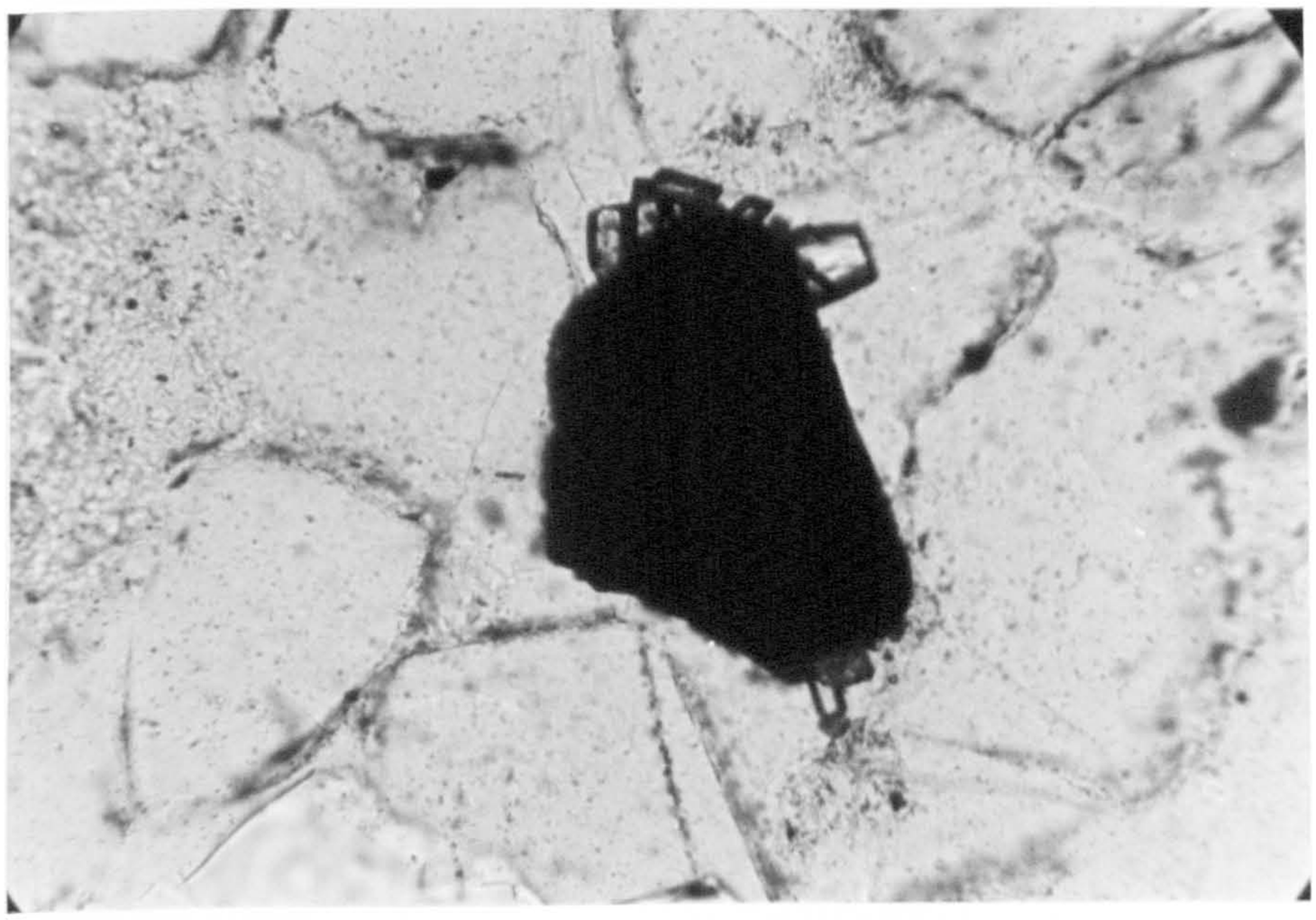

0.25 mm

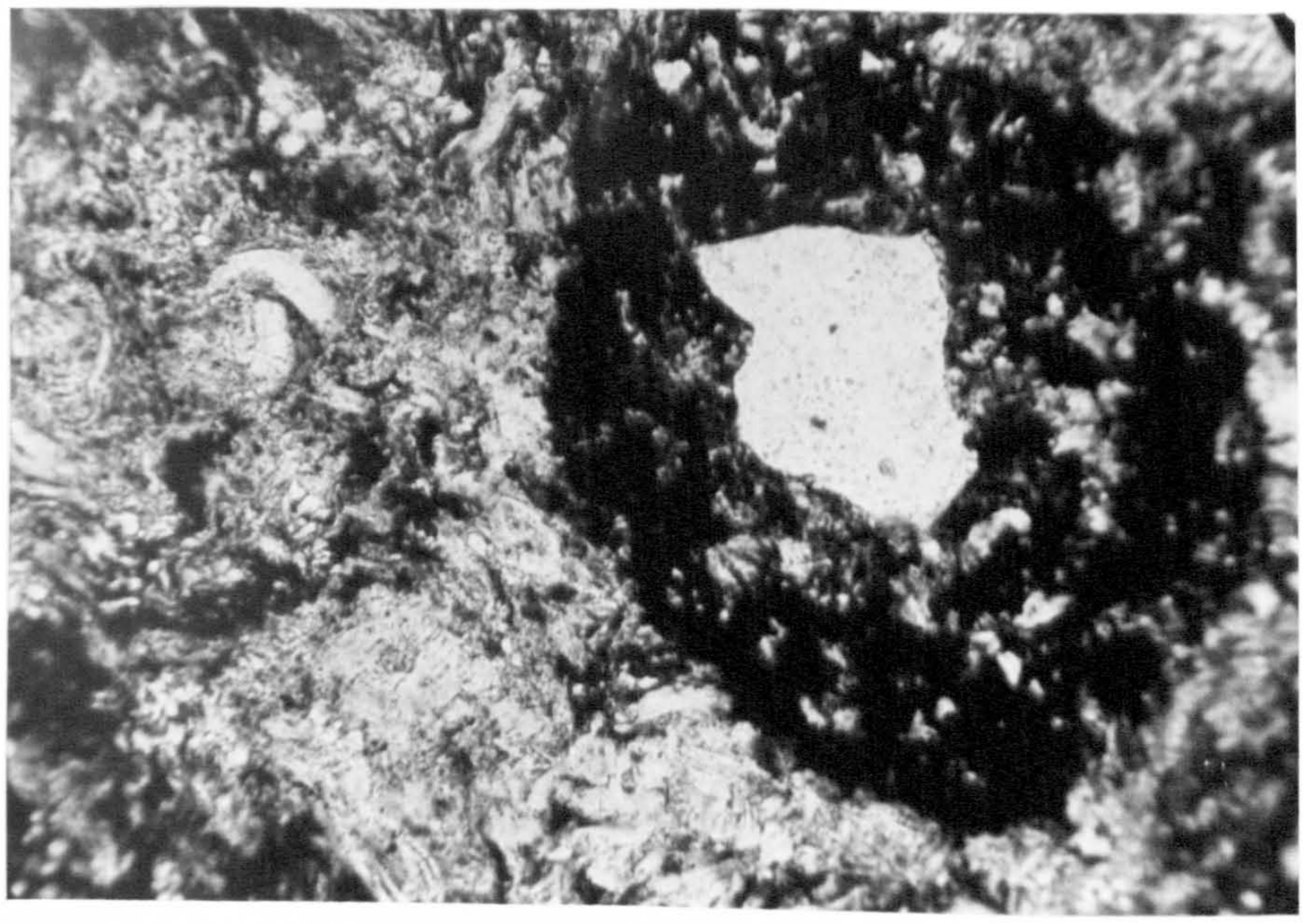

0.3 mm

Plate 6. 5. Photomicrograph of a medium - grained sublitharenite , cemented mainly by iron oxides; some of the quartz grains appear to have been reworked. The interstices are occupied partially by kaolin booklets after feldspar . Crossed polars, sample No. U 11 00.

Plate 6..6. Photomicrograph of a medium - grained lithic subarkose, showing the original subrounded grains of quartz modified by authigenic overgrowths. The margin of the original detrital cores is occupied by a film of clay minerals. Polarised light, sample No. U 13 07.

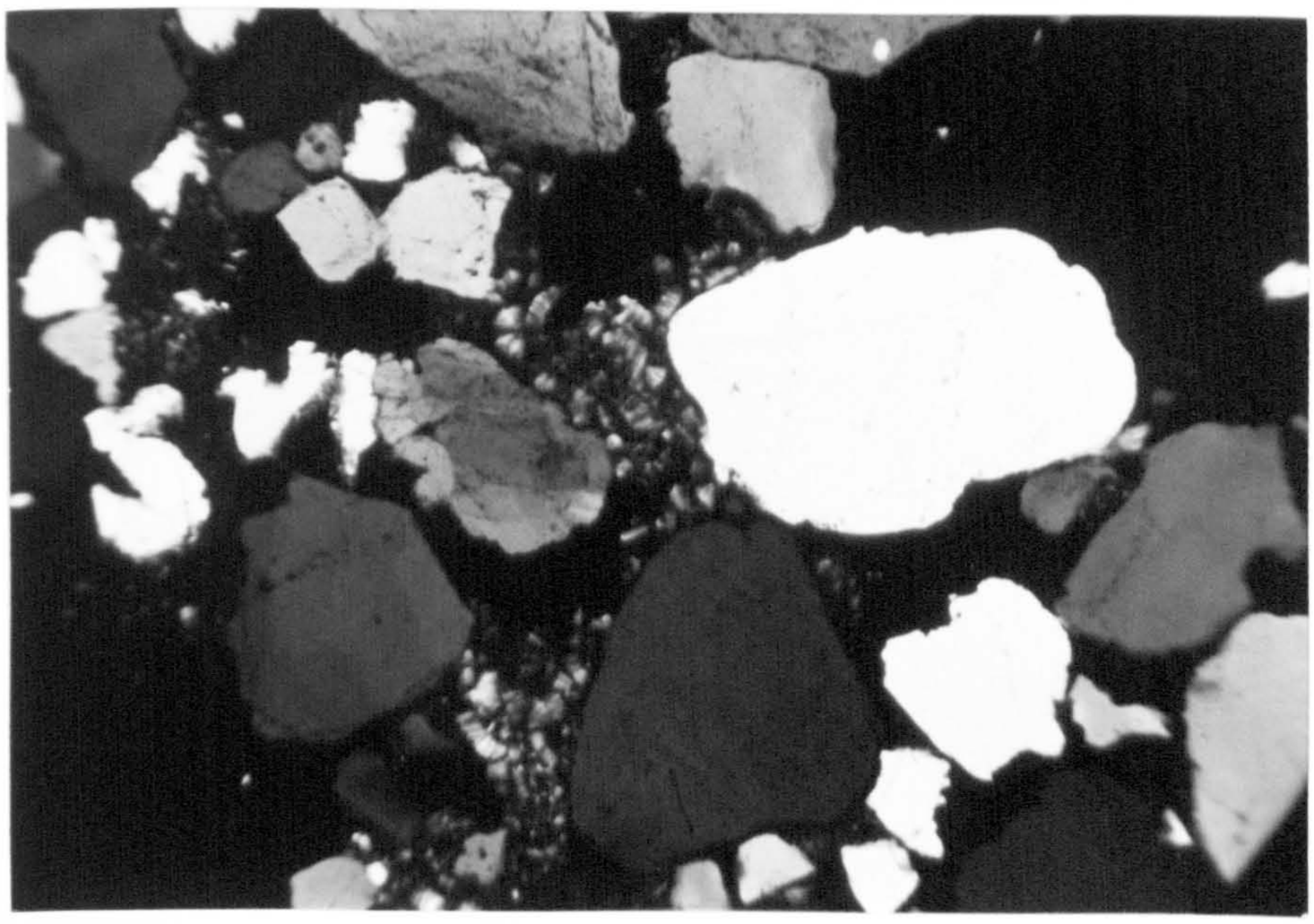

0.8 mm

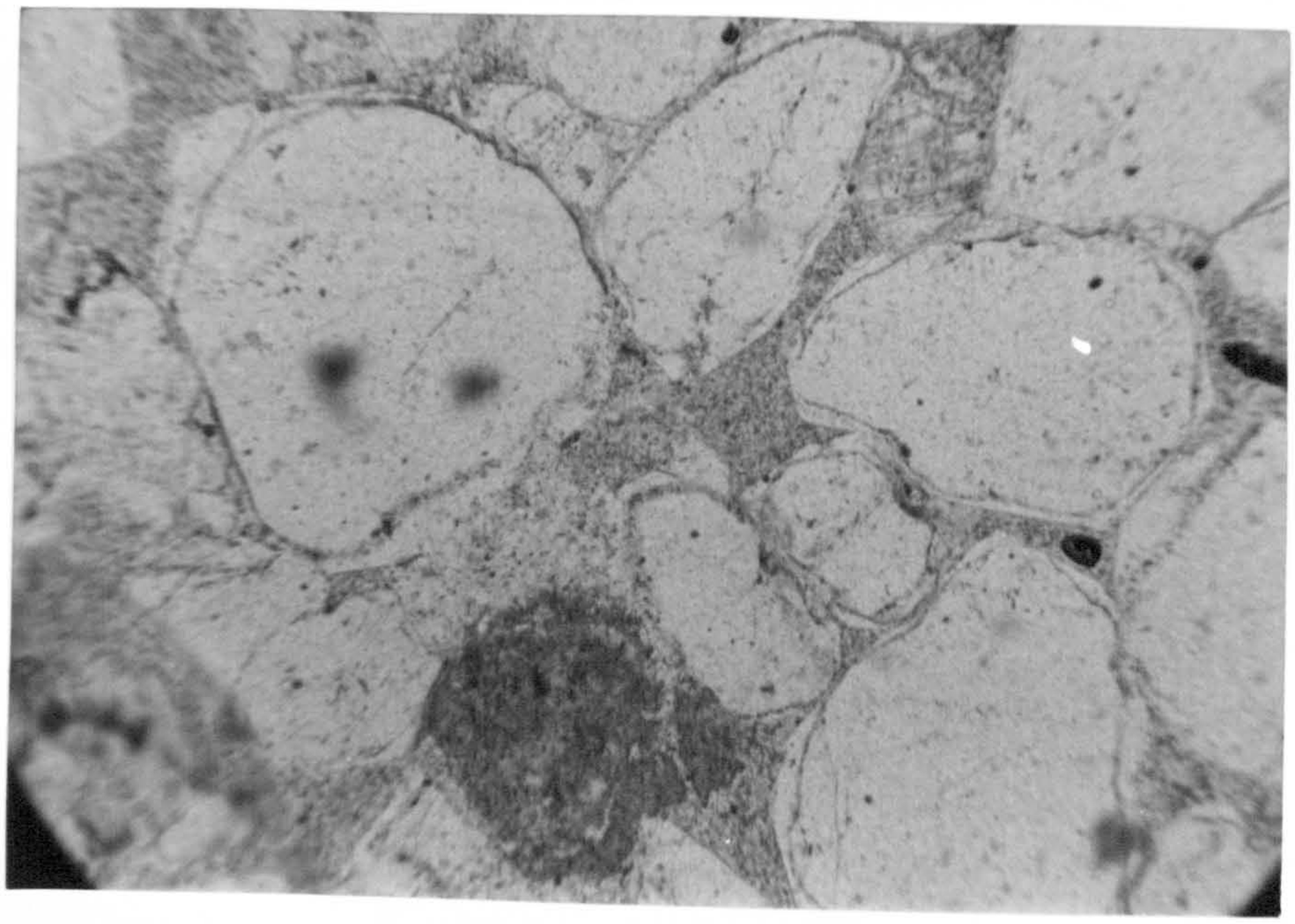

0.7 mm

Plate 6. 7. Photomicrograph of a coarse - grained subarkose, cemmented by ferroan dolomite. A dolomite rhomb is well developed (centre). An orthoclase grain (bottom left) shows marked evidence of corrosion by percolating carbonate - rich pore waters. Polarised light, sample No. U 06 05a.

Plate 6. 8. Photomicrograph of a fine - grained lithic subarkose, showing well - sorted, subrounded to subangular quartz grains, with orthoclase and microline (centre right), cemented by iron oxide and quartz authigenic overgrowths. The interstices are occupied partially by kaolin. Crossed polars, sample No. U 06 10.

0.3 mm

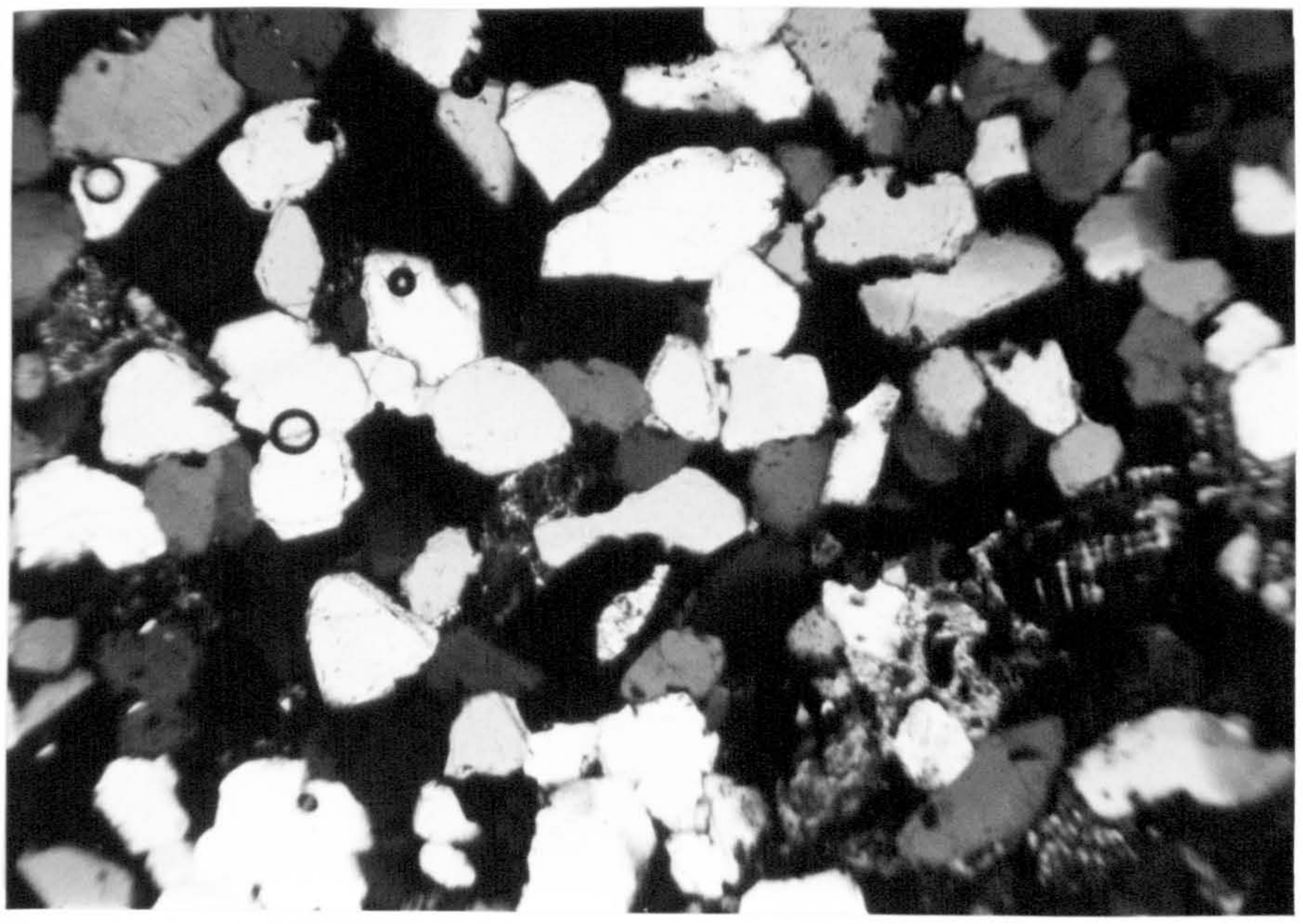

0.6 mm

Plate 6. 9. Photomicrograph of a coarse silty arkose, showing well - sorted, subrounded to subangular quartz grains, with orthoclase and twinned plagioclase (centre), cemented by iron oxide and ferroan dolomite, with some scattered dolomite rhombs (centre). Crossed polars, sample No. H 11 15.

Plate 6.10. Photomicrograph of a coarse silty arkose, consisting of a moderately sorted mixture of angular to subangular quartz and feldspar grains together with a little mica set in a ferroan dolomite cement and clotlike (black) hematite matrix. Abundant, though not clearly shown in the figure, are rhombic dolomite euhedra (centre). Polarised light, sample No. H 07 07.

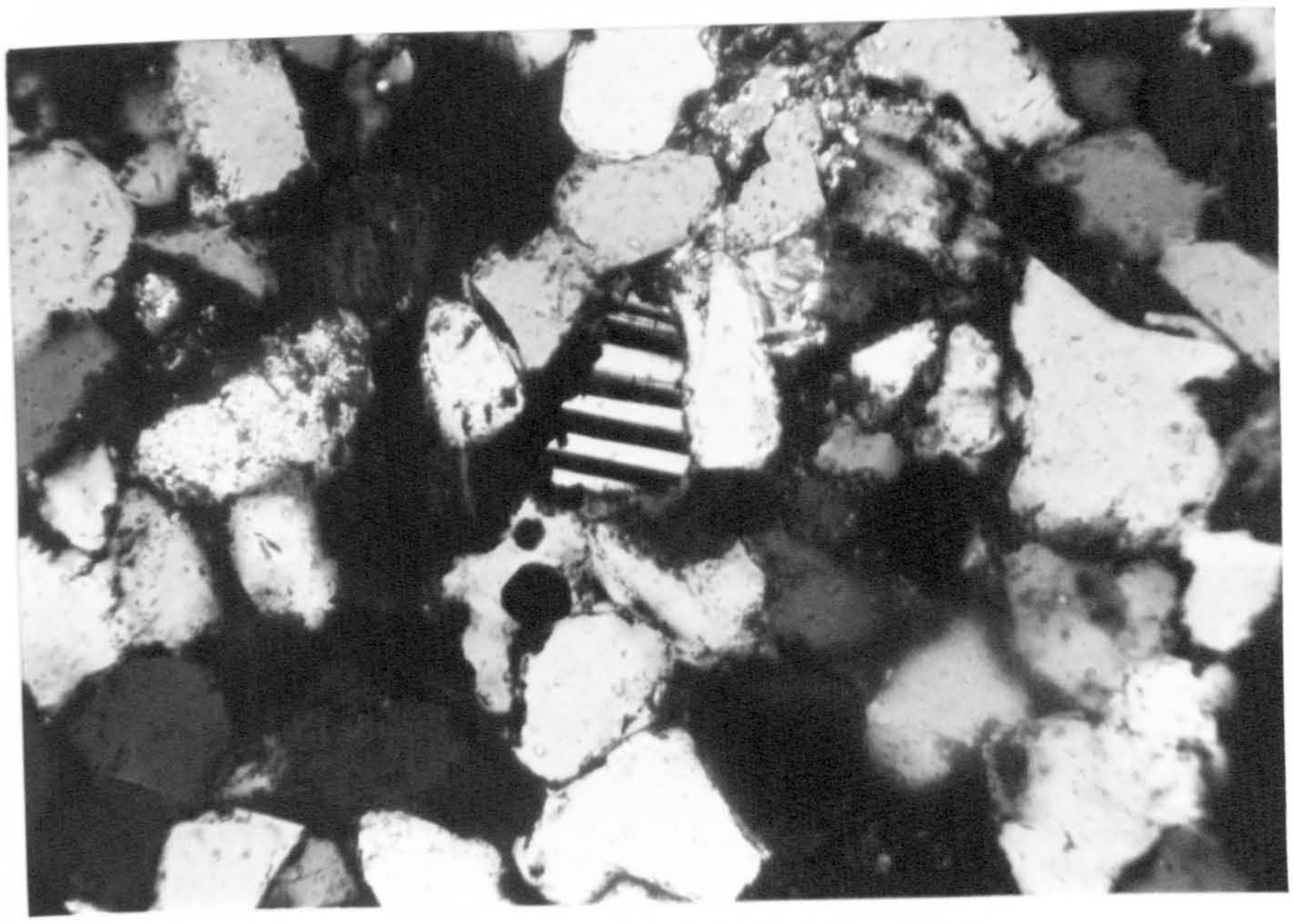

0.15 mm

0.16 mm

Plate 6.11. Photomicrograph of a medium - grained calcarenaceous orthoquartzite, cemented by dolomite and showing a fuziform foraminiferal tests (centre) with further recrystallisation. Brachiopod debris (top left) and floating quartz grains in a dolomitic cement are also visible. Polarised light, sample No. N 10 10a.

Plate 6.12. Photomicrograph of a medium - grained calcarenaceous orthoquartzite, cemented by dolomite. Skeletal debris includes bryzoan fragment (centre) showing dolomite recrystallisation. Polarised light, sample No. N 10 10b.

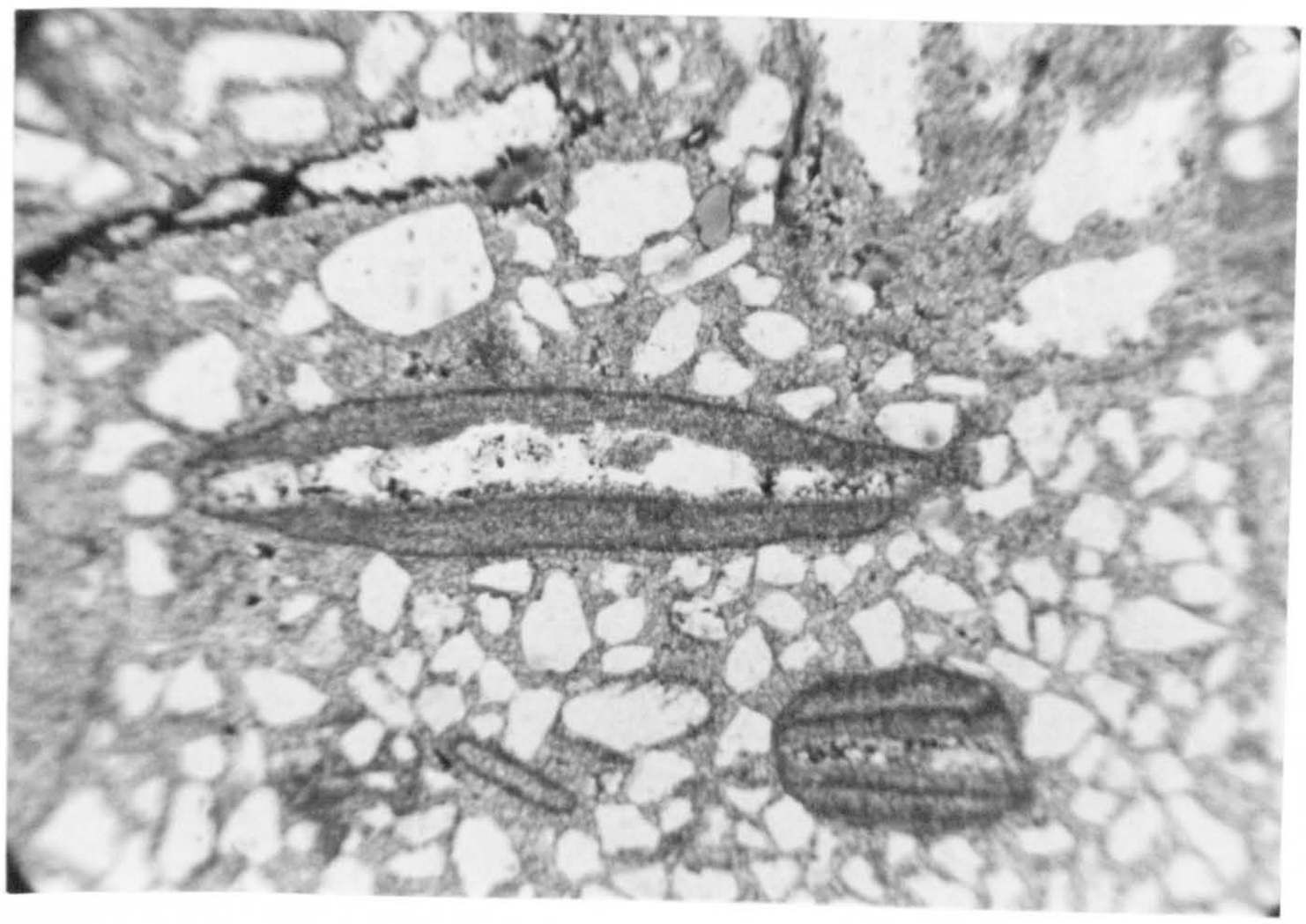

0.4 mm

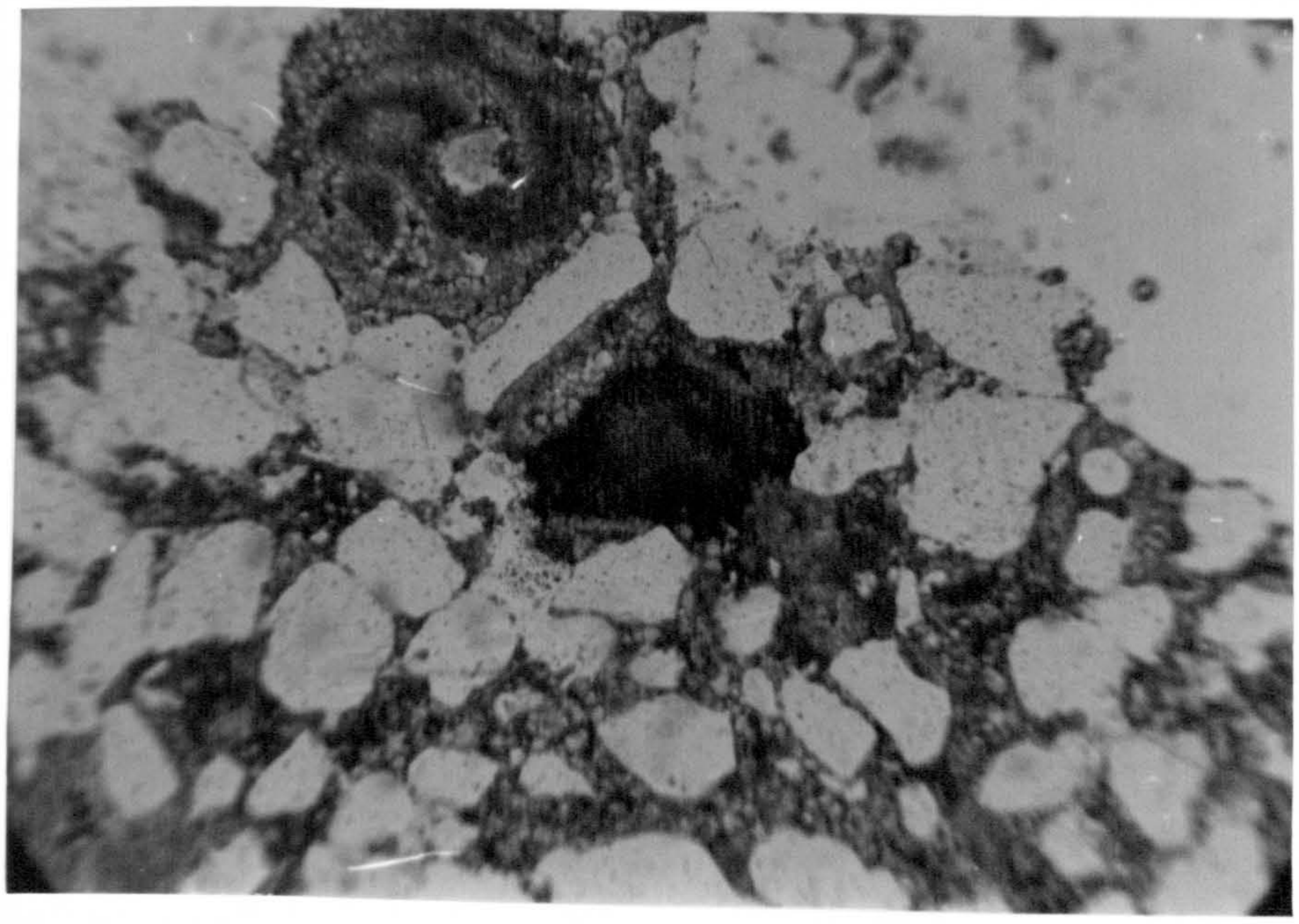

0.4 mm

Plate 6.13. Photomicrograph of a medium - grained calcarenaceous orthoquartzite, cemented by dolomite. Moderately - sorted, subrounded quartz grains appear to be floating in the dolomite cement. Spherical oncoliths with a concentric structure are embedded in dolomitic cement; some of them have a single quartz nucleus or a shell fragment. Polarised light, sample No. N 07 08.

Plate 6.14. Photomicrograph of a calcarenaceous orthoquartzite, showing elongate fragment of brachiopods, oncoliths and quartz grains floating in a dolomite cement. Polarised light, sample No. N 07 08.

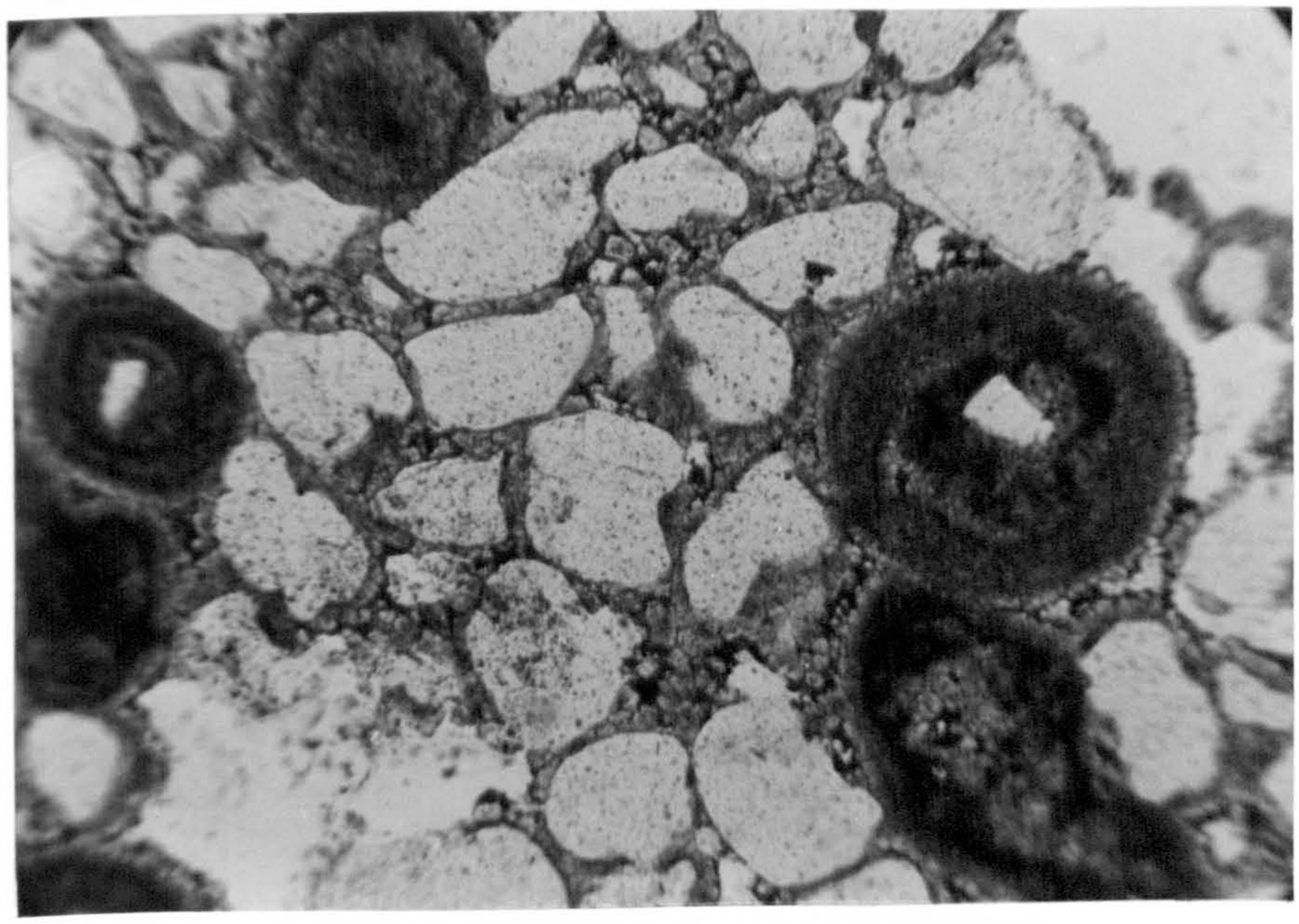

0.7mm

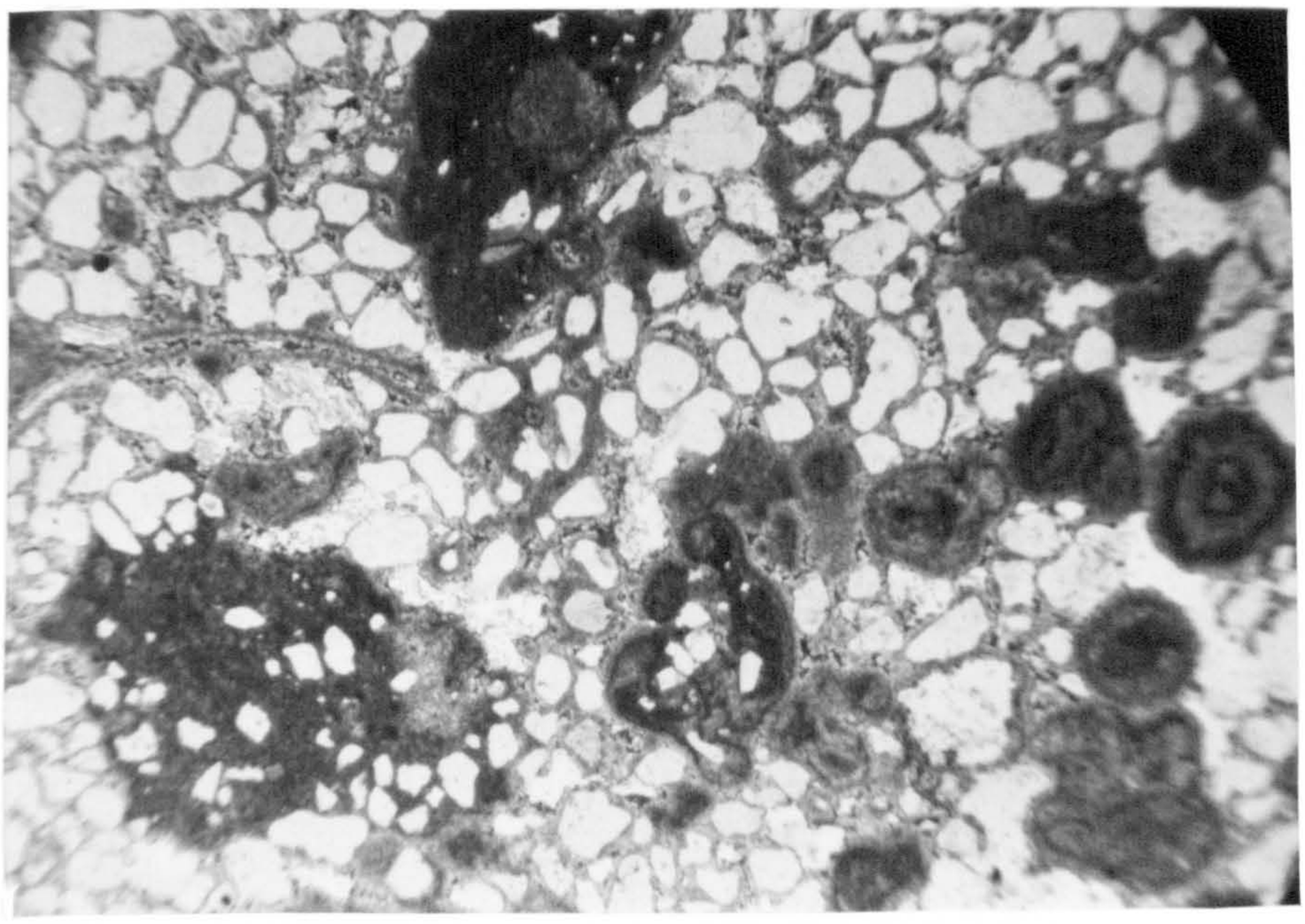

1.1mm

CHAPTER SEVEN

CONCLUSIONS

CHAPTER SEVEN

CONCLUSIONS

7.1 UPPER CAMBRIAN MODEL

The Upper Cambrian rocks can be divided into two facies: arenite and heterolithic facies, each facies being characterised by a particular association of sedimentary structures and textures. These two facies are arranged in six major couplets, reflecting six successive episodes of minor transgressions and regressions interacting with an extensive distal braided alluvial plain and adjacent tidal flat, along a NE - SW orientated palaeoshorelines (Fig. 7. 1).

The quartzarenite facies forms multilateral multistorey sheet sandbodies internally structured by erosively bounded, vertically stacked sandstones containing mainly trough cross - bedding, deposited as channel floor dunes in a sandy bedload dominated braided river system, similar to the braided South Saskatchewan River. In the South Saskatchewan River sinous to irregularly crested megaripples are the most common bedform in the major channels at almost all stages of flow and the scale of the megaripples is directly related to channel depth (Cant and Walker, 1978).

The quartzarenite facies is interpreted to have formed on the distal reaches of an unconfined braidplain sloping gently towards the northwest

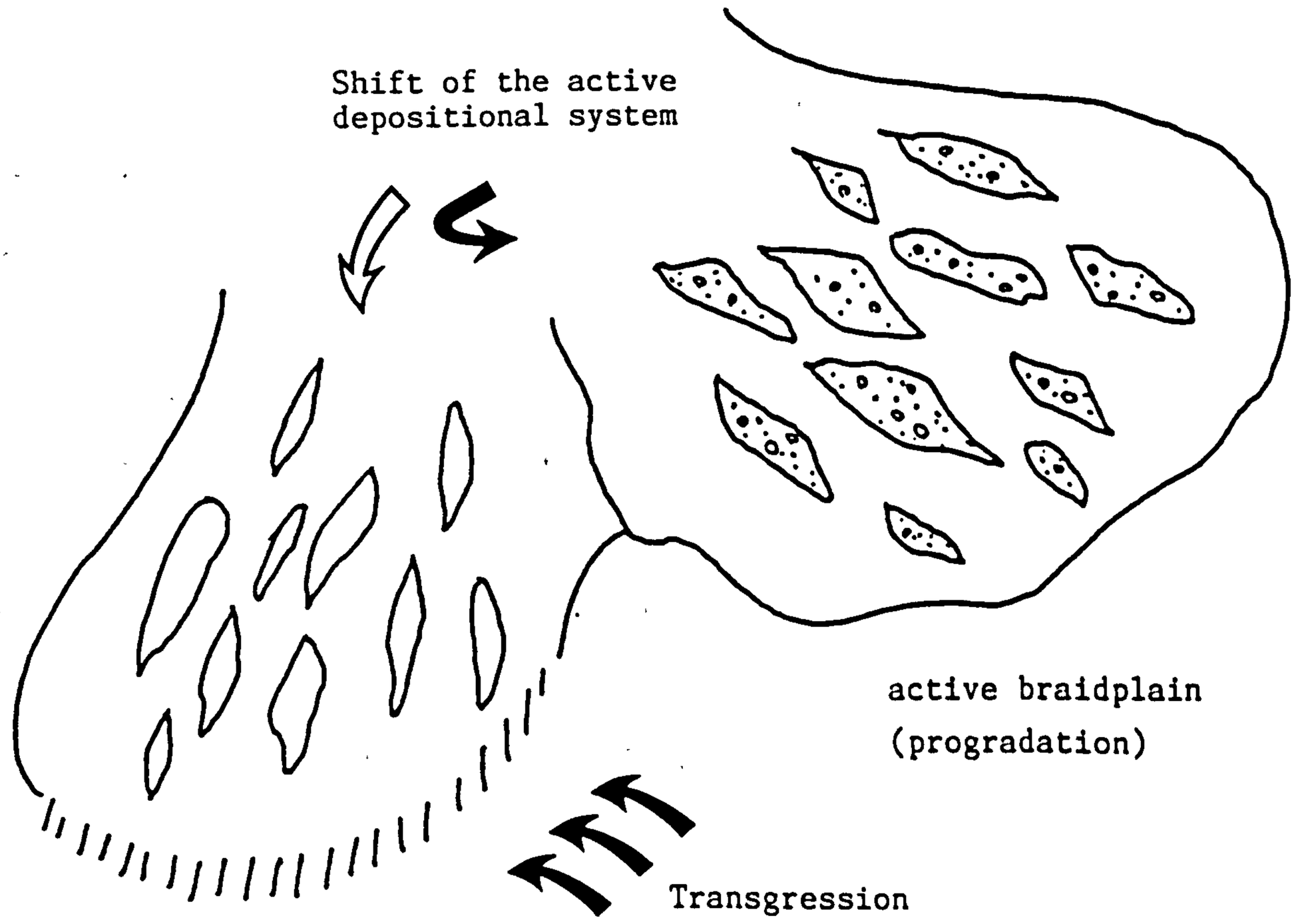

Fig. 7.11. Depositional model for the Upper Cambrian succession showing tidal flats developed on the inactive braidplain after channel shifting or during periods of weak detrital influx.

from an elevated provenance in the southeast, probably the Arabo - Nubian Shield. The paucity of fines may be due to rapid shifts of the active channel tracts giving rise to vertical and lateral stacking of the braided arenite sheets (Fig. 7. 1), or it may be due to the lack of topographic diversity on the distal braidplain, which was unable to trap the fines.

Reference to the braided river models (Fig. 2. 5) proposed by Miall (1978) shows that the Upper Cambrian braided model does not readily fit any of them. Although the present model resembles the Saskatchewan model in that both are of braided pattern and have high sand/mud ratios, they differ in their preservation potential of the fine material which is almost lacking in the present model. Another notable difference is the dominance of trough cross - bedding in the Upper Cambrian model.

Depositional conditions were variable during Upper Cambrian times with the source area providing a supply of mostly mature, recycled, lithologically uniform sediment to the depositional site. As the distal fluvial system shifted,the braidplain became inundated by the sea giving rise to the formation of the heterolithic facies, which comprises thin alternating beds of sandstone, siltstone and mudstone, but with the fines predominating. The heterolithic facies is interpreted to have formed by tidal currents acting on the distal margin of the alluvial braidplain during periods of repeated minor transgressions. These transgressions must have been shortlived and of fairly low energy

judging by the thickness of the heterolithic facies, the sedimentary structures, textures and biogenic features. The repetitive pattern of fluvial and tidal sedimentation could be related to tectonism or shifting of the depositional system. During periods of active tectonism and elevation of the source area, gradients and detrital influx increased resulting in progradation of the braidplain. During periods of reduced tectonism, gradients and sediment input declined resulting in abandonment of the braidplain after which transgression occured. Rapid shifting and abandonment of the active braidplain due to gradient advantages was followed by subsidence, inundation and reworking of the abandoned part of the braidplain by marine currents (Fig. 7. 1). The thickness of the heterolithic facies and their variation in thickness suggests that shifting rather than tectonism was the most important reason for the limited transgressive events.

A depositional model for the Upper Cambrian succession comprises thin tidal deposits associated with thick braided fluvial sequences. The juxtaposition of tidal and fluvial deposits indicates their occurrence to be in response to marine processes operating on a shoreline whose morphology is determined by the fluvial system. The depositional model proposed is one of an open, shallow, gently shelving braidplain. Intertidal flats probably developed in response to weak tidal action on the margins of the inactive braidplain after channel shifting, or during reduced detrital influx. Similar open non - barred, tidal flats are developed in shallow, gently shelving embayments in

Shark Bay, Western Australia, where the tidal range is less than one meter (Logan et al., 1970), and on the inner margins of interdistributary embayments of the Precambrian Waterberg succession, South Africa (Vos and Eriksson, 1977). Similarly interbedded fluvial and tidal sediments were described by Miall (1976) from the Proterozoic of Canada (Glenelg Formation of Banks and Victoria Islands, Artic Canada).

7.2 PERMO - TRIASSIC MODEL

Facies and palaeocurrent analysis of the Um Irna Formation indicates that deposition occurred on the lower to middle reaches of an unconfined humid braidplain sloping gently westwards from an elevated source area in the south and east. The lithological similarity of the sediments throughout the area suggests that the braidplain was supplied with detritus from granites and metamorphics of the Arabo - Nubian Shield located a few tens of kilometres to the south and east. The westward palaeocurrent trend is consistent with a single drainage system, with the lowermost facies regarded as a distal equivalent of the overlying coarser grained facies in the succession. The greater proportion of fines in the more proximal of the two facies may be attributed to the trapping of fines by vegetation on the more topo - graphically diverse middle reaches of the braidplain (Fig. 7. 2).

The general uniformity of facies types points to the existence of a broad gentle upwarp of the provenance rather than localised areas

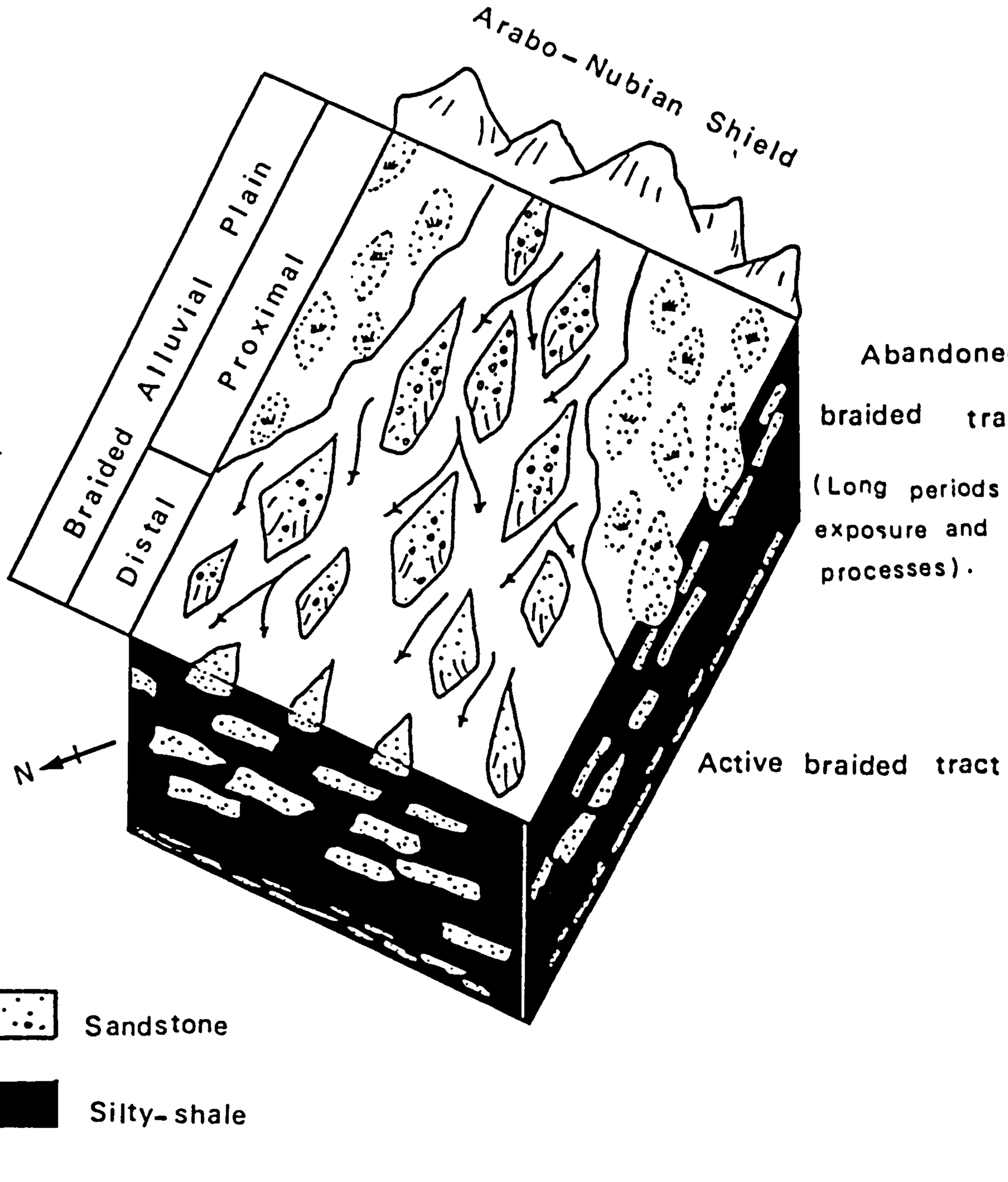

Fig. 7.12. Diagram showing subenvironments of the Permo - Triassic (Um Irna Formation), associated with deposition on distal and proximal parts of a braided alluvial plain.

of strongly contrasting relief. This relationship argues against the extensive development of alluvial fans marginal to the source terrane at this time, but favours instead the existence of a more gently sloping middle to upper braidplain environment in the proximal reaches of the depositional system. This in turn implies that deposition was largely a function of periodic shifts of the active channel tract, superimposed on a gradually increasing source area elevation promoting basinwide progradation and vertical stacking of the two major facies components in the succession. This increase in source area elevation and gradients is reflected in the upward increase in bed thickness and the size and abundance of small pebbles in the succession. Elevation of the source may also have influenced climate and the length of the alternating wet and dry seasons essential for the formation of ferruginous concretions (pisoliths). The development of Fe- pisoliths also reflect the seasonal rainfall conditions responsible for leaching and precipitation processes (see section 3.3). The upward increase in abundance of pisoliths and the associated development of carbonaceous shale with plant remains and coaly stringers near the top of the succession indicate an increase in the length of the rainy season and possibly the level of the groundwater table.

Marine sediments in the lower part of the succession some 50 km northeast of the Dead Sea (Bandel and Khoury, 1981) represent a shallow water marine depository into which the fluvial depositional system drained. Lack of adequate outcrop and subsurface data in this direction

preclude the recognition of any contemporaneous shoreline facies. Evidence of the existence of this depository during deposition of the upper part of the Um Irna (Upper Member) is lacking, presumably because of the shift of facies tracts concomitant with progradation of the depositional system in this direction. The Um Irna records a period of cratonic instabilty when continental conditions were well established on the eastern side of the Dead Sea rift, flanked further north and west by shallow water marine conditions. Following this, deposition was dominated by marine clastics and carbonates (Bandel and Khoury, 1981) as the Tethys seaway encroached southwards, punctuated by minor regressive and transgressive phases, possibly controlled by mild vertical oscillations of the craton (Garfunkel, 1978).

7.3 LOWER TRIASSIC MODEL

The Ma'in Formation is the lowermost Triassic lithostratigraphic unit dealt with in the present study. Facies analysis shows that most of the formation was deposited in a shallow water marine and intertidal environment. Clastic detritus was supplied from the south-east (Arabo - Nubian Shield) and reworked by shoreline processes into a series of northeast - southwest trending facies tracts. A shallow shelf sea (Tethys) existed to the northwest, giving rise to a major transgressive event at the begining of Lower Triassic sedimentation (Fig. 7. 3).

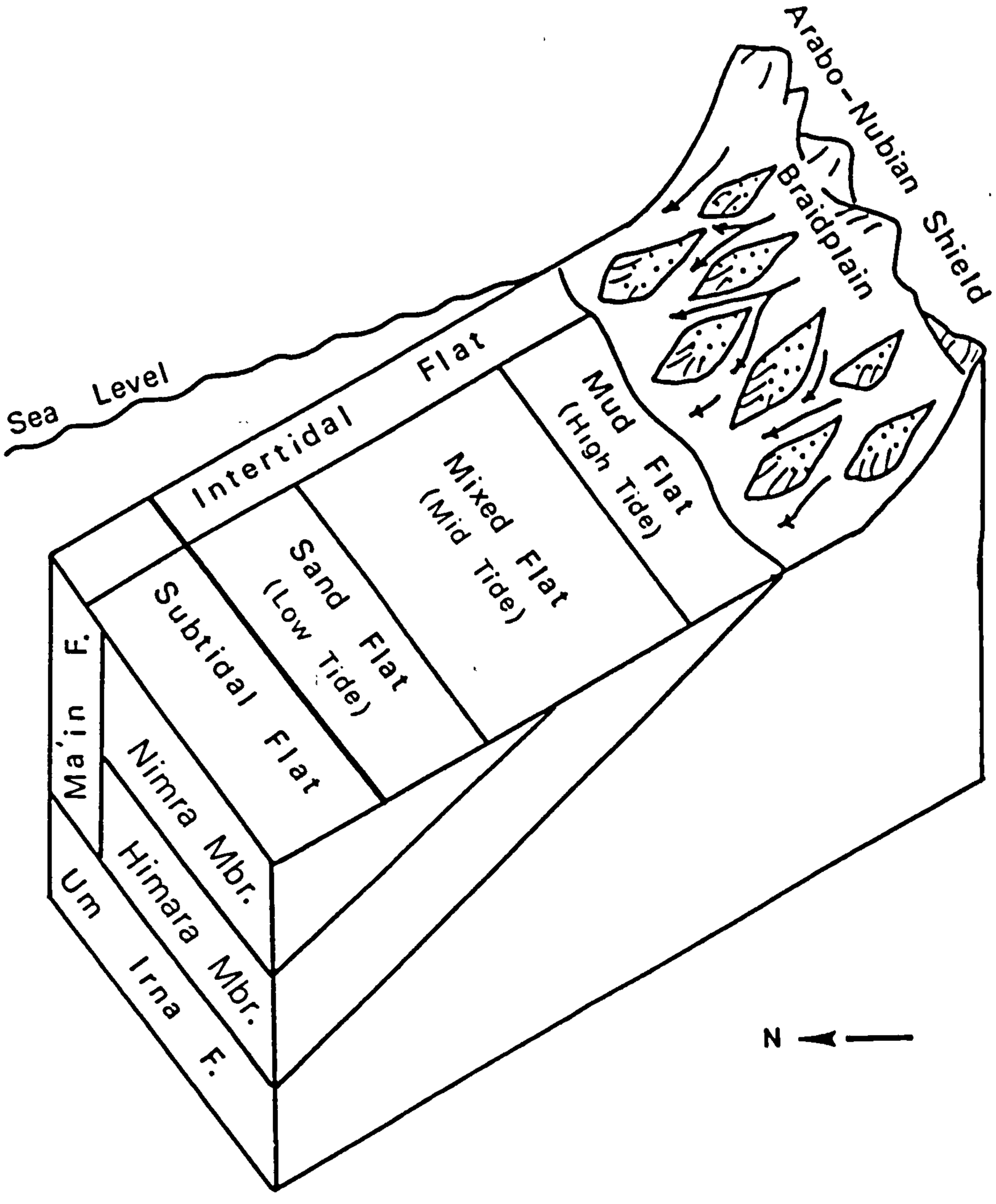

Fig. 7.3. Schematic depositional model of Ma'in Formation environment indicating inferred relationship to Um Irna Formation.

Conditions during deposition of the Nimra and Himara Members of the Ma'in Formation differed in that water depths gradually increased and there is no evidence of subaerial emergence during deposition of the Nimra Member (Fig. 7. 4).

7.3.1. Himara Member

Most of the clastic sedimentation associations consist of clay - stones, siltstones and fine to medium - grained sandstones, arranged in a major fining-upward sequence. Superimposed on this are smaller fining - upward intertidalite facies sequences, which are interpreted as a product of seaward progradation of the tidal flat. Stacking of these sequences indicates a series of minor local transgressive and regressive events attributed to a reduction in sediment supply to the coastal plain. This may be due to shifting of the active part of the braided fluvial system in response to gradient advantages, or to tectonism. Shifting of the depositional system leads to abandonment of the inactive part of the coastal plain, followed by subsidence and transgression. Tectonic uplift increases gradients (on a more regional scale) and the sediment supply, promoting progradation of the depositional system. As tectonism wanes gradient and sediment supply decrease and transgression occurs. Transgression without any concomitant rise in sea level (e.g. due to coastline erosion) or with a slow rise in sea level results in erosion and destruction of the shoreline system, prior to the next progradational phase. Thus, any barrier island that

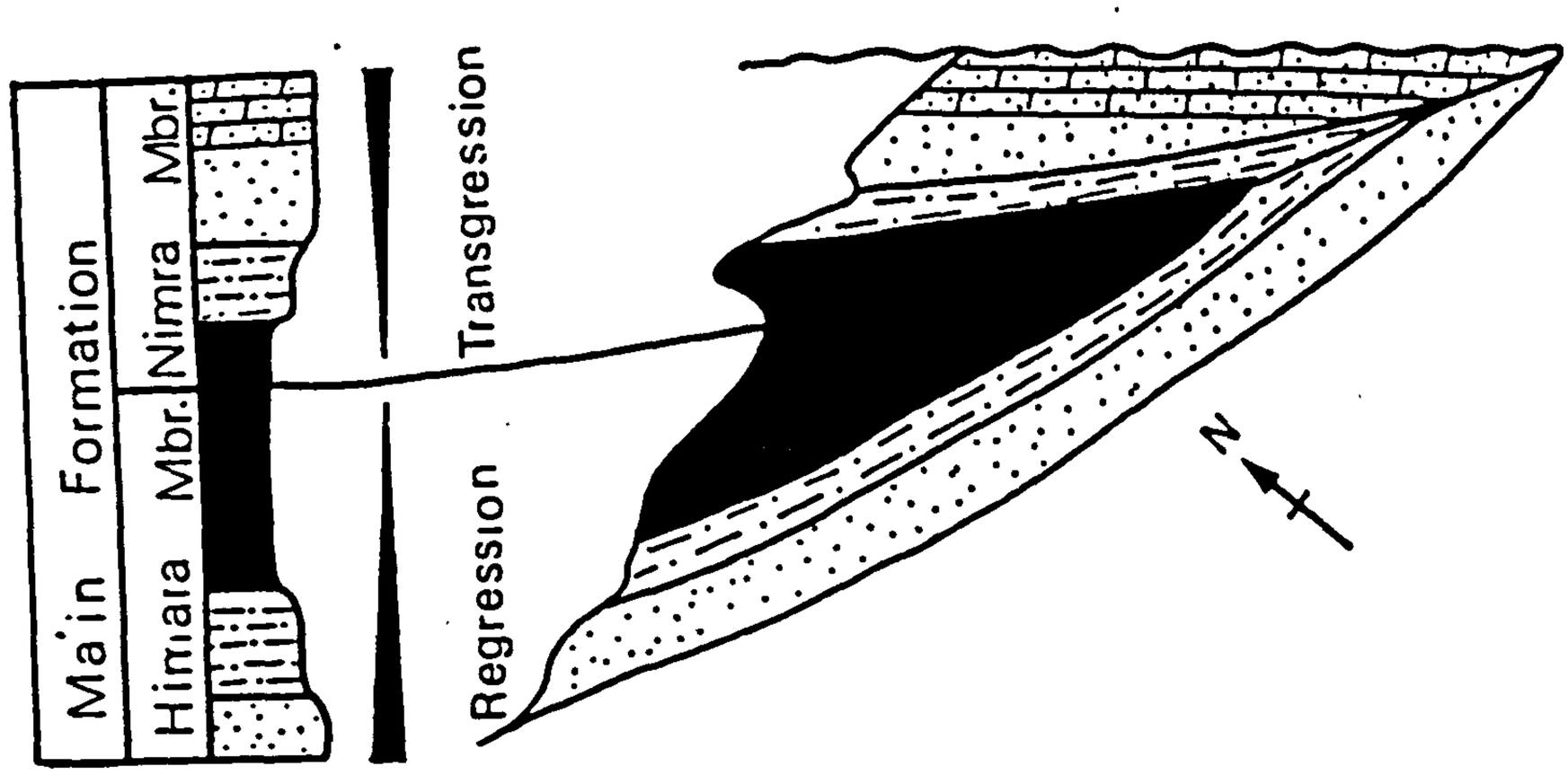

Fig. 7..4. Vertical sequences of regressive deposits of Himara Member and transgressive deposits of Nimra Member.

might have been protecting the tidal flats is destroyed and is not preserved in the rock record. These regressive - transgressive events must have been superimposed on the larger scale (tectonically controlled?) fining-upward regressive trend (Fig. 7. 4).

A marginal intertidal flat environment (Fig. 7. 5 A) is proposed for the Himara Member based on the features shown by the sediment associations which have much in common with modern clastic intertidal flats, especially the subenvironments of the Dutch Wadden sea tidal flats (Van Straaten, 1949, 1950 a, 1950b, 1951, 1952, 1953, 1954a, 1954b, 1959, 1961; Van Straaten and Kuenen, 1958; Klein and Sanders, 1964) and the Bay of Fundy intertidal zone (Klein, 1963, 1970a, 1970b, 1971, 1977; Klein and Saunders, 1964). These features are summarised as follows; (1) rhythmic beds of sand, silt and clay "tidal bedding" (Reineck and Wunderlich, 1968), flaser and lenticular bedding, and clay drapes over ripples, (2) late stage emergence run off features (e.g. interference ripples, "current ripples superimposed at 90° on current ripples", ladder-back ripples" small - scale ripples on larger ripples" (Plates 5.10 - 5.13), (3) reversing tidal currents as shown by herring-bone cross - strata with sharp set boundaries produced by bedload transport by tidal currents of nearly equal strength,as indicated by the equal thickness of cross - bed sets (Plate 5.15), (4) subaerial exposure (e,g. mudcracks, raindrop imprints, runzel marks, and oxidised deep maroon colour, Plates 5. 6 - 5. 9, 5.14), (5) bioturbation and shells oriented convex side upward (Plate 5.18), and (6) calcareous

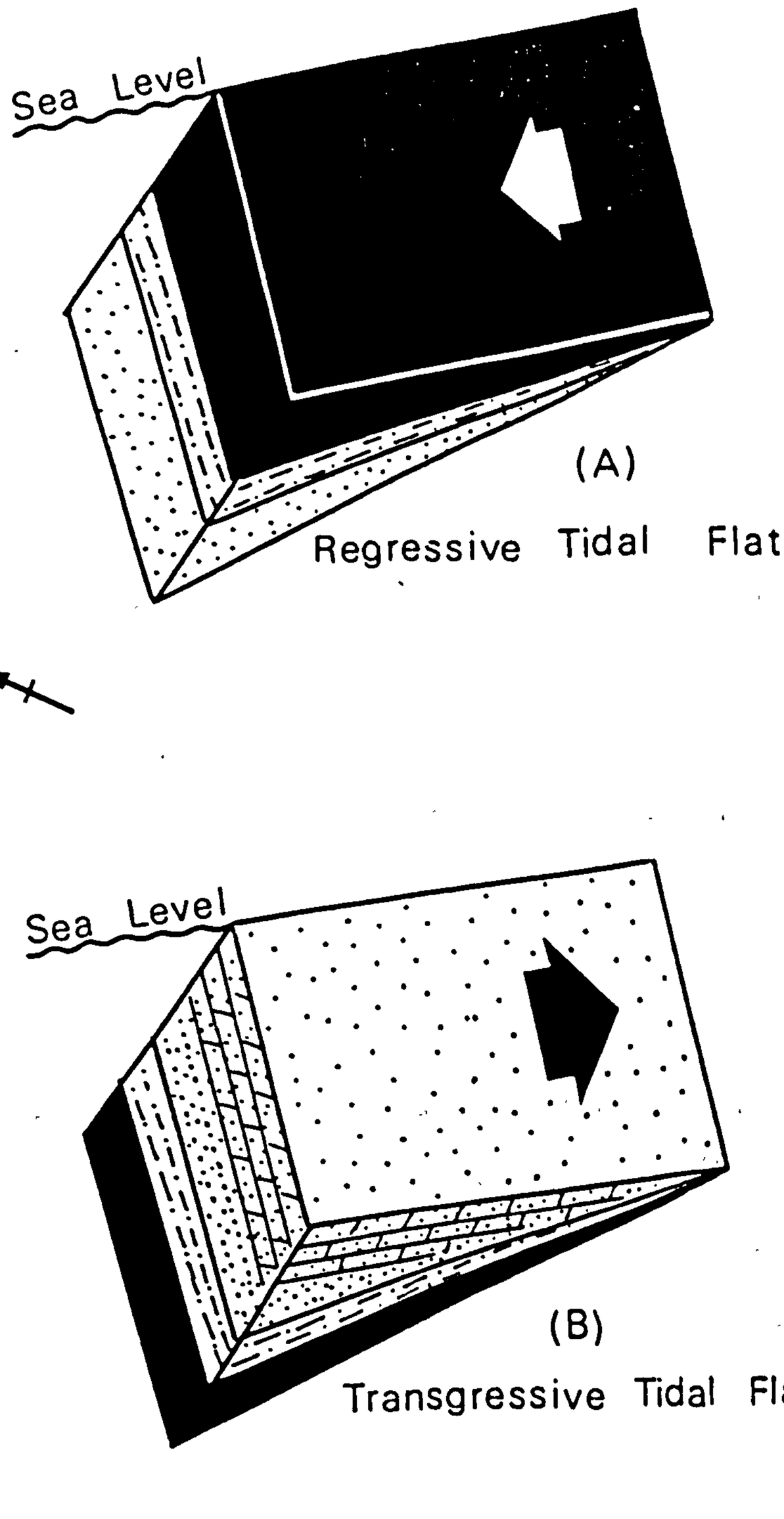

Fig. 7.5. (A) Regressive tidal flat model illustrating the development of the Himara Member, and (B) Transgressive tidal flat model illustrating the development of the Nimra Member (see Fig. 7. 4 for legend).

horizons, mostly dolomitic.

On the basis of the ratio of coarse to fine clastics the intertidal environment can be subdivided into three subenvironments of deposition (Table 2.5); sand flats (lower tidal flat), mixed flat (midtidal flat), and mud flat (high tidal flat) (Reineck, 1975; Klein, 1977). The coarse (sandstone) to fine (siltstone and mudstone) ratio within the Himara Member succession is approximately 2 to 1 in the lower part and 1 to 5 in the upper part (Fig. 5. 3). The clastic ratios place it in the mixed flat (mid tidal flat) subenvironment in which the lower sandy facies (quartz arenite) is deposited closely to the low tide zone possibly associated with tidal channels and their lateral migration, and the upper shaly facies (heterolithic) is deposited closely to the high tide zone (Fig. 5. 7, 7. 3).

The depositional model proposed is one of a microtidal to mesotidal coastline, with a palaeotidal range of 0·45 m to 2·35 m (Hayes, 1975; Klein, 1971). The coastline is inferred to have been interacting with a braided fluvial plain, which fed in quartzitic sediment from the southeast as indicated by the palaeocurrent rose diagram (Fig. 5. 6) see also section 5.2.2.

The coquinas probably represent lag concentrates, moved onshore and buried by new sediments. Low faunal diversity is typical of tidal flats due to changes in temperature, salinity and water cover.

Another factor is restricted circulation particularly where the tidal flats are protected by a barrier (Hayes and Kana, 1976). The absence of open mudflats seems to be characteristic of arid and semi - arid environments. However, the absence of evaporites suggests a semi - arid and strongly seasonal climate (Flemming, 1977).

7.3.2. Nimra Member

The Nimra Member comprises two distinct facies; the lower (Heterolithic facies) and the upper (Quartz arenite facies).

Heterolithic Facies

The boundary between this facies and the heterolithic facies of the Himara Member is gradational (Fig. 7. 5), both facies have similar lithologies and similar sedimentary structures such as tidal bedding (alternation of sand, silt and clay), flaser, lenticular and rippled bedding and varicoloured (red, cream, yellowish, grey), beds. Nevertheless, the heterolithic facies of the Nimra differ from the Himara heterolithic facies in that (1) the colour becomes more whitish and greyish, while the red colour diminishes upward, and (2) the subaerial exposure structures (mudcracks, raindrop imprints) decrease compared to the lower facies.

The above mentioned features of the Nimra heterolithic facies

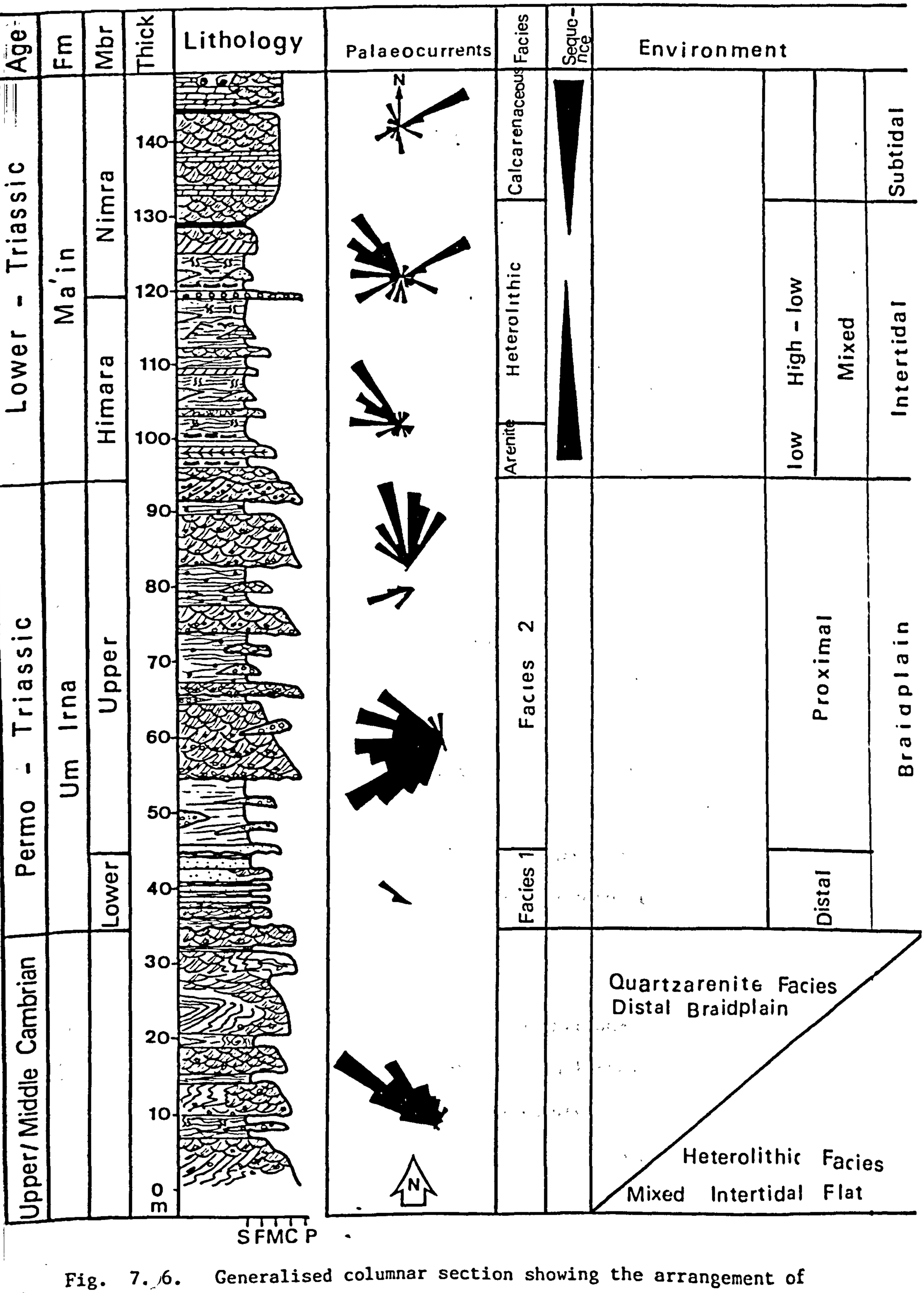

Fig. 7.6. Generalised columnar section showing the arrangement of the different rock units studied, their palaeocurrents and depositional environments.

in addition to the mixed bedload and suspension sediments place it in the mixed flat in the intertidal depositional environment (Hayes, 1975; Klein, 1977) (Figs. 5.17, 7.8, 7.15B).

Quartz Arenite Facies

The proposed model of depositional environment for the upper sandy facies of the Nimra Member is a shallow marine (subtidal shelf) influenced by an influx of clastic sedimentation through areas, which might be river mouths extending subaqueously into the sea (subtidal channels) (Figs. 7.3, 7.15B). The abundance of quartz grains in the carbonates emphasises the strong influence of detrital, continental derived material in the nearshore environment. Since the sandstones are clean and quartzitic it is inferred that they were winnowed by marine currents (tidal and longshore currents) (Weggel, 1972), with the fine particles probably carried in suspension further seawards where they settled out in the distal shelf areas. This suggests the possible presence of offshore shelf shales towards the west as a distal facies equivalent of the more proximal sandy facies.

The shallow nature of the open marine environment is indicated by the presence of ooliths, foraminifera, lamellibranchs, echinoids, bryozoa and gastropod fragments cemented mainly by dolomite (Plates 5.11 - 5.14). The oolitic lithofacies possibly represent a subtidal

shoal in agitated waters (Illing, 1954).

This facies lacks the features typical of subaerial exposure and late stage emergence run off, while the red colour is totally absent. The ratio of sandstone to shale in the Nimra Member decreases northward as shown in the Suweilih well logs (Bandel and Khoury, 1981) as one moves away from the clastic provenance situated in the southwest (as shown by the rose diagram) (Fig. 7.6).

The overall model proposed for the Ma'in Formation is that of an intertidal flat environment (Himara Member) located between a braided alluvial plain (Um Irna Formation) and a subtidal marine shelf environment (Nimra Member) (Fig. 7.3). The thickness of the intertidal facies added to that of the overlying subtidal facies corresponds to the rise in sea level or magnitude of basin subsidence during transgression (Reineck and Singh, 1973). The coarsening - upward trend in the succession is consistent with a gradual trans - gression and subsidence of the basin, as the subtidal shelf deposits encroached landward across the tidal flats.

7.4 STRATIGRAPHY AND REGIONAL CORRELATION OF PERMIAN AND TRIASSIC

The Triassic and Permo - Triassic succession in Jordan, east of the Dead Sea Rift, consists of more than 1000 m of mainly clastic sediments assigned to nine formations (Bandel and Khoury, 1981).

However, only the lower 500 m of the succession, along the northeastern margin of the Dead Sea basin is well exposed. The rest of the succession is known only from subsurface well data.

The succession is generally flat - lying, but is broken by faults and intruded by a few igneous dykes and sills. The sediments are considered to have been deposited in terrestrial, nearshore and shallow water marine environments. Fluvial sediments prograded northwards into a shallow marine shelf environment during deposition of the lower part of the succession, in response to tectonic activity in the Arabo - Nubian Shield in the south. This was followed by a period of tectonic quiescence, when the Arabo - Nubian Shield exerted little influence on patterns of sedimentation (Bandel and Khoury, 1981).

Most of the Mesozoic sediments in Jordan, Palestine, Sinai, Egypt and Iraq were deposited in shallow waters covering the margins of the Arabo - Nubian Shield. A hinge belt running parallel to the present shoreline of Palestine and Sinai designates facies changes from shallow water to open and deep marine sediments. This hinge belt has been interpreted as a continental edge of the Arabo - Nubian Shield (Wetzel and Morton, 1959; Druckman, 1977), whereas adjacent to the shoreline, intertidal and subtidal environments prevailed (Figs. 7. 7).

The purpose of this section is to discuss lithostratigraphic

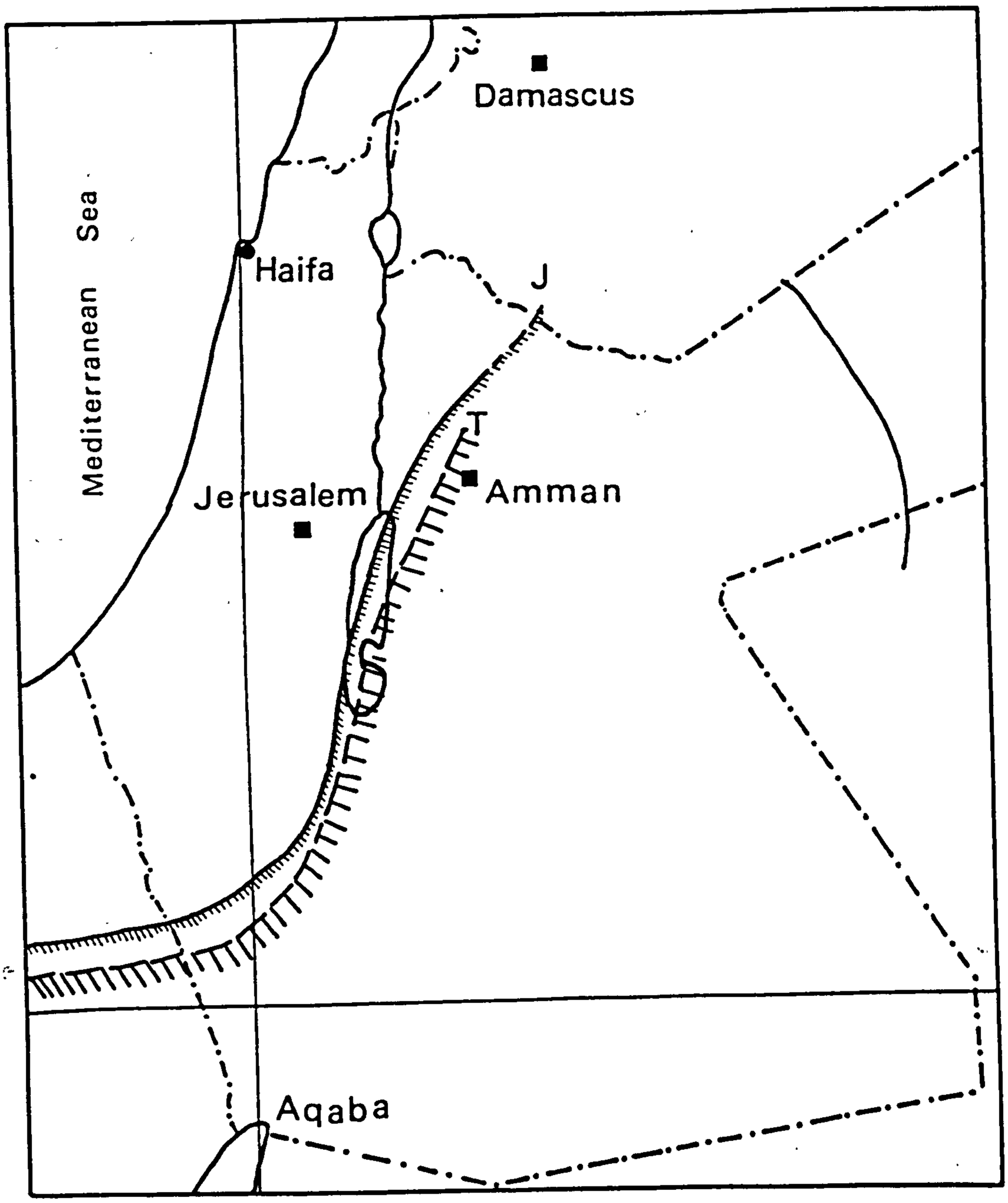

Fig. 7. 7. Shorelines of the Jurassic (J) and the Triassic (T). (Wetzel and Morton, 1959). Shading is to landwards on both shorelines.

relationships across the Middle East in order to try and establish grounds for regional comparison and correlation of the stratigraphic column along the Permo - Triassic Tethys shoreline.

Comparison of the Triassic sediments with those on the western side of the Dead Sea Rift show that correlatives of the fluviatile Um Irna Formation are lacking, and the succession is almost exclusively marine in character (Garfunkel, 1978). Possible marine facies equivalents of the Um Irna are precluded by the fact that the lowermost Triassic Formation in the central Naqab, the Zafir is of Scythian age (Druckman, 1974; Garfunkel, 1978). Nevertheless, such facies equivalents must have existed on the western side of the rift according to the sediment dispersal patterns. A possible correlative is the poorly known Permo - Triassic Yamin Formation in the central Naqab, (Table 7. 1), which consists of marine carbonates in the north, becoming more sandy and continental in character in the south where it is truncated by an early Cretaceous unconformity (Garfunkel, 1978). Assuming a relative displacement (left lateral) of the rocks on either side of the Dead Sea Rift of the order of 100 km (Freund et al., 1970; Bandel and Khoury, 1981) a northeast - southwest facies tract can be delineated (Druckman, 1974) with continental conditions predominating in the east on the Jordanian side and marine conditions in the west in central Naqab (Fig. 7. 7).

In 1984 Goldbery and Beyth studied the Triassic Budra Formation

of south - western Sinai, which could be considered as a possible lateral equivalent of the Um Irna Formation (Fig. 7. 8). The Budra Formation occurs on the Um Bogma Plateau (Gebel Mussaba Salama), south - western Sinai, and Wadi Budra to the south. The Budra Formation varies in thickness from 74 to 327 m, and comprises thick intervals of buff/white, medium to coarse - grained quartz arenites succeeded by finer grained clastics comprising fine sandstones and siltstones which are red and mottled purple - red and white colour. These clastics are arranged in fining-upward cycles, with basal lag deposits. Bedding is dominated by large - scale cross - bedding with frequent occurrence of plane lamination presumed to have formed under upper flow regime conditions (Goldbery and Beyth, 1984). The overbank facies of the Budra Formation is represented by finely laminated siltstone and fine sandstone red beds containing mudcracks and evidence of biogenic activity. Ferruginous concretions are common (Table 7. 2).

To the north, the influence of the Tethys ocean is well marked by lateral facies changes from the continental sandstones of the Budra Formation into supratidal and shallow shelf carbonates and evaporites of the Mohilla Formation (Druckman et al., 1970). The Budra Formation is considered by Druckman et al., (1970) to be of Triassic age (Table 7. 1), on the basis of palynological assemblages characteristic of the ."Taeniaesporites Kraeuseli" zone of Middle to Upper Triassic age (Horowitz, 1970).

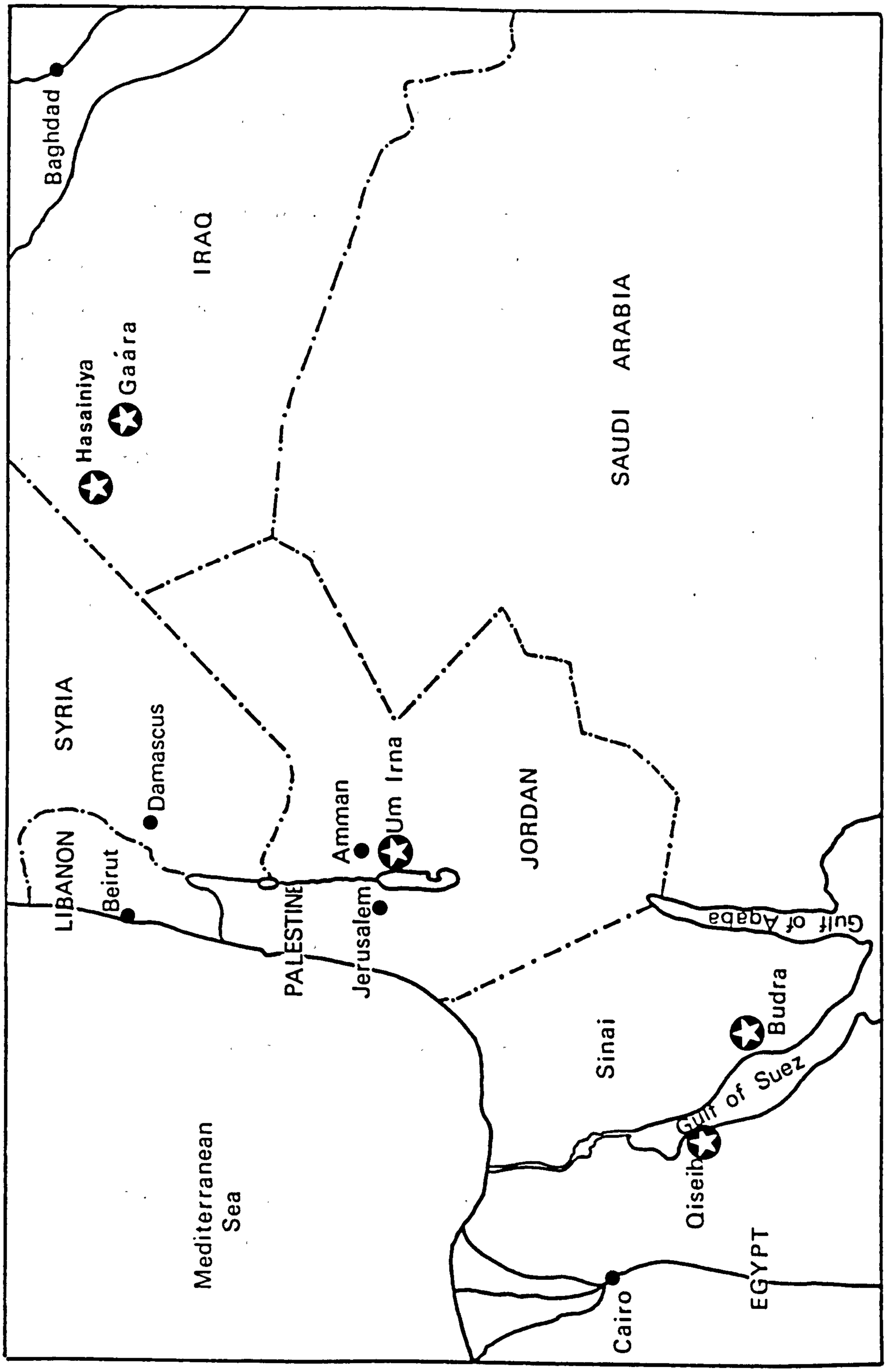

Fig. 7.8. Regional map showing the location of Um Irna Formation and the equivalent formations (stars) in the neighbouring countries.

At the second Jordanian Geological Conference held in Amman in 1985, El Barkooky presented an abstract on the lithostratigraphy and depositional environment of the "Nubian Sandstone" in west - central Sinai. In that note he described a sequence of clastic rocks of Permian ? to Early Cretaceous age, exposed along the foothills of the south-western scarp of the Tih Plateau. He subdivided the sequence into four formal rock units, arranged from base to top as follows: (1) Qiseib Formation,(2) Raqaba Formation,(3) Temmariya Formation, and (4) Malha Formation.

The Qiseib Formation (Fig. 7. 8) seems to be identical to those observed on the northeastern margin of the Dead Sea (Um Irna Formation) in possessing a similar Permo - Triassic age and similar features such as (1) fluvial environment of deposition (mostly braided system), (2) fining upward sequences, (3) cross - bedded and pebbly sandstones, (4) ferruginous concretions (pisoliths), and (5) carbonaceous shales.

Druckman (1970) considered the Qiseib Formation as the lateral equivalent of the Budra Formation in southwestern Sinai, both of which may be correlatives of the Um Irna Formation (Table 7. 1).

In Iraq, similar deposits were recorded in the Gaara depression (Western Desert). The Gaara sandstone Formation is more than 770 m thick, but 100 m only are exposed. The thickness gradually decreases

Table 7. 1

Regional Correlation Of Some Lithostratigraphic Units In The Middle East.
Data From Bender,1974;Druckman et al.,1970;Goldbery and Beyth,1984;Bandel and Khoury,1981;Weissbrod,1968;Jewad,1980.

Age	Eastern Eygpt (Wadi Qiseib)	Southern Sinia (Wadi Budra)	Palestine (Neqab)	Jordan (Dead Sea area)	Iraq (Western Desert)
Lr.Cretaceous	Malha F.	Hatira F.		Kurnub Sst.F.	
Tri-assic: Rhaetian, Norian, Carnian		Budra F.*	Mishhor F. Mohilla F. Saharonim F.		
Tri-assic: Ladinian			Gevanim F.	Mukheiris F.	
Tri-assic: Anisian			Raa'f F.	Hisban F.	
Tri-assic: Seythian				Ain Musa F. Dardur F.	
			Zafir F.	Ma'in F.	
Permo -Triassic	Qiseib F.*		Yamin F.	Um Irna F.*	
				--U.C--	Ga'ara F.
Permo-Carboniferous Carboniferous		Ataqa F.			
Up.				Brownish Weatherd Sst.	
Cambrian Mid				Burj F.	
Lr					

towards the west. It was found to be only 2 m thick in the bore hole KH 5 - 6 west of Rutba (Fig. 7..8). It was given an Uppermost Carboniferous and / or Permian age by Clyrocky (1973) on the basis of fossil plant remnants. This was confirmed by Dr. J. Setik, who determined new plant fossil remnants and a post Stephanian age was given.

The Gaara Formation sediments consists of two main lithologies, sandstones and mudstones which form beds and lenticular layers of different thickness, varying from several centimeters to tens of meters. They alternate many times within the profile of the unit. The majority of sandstones are cross - bedded and locally pebbly. Basal planes of sandstone layers are often sharp and uneven. Clay fragments occur commonly at the bottom of the sandstone bands. Sandstones were several times reworked, and are mature in both granularity and mineralogical composition. They are of monomineralic character and could be called quartzarenite to quartzwacke.

Siltstones and subordinate mudstones are usually varicoloured; violet colour is most common, but also red, pink, yellowish, ochre, greenish, bluish-grey and white colours as well as conspicous mottling are commonly present. Pure claystones usually of white colour composed of kaolinite or kaolinite - illite are rare (Abboud and Raouf, 1972; Kadir and Santrucek, 1975; and Salman, 1977).

Thin lenticular layers of Fe- ores (hematite and goethite) usually several centimeters to tens of decimeters in thickness (maximum about one metre) occur at different levels within the formation, both in the sandstone and mudstone. The most common occurrence of these iron ores is at the boundary of the mudstone and overlying sandstone. Fe - ores seem to have originated from colloidal solutions during the quiet period of sedimentation, which was interrupted by the deposition of a new overlying sandstone layer (Table 7. 2).

Relatively rare leaves of fossil plants occur within pelite layers at different levels. Small fragments of fossil plants are scattered on bedding planes of some siltstone and fine sandstones. Stems and logs have been found both in pelitic and psammitic rocks. Some are incrustated by Fe - oxide. Also bioglyphs, small worm - burrows and trails on bedding planes, occur commonly within mudstone beds. Coal seams are not known from the outcrops of the Gaara Formation, although thin coal beds (max. 50 cm thick), composed of impure fusitic coal, were penetrated by the bore hole K 5 - 2 in two levels.

The sediments of the Gaara Formation were deposited in continental fluviatile and lacustrine environments. The sandy and clayey material was delivered to the depositional site by a large river or more likely by several rivers, from the south or southwest (Salman,

Table 7. 2

The Average Concentration Of Major,Minor And Trace Elements Of Iron Ores In Um Irna,Budra,Gaara And Hasainiya Formations(Budra Data From Goldbery And Beyth,1984;Gaara And Hasainiya From Jawad,1980).

	Jordan	SW Sinai	Iraq	
	Um Irna	Budra	Gaara	Hasainiya
SiO2	21.85	28.95	41.80	48.48
Al2O3	8.27	15.81	9.52	14.20
Fe2O3	62.87	48.48	35.50	18.90
MgO	0.20	-	1.78	1.70
CaO	0.16	-	2.07	2.14
Na2O	0.06	-	0.68	0.73
K2O	0.23	-	0.52	0.55
LOI	5.13	3.81	-	-
TiO2	0.74	1.16	-	-
MnO	0.05	0.01	-	-
P2O5	0.03	-	-	-
Cr ppm	177	-	256	130
Li ppm	41	-	-	-
Ni ppm	86	-	85	143
Co ppm	35	-	34	34
Zn ppm	79	-	-	-
Be ppm	12	-	-	-
Cu ppm	13	-	-	-
V ppm	835	-	297	434
Sc ppm	27	-	-	-
Rb ppm	6	-	-	-
Mn ppm	-	-	222	131
Ti ppm	-	-	<1	1

1977). The source area is presumably the Arabian Shield, formed both by plutonic and metamorphic rocks.

7.5 DISCUSSION

Fluvial red beds of Carboniferous, Permian and Triassic ages, representing part of the continental sedimentation regime occur on the edges of the Arabo - Nubian Shield, whilst Tethian marine sedimentation occurs to the north and west (Fig. 7. 8). The continental sediments are represented by:

(1) Um Irna Formation, Permo - Triassic, Jordan,

(2) Gaara Formation, Permo - Carboniferous, Iraq,

(3) Mishhor Formation, Upper Triassic, Palestine,

(4) Budra Formation, Middle to Upper Triassic, Sinai, and

(5) Qiseib Formation, Permo - Triassic, Egypt.

These red beds are of regional significance and attest to important sedimentological and palaeoclimatic events in the Middle East. The correlation among the different formations is reasonably reliable on the basis of available lithological and palaeontological data (Fig. 7.)9).

During the Permian, the terriginous facies reached its maximum geographic extent, covering the western desert of Iraq (NE) and extending east of the Dead Sea (Jordan) into southwestern Sinai

and eastern Egypt. In all these areas a group of ferrugeneous clay and silt sediments occur which may be significant indicators of nonmarine weathering crusts or soil forming processes. These may be explained by descending and / or ascending solutions leaching part of the iron from the ferruginous beds and redepositing it as iron concretions with soft ferricrusts (Goldbery and Beyth, 1984).

Towards the end of the formation of the Um Irna a transgression of the Tethys ocean covered most of the Middle East area. This major transgression marks the end of the Permo - Triassic facies. The sea transgressed from the northwest and deposited the predominantly carbonate sequence of the Ma'in Formation which is the lowermost dated marine Triassic Formation (Scythian) deposited on the continental Um Irna Formation.

In Palestine, marine sediments prevailed in the Naqab continuously throughout the Upper Permian to Lower Triassic (Yamin and Zafir Formations). No sedimentologic break has yet been detected within the sequence (Druckman, 1974).

The Ma'in Formation should be considered as the facies equivalent of the Zafir Formation in Palestine. The theory of sinistral movement, 100 km along the Dead Sea Rift valley (Quennel, 1958, 1983; Freund et al., 1970) seems to be supported by the occurrence of a Ma'in time equivalent Zafir Formation in the northern Naqab in Palestine (Druckman, 1974).

CONCLUSIONS

1. The Upper Cambrian rocks were divided into two facies: arenite and heterolithic facies. The quartzarenite facies is interpreted to have formed on the distal reaches of an unconfined braidplain sloping gently towards the northwest from an elevated provenance in the southeast, probably the Arabo-Nubian Shield. The heterolithic facies is interpreted to have formed by tidal currents acting on the distal margin of alluvial braidplain during periods of repeated minor transgressions.

2. Facies and palaeocurrent analysis of the Um Irna Formation indicates that deposition occurred on the lower to middle reaches of an unconfined humid braidplain sloping gently westwards from an elevated source area in the south and east. The lowermost facies is regarded as a distal equivalent of the overlying coarser grained facies in the succession.

3. The overall model proposed for the Ma'in Formation is that of an intertidal flat environment (Himara Member) located between a braided alluvial plain (Um Irna Formation) and a subtidal marine shelf environment (Nimra Member).

The results of this research suggest that more research work needs to be done along the following lines:

1. Extend the work lower down in the succession to include the lower part of the Upper Cambrian Ishrin Formation and the Early Middle Cambrian Burj Formation, and try to establish more precisely age relationships.

2. Extend the work to the south to try and establish stratigraphic and lithofacies relationships (proximal and distal facies equivalents).

3. More detailed study of sedimentary petrography, including heavy mineral analysis to try and establish whether the Arabo-Nubian Shield was exposed or covered during Permo-Triassic times. This may also help to determine whether the source area was tectonically active at this time, and whether the sediments were recycled or not.

4. Further detailed study of the finer grained heterolithic facies in the Upper Cambrian could be useful in order to refine the environmental interpretation. This may also yield more palaeontological evidence of the age of the sediments.

5. A more detailed clay mineral/geochemical study of the Permo-Triassic Um Irna is needed to define the nature of pedogenic processes operating at this time.

APPENDIX A

MODAL ANALYSES

Appendix A

Table A.1

Modal Analysis Of Upper Cambrian Sandstones

Constituents	C03 22	C03 18	C03 16	C03 17	C03 19	C03 20	C05 14	C08 15	C00 24	Average
Monocryst.Quartz	46.8	57.0	64.0	57.8	68.4	58.8	70.6	34.0	63.8	58.0
Polycryst.Quartz	1.2	4.2	2.0	1.9	9.2	3.2	11.2	0.0	1.4	3.8
Silica Overgrowth	0.2	12.0	8.8	6.4	14.0	4.8	13.6	0.2	8.4	7.6
Chert	0.0	0.0	1.4	2.7	0.0	2.0	0.6	0.0	0.0	0.7
K-Feldspar	4.2	2.2	13.8	3.0	0.0	3.0	0.0	3.8	6.6	4.0
Plagioclase	0.6	0.2	1.2	0.0	0.0	0.6	0.0	1.6	0.2	0.5
Mica	2.0	0.4	0.4	0.2	0.2	0.6	0.0	2.4	0.2	0.7
Heavy Minerals	1.8	2.0	1.0	2.6	2.0	2.0	0.2	5.6	2.5	2.2
Lithic Fragments	0.0	5.6	2.2	3.0	5.2	0.8	1.8	0.6	1.4	2.3
Kaolin	34.2	14.6	3.6	20.2	0.6	9.4	1.4	29.4	9.0	13.6
Iron Oxide	9.0	1.8	1.6	2.2	0.4	14.8	0.6	22.4	6.4	6.6

Table A.2

Modal Analysis Of Permo-Triassic Sandstones (Um Irna Formation)

Constituents	U06 10	U06 09	U06 06	U06 04	U06 01	U06 05a	U11 07	U11 05	U11 04	U11 01	U11 00	U13 06	U13 07	U12 01	Average
Monocryst.Quartz	45.6	50.6	59.4	56.2	46.2	39.8	46.0	51.8	45.6	51.6	52.0	56.8	45.8	30.8	49.8
Polycryst.Quartz	3.2	1.4	2.0	3.0	2.4	17.2	4.0	3.4	5.4	2.6	7.2	24.6	12.4	0.6	7.0
Silica Overgrowth	4.6	8.0	5.2	2.8	10.4	0.0	1.0	4.4	0.8	2.4	4.0	2.2	11.6	0.0	4.4
Chert	0.4	0.0	0.0	0.0	0.0	0.4	0.4	0.8	1.2	0.4	0.0	1.4	0.0	0.0	0.4
K-Feldspar	16.0	15.4	4.4	8.4	13.6	10.8	21.8	15.2	22.2	11.8	0.6	0.2	10.0	0.0	11.6
Plagioclase	0.4	0.2	0.0	0.0	0.0	0.2	0.4	0.2	0.0	0.2	0.0	0.0	0.0	0.0	0.2
Mica	0.8	1.0	0.2	0.8	1.0	0.8	0.2	1.2	1.4	1.0	0.2	0.8	0.2	0.0	0.8
Heavy Minerals	2.4	2.4	1.6	3.4	3.8	0.4	0.0	2.2	1.0	1.8	0.2	1.0	1.4	1.0	1.8
Lithic Fragments	0.0	0.8	0.2	0.2	0.2	1.4	0.6	1.2	0.0	0.2	0.2	0.6	0.4	0.0	0.5
Kaolin	18.6	14.4	25.0	20.6	12.4	0.2	3.0	12.4	17.6	8.8	7.2	10.2	14.8	10.4	12.7
Iron Oxide	8.0	5.8	2.0	4.6	10.0	7.4	22.4	7.2	4.8	5.8	27.6	2.2	3.4	57.2	8.0
Dolomite	0.0	0.0	0.0	0.0	0.0	21.4	0.2	0.0	0.0	13.4	0.8	0.0	0.0	0.0	2.8

Table A.3

Modal Analysis Of Lower Triassic Sandstones (Ma'in Formation)

Constituents	H11 15	H07 07	H07 22	H06 30	HN07 23	N07 08	N10 10a	N11 16	Average (H)	Average (N)	Average (Total)
Monocryst.Quartz	47.6	24.0	37.6	44.4	70.0	47.0	43.0	52.8	38.4	47.6	43.0
Polycryst.Quartz	0.4	0.4	2.4	1.2	4.6	2.4	4.2	3.0	1.0	3.2	2.1
Silica Overgrowth	3.6	0.4	6.2	8.2	18.6	0.4	1.6	0.0	4.6	0.7	2.6
Chert	0.0	0.0	0.0	0.8	0.8	0.0	0.0	0.0	0.4	0.0	0.2
K-Feldspar	16.6	14.8	15.4	19.2	2.0	0.0	2.0	0.0	16.5	0.7	8.6
Plagioclase	5.6	10.6	5.8	4.8	0.0	0.0	1.2	0.0	6.7	0.4	3.5
Mica	0.4	1.4	1.8	3.0	1.0	0.0	0.0	0.2	1.6	0.1	0.9
Heavy Minerals	3.0	2.0	3.4	5.4	1.8	0.2	0.8	0.2	3.5	0.4	2.0
Lithic Fragments	0.6	0.2	1.0	1.6	0.0	0.0	0.0	0.0	0.9	0.0	0.5
Kaolin	0.0	1.0	0.0	0.0	0.0	0.0	0.0	0.0	0.3	0.0	0.2
Iron Oxide	10.6	10.8	7.4	10.6	1.2	0.4	1.2	1.0	9.8	0.8	5.3
Dolomite	11.6	31.4	18.0	0.0	0.0	35.6	30.8	42.8	15.3	36.4	25.8
Bioclasts	0.0	3.0	1.0	0.8	0.0	2.4	8.8	0.0	1.0	3.7	2.3
Oolite	0.0	0.0	0.0	0.0	0.0	11.6	6.4	0.0	0.0	6.0	3.0

APPENDIX B

MEAN FRAMEWORK MODES

Appendix B

Table B.1

Mean Framework Modes Of Studied Sandstones Of Upper Cambrian

Sample Number	Q	F	L	Qm	F	Lt	Qm	P	K
C 03 22	48.2	5.5	39.3	64.3	6.6	29.1	90.7	1.2	8.1
C 03 18	73.0	2.9	24.1	82.4	3.5	14.1	96.0	0.3	3.7
C 03 16	76.4	17.0	6.6	75.7	17.7	6.6	81.0	1.5	17.5
C 03 17	70.4	3.4	26.2	84.5	4.4	11.1	95.0	0.0	5.0
C 03 19	93.0	0.0	7.0	82.6	0.0	17.4	100.0	0.0	0.0
C 03 20	82.3	4.6	13.1	86.0	5.3	8.7	86.0	5.3	8.7
C 05 14	96.3	0.0	3.7	83.8	0.0	16.2	100.0	0.0	0.0
C 08 15	49.0	7.8	43.2	85.0	13.5	1.5	86.3	4.1	9.6
C 00 24	79.1	8.3	12.6	71.4	20.2	8.4	78.0	0.6	21.4
Average	91.1	5.9	3.0	84.5	6.5	9.0	92.8	0.8	6.4

Table B.2

Mean Framework Modes Of Studied Sandstones Of Permo-Triassic (Um Irna Fm.)

Sample Number	Q	F	L	Qm	F	Lt	Qm	P	K
U 06 10	58.4	19.5	22.1	69.5	25.0	5.5	73.5	0.6	25.9
U 06 09	62.8	18.8	18.4	74.2	22.9	2.9	76.4	0.3	23.3
U 06 06	67.5	4.8	27.7	90.0	6.7	3.3	93.1	0.0	6.9
U 06 04	67.0	9.5	23.5	82.9	12.4	4.7	87.0	0.0	13.0
U 06 01	65.0	18.2	16.8	74.0	21.8	4.2	77.3	0.0	22.7
U 06 05a	82.0	15.7	2.3	57.0	15.8	27.2	78.3	0.4	21.3
U 11 07	66.2	29.1	4.7	62.8	30.3	6.9	67.4	0.6	32.0
U 11 05	65.9	18.1	16.0	71.3	21.2	7.5	77.0	0.3	22.7
U 11 04	53.9	22.9	23.2	57.6	28.0	14.4	67.3	0.0	32.7
U 11 01	72.2	15.9	11.9	77.2	18.0	4.8	81.1	0.3	18.6
U 11 00	88.1	0.9	11.0	86.7	1.0	12.3	98.9	0.0	1.1
U 13 06	88.3	0.2	11.5	67.9	0.2	31.9	99.6	0.0	0.4
U 13 07	69.8	12.0	18.2	66.8	14.6	18.6	82.1	0.0	17.9
U 12 01	75.1	0.0	24.9	98.0	0.0	2.0	100.0	0.0	0.0
Average	83.3	16.0	0.7	72.0	17.0	11.0	80.9	0.3	18.8

Table B.3

Mean Framework Modes Of Studied Sandstones Of Lower-Triassic (Ma'in Fm.)

Sample Number	Q	F	L	Qm	F	Lt	Qm	P	K
H 11 15	67.8	31.4	0.8	67.2	31.4	1.4	68.2	8.0	23.8
H 07 07	45.2	47.0	7.8	44.4	47.0	8.6	48.6	21.5	29.9
H 07 22	63.3	33.5	3.2	59.5	33.5	7.0	64.0	9.9	26.1
H 06 30	63.7	33.0	3.3	61.0	33.0	6.0	65.0	7.0	28.0
HN 07 23	97.4	2.6	0.0	90.4	2.6	7.0	97.2	0.0	2.8
N 07 08	77.9	0.0	22.1	74.1	0.0	25.9	100.0	0.0	0.0
N 10 10a	71.9	4.9	23.2	65.5	4.9	29.6	93.1	2.6	4.3
Average	79.2	20.0	0.8	74.5	21.0	4.5	78.0	6.4	15.6

APPENDIX C

TRIANGLUAR PLOTS

Appendix C

Table C.1

Qm-Qp-Chert , Qm-Qp-Silica Overgrowth , and Kaolin- Fe Oxide- Carbonate Triangular Plot Of the Upper Cambrian , Permo-Triassic (Um Irna Formation) and Lower Triassic(Ma'in For--mation) Sandstones .

	Qm	Qp	C	Qm	Qp	Si	Kl	Fe	Ca
Cambrian	92.8	6.1	1.1	83.5	5.5	11.0	67.3	32.7	0.0
Permo-Triassic	87.1	12.2	0.7	81.4	11.4	7.2	54.0	34.1	11.9
Lower Triassic	94.9	4.6	0.5	90.1	4.4	5.5	0.5	14.5	85.0

APPENDIX D

CHEMICAL ANALYSES

Appendix D

Table D.1

Chemical Analyses Of Major,Minor And Trace Elements Of Ferruginous Pisoliths From The Um Irna Formation

	BT1	BT2	BT3	BT4
SiO2	20.2	29.0	18.9	19.3
Al2O3	6.1	11.2	6.1	9.7
Fe2O3	67.4	54.9	67.8	61.4
MgO	0.16	0.17	0.17	0.31
CaO	0.16	0.18	0.14	0.16
Na2O	0.07	0.06	0.07	0.05
K2O	0.22	0.19	0.22	0.29
LOI	4.43	4.14	4.40	7.56
TiO2	0.74	0.89	0.74	0.60
MnO	0.02	<0.01	0.02	0.14
P2O5	0.04	0.03	0.03	0.04
Cr ppm	155	300	148	109
Li ppm	24	74	28	38
Ni ppm	65	69	76	134
Co ppm	27	14	32	68
Zn ppm	88	41	113	75
Be ppm	11	6	13	16
Cu ppm	16	5	16	14
V ppm	687	863	769	1020
Sc ppm	25	30	28	25
Rb ppm	8	3	9	5
Total	99.54	100.77	99.33	99.55

Table D.2

The Range And Average Concentration Of Major ,Minor And Trace Elements Of Ferruginous Pisoliths In The Um Irna Formation.

	Range	Average
SiO2	18.9 - 29.0	21.85
Al2O3	6.1 - 11.2	8.27
Fe2O3	54.9 - 67.8	62.87
MgO	0.16 - 0.31	0.20
CaO	0.14 - 0.18	0.16
Na2O	0.05 - 0.07	0.06
K2O	0.19 - 0.29	0.23
LOI	4.14 - 7.56	5.13
TiO2	0.60 - 0.89	0.74
MnO	0.01 - 0.14	0.05
P2O5	0.03 - 0.04	0.03
Cr ppm	109 - 300	177
Li ppm	24 - 74	41
Ni ppm	65 - 134	86
Co ppm	14 - 68	35
Zn ppm	41 - 113	79
Be ppm	6 - 16	12
Cu ppm	5 - 16	13
V ppm	687 - 1020	835
Sc ppm	25 - 30	27
Rb ppm	3 - 9	6

APPENDIX E

URANIUM MEASUREMENTS

Appendix E

Table E.1

Uranium Measurements In The Um Irna Formation And Adjacent Rocks

Formation	Member	Facies	Section	Rock Type	Uranium	Minute
Um Irna	Upper	2	11	Pebbly Sandstone	14 ppm	4
Um Irna	Upper	2	11	Pebbly Sandstones	28 ppm	4
Um Irna	Upper	2	11	Pisolite	20 ppm	4
Um Irna	Upper	2	11	Pisolite	27 ppm	4
Um Irna	Upper	2	11	Siltstone	21 ppm	4
Um Irna	Upper	2	11	Green Shales	72 ppm	4
Um Irna	Upper	2	11	Green Shales	44 ppm	4
Um Irna	Lower	1	13	Sandclasts	30 ppm	4
Um Irna	Upper	2	13	Pisolite	54 ppm	4
				Travertine	40 ppm	4

APPENDIX F

X - RAY DIFFRACTION

Appendix F

Table F.1

X-ray Diffraction For Um Irna Formation At Three Sections
(See Fig. 1.07 For Location)

Section	Sample	Member	Rock Type	Major Mineral Components
11	U 11 10a	Upper	Pisoliths	Hematite,Goethite
	U 11 09a	Upper	Claystone	Quartz,Kaoline
	U 11 07	Upper	Sandstone	Quartz,Kaoline,Feldspar,Hematite
	U 11 05	Upper	Sandstone	Quartz,Feldspar,Kaoline
	U 11 03	Upper	Sandstone	Quartz,Kaoline,Feldspar
	U 11 02	Upper	Sandstone	Quartz,Kaoline,Feldspar
	U 11 01a	Upper	Sandstone	Quartz,Calcite
6	U 06 15	Upper	Silty-Shale	Quartz,Kaoline
	U 06 14	Upper	Silty-Shale	Quartz,Kaoline,Hematite
	U 06 10	Upper	Sandstone	Quartz,Feldspar,Gypsum,Kaoline
	U 06 07	Upper	Sandstone	Quartz,Feldspar,Kaoline
	U 06 05	Upper	Sandstone	Quartz,Kaoline,Calcite
	U 06 02	Lower	Sandstone	Quartz,Kaoline
	U 06 01	Lower	Siltstone	Quartz,Kaoline
	U 06 05a	Upper	Sandstone	Quartz,Dolomite,Feldspar,Calcite
13	U 13 07	Upper	Sandstone	Quartz,Feldspar,Kaoline
	U 13 06	Upper	Sandstone	Quartz,Kaoline

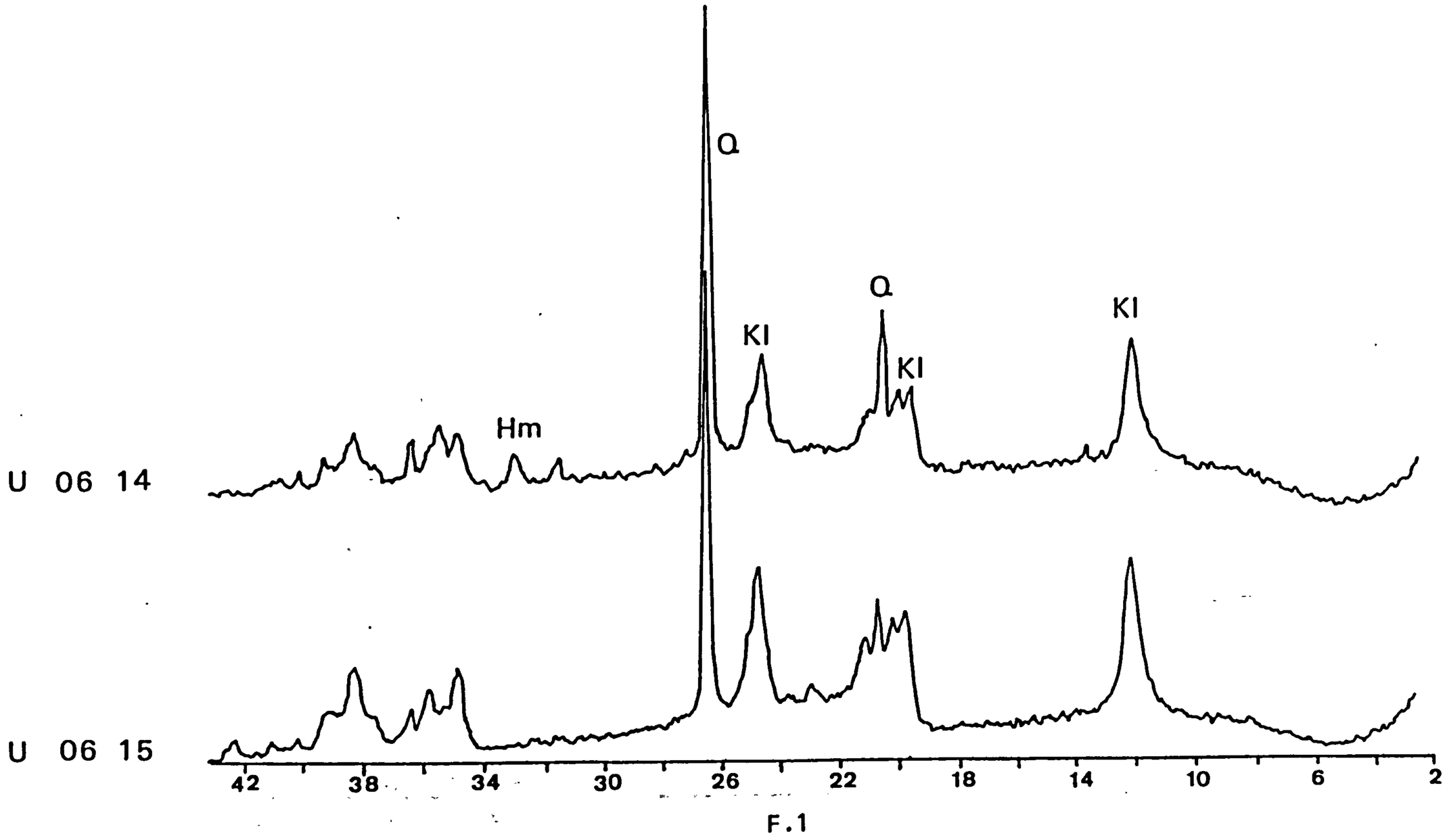

F.1

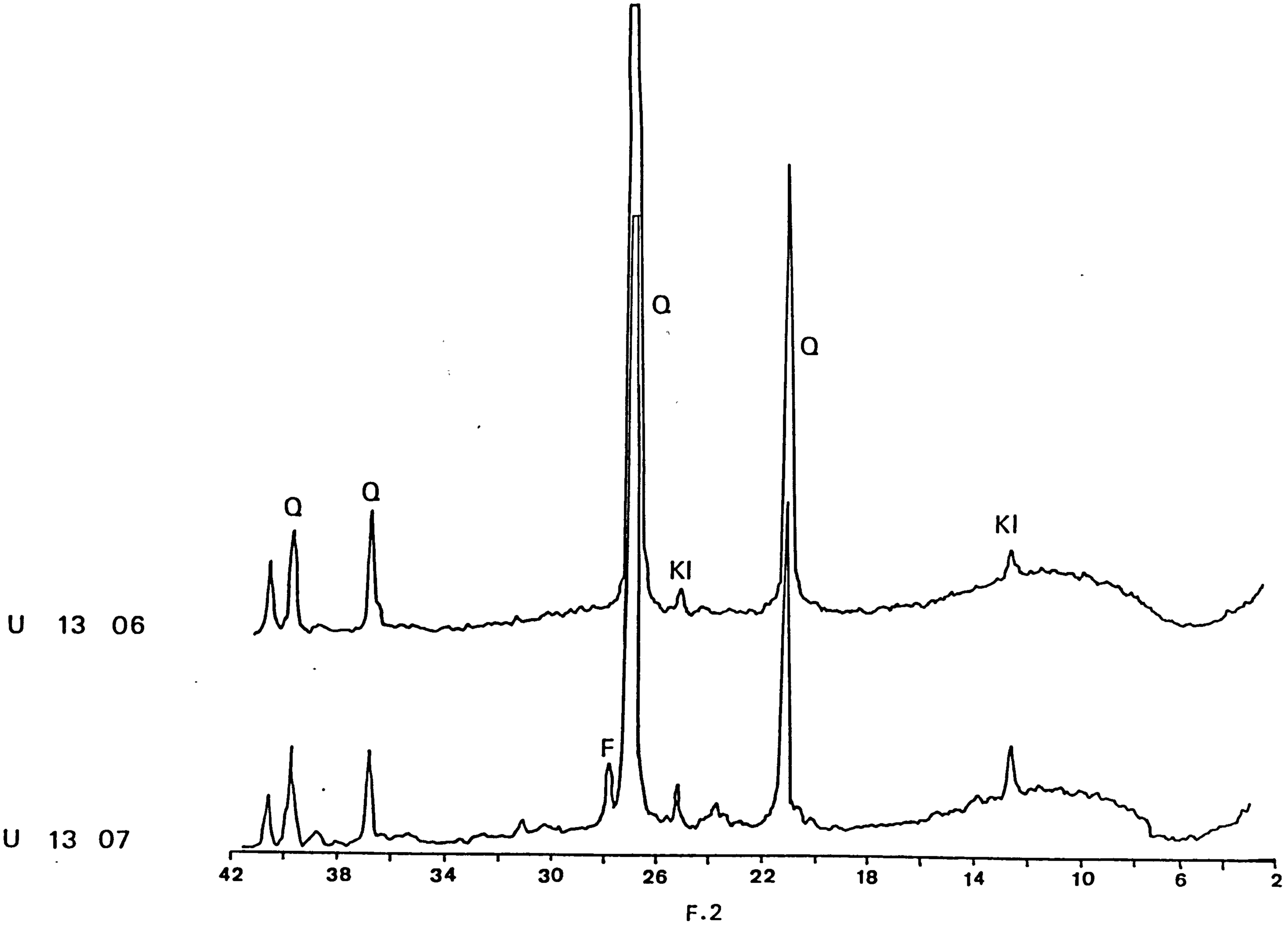

F.2

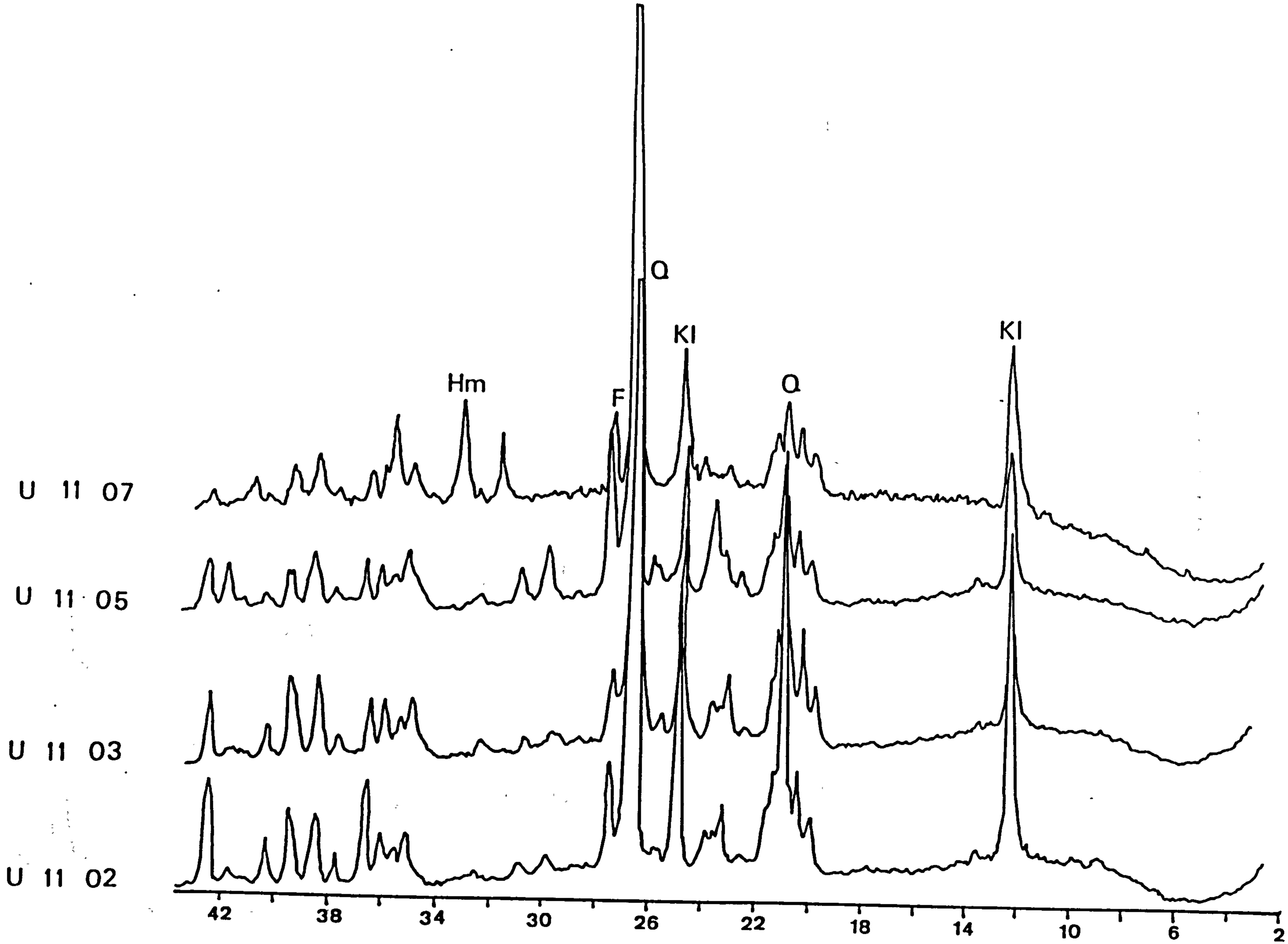

F.3

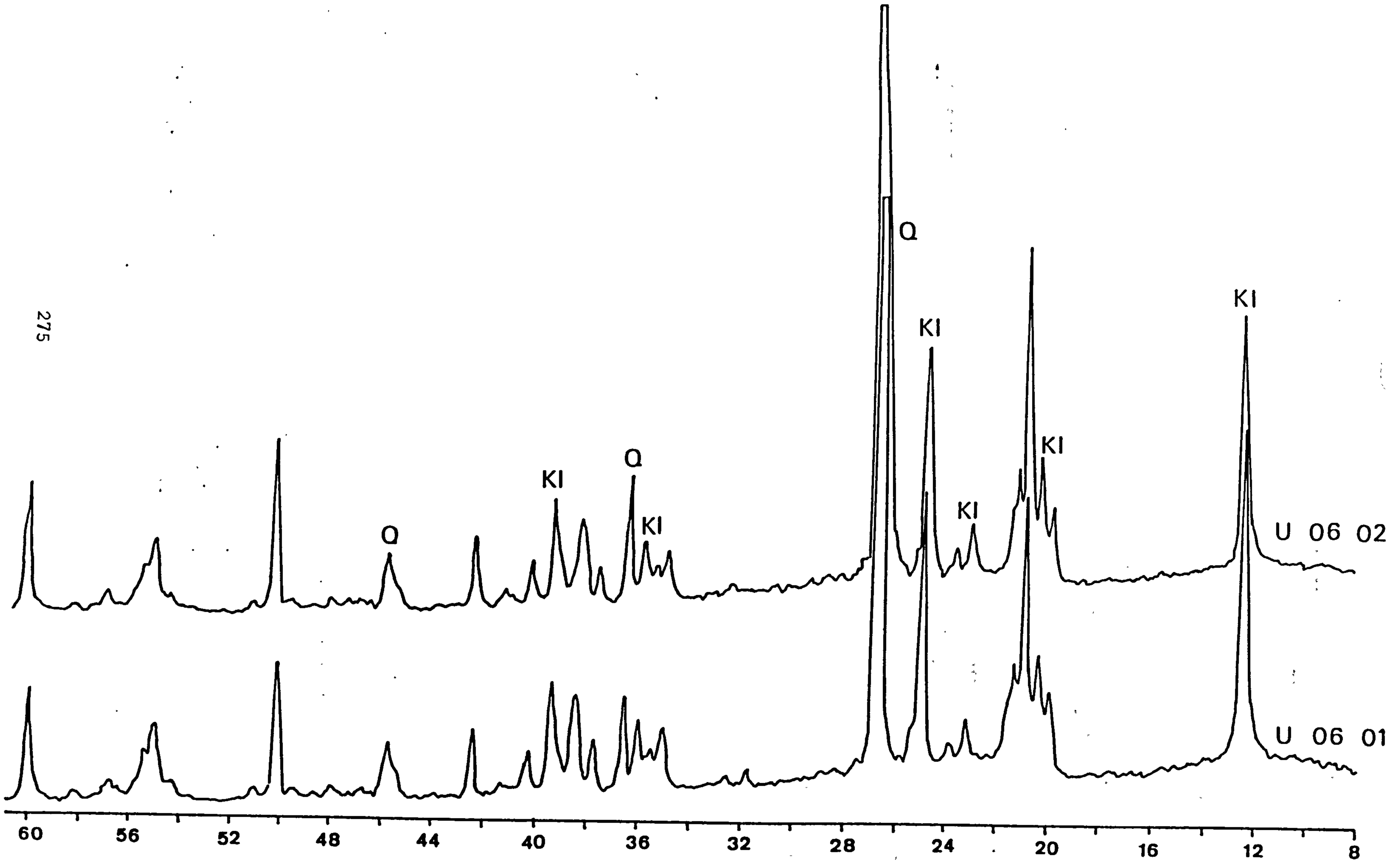
Q
KI
KI
Q
KI
Q
KI
KI
KI
U 06 02
U 06 01
60
56
52
48
44
40
36
32
28
24
20
16
12
8

F.4

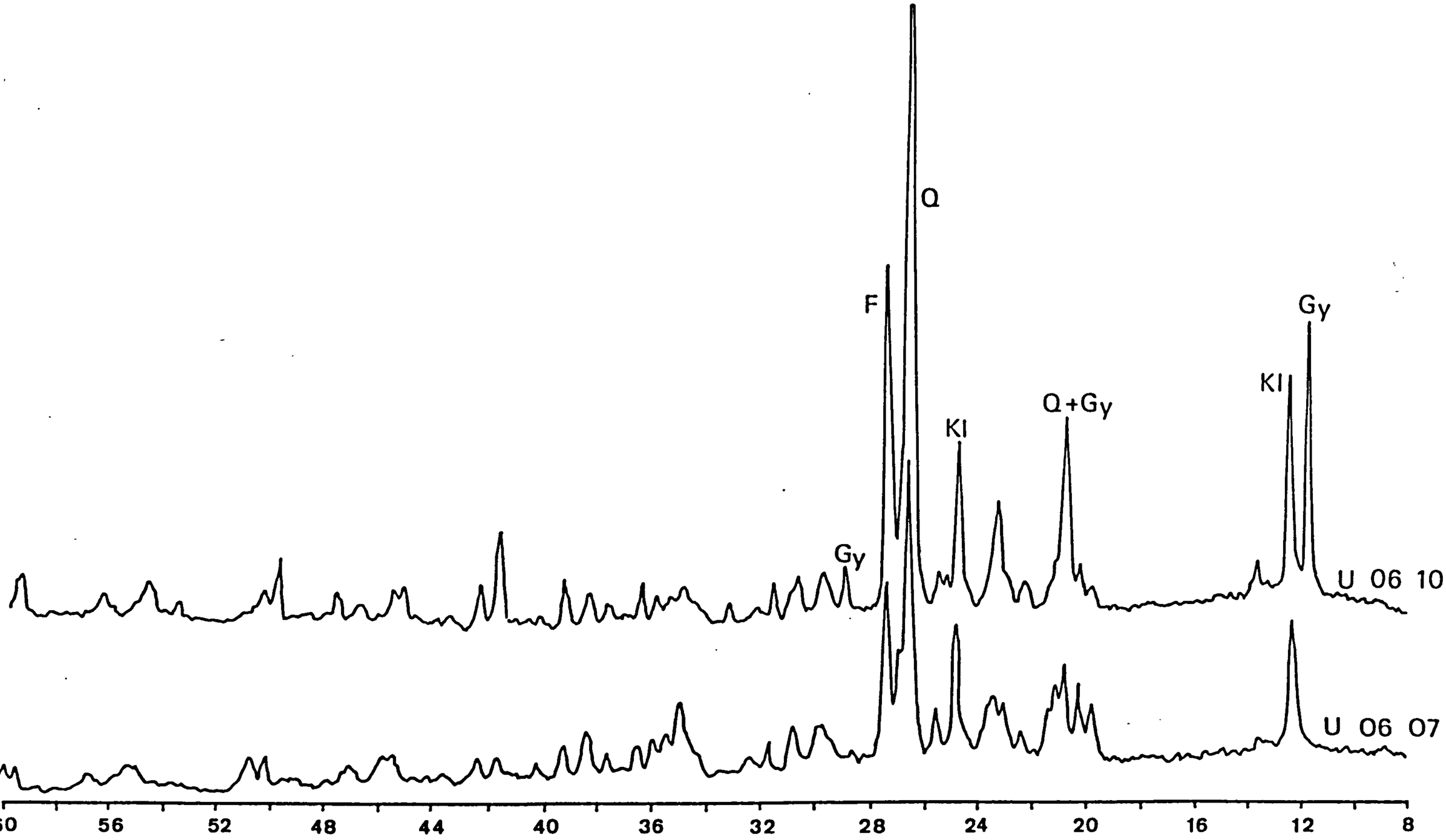
F
Q
Gy
KI
Q+Gy
KI
Gy
U 06 10
U 06 07
60
56
52
48
44
40
36
32
28
24
20
16
12
8

F.5

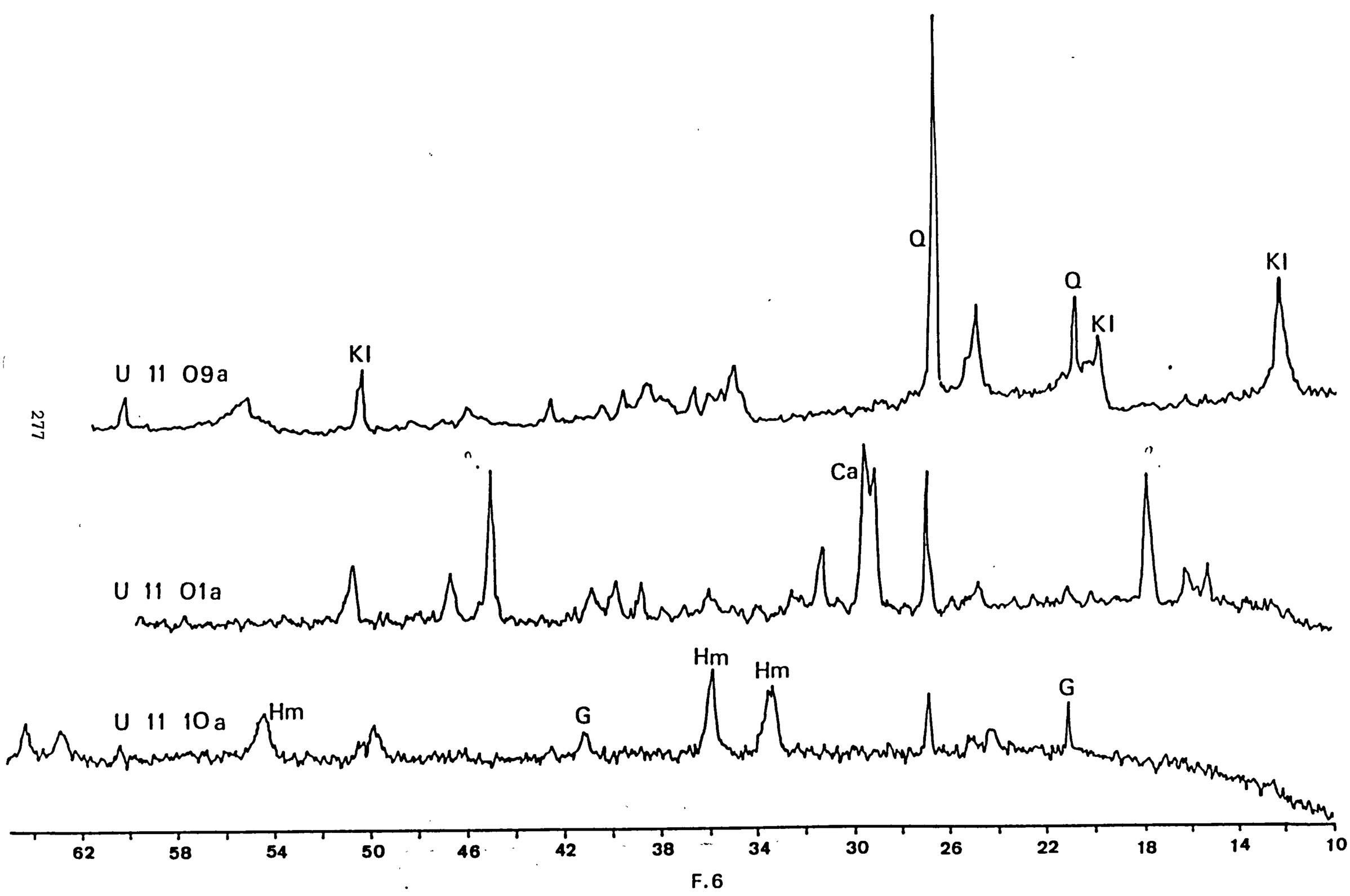
U 11 09a
KI
Q
Q
KI
KI
Ca
U 11 01a
U 11 10a
Hm
G
Hm
Hm
G
62
58
54
50
46
42
38
34
30
26
22
18
14
10

F.6

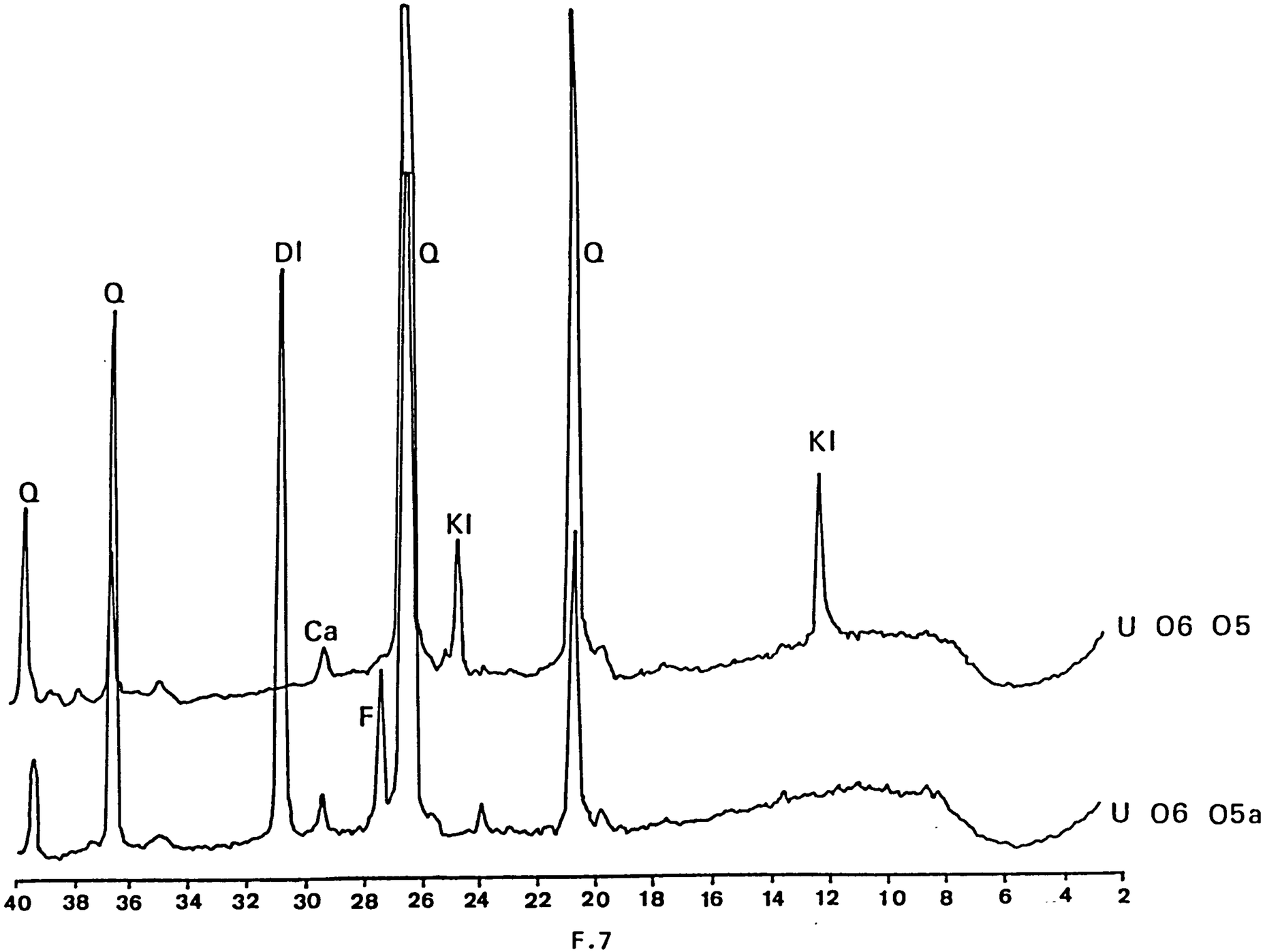
Q
DI
Q
Q
KI
Q
KI
Ca
F
U 06 05
U 06 05a
40 38 36 34 32 30 28 26 24 22 20 18 16 14 12 10 8 6 4 2

F.7

APPENDIX G

STRATIGRAPHY AND MEASURED SECTIONS

STRATIGRAPHY

I. The Upper - Middle Cambrian Sediments

These occur along the northeastern margin of the Dead Sea, and are exposed between Wadi Manshala and Wadi Abu Khusheiba. They are 110 m thick, with the upper 55 m best exposed in Wadi Manshala. They conformably overly the Middle Cambrian sediments of the Burj Formation. This boundary is exposed 1 km north of the mouth of Wadi Zarqa Ma'in, where it is marked by a change from thin bedded grey shale and marl to thick bedded brownish weathered sandstones (Plate 2.2). The upper contact is unconformable with the Permo - Triassic (Um Irna Formation) Plate 2.1.

The Upper - Middle Cambrian sediments comprise cream to brownish weathered massive quartzarenites, interbedded with minor amounts of siltstone and mudstone (Heterolithic facies) Plates 2.3, 2.4. Fossils are very rare except for a few badly preserved trilobites and bivalves ?lingula S_p in the heterolithic facies.

II. The Permo - Triassic Sediments (Um Irna Formation)

occurs at the northeastern margin of the Dead Sea, exposed between Wadi Mukheiris and Wadi Atun. They are about 60 m thick and are best exposed ay Wadi Himara (about 1 km to the east of the Dead

Sea, above the waterfall).

The Permo - Triassic sediment unconformably overlies the Upper - Middle Cambrian sediments. The lower contact is erosional and marked by a change from cream / light brown coloured quartzarenites to dark chocolate brown sandstone and shale interbeds and local pisoliths (iron oxide concretions). The upper contact is marked by the deep maroon bioturbated rhythmites of the Ma'in Formation (Himara Member) Plate 2. 1.

The Um Irna Formation comprises two sedimentary facies, which correspond to the informally designated lower and upper members. The Lower Member consists of about five fining - upward sequences composed of pebbly sandstones and pisolitic silty - shale, locally carbonaceous.

An Upper Permian age was attributed to the Um Irna Formation sampled at Bassat en Nimra by Dr. W. A. Brugman (Utrecht) on the basis of pollen grains, who determined "Lueckisporites virkklae" (Potenie et Klaus 1954) "Nuskoisporites dulhuntyi" and "Playfordiaspora crenulata" (Wilson, Forster 1979) from the dark argillaceous shales above the contact with Cambrian sandstones (Bandel and Khoury, 1981).

The Upper Permian age attributed to the Um Irna Formation is confirmed in this study by Dr. H. A. Armstrong of Newcastle upon Tyne University (personal communication, 1985) who described the pollen

grains in two samples (near the base of the Upper Member of the Um Irna Formation);

i) Sample 524 (BRT 1)

Abundant comminuted plant debris, small angular fragments of cuticle predominate, "Gymnosperm tracheids" are also common. Spores are present but generally poorly preserved. The microflora comprises bisaccate grains including; "Protohaploxipinus sp.", "Striatopodocarpites sp." and "Taeniaesporites sp.?". Generally these are badly affected by pyrite damage and have been identified using sac size to central body size characteristics. Also common are simple circulate Hiletespores but are poorly preserved and difficult to identify. "Cordailina sp.?" , "Vesicaspora sp.", "Punctatisporites sp.?".

ii) Sample 525 (BRT 2)

Better preserved, pale brown (? slightly oxidised) organic material, consisting of cuticle fragments (showing structures) and structureless material. Spores are almost absent; a few simple circular trilete spores are present, plus what might be the detached central bodies of bisaccate grains, nothing age diagnostic.

General comments (Dr. H. A. Armstrong); (1) both samples contain abundant terrestrial organic debris, (2) Spores in both are not particularly age diagnostic, (3) sample (BRT 1) contains what might be considered a moderately diverse assemblage if presented to a Gondwana specialist might yield a reasonable age, (4) The microflora is considered to be typical Gondwana Permian - ??? striatit. flonzone (Upper Permian).

III The Lower Triassic (Ma'in Formation)

Occurs at the northeastern margin of the Dead Sea, between Wadi Mukheiris and Wadi Abu Khusheiba. It is 55 m thick and best exposed at the mouth of Wadi Mukheiris.

The Ma'in Formation overlies the Permo - Triassic (Um Irna Formation), and is conformably overlain by the Dardur Formation. The lower contact is marked by an erosional surface underlain by a pebbly bed and pisolitic iron concretions of Um Irna Formation. The upper contact is marked by a change from thick bedded cream calcarenaceous sandstones to the thinly bedded marly shales of the Dardur Formation.

The Ma'in Formation was divided into two members; the Lower Member (Himara), 30 m thick; consists of deep maroon rhythmites associated with varicoloured shales. The Upper Member (Nimra) , 25 m thick; consists mainly of thick bedded cream coloured calcarenaceous sandstones; the lower part consists of varicoloured shales.

The existence of Lower Triassic conodonts in Jordan has been known since Huckride and Stoppel (Bender, 1974) discovered "Hadrodont-ina anceps", "H. biserialis", "Pachycladina inclinata", "P. obliqua" and "P. symmetrica" in the lower part of the Triassic succession at Wadi Zarqa Ma'in. placing these beds in the Scythian.

Trough cross-bedding

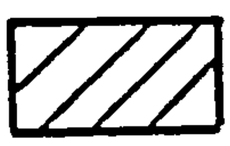

Planar cross-bedding

Herringbone cross-bedding

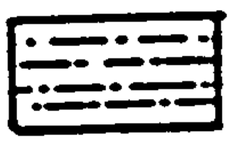

Structureless silty-shale

Rippled silty-shale

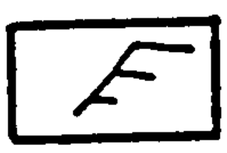

Rippled

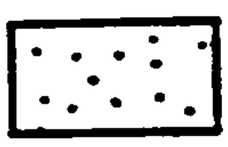

Structureless sandstone

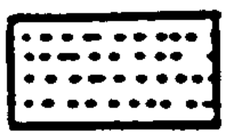

Laminated sandstone

Pebbly sandstone

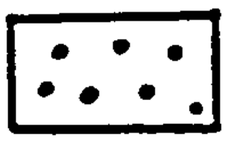

Pisoliths

Flaser bedding

Lenticular bedding

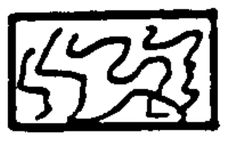

Deformed cross-bedding

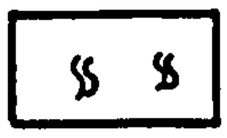

Bioturbation

Volcanic sill

Overturned cross-bedding

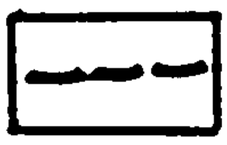

Mudcracks

Intraclasts

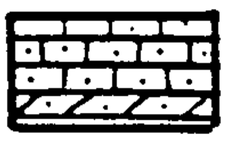

Calcareous sandstone

Erosional surface

Rippled surface

Notations

S = Silty-shale

F = Fine sandstone

M = Medium sandstone

C = Coarse sandstone

P = Pebbly sandstone

M = Thickness in metres

Key showing lithology, sedimentary structures and other notations used in Appendices.

G.1 - Section 8

Age	Lithology	Age	Lithology	Age	Lithology
Upper Cambrian	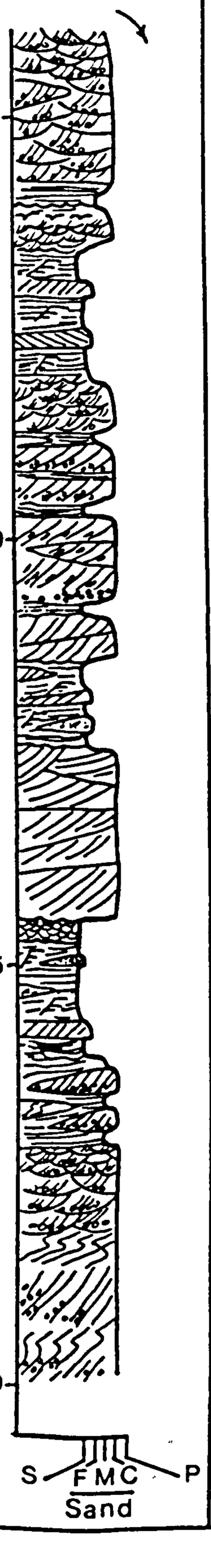		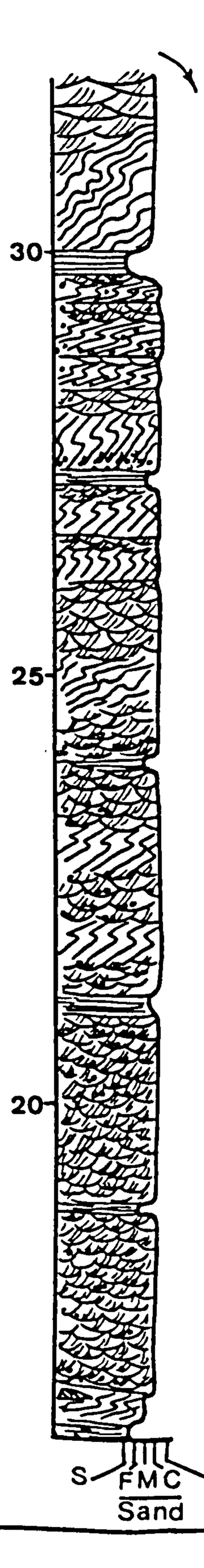		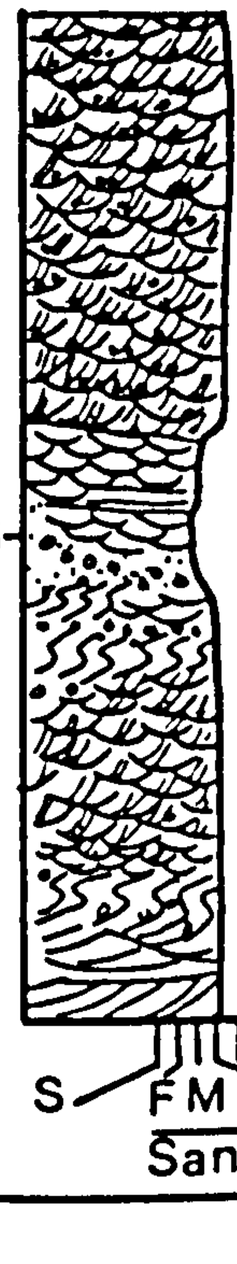

G.2 - Section 5

Age	Lithology	Age	Lithology
Upper Cambrian	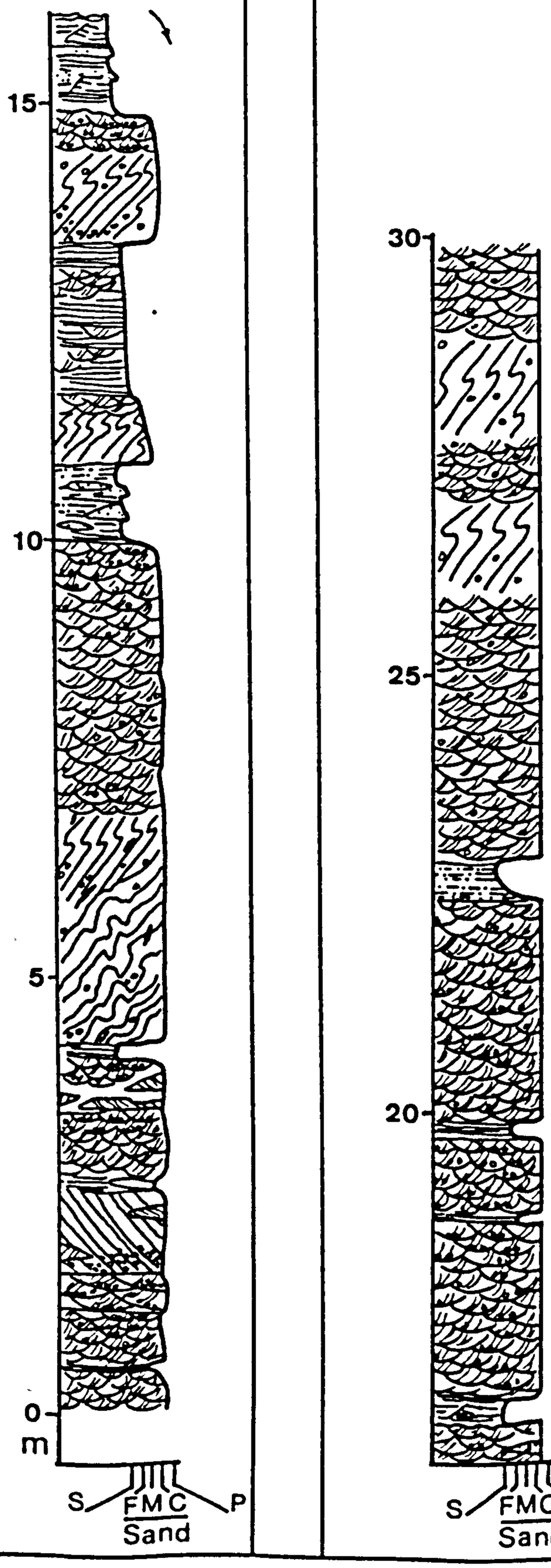		

G.3 - Section 6

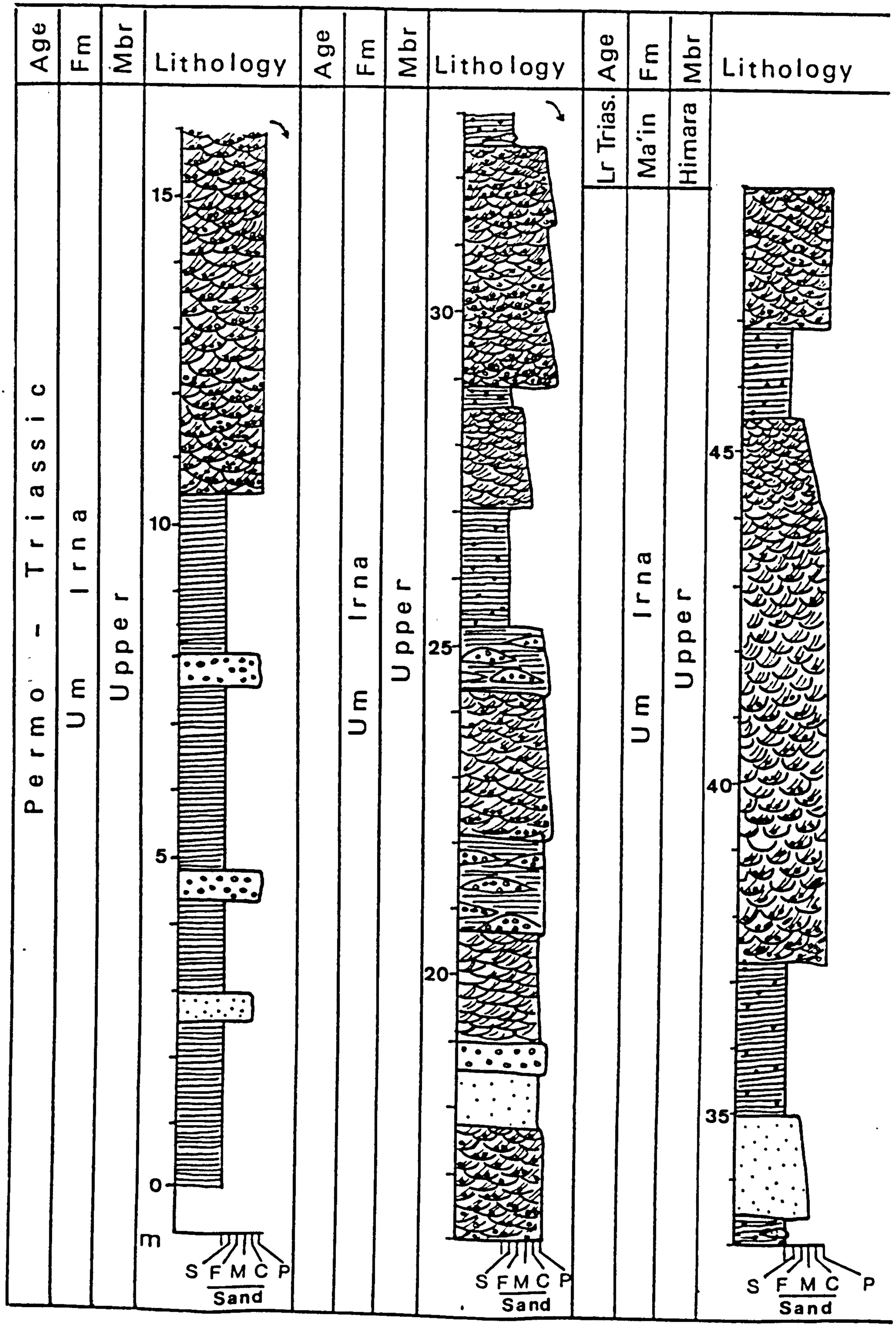
Age
Fm
Mbr
Lithology
Permo - Triassic
Um Irna
Upper
Lr Trias.
Ma'in
Himara
0
5
10
15
20
25
30
35
40
45
m
S F M C P
Sand

G.4 -Section 10

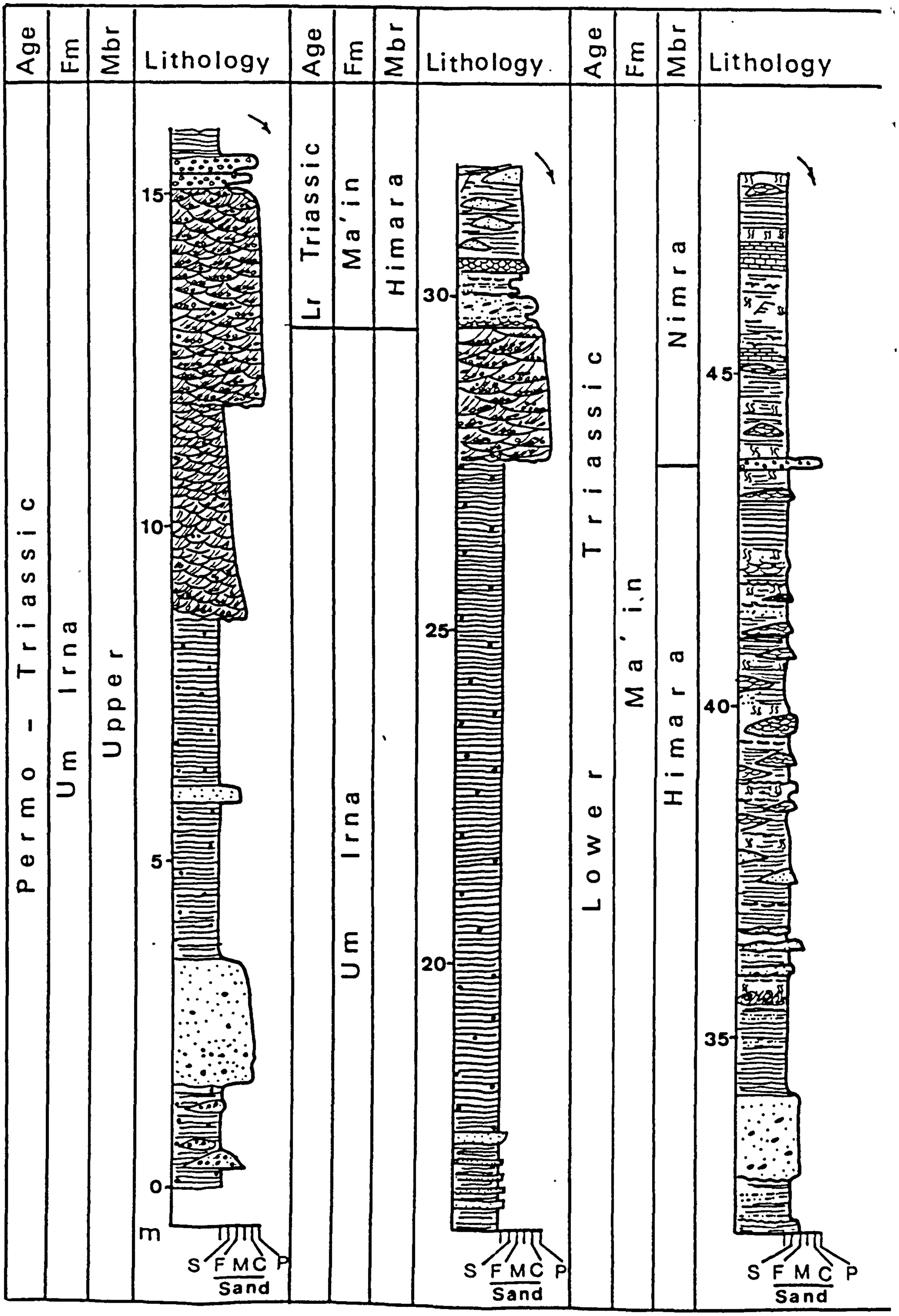

G.4-Section 10 (continued)

Age	Fm	Mbr	Lithology	Age	Fm	Mbr
Lower Triassic	Ma'in	Nimra	60 55 50 S F M C P Sand	Ma'in	Dardur	Nimra

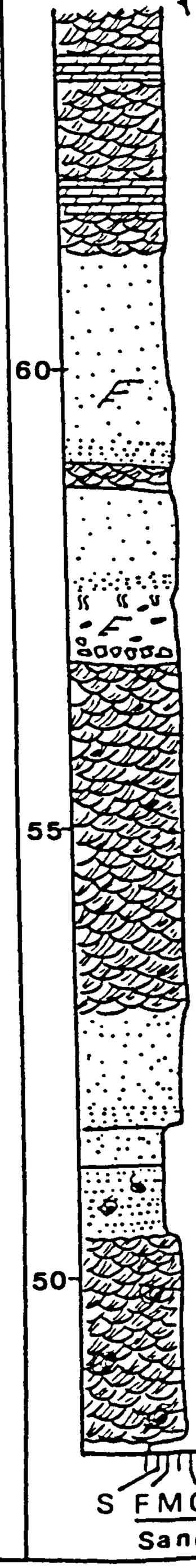

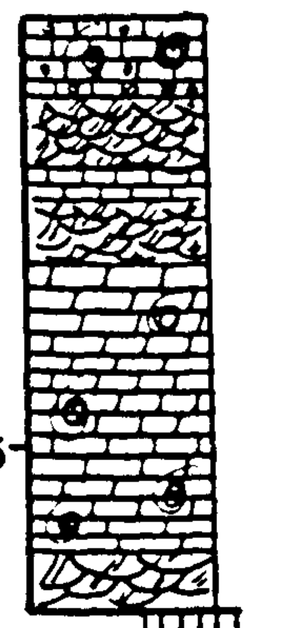

G.5 - Section 11

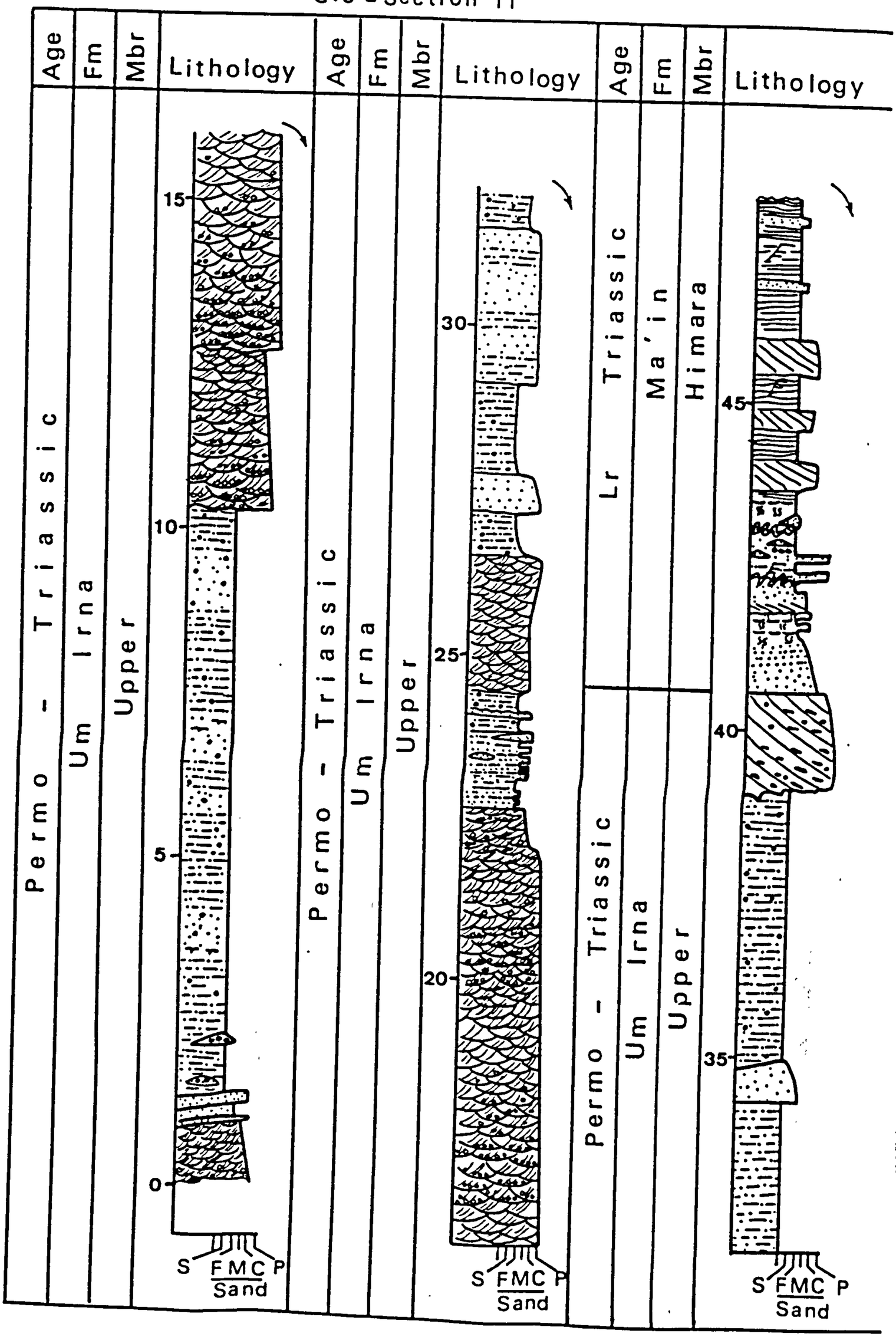

G.5 - Section 11 (continued)

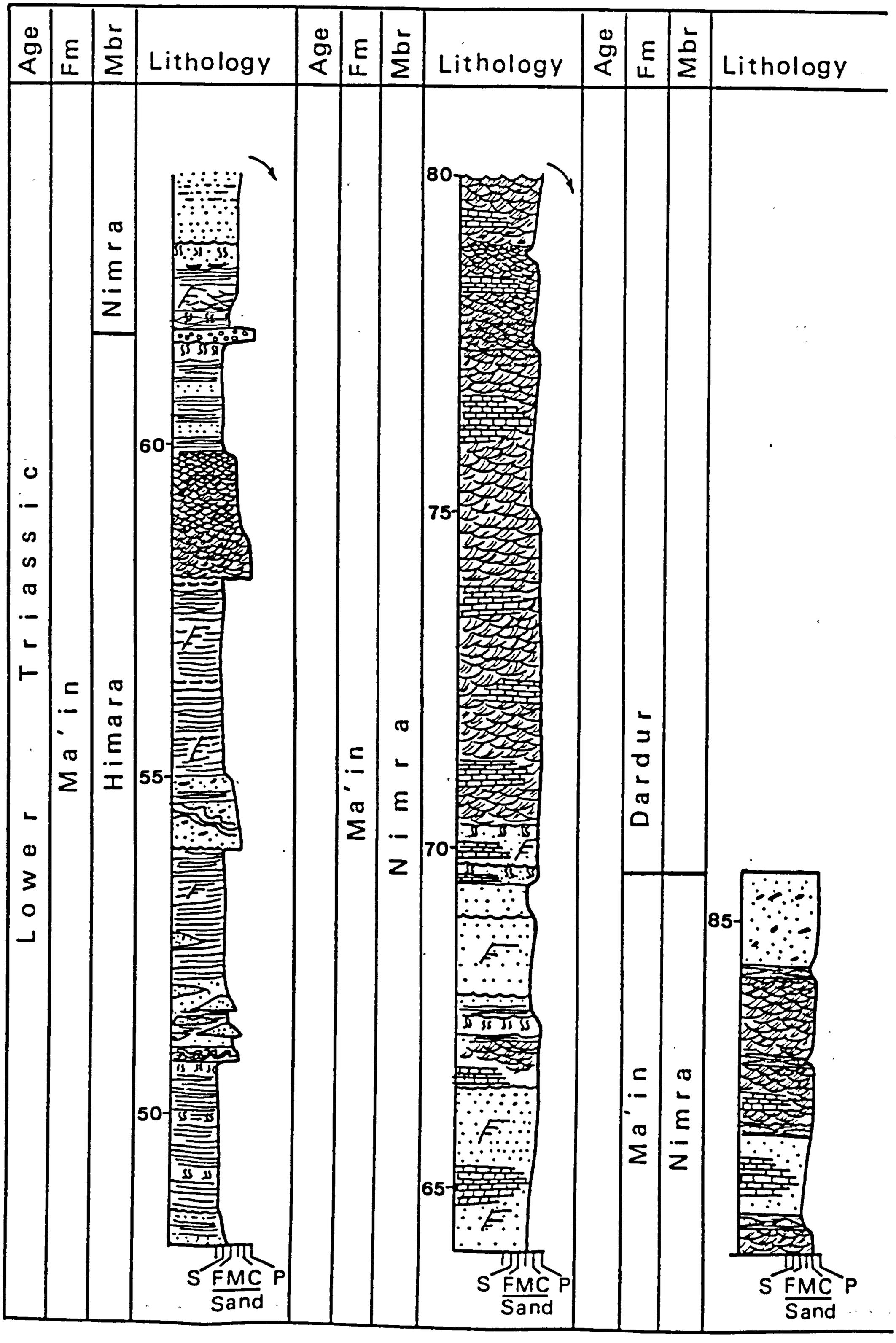

G.6 - Section 7

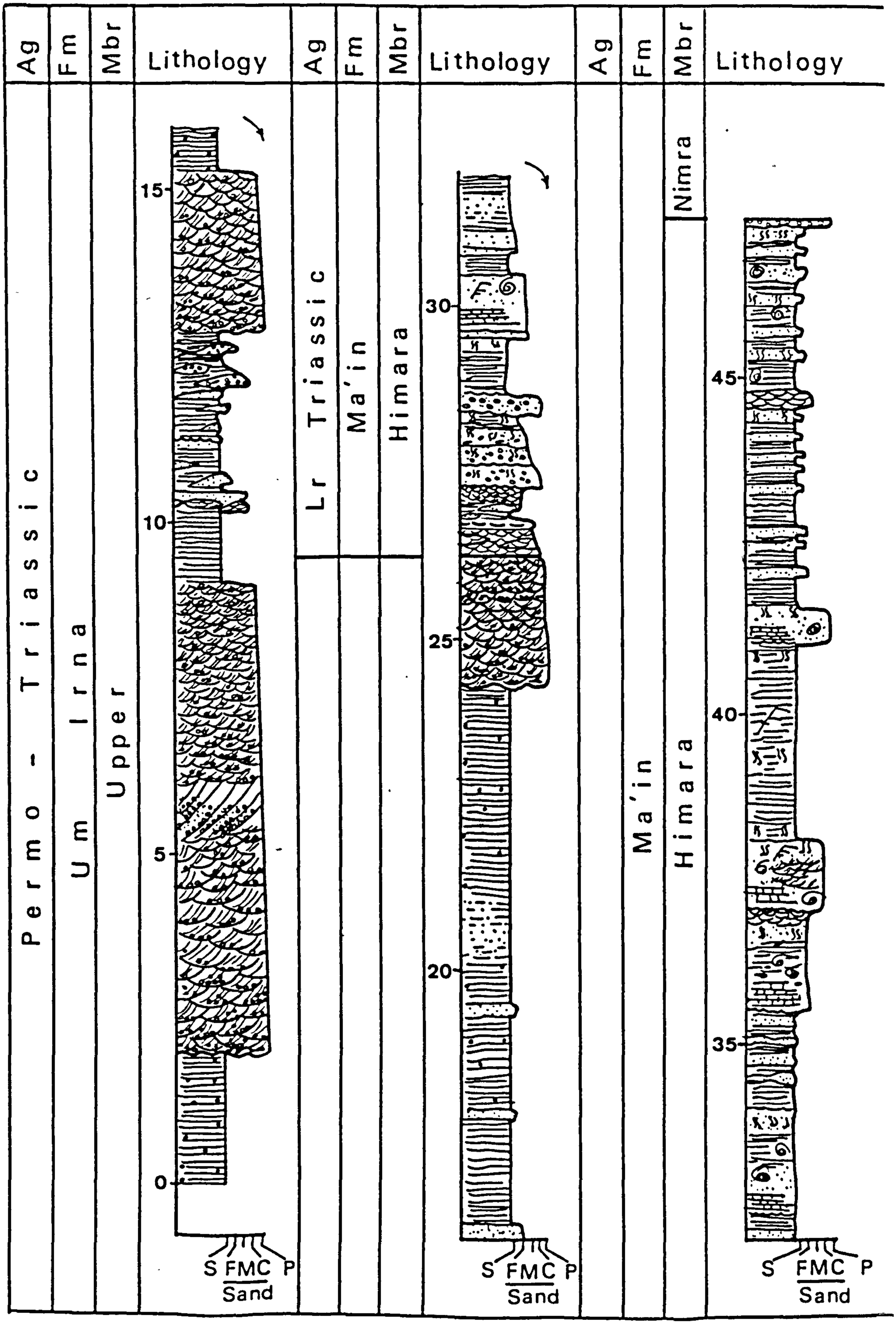
Ag
Fm
Mbr
Lithology
Permo - Triassic
Um Irna
Upper
Lr Triassic
Ma'in
Himara
Nimra
0
5
10
15
20
25
30
35
40
45
S FMC P
Sand

G.7 - Section 1

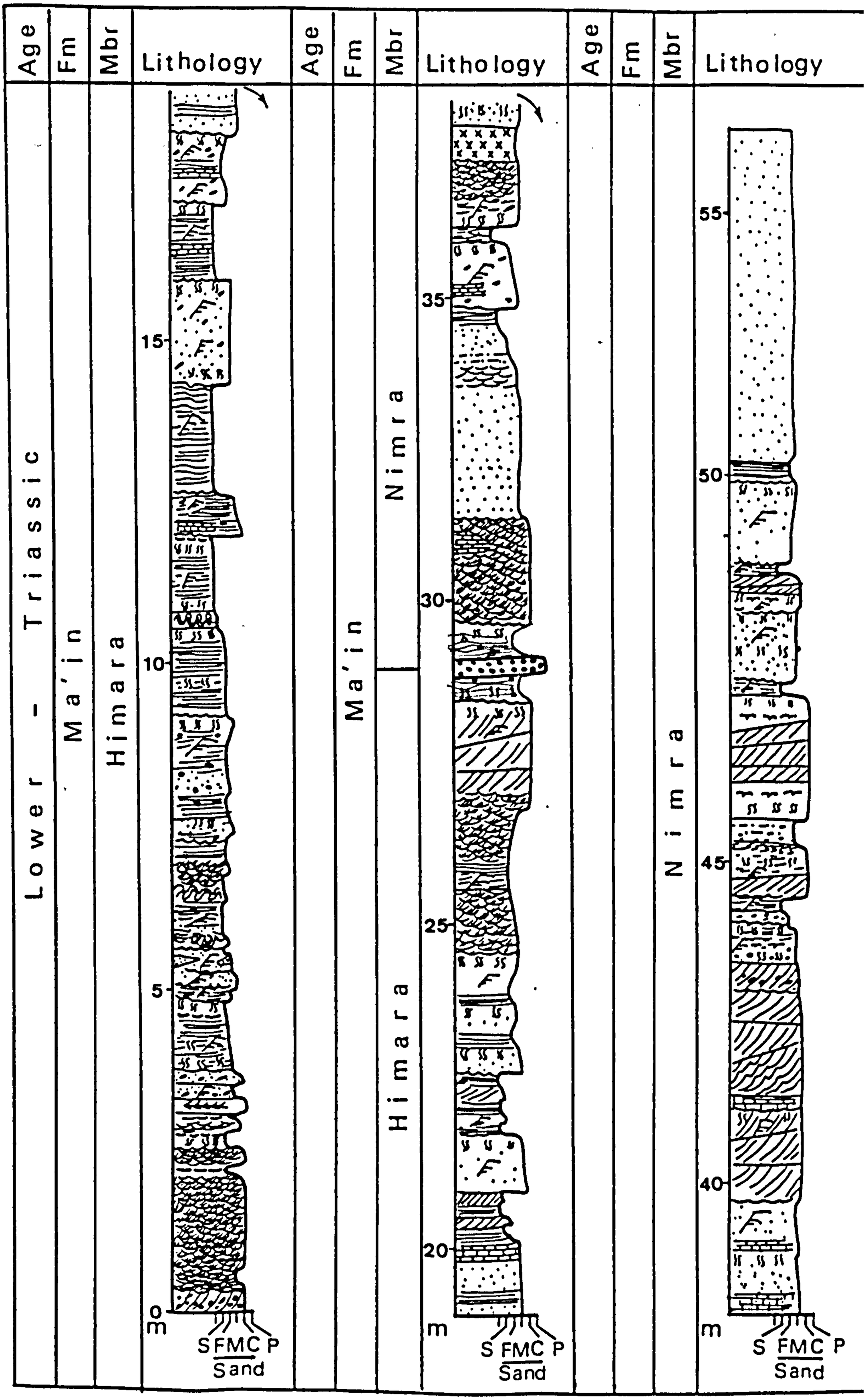
Age
Fm
Mbr
Lithology
Lower - Triassic
Ma'in
Himara
Nimra
0
5
10
15
20
25
30
35
40
45
50
55
m
S FMC P
Sand

G.8 - Section 4

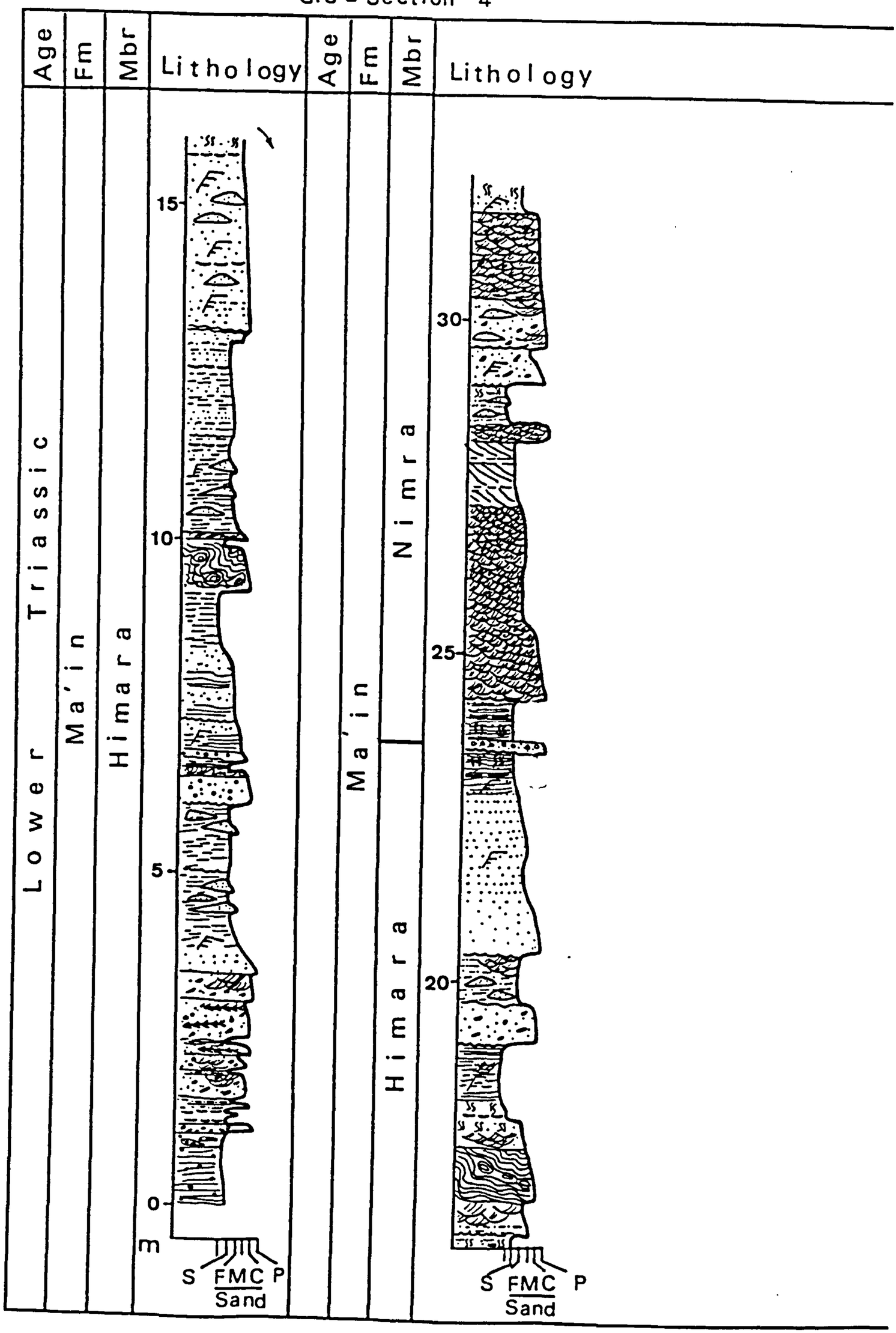
Age
Fm
Mbr
Lithology
Lower Triassic
Ma'in
Himara
Nimra
m
0
5
10
15
20
25
30
S
FMC
Sand
P

APPENDIX H

PALAEOCURRENT MEASUREMENTS

Appendix H

Table H.1

Palaeocurrent Measurements Of The Upper Cambrian

Section 3

Orientation Of Trough Cross-Bedding

324	10	150	350	328	348	330	332	357	328	16	40
355	341	320	327	302	310	340	320	295	327	326	333
310	300	290	320	308	326	290	341	332	335	342	336
337	336	331	321	346	348	344	340	358	14	342	354
10	356	345	00	344	4	7	11	354	348	338	

Orientation Of Overturned Cross-Bedding

325	324	332	28	300	70	52	60	326	320	327	66
332	315	334	350	52	35	320	127	321	328	338	337

Orientation Of Ripple Marks

316	295	300	398	326	290	312	318

Mudclast Imbrication

346

Table H.1

Palaeocurrent Measurements Of The Upper Cambrian(continued)

Section 5

Dip/Stike(Mean) 15/268

Orientation Of Trough Cross-Bedding

298	292	298	310	300	302	304	302	310	288	355	314
354	280	302	304	358	344	285	288	300	300	306	298
294	320	304	315	314	00	356	5	303	300	304	324
322	300	302	302	305	292	14	15	302	319	366	294
311	323	5	36	352	346	00	320	314	302	284	300
280	300	270	294	303	292	290	296	295	294	300	

Orientation Of Overturned Cross-Bedding

310	323	288	300	313	306	286	300	303	36	358	2
306	310	310	308	302	310	300	320	302	312	306	307
312	289	295	30	22	24	30					

Orientation Of Ripple Marks

278

Pebble Imbrication

312 310

Table H.1

Palaeocurrent Measurements Of The Upper Cambrian (continued)

Section 8

Dip/Stike(Mean) 11/229

Orientation Of Trough Cross-Bedding

42 20 38 17 282 280 284 293 262 297 297 310

300 306 325 291 290 298 292 292 278 294 318 306

325

Orientation Of Overturned Cross-Bedding

300 325 22 320 305 285 40 55 38 320 304 348

282 35 235

Orientation Of Planar Cross-Bedding

312

Orientation Of Ripple Marks

290 298

Appendix H

Table H.2

Palaeocurrent Measurements Of The Permo-Triassic (Um Irna Fm.)

Section 6

Orientation Of Trough Cross-Bedding

280 268 252 250 260 224 206 214 245 220

Section 7

Dip/Strike (Mean) 11/321

Orientation Of Trough Cross-Bedding

330 340 308 346 324 306 329 334 352 36 14 32

Pebble Imbrication

360 12 14 347 380 4 32 30 5 340 348 348

320 344 2 36 7 28 320 20 15 14 300

Section 11

Orientation Of Trough Cross-Bedding

266 220 218 336 230 234 202 302 300 304 285 245

274 266 230 270 208 280

Orientation Of Planar Cross-Bedding

248 258

Section 13

Orientation Of Trough Cross-Bedding

324 300 290 280 282 287 288 300 294 304 290 292

Section 14

Orientation Of Trough Cross-Bedding

350 320 318 162 356 238 218 262 238 234 224 248

254 206 222 240 226 236 272 214 246 220

Appendix H

Table H.3

Palaeocurrent Measurements Of The Lower-Triassic (Ma'in Fm.)

Section 1

Dip/Strike 20/250
Orientation Of Trough Cross-Bedding
320 330 110 320 80 70 65 66 68 70 62 76
118 340
Orientation Of Ripple Marks
328 240 225

Section 2

Dip/Strike (Mean) 12/212
Orientation Of Trough Cross-Bedding
82 110 210 240 254 266

Orientation Of Ripple Marks
175

Section 4

Dip/Strike (Mean) 11/287
Orientation Of Trough Cross-Bedding
16 20 104 292 320 120 218
Orientation Of Ripple Marks
325

Section 7

Dip/Strike 10/212
Orientation Of Ripple Marks
242

Section 11

Dip/Strike (Mean) 12/175
Orientation Of Trough Cross-Bedding
312 250 176 182 248
Orientation Of Planar Cross-Bedding
270

Orientation Of Ripple Marks
316

APPENDIX I

LIST OF ABBREVIATIONS

Appendix I

List Of Abbreviations

Q : Quartz mono and polycrystalline

Qm : Quartz monocrystalline

Qp : Quartz polycrystalline

Si : Silica overgrowth

C : Chert

F : Feldspar

K : K-Feldspar

P : Plagioclase

M : Mica

H : Heavy minerals

L : Lithic fragments

Kl : Kaolinite

Fe : Iron oxide

D,Dl,Dol : Dolomite

B,Bio: Bioclasts

Ool: Oolite

Ca : Calcite

Hm : Hematite

G : Goethite

Gy : Gypsum

C : Upper Cambrian

U : Permo Triassic(Um Irna Fm.)

H : Himara Member

N : Nimra Member

HN : Contact between H and N

Mbr: Member

F,Fm.: Formation

APPENDIX J

REFERENCES

REFERENCES

Abboud, D.Y. and Raouf, K.A., 1972. Geological investigation carried out on clay deposits of Samhat area, Middle Western rim of Al-Gaara Depression. MS Report, SOM Library, No.5581. Baghdad.

Abed, M.A., 1983. Mediterranean-Dead Sea canal and the Dead Sea water budget. Proc. of the first Jordanian Geological Conference, Amman : 617-640.

Abed, M.A., 1985. New evidence for horizontal movement along the Jordan Rift. Arab Gulf J. Scient. Res., 3, 539-551.

Allen, J.R.L., 1964. Studies in fluviatile sedimentation : six cyclothems from the Lower Old Red Sandstone, Anglo-Welsh Basin. Sedimentology, 3, 163-198.

Allen, J.R.L., 1965. A review of the origin and characteristics of recent alluvial sediments. Sedimentology, 5, 89-191.

Allen, J.R.L., 1968. Current ripples. North-Holland, Amsterdam, 433.

Allen, J.R.L., 1970. Studies in fluvial sedimentation : a comparison of fining-upwards cyclothems with special reference to coarse member composition and interpretation. J. Sediment. Petrol., 40, 298-323.

Allen, J.R.L., 1982. Sedimentary structures : their character and physical basis. Vol.1, Elsevier, Amsterdam, 593.

Allen, J.R.L. and Banks, N.L., 1972. An interpretation and analysis of recumbent-folded deformed cross-bedding. Sedimentology, 19, 257-283.

Anderson, D.W. and Picard, M.D., 1974. Evolution of synorogenic clastic deposits in the Intermontane Uinta Basin of Utah. S.E.P.M. Spec. Publ., 22, 167-189.

Balazs, R.J. and Klein, G. de V., 1972. Roundness-mineralogical relations of some intertidal sands. J. Sediment. Petrol., 42, 425-433.

Bandel, K., 1981. New stratigraphical and structural evidence for lateral dislocation in the Jordan Rift Valley connected with a description of the Jurassic rock column in Jordan. N. Jb.Geol. Palaont. Adh. Stuttgart, 161, 3, 271-308.

Bandel, K. and Khoury, H., 1981. Lithostratigraphy of the Triassic in Jordan. Erlangen, Facies, 4, 1-26.

Banks, N.L., Edwards, M.B., Geddes, W.P., Hobday, D.K. and Reading, H.G., 1971. Late Precambrian and Cambro-Ordovician sedimentation in East Finnmark. In: The Caledonian Geology of Northern Norway. Roberts, D. and Gustavson (Eds.). 197-236.

Bender, F. et al., 1968. Geological map of Jordan 1:250 000. 5 sheets, Geol. Surv. of Fed. Rep. Germany, Hanover.

Bender, F., 1974. Geology of Jordan, Gebruder Borntraeger, Berlin, 196.

Bender, F., 1983. On the evolution of Wadi Araba, Jordan Rift. In: Abed, A.M. and Khalid, H.M. (Eds.). Proc. 1st Jordanian Geol. Conf. Amman, 415-445.

Blake, G.S., 1936. The stratigraphy of Palestine and its building stones. Printing and Stationery Office, Jerusalem, 133.

Blakey, R.C. and Gubitosa, R., 1984. Controls of sandstone body geometry and architecture in the Chinle Formation (Upper Triassic), Colorado Plateau. Sediment. Geol., 38, 51-86.

Blatt, H., Middleton, G.V. and Murray, R.C., 1980. Origin of Sedimentary Rocks : 2nd ed., Englewood Cliffs, N.J., Prentice Hall, 782.

Boothroyd, J.C. and Ashley, G.M., 1975. Process, bar morphology and sedimentary structures on braided outwash fans, Northeastern Gulf of Alaska. In: Glaciofluvial and Glaciolacustrine sedimentation Jopling, A.V. and McDonald, B.C. (Eds.). S.E.P.M. Spec. Publ., 23, Tulsa, 193-222.

Bown, T.M. and Kraus, M.J., 1981. Lower Eocene palaeosols (Willwood Formation, north-west Wyoming, U.S.A.) and their significance for palaeoecology, palaeoclimatology and basin analysis. Palaeogeogr., Palaeoclimatol., Palaeoecol., 34, 1-30.

Brenchley, P.J. and Newall, G., 1977. The significance of contorted bedding in the Upper Ordovician sediments of the Oslo region, Norway. J. Sediment. Petrol., 47, 819-833.

Burdon, D.J., 1959. Handbook of the geology of Jordan to accompany and explain the three sheets of the 1:250 000 geological map east of the Rift by A.M. Quennel, Colchester (Benham) 82.

Cooper, G.A., 1976. Lower Cambrian Brachiopods from the Rift Valley (Israel and Jordan). J. Palaeont., 50, 269-289.

Campbell, C.V., 1976. Reservoir geometry of a fluvial sheet sandstone. Bull. Am. Assoc. Petrol. Geol., 60, 1009-1020.

Cant, D.J. and Walker, R.G., 1976. Development of a braided-fluvial facies model for the Devonian Battery Point Sandstone, Quebec. Can. J. Earth Sci., 13, 102-119.

Cant, D.J. and Walker, R.G., 1978. Fluvial processes and facies sequences in the sandy braided South Saskatchewan River, Canada. Sedimentology, 25, 625-648.

Cant, D.J., 1978. Development of a facies model for sandy braided river sedimentation. Comparison of the South Saskatchewan River and the Battery Point Formation. In: Miall, A.D. (Ed.). Fluvial Sedimentology. Can. Soc. Petrol. Geol. Mem. 5, 627-641.

Chayes, F., 1956. Petrographic modal analysis. An elementary statistical appraisal. Wiley and Sons, New York.

Clifton, H.E., Hunter, R.E. and Phillips, R.L., 1971. Depositional structures and processes in the non-barred high-energy nearshore. J. Sediment. Petrol., 41, 651-670.

Coleman, J.M., 1969. Brahmaputra River : Channel processes and sedimentation. Sediment. Geol. (special issue), 3, 122-239.

Collinson, J.D. and Lewin, J., 1983 (Eds.). Modern and Ancient Fluvial Systems. Spec. Publ. No.6. Int. Assoc. of Sediment., Blackwell Scientific Publications, Oxford, London, 575.

Cotter, E., 1978. The evolution of fluvial style, with special reference to the central Appalachian Palaeozoic. In: Miall, A.D. (Ed.), Fluvial Sedimentology. Can. Soc. Petrol. Geol. Mem. 5, 361-383.

Cox, L.R., 1924. Triassic fauna from the Jordan Valley. Ann. Mag. Nat. Hist., London (9), 14, 52-96.

Cox, L.R., 1932. Further notes on the Transjordan Trias. Ann. Mag. Nat. Hist., London, (10), 10, 93-113.

Crook, K.A.W., 1974. Lithogenesis and tectonics : the significance of compositional variation in flysch arenites (graywackes). In: S.E.P.M. Spec. Publ., 19, 304-310.

Daniel, E.J., 1959. Stratigraphic Lexicon of Palestine. (unpublished draft).

Daniel, E.J., 1963. Lexique Stratigraphique International Jordanie. Vol. III. Centre National de la Researche Scientifique. Paris, Fasc.10C, 295-437.

Davies, J.L., 1964. A morphogenetic approach to world shorelines. Zeits. Geomorph., 8, 127-142.

Desio, A., 1935. Studi geologici sulla Cirenaica sul de serto libico, sulla Tripolitania e sul Fezzan orientali : Rome, Missione Scient. Reale Acc. d'Italia a Cufra (1931), V.I, 464.

Dickinson, W.R., 1982. Compositions of sandstones in Circum-Pacific subduction complexes and fore-arc basins. Bull. Am. Ass. Petrol. Geol., 66, 121-137.

Dickinson, W.R. and Suczek, C.A., 1979. Plate tectonics and sandstone compositions. Bull. Am. Ass. Petrol. Geol., 63, 2164-2182.

Doe, T.W. and Dott, R.H., 1980. Genetic significance of deformed cross-bedding with examples from the Navajo and Weber sandstones of Utah. J.Sediment. Petrol., 50, 793-812.

Druckman, Y., 1974. The stratigraphy of the Triassic sequence in southern Israel. Geol. Surv. Isr. Bull., 64, 92.

Druckman, Y., 1977. Differential subsidence during deposition of the Lower Jurassic Ardon Formation in Western Jordan, Southern Israel and Northern Sinai. Isr. J. Earth-Sci., 26, 45-54.

Druckman, Y., Weissbrod, T. and Horwitz, A., 1970. The Budra Formation : A Triassic Continental deposit in south-western Sinai. Rep. Geol. Surv. Isr., No. OD/3/70, 20.

Dunham, R.J., 1965. Vadose pisolite in the Capitan Reef (Permian), New Mexico and Texas. S.E.P.M. Spec. Publ. 14, 182-191.

Dypvik, H. and Vollset, J., 1979. Petrology and diagenesis of Jurassic sandstones from Norwegian Danish Basin, North Sea. Bull. Am. Ass. Petrol. Geol., 63, 182-193.

Ethridge, F.G., 1985. Surface and subsurface methods of investigation and classification of fluvial systems. In: S.E.P.M. Short Course No.19, Recognition of fluvial depositional systems and their resource potential, 9-32.

Figari Bey, A., 1864. Studii scientifici sull'Egitto e sue adjacenze compresa la penisola dell'Arabia Petraea : Lucca, tipografia di Giuseppe Giusti.

Flemming, B.W., 1977. Langebaan Lagoon : a mixed carbonate-siliciclastic tidal environment in a semi-arid climate. Sediment. Geol., 18, 61-95.

Flores, R.M., 1985. Introduction. In: S.E.P.M. Short Course No.19, Recognition of fluvial depositional systems and their resource potential, 1-8.

Freund, R. and Garfunkel, Z., 1981. (Eds.). The Dead Sea Rift. Tectonophysics, 80, Nos. 1-4, 304.

Freund, R., Garfunkel, Z., Zak, I., Goldberg, M., Weissbrod, J. and Derin, B., 1970. The shear along the Dead Sea Rift. Phil. Trans. Royal Soc., London, A267, 107-130.

Friend, P.F., 1983. Towards the field classification of alluvial architecture or sequence. In. Collinson, J.D. and Lewin, J. (Eds.), Modern and ancient fluvial systems. Internat. Assoc. Sedimentologists, Spec. Publ.6.

Friend, P.F., Slater, M.J. and Williams, R.C., 1979. Vertical and lateral building of river sandstone bodies, Ebro Basin, Spain. J. Geol. Soc., London, 136, 39-46.

Garfunkel, Z., 1978. The Negev-Regional Synthesis of sedimentary basins. Pre-Congress Excursion Guidebook, Israel, 35-110. Tenth Int. Congr. on Sedimentology, Jerusalem.

Gindy, A.R., El-Askary, M.A. and El-Fishawi, N.M., 1982. The Skewness-Median environmental discriminator for some recent and ancient sediments from Egypt. N. Jb. Geol. Palaont. Mh., H., 12, 705-722, Stuttgart.

Girdler, R.W., 1983. The importance of the Jordanian Rift to studies of the Red Sea and Gulf of Aden. In: Abed, A.M. and Khalid, H.M. (Eds.). Proc. 1st Jordanian Geol. Conf., Amman, 503-520.

Goldbery, R. and Beyth, M., 1984. Laterization and ground water alteration phenomena in the Triassic Budra Formation, south-western Sinai, Sedimentology, 31, 575-594.

Harms, J.C., Southard, J., Spearing, D.R. and Walker, R.G., 1975. Depositional environments as interpreted from primary sedimentary structures and stratification sequences. Lecture notes : Soc. Econ. Palaeont. Miner., Short Course 2, Dallas, 161.

Harms, J.C., Southard, J.B. and Walker, R.G., 1982. Structures and sequences in clastic rocks. Soc. Econ. Palaeont.Miner. Short Course No.9.

Haszeldine, R.S., 1983. Descending tabular cross-bed sets and bounding surfaces from a fluvial channel in the Upper Carboniferous coalfield of north-east England. In: Collinson, J.D. and Lewin, J. (Eds.), Spec. Publ. Int. Ass. Sediment., 6, 449-456.

Hayes, M.O., 1975. Morphology of sand accumulations in estuaries. In: Estuarine Research, Cronin, L.E. (Ed.). New York : Academic Press, 3-22.

Hayes, M.O., 1979. Barrier island morphology as a function of tidal and wave regime. In: Leatherman (1979), 1-27.

Hayes, M.O. and Kana, T.W., 1976. Terrigenous Clastic Depositional Environments - some modern examples. Tech. Rep. 11-CRD, Coastal Res. Div., Univ. South Carolina, I-131, II-184.

Helal, A.H., 1964. On the occurrence of lower Palaeozoic rocks in Tabuk area, Saudi Arabia : Neues Jahrb. Geologie U. Palaontologie Montash, Heft 7, 391-414.

Hendry, H.E. and Stauffer, M.E., 1975. Penecontemporaneous recumbent folds in trough cross-bedding in Pleistocene sands in Saskatchewan, Canada. J. Sediment. Petrol., 45, 932-943.

Hendry, H.E. and Stauffer, M.E., 1977. Penecontemporaneous folds in cross-bedding : Inversion of facing criteria and mimicry of tectonic folds. Bull. Geol. Soc. Am., 88, 809-812.

Hirsch, F., 1975. Lower Triassic conodonts from Israel. Geol. Survey Isr. Bull., Tel Aviv, 66, 39-49.

Horwitz, A., 1970. Palynostratigraphy of the Upper Paleozoic - Lower Mesozoic sequence in Zohar 8 Borehole (Southern Israel). Rep. Geol. Surv. Isr., P/1/70; Rep. Inst. Petrol. Res. Geophys. 1038, Jerusalem, 9.

Hull, E., 1886. Memoirs on the geology and geography of Palestine. (London : Palestine Exploratoin Fund).

Illing, L.V., 1954. Bahaman calcareous sands. Bull. Am. Assoc. Petroleum Geol., 38, 1-95.

Ionides, M.G. and Blake, G.S., 1939. Report on the water resources of Transjordan and their development, local report. Government of Transjordan, 372.

Issawi, B., 1971. Nubian Sandstone : discussion. Bull. Am. Assoc. Petrol. Geol., 55, 885-887.

Jackson, R.G., 1975. Velocity-bedform texture patterns of meander bends in the lower Wabash River of Illinois and Indians. Bull. Geol. Soc. Am., 86, 1511-1522.

Jackson, R.G., 1976. Large scale ripples of the Lower Wabash River. Sedimentology, 23, 593-623.

Jackson, R.G., 1978. Preliminary evaluation of lithofacies models for meandering alluvial streams. In: Miall (1978), 543-576.

Jeward, A.M., 1980. Geochemistry and mineralogy of Ubaid Formation in the western desert. Unpubl. M.Sc. Thesis, Baghdad Univ., Iraq.

Kadir, S.J.A. and Santrucek, P., 1975. Report on the geological investigation of clay deposit of Duekhla area - Southern rim of Al-Gaara Depression. MS report, SOM Library No. 699, A-12, Baghdad.

Kessler, L.G., 1971. Characteristics of the braided stream depositional environment with examples from the South Canadian River, Texas. Western Geol. Ass. Earth Sci. Bull., 4, 25-35.

Klein, G. de V., 1963. Bay of Fundy intertidal sediments. J. Sediment. Petrol., 33, 844-854.

Klein, G. de V., 1967. Comparison of recent and ancient tidal flat and estuarine sediments. In: Lauff, G.H. (Ed.). Estuaries. Am. Assoc. Adv. Sci. Publ. 83, 207-218.

Klein, G. de V., 1970a. Tidal origin of a Precambrian quartzite - the lower Fine-grained Quartzite (Middle Dalradian) of Islay, Scotland. J. Sediment. Petrol., 40, 973-985.

Klein, G. de V., 1970b. Depositional and dispersal dynamics of intertidal sand bars. J. Sediment. Petrol., 40, 1095-1127.

Klein, G. de V., 1971. A sedimentary model for determining paleotidal range. Bull. Geol. Soc. Am., 82, 1585-2592.

Klein, G. de V., 1977a. Tidal circulation model for deposition of clastic sediment in epeiric and mioclinal shelf seas. Sediment. Geol., 18, 1-12.

Klein, G. de V., 1977b. Clastic Tidal Facies : Continuing Education Publication Co., 149.

Klein, G. de V. and Sanders, J.E., 1964. Comparison of sediments from Bay of Fundy and Dutch Wadden Sea tidal flats. J. Sediment. Petrol., 34, 18-24.

Krynine, P.D., 1946. Microscopic morphology of quartz types. Pan. American Cong. Min. and Geol. Engineers. Annals of 2nd comm., 36-49.

Kuenen, P. H., 1953. Significant features of graded bedding. Am. Assoc. Petroleum Geologists. Bull. 37, 1044-1066.

Lachenbruch, A.H., 1962. Mechanics of thermal contraction cracks and ice-wedge polygons in permafrost. Geol. Soc. Am. Spec. Paper 70, 1-69.

Lachenbruch, A.H., 1963. Contraction theory of ice-wedge polygons : a qualitative discussion. Nat. Acad. Sci. Natl. Res. Counc. Publ. No. 1287, 63-71.

Lapparent, A.F. de., 1952. Etat actuel de nos connaissances sur la stratigraphie, la paleontologie et la tectonique de Gres de Nubie du Sahara Central : 19th Internat. Geol. Cong., Algiers, fasc. 21 (Alger 1954), 113-127.

Lartet, L., 1869. La geologie de la Palestine, Ann. Sci. Geol. Paris, 1.

Leeder, M.R., 1982. (Ed.). Sedimentology process and product. George Allen and Unwin, London, 344.

Leopold, L.B. and Wolman, M.G., 1957. River channel patterns : braided, meandering and straight. US Geol. Surv. Prof. Pap. 282-B, 39-85.

Lillich, W., 1964. Stratigraphical investigations on the Paleozoic and Mesozoic sandstones on the east side of the Dead Sea. Unpublished report. Deutsche Geol. Mission Jordanien, Arch. Bundesant. Bodenforsch, Hanover.

Lloyd, J.W., 1969. The hydrogeology of the southern desert of Jordan. UNDP/FAO 212, Technical Report No.1.

Logan, B.W., Rezak, R., and Ginsburg, R.N., 1962. Classification and environmental significance of algal stromatolites. J. of Geol., 72, 68-83.

Logan, B.W., Davies, G.R., Read, J.F. and Cebulski, D.E., 1970. Carbonate sedimentation and environment, Shark Bay, Western Australia. Mem. Am. Assoc. Pet. Geol., 13, 223.

Lowe, D.R., 1976. Subaqueous liquefied and fluidized sediment flows and their deposits. Sedimentology, 23, 285-308.

Lowe, D.R. and Lo Piccalo, R.D., 1974. The characteristics and origins of dish and pillar structures. J. Sediment. Petrol., 44, 484-501.

McBride, E.F., 1963. A classification of common sandstones. J. Sediment. Petrol., 33, 664-669.

McKee, E.D., 1962. Origin of the Nubian and similar sandstones. Geol. Rundschau, Bd. 52, Hft. 2, 551-587.

McKee, E.D., Reynolds, M.A. and Baker, C.H., Jr., 1962. Experiments on intraformational recumbent folds in cross-bedded sand. US Geol. Surv. Prof. Pap. 450 D, D155-D159.

McKee, E.D. and Bigarella, J.J., 1972. Deformational structures in Brazilia Coastal Dunes. J. Sediment. Petrol., 43, 670-681.

Miall, A.D., 1970. Devonian alluvial fans, Prince Edward Island, Arctic Canada. J. Sediment. Petrol., 40, 556-571.

Miall, A.D., 1976. Proterozoic and Palaeozoic Geology of Banks Island, Arctic Canada. Geol. Surv. Can. Bull. 258, 77.

Miall, A.D., 1977. A review of the braided river depositional environment. Earth Sci. Rev. 13, 1-62.

Miall, A.D., 1978. Lithofacies types and vertical profile models in braided river deposits : a summary. In: Miall, A.D. (Ed.). Fluvial Sedimentology, Can. Soc. Petrol. Geol. Mem. 5, 597-604.

Mills, P.C., 1983. Genesis and diagnostic value of soft-sediment deformation structures - A review. Sediment. Geol. 35, 83-104.

Miall, A.D., 1985. Architectural-element analysis : A new method of facies analysis applied to fluvial deposits. Earth Sci. Rev., 22, 261-308.

Parker, D.H., 1970. Sandstone aquifers of East Jordan. FAO, Technical report, Rom.

Pearce, A.J., 1976. Geomorphic and hydrologic consequences of vegetation destruction, Sudbury, Ontario : Can. J. Earth Sci., 13, 1358-1373.

Pettijohn, F.J., 1957. Sedimentary rocks, 2nd ed., New York, Harper and Row, 718.

Pettijohn, F.J., Potter, P.E. and Siever, R., 1972. Sand and Sandstone. New York, Springer-Verlag, 618.

Picard, L., 1938. Synopsis of stratigraphic terms in Palestinian geology. Hebrew Univ. Geol. Dept. Bull. V.2, No.2, 24.

Picard, L., 1943. Structure and evolution of Palestine. Hebrew Univ., Jerusalem, Geol. Dept. Bull, 4, 135.

Pomeyrol, R., 1968. 'Nubian Sandstone'. Bull. Am. Assoc. Petrol. Geol., 52, 589-600.

Potter, P.E. and Pettijohn, F.J., 1977. Palaeocurrents and basin analysis. New York : Springer-Verlag, 425.

Quennell, A.M., 1951. The geology and mineral resources of (former) Transjordan : London, Colonical Geol. Min. Resour. 2, No.2.

Quennell, A.M., 1958. Structures and geomorphic evolution of the Dead Sea Rift, Q.J. Geol. Soc., Lond., 64, 1-24.

Quennell, A.M. 1959a. Tectonics of the Dead Sea Rift. 20th Int. Geol. Cong., Mexico, 385-405.

Quennell, A.M., 1959b. Geological map of Jordan (East of the Rift Valley). 1:250,000 Sheets. Amman, Karak, Ma'an (Amman : Jordan Government) (Ref. Burdon, 1959).

Quennell, A.M., 1983. In the evolution of the Dead Sea Rift - a review. In: Abed, A.M. and Khalid, H.M. (Eds.). Proc. 1st Jordanian Geol. Conf. Amman, 460-482.

Reading, H.G. (Ed.), 1978. Sedimentary environments and facies. Oxford : Blackwell Scientific Publications, 557.

Reineck, H.E., 1967. Layered sediments of tidal flats, beaches, and shelf bottoms of the North Sea. In: Lauff, G.H. (Ed.). Estuaries, Washington, D.C., Am. Assoc. Adv. Sci., Spec. Publ., 83, 191-206.

Reineck, H.E., 1972. Tidal flats. In: Recognition of Ancient Sedimentary Environments. Rigby, J.K. and Hamblin, W.K. (Eds.). Spec. Publ. Soc. Econ. Palaeont. Miner., 16, Tulsa, 146-159.

Reineck, H.E., 1975. German North Sea tidal flats. In: Tidal Deposits. Ginsburg, R.N. (Ed.). Springer-Verlag, New York, 5-12.

Reineck, H.E. and Wunderlich, F., 1968. Classification and origin of flaser and lenticular bedding,. Sedimentology, 11, 99-104.

Reineck, H.E. and Singh, I.B., 1972. Genesis of laminated sand and graded rhythmites in storm-sand layers of shelf mud. Sedimentology, 18, 123-128.

Reineck, H.E. and Singh, I.B., 1973 (Eds.). Depositional Sedimentary Environments : New York-Heidelberg-Berlin, Springer-Verlag, 439.

Rigassi, A.D., 1969. 'Nubian Sandstone' : discussion. Should the term 'Nubian Sandstone' be dropped? Bull. Am. Assoc. Petrol. Geol., 53, 183-184.

Robson, D.A., 1956. A sedimentary study of the Fell Sandstone of the Coquet Valley, Northumberland. Q. J. Geol. Soc., Lond., 112, 241-262.

Rüssegger, J., 1837. Kreide und Sandstein : Enfluss Von Granit auf letzteren : Neues Jahrb. Mineralogie Abh. 665-669.

Rüssegger, J., 1847. Reisen in Europa, Asien und Afrika, mit besonderer Ruecksicht auf die naturwissenschaftlichen Verhaeltnisse der betreffenden laender, untermommen in der Jahren 1835 bis 1841, mit einem Atlas, enthaltend geographische Karten, Bd. 3, Reisen in unter-Eggpten, auf der Halbinsel der Sinai und im gelobten Land : Stuttgart, E. Schweizzerbart, 1-292.

Rust, B.R., 1978. Depositional models for braided alluvium. In: Miall, A.D. (Ed.). Fluvial Sedimentology. Can. Soc. Petrol. Geol. Spec Publ. 5, 605-625.

Said, R., 1962. The Geology of Egypt. New York, Elsevier Pub. Co., 377.

Salmon, H.H., 1977. Sedimentology of the upper part of Gaara Formation, Western Iraq., M.Sc., Thesis, Baghdad Univ.

Sanders, J.E., 1960. Origin of convoluted laminae. Geol. Mag., 97, 409-421.

Saxena, R.S., 1976. Sand bodies and sedimentary environments of the modern Mississippi Delta - An excellent model for exploration in deltaic sandstone reservoirs. Egypt General Petroleum Corp., Exploration Seminar, Cairo, Egypt, 15-17.

Schneider, W., Abed, A.M. and Salamek, E., 1984. Mineral content and diagenetic pattern - Useful tools for lithostratigraphic subdivision and correlation of the Nubian series - Results of work in the Wadi Zarga Main area, Jordan. Geol. Jb. B53, 55-75, Hanover.

Schumm, S.A., 1967. The disparity between present rates of denudation and orogeny. US Geol. Surv. Prof. Pap. 454-H, 13.

Schumm, S.A., 1968. Speculations concerning paleohydrologic controls of terrestrial sedimentation. Geol. Amer. Bull. 79, 1573-1588.

Schumm, S.A., 1972. Fluvial palaeochannels. In: Recognition of Ancient Sedimentary Environments. Rigby, J.K. and Hamblin, W.K. (Eds.). Spec. Publ. Soc. Econ. Palaeont. Miner., 16, Tulsa, 98-107.

Schumm, S.A., 1981. Evolution and response of the fluvial system, sedimentological implications. In: Ethridge, F.G. and Flores, R.M. (Eds.). Recent and ancient nonmarine depositional environments : Models for exploration. Soc. Econ. Paleon. Miner. Spec. Publ. 31, 19-30.

Schwab, F.L., 1975. Framework mineralogy and chemical composition of continental margin-type sandstone. Geology, 3, 487-490.

Seed, H.B., 1968. Landslides during earthquakes due to soil liquefaction. Proc. Am. Soc. Civ. Eng. J. Soil Mech. Found. Div., 94, 1055-1122.

Selley, R.C., 1969. Torridorian alluvium quick sands. Scott. J. Geol. 5, 328-346.

Selley, R.C., 1972. Diagnosis of marine and non-marine environments from the Cambro-Ordovician sandstones of Jordan. J. Geol. Soc. 128, 135-150.

Selley, R.C., 1976. An Introduction to Sedimentology. Academic Press, London, 408.

Selley, R.C. and Shearman, D.J., 1962. Experimental production of sedimentary structures in quick sand. Proc. Geol. Soc. London, 1599, 101-102.

Shawa, M.S., 1969. 'Nubian Sandstone' : discussion. Bull. Am. Assoc. Petrol. Geol., 53, 182.

Shawa, M.S., 1970. Reply : Bull. Am. Assoc. Petrol. Geol., 54, 530-531.

Smith, N.D., 1970. The braided stream depositional environment : comparison of the Platte River with some Silurian clastic rocks, North Central Appalachians, Geol. Soc. Amer. Bull., 81, 2993-3014.

Smith, N.D., 1971. Transverse bars and braiding in the lower Platte River, Nebrasks. Geol. Soc. Am. Bull, 82, 3407-3420.

Smith, N.D., 1972. Some sedimentological aspects of planar cross-stratification in a sandy braided river. J. Sediment. Petrol., 42, 624-634.

Straaten, L.M.J.U.Van, 1949. Occurrence in Finland of structures due to subaqueous sliding of sediments. Bull. Comm. Geol. Finlande, 144, 9-18.

Straaten, L.M.J.U.Van, 1950a. Environment of formation and facies of the Wadden Sea sediments. Koninkl. Ned. Aardrijksde Genoot. 67, 49-108.

Straaten, L.M.J.U. Van, 1950b. Giant ripples in tidal channels. Koninkl. Ned. Aardrijkskde Genoot. 67, 336-341.

Straaten, L.M.J.U.Van, 1951. Longitudinal ripple marks in mud and sand. J. Sediment. Petrol. 21, 47-54.

Straaten, L.M.J.U.Van., 1952. Biogenic textures and the formation of shell beds in the Dutch Wadden Sea. Proc. Koninkl. Ned. Akad. Wetenschap. Amsterdam, Ser. B55, 500-516.

Straaten, L.M.J.U.Van, 1953. Rhythmic pattern on Dutch North Sea beaches. Geol. Mijnbouw 15e, 31-43.

Straaten, L.M.J.U.Van., 1954a. Composition and structure of recent marine sediments in the Netherlands. Leidse Geol. Mededel. 19, 1-110.

Straaten, L.M.J.U.Van., 19544b. Sedimentology of recent tidal flat deposits and the psammites due Condroz (Devonian). Geol. Mijnbouw 16, 25-47.

Straaten, L.M.J.U.Van, 1959a. Minor structures of some recent littoral and neritic sediments. Geol. Mijnbouw, 21, 197-216.

Straaten, L.M.J.U.Van., 1961. Sedimentation in tidal flats area. Alberta Soc. Petrol. Geol. J., 9, 204-226.

Straaten, L.M.J.U.Van and Kuenen, Ph. H., 1957. Accumulation of fine-grained sediments in the Dutch Wadden Sea. Geol. en. Mijnb., 19, 329-354.

Straaten, L.M.J.U.Van and Kuenen, Ph. H., 1958. Tidal action as a cause of clay accumulation. J. Sediment. Petrol., 28, 406-413.

Tankard, A.J. and Hobday, D.K., 1977. Tide-dominated back-barrier sedimentation, early Ordovician Cape Basin, Cape Peninsula, South Africa. Sediment. Geol., 18, 135-159.

Tate, R., 1871. On the age of the Nubian Sandstone. Geol. Soc., London. Quart. J., 27, No.108, 404-406.

Termier, H. and Termier, G., 1952. Histoir geologique du Cambrien au Quaternaire dans histoir geologique de la biosphere. Paris, Masson et cie, 721.

Terzaghi, K., 1956. Varieties of submarine slope failures. Proc. Texas Conf. Soil. Mech. Found. Eng., 8, 41-52.

Turner, B.R., 1981. Deformed cross-bedding patterns in the Upper Triassic Molteno Formation in the main Karoo Basin, South Africa : a model for their genesis. Geol. Rundschau, 70, 910-924, Stuttgart.

Turner, B.R., 1983. Braidplain deposition of the Upper Triassic Molteno Formation in the main Karoo (Gondwana) Basin, South Africa. Sedimentology, 30, 77-89.

Turner, B.R., 1986. Tectonic and climatic controls on continental depositional facies in the Karoo Basin of Northern Natal, South Africa. Sediment. Geol., 46, 231-257.

Turner, B.R. and Monro, M. (in press). Channel emplacement and migration by mass flow processes in the lower Carboniferous fluviatile Fell Sandstone Group, north-east England. Sedimentology.

Vos, R.G. and Eriksson, K.A., 1977. An embayment model for tidal and wave swash deposits occurring within a fluvially dominated middle Proterozoic sequence in South Africa. Sediment. Geol., 18, 161-173.

Wagner, G., 1934. Deutscher Muschelkalk am Toten Meer. Natur U. Volk 64/2, 449-454, Frankfurt.

Walker, R.G., 1979 (Ed.). Facies models : Geosci. Can. Reprint Series 1, Geol. Assoc. Can, 211.

Walker, R.G. and Harms, J.C., 1971. The Catskill 'Delta' - a prograding muddy shoreline in central Pennsylvania. J. Geol., 79, 381-399.

Walker, R.G. and Harms, J.C., 1975. Shorelines of weak tidal activity : Upper Devonian Catskill Formation, Central Pennsylvania. In: Ginsburg, R.N. (Ed.). Tidal Deposits, 103-108.

Walker, R.G. and Cant, D.J., 1984. Sandy fluvial systems. In: Walker, R.G. (Ed.). Facies models, second edition, Geoscience Canada Reprint Series, 1, 71-89.

Wegener, A., 1924. The origin of continents and oceans. 3rd ed. English translation by J.G.A. Skerl. Methuen, London.,212.

Weggel,J.R., 1972. An introduction to oceanic water motions and their relation to sediment transport. In: Swift, D.J.P., Duane, D.B. and Pilkey, O.H. (Eds.). Shelf sediment transport : process and pattern, Stroudsburg, Pa., Dowden, Hutchinson and Ross, 1-20.

Weissbrod, T., 1970. 'Nubian Sandstone' : discussion. Bull. Am. Assoc. Petrol. Geol., 54, 526-529.

Weissbrod, T., 1978. Criteria for the recognition of lithostratigraphic units in the Nubian Sandstone Sequence. Proc. Tenth Intern. Congress on Sedimentology, Jerusalem, 1978 (Abs.).

Wentworth, C.K., 1922. A scale of grade and class terms for clastic sediments. J. Geol., 30, 377-392.

Wetzel, R., 1947. Stratigraphic sections of Jordan Valley and Dead Sea. Unpubl. Rep. Petrol. Develop. (Transjord.) Paris.

Wetzel, R. and Morton, D.M., 1959. Contribution a la geologie de la Transjordanie. Note Mem. Moyen. Orient. V.7, 95-191, Paris.

Whiteman, A.J., 1969. The Geology of Sudan Republic. Oxford, Clarendon Press.

Whiteman, A.J., 1970. Nubian Group : Origin and Status. Bull. Am. Assoc. Petrol. Geol., 54, 522-526.

Williams, G.E., 1971. Flood deposits of the sand-bed ephemeral streams of Central Australia. Sedimentology, 17, 1-40.

Williams, P.F. and Rust, B.R., 1969. The sedimentology of a braided river. J. Sediment. Petrol., 39, 649-679.

Wilson, M.D. and Pittman, E.D., 1977. Authigenic clays in sandstones : recognition and influence on reservoir properties and paleoenvironmental analysis. J. Sediment. Petrol., 47, 3-31.

Wunderlich, F., 1970. Genesis and environment of the 'Nellenkopfenschichten' Lower Emsian, Rheinian (Devonian) of Locus typicus in comparison with modern coastal environments of the German Bay. J. Sediment. Petrol., 40, 102-130.

Zittel, K.A., 1883. Beiträge zur Geologie und Palaeontologie der Libyschen Wüste und der angrenzenden Gebiete von Aegypten : Stuttgart, Paleontographica. Bd. 30, Hft. 1, 1-112.

* * *